INTERACTIONS BETWEEN CANCER CELLS AND INORGANIC MATERIALS

GRAHAM J. HICKMAN

A thesis submitted in partial fulfilment of the requirements of Nottingham Trent University for the degree of Doctor of Philosophy

December 2013

Abstract

Cancer is a complex multi-faceted disease that poses a significant threat to world health. However, as our understanding of the disease improves so does the complexity of this threat. One aspect of complexity is tumour heterogeneity, subpopulations of which have been identified as being fundamental to the understanding the formation, progression and treatment of the disease. Cancer stem cells and cells undergoing epithelial to mesenchymal transition are two such subpopulations. However, the study of these populations is complicated by difficulties in the isolation and sustainment of these cell types *in vitro* due to the scarcity and transience of their nature.

The importance of the cells local environment or 'niche' in driving cell responses has been made increasingly apparent in recent years, specifically the role of the surfaces to which the cell is in contact. Many cellular processes, even the survival of the cell itself, have been shown to be dependent on cues taken from the surface and the biological entities (proteins etc.) which can interact with surfaces independently of the cell. This understanding opens the possibility that surface chemistry can be applied to the precise control of cells for specific applications.

Using this premise, this work developed a range of surface materials based around silica which are both compatible with *in vitro* culture and capable of presenting a range of surface chemistries (hydroxyl, methyl. phenyl, amino) to which the cell response in terms of proliferation, adhesion, motility and morphology was measured. Specific surfaces determined from these assays where then examined to explore the influence of surface chemistry on the sub-populations of the human prostate cell line OPCT1.

The data obtained shows that silica materials, including those of extreme properties (such as super-hydrophilicity) can support the adhesion and growth of tumour cell lines, likely due to enhanced protein adsorption. Distinct surface chemistries were found to influence the adhesion and proliferation of these cell lines differently. The surfaces were also found to influence the adsorption of specific proteins such as fibronectin. In response to cell selection, surfaces (3-aminopropyl and a glass substrate) were identified which could selectively enrich epithelial and mesenchymal populations from co-culture, fulfilling the initial aims of the study.

Dedication

To my family and friends without which any of this would be impossible.

"I do not have much patience with a thing of beauty that must be explained to be understood. If it does need additional interpretation by someone other than the creator, then I question whether it has fulfilled its purpose"

Sir Charles S. Chaplin, KBE (16th April 1889 – 25th December 1977)

Acknowledgements

Firstly I acknowledge the support of my supervisory team, Prof's Carole C. Perry, Robert C. Rees & Dr. David J. Boocock, who have been an enduring supply of encouragement and inspiration throughout my studies.

I acknowledge the following contributions:

- Dr Akhilesh Rai for his initial support and assistance with the AFM, protein and molybdic acid assays presented in chapter three
- Dr. David J. Belton for constant support and knowledge
- Dr. Naomi Dunning-Foreman for her pioneering work on EMT
- Dr. Stephanie E.B. McArdle for flow cytometry method development

The support of collaborators Dr. R. R. Naik & Mr J. Slocik (XPS), Dr. A. El Hadad (osteoblast related studies) & Prof. M. R. Clench (MALDI imaging) for their invaluable contributions and the opportunities they represent.

I acknowledge an invaluable team of support staff; Miss C. Coveney, Mr S. Reeder, Mrs A Schneider, C Johnson & P. Whitehall & Mr G Arnott. I acknowledge the advice and support of; Prof A. G. Pockley & G. Ball. Dr O. Deschaume, S. V. Patwardhan, N. J. Shirtcliffe, P. Roach, V. Puddu, M. Demurtas, L. L. S. Canabady-Rochelle, A. K. Miles, M. G. Mathieu, M. Ahmad, T. Regad, D. L. Tong & B. Matharoo-Ball.

I acknowledge the support and advice of my fellow Ph.D students; Mr J. Vadakekolathu, Miss E. Boix-Lopez & M. Limo, Mr R. Ramasany, Mrs & Mr A. Sola-Rabada & M. Gimeno-Fabra, Mr M. Parambath, Mrs S. Malhi, Miss V. Phatak, Mr G. Dhondalay, Dr. A. Linley, B. Vafader-Isfahani & S. Laversin, Miss S. Rane, Mr B. Alshehri, Mrs J. Saif, Miss Y. Dede, Mr S. Hood, M. Ponniah & I. Burhan, Miss D. Agarwal, Mr M. Nicklin, Dr. M. K. Liang, M. S. Zafer, S. Gill & T. Green & Mr T. Kriese. Mr T. Resinger, Miss M. P. Borras, Mr A. Prashar & D. Nagaranjan.

Special mention to the support of external presences Dr. A. Fenton (landlord), Mr M. Capeness, Mr J. White, Dr. A. Fernandes & the assorted members of 'Sockett Lab'.

Contents

Chapter 2: Experimental Methods

2.1 Ultraviolet-visible spectrophotometry, luminometry and fluorometry

Chapter 3: Development of Silica Surfaces for Tissue Culture: Fabrication, Characterisation & Performance in Culture

Chapter 4: Response of Tumour Cell Lines to Silica Materials of Varying Chemical Properties

Chapter 5: Applying Cell Response to Inorganic Materials: Developing a Selective Surface

Chapter 6: Moving to a Mechanistic Understanding of Cell Responses & Selection Effects with Respect to Surface Properties

List of figures

xii

xiii

List of tables

Chapter One

Introduction

1.1 Silica in chemistry & biology

1.1.1 Silica chemistry & synthesis

Silica (SiO_2) or silicon dioxide is an abundant inorganic compound. Present in a wide variety of forms and phases, silica can be crystalline (such as quartz or cristobalite) or amorphous (vitreous silica, micro-amorphous silica) in nature and these forms can be further sub-divided into hydrated and anhydrous forms such as magadiite a hydrated crystalline silica and fumed silica an amorphous anhydrous silica (Iler, 1976). Of particular interest in this study is the common amorphous class of micro-amorphous silica's formed by polymerisation of silica monomer in aqueous conditions.

Silica itself is weakly soluble in water (70-150 ppm) with potable water generally containing around 6 ppm of soluble silica leached from surrounding minerals (Iler, 1976). The soluble form of silica is the weak acid $Si(OH_4)$ (monosilicic acid), which is stable under neutral and mildly acidic conditions at low concentration. However at concentrations greater than two millimolar, monosilicic acid will readily polymerise to form oligomers of the monomer or polysilicic acid which can further polymerise to a colloid or form a silica gel network (Iler, 1976).

The polymerisation of silica can be described as a nucleophilic condensation process as water is liberated as a result of the reaction between two silanol (SiOH) groups of monosilicic acid to form a siloxane bond as described in fig. 1.1A. The process is initiated by protonation of a silanol, resulting in the silanol taking on a more acidic character, withdrawing electrons from the silicon atom, making itself vulnerable to a nucleophilic species such as the oxygen of another silanol. Under basic conditions (fig. 1.1B) this process starts with deprotonation of a silanol, negatively charging oxygen which can attack another silicon atom (Harrison, 1993).
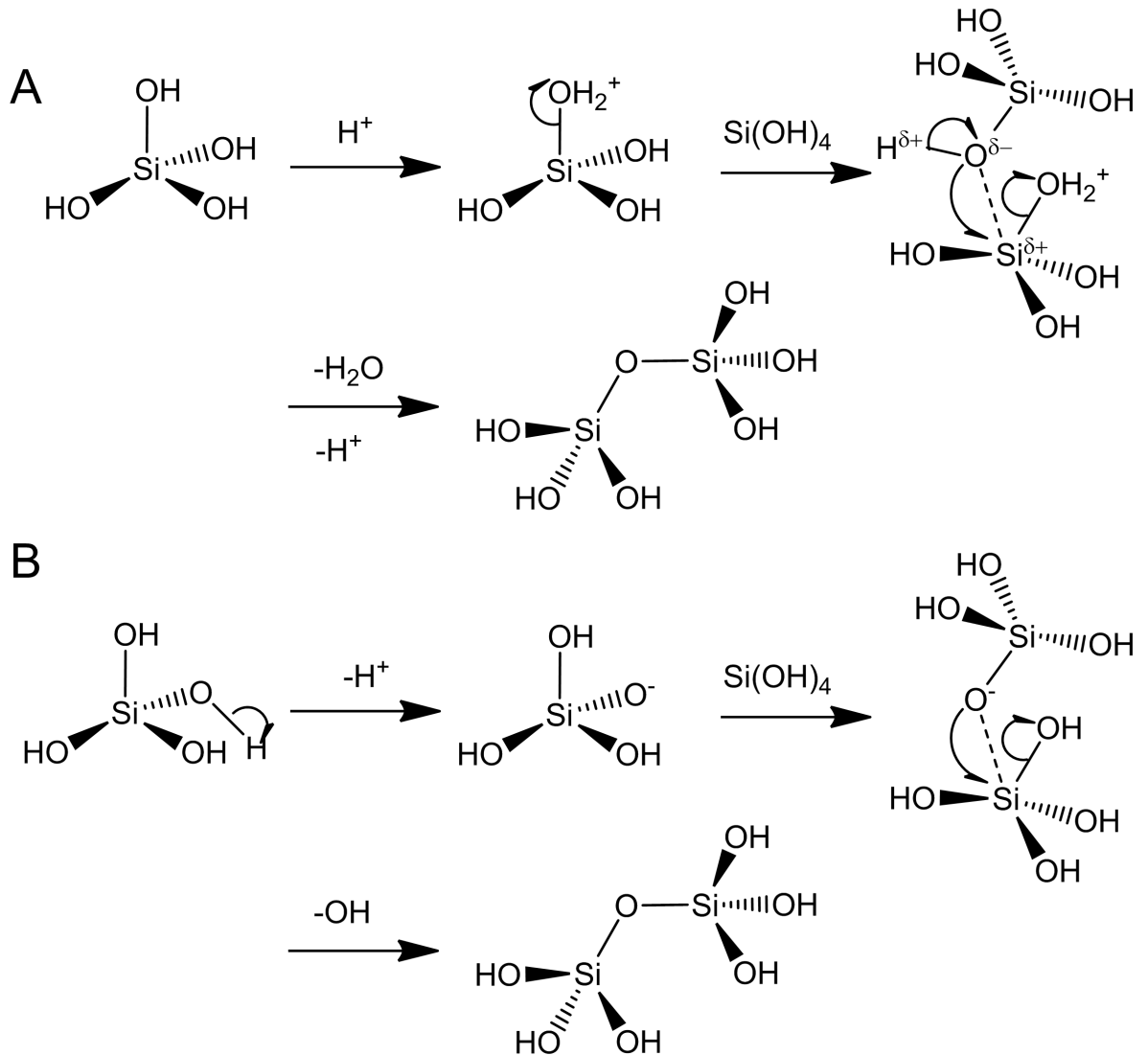
Figure 1.1: Condensation mechanisms of silicic acid under (A) low and (B) high pH conditions. Figure adapted from Harrison 1993.

The general polymerisation behaviour of silica is further described in fig. 1.2 where under condensing conditions silicic acid after forming polysilicic acid will eventually form discrete primary particles (> 1 nm) which can, depending on the conditions, form a colloid with particles many micrometres in diameter or a three dimensional gel network (Iler, 1976). Overall this latter process can be described as a sol-gel method; the sol being the initial colloidal system of discrete particles and the gel the transformation of this system to a network of interlinked particles (Hench & West, 1990).

The source of silicic acid for the polymerisation process is most commonly derived from the hydrolysis of an alkoxide precursor (common precursors being tetramethoxysilane

[TMOS] and tetraethoxysilane [TEOS]). In the presence of water or acid these precursors hydrolyse by a nucleophilic substitution reaction with a hydroxyl group replacing the alkoxy group after protonation. In the case of TMOS four molecules of methanol are liberated for complete hydrolysis to silicic acid. While TMOS hydrolyses readily, precursors with longer alkyl groups suffer a reduction in the rate of hydrolysis due to steric effects (Schmidt *et al.*, 1984).
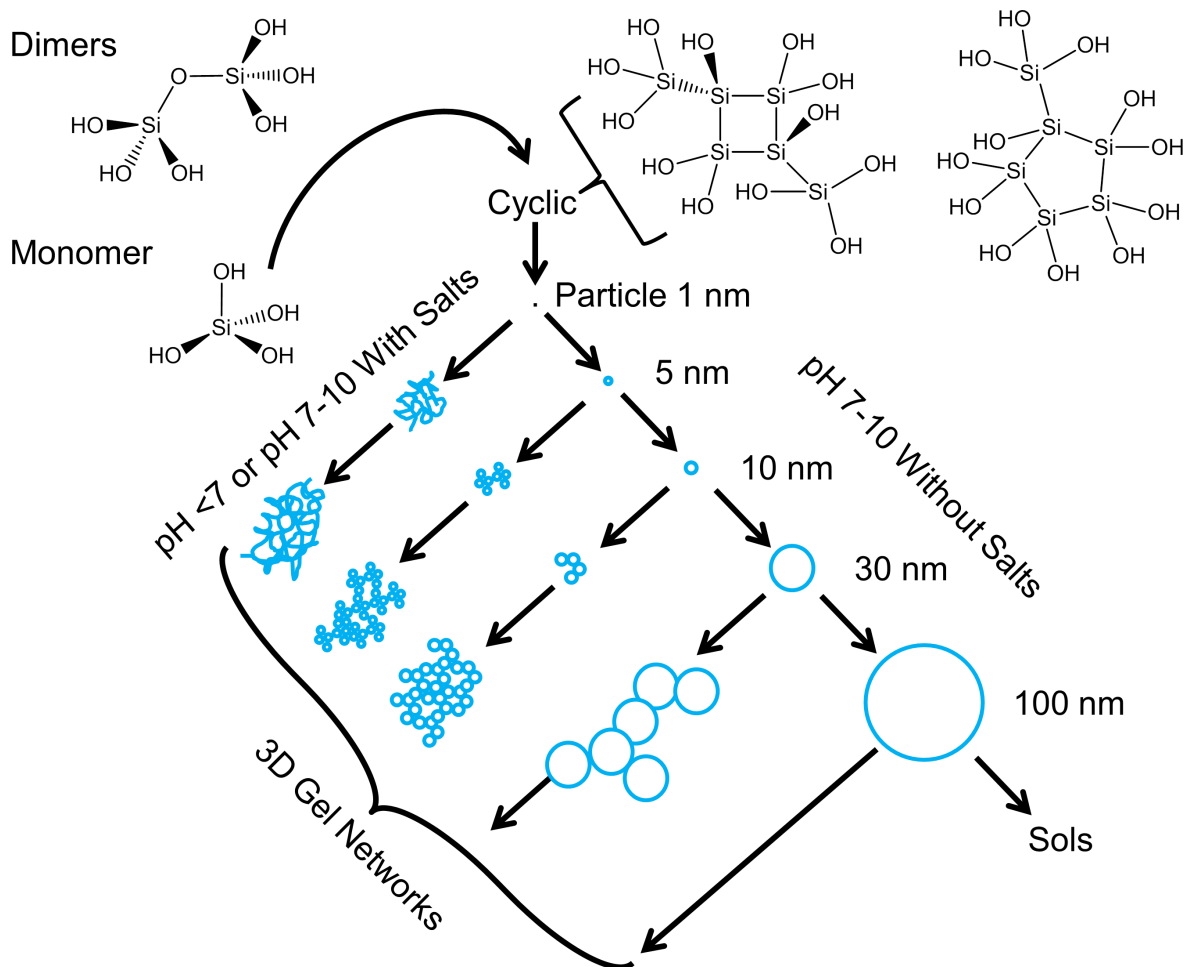
Figure 1.2: Polymerisation behaviour of silicic acid in differing conditions, proceeding from monomer to polysilicic acid. Polysilicic acid may go on to form discrete particles or gel networks depending on local conditions. Figure adapted from Iler, 1976.

The resulting materials produced by the sol-gel mechanism can vary considerably in their properties and forms as shown above. Further variation can be introduced by modifying the solution chemistry, such as pH, temperature, solvent, pre-cursor, rate of hydrolysis and condensation, etc. (Schmidt, 1988; Brinker & Scherer, 1998). Pre-processing techniques

like sonication and post-processing techniques such as drying to remove solvents from the gels can also further modify the resulting product, in for example porosity, forming microporous, mesoporous and macroporous silica's such as aerogels and xerogels (Salinas *et al.*, 2009; Fidalgo *et al.*, 2003).

Of the bulk silica material produced condensation will generally be incomplete with a variety of differently condensed species (Q_{1-4}) within and on the surface of the material. Accessible silanols may act as sites for further condensation and in sufficient density may condense by themselves under appropriate conditions ($\geq 180°C$) (Zhuravlev, 2000). The degree of condensation will influence the properties of the material, for example the number of silanol groups available on the surface influences hydrogen bonding. For the surface of amorphous silica the number of silanols per square nanometre was initially assessed as 7.8 for fully hydroxylated silica, based on geometry and density, though later revised downwards to 4.9 silanols from experimental data (Iler, 1976; Zhuravlev, 2000). Siloxane groups in contrast are very stable under most conditions and essentially hydrophobic in nature, rehydration occurring slowly unless catalysed by an alkali and is dependent on residual silanols (Iler, 1976). It is these different chemical species on the surface of amorphous silica, together with the form of the material, which dictates the adsorption of different molecules, including interactions with those of a biological origin.

1.1.2 Silica's biological role & interactions

The role of silica is not limited to being a resource for industrial and scientific endeavours; silica plays a key role in several aspects of organic life. Silica has been isolated and studied in a wide range of organisms from simple single cell organisms like *Diatomophyceae* to more complex multicellular plants like *Equisetum* (Currie & Perry, 2007; Hildebrand, 2003). Not limited to the kingdom *Plantae*, silica has also been studied in *Eukaryotic* organisms from *Porifera* to *Mammalia*, including *Homo Sapiens*.

The biological role of silica in many of these organisms is poorly understood and it would be difficult to consider silica to be broadly essential to life, especially in certain *Eukaryotic* organisms like man. However involvement in osteogenesis has been observed with altered bone growth noted in silica deficient rats (Jugdaohsingh *et al.*, 2008). A relationship between silica and biometals such as aluminium, calcium and iron, have also been noted in bone mineralisation (Perry & Keeling-Tucker, 1998).

Indication of a biological role for silica in certain species derives from its isolation to some degree from most organisms, silica is generally regarded to be non-cytotoxic and biologically compatible. However there are exceptions, primarily the incidence of silicosis; a respiratory disease resulting from inhalation of crystalline silica particulates (Leung *et al.*, 2012). The mechanism of silica toxicity in this disease is understood to be an inflammatory response to the ingestion of silica particles by macrophages in the alveoli and the inability of the lungs to clear these particulates. The cytotoxic effect seen for macrophages after phagocytosis of the particles is believed to be caused by free radical production by the silica surface once inside the cell and lysosome instability after ingestion (Hamilton *et al.*, 2007). It is noted that the cytotoxic effects of silica on macrophages can be achieved with other materials of an appropriate form such as latex beads, indicating that cytotoxic effect is not necessarily due to 'silica' itself but rather its form and as such part of the wider debate on the health effects of nanoparticles (Oberdörster *et al.*, 2005).

The quantity of silica accumulated within the cell varies from species to species; this has been shown to be related in part by the organism's ability to acquire it. Tomatoes, for example, acquire silica by passive diffusion of silicic acid and have lower silica concentrations than rice which actively uptakes silicic acid from its environment through the transporter protein Lsi1 (Mitani & Ma, 2005). In organisms where silica is found in abundance like *Diatomophyceae* and *Porifera* the role of silica is clearly structural in nature, forming part of the cell wall and skeleton of the organism, to the point that the historical remains of these organisms like diatomaceous earth are valued sources of silica for industrial application (Losic *et al.*, 2009).

In *Equisetum* for example, once bioavailable silicic acid has been imported in sufficient concentration (~100-200 mg kg^{-1}), it polymerises within the plant to form silica (Perry & Keeling-Tucker, 2003). This silica may be incorporated in the cell wall, with a range of biomolecules (such as proteins and polysaccharides) suspected of mediating polymerisation (Currie & Perry, 2007). Bioavailable silica has been shown to have a restorative effect on plants suffering from stress (drought, heavy metal toxicity etc.) by sequestering metal ions within the cell and activating antioxidant pathways (Liang *et al.*, 2007). Silica deficiency is suggested to increase the susceptibility of plants to stress and disease (Nakata *et al.*, 2008).

The ability of certain organisms to sequester silica is interesting as bioavailable silica is present in low concentrations (on average 220 µM for groundwater and 70 µM for seawater) in the environment due to its weak solubility (Exley, 1998; Treguer *et al*., 1995). Study of these organisms has uncovered several different classes of biomolecule that have been shown to interact with silica in the organism, and these have been extensively studied in the laboratory for their ability to manipulate silica chemistry (Yamaji & Ma, 2007). These biomolecules fall across several categories including proteins, like silaffins and silicateins in addition to long chain polyamines; a summary of which is given in table 1.1 below (Sumper & Kröger; 2004, Belton *et al*., 2008).

While many biomolecules have been shown to act as a catalyst or control agent for biosilica formation, there has been considerable study on the potential of a silica enzyme, a protein that may metabolise silica, not just condensing but potentially remodelling silica within the cell. Of the different biomolecules that interact with silica, silicatein α, a protein isolated from the spicules of sea sponges is the most promising (Shimizu *et al*., 1998).

Extensive study of silicatein α has revealed its physical structure and its homology to the cysteine protease cathepsin L (Shimizu *et al*., 1998). The expression of this protein within *Suberites domuncula* has been directly linked to the abundance of silicate in the environment (Krasko *et al*., 2000). The ability of silicatain α to catalyse the hydrolysis of tetraethoxysilane is given as an indicator of its bioactivity. This is interesting as tetraethoxysilane is a wholly artificial molecule, though its ability to direct the condensation of silica from monomer has also been shown (Rai & Perry, 2010). It should be noted that the biological role of certain biosilica related proteins (e.g. silicatein) is deduced largely from the proteins association with silica during isolation; to my understanding no gene knock-outs have yet been demonstrated which induce a functional loss or morphological change for the organism. The active site of the protein for the hydrolysis of tetraethoxysilane was believed to involve the hydroxyl group of serine-26 and the imidazole of histidine-126 (Zhou *et al*., 1999). This mechanism was further refined through the solving of the crystal structure of a cathepsin L chimera altered to resemble silicatein α, consisting of stabilisation of a deprotonated silicic acid by histidine allowing nucleophilic attack of another silicic acid inducing condensation, fig. 1.3 (Fairhead *et al*., 2008).

Table 1.1: Biomolecules implicated in silica interactions

Molecule	Type	Role	Size	pI	Reference
Polysaccharides					
Cellulose	Beta (1-4) glucan polysaccharide	Cell wall structure	10^3-10^4 monomer units	-	Perry & Lu, 1992
Proteins					
Silicatein-α, β and γ	Cathepsin L like protein	Biosilisification of *Tethya aurantia* spirucules	~2-27 kDa	~pH 5	Shimizu *et al*., 1998
Frustulins	Glycoproteins	Biosilisification of diatom cell wall	~40-200 kDa	-	Baeuerlain, 2000; Kröger *et al*., 1996
Pleuralins (formerly HF-extractable proteins proteins)	Protein	Biosilisification of diatom cell wall	~150-200 kDa	~pH 4	Baeuerlain, 2000
Silaffins	Lysine (N-methylated) modified polypeptides	Biosilisification of diatom cell wall	~4-40 kDA	< pH 4.5	Kröger *et al*., 1999; Poulsen & Kröger, 2004
Silicic acid transporters	Transmembrane sodium/silica symporter	Diatom silica transporter	-	-	Baeuerlain, 2000
Silica induced protein	Fe^{3+}-binding protein homologue	Unknown, expression induced by super-saturated silica	~35 kDa	~9.5	Doi *et al*., 2009
Low silica 1/2	Aquaporin's	Silica transporter	~23-31 kDa	-	Mitani & Ma, 2005; Maurel *et al*., 2008
Polyamines					
Polyamines	Oligo (N-methylated) polypropyleneimine	Various metabolic and proliferative roles	>20 units	-	Belton *et al*., 2008

From table 1.1 it can be inferred that some of the proteins identified and the polyamine class would be positively charged under biological conditions. Their amine rich nature, with an abundance of arginine and lysine residues for the proteins, can be attributed to this property. For those isolated from the diatom the pI is below standard biological conditions. However the site of silica condensation in diatoms; the silica deposition vesicle is mildly acidic in nature, likely also giving these molecules a positive charge (Otzen, 2012).

While the precise mechanism of interaction between silica and cationic biomolecules is poorly understood, silicic acid monomers in solution carry a negative charge under most conditions, having an isoelectric point around pH 2 ± 0.5 (Iler, 1976). The difference in charge between these different species drives an electrostatic interaction by which silicic acid monomers are attracted to the surface of positively charged cationic molecules. Once silicic acid is at sufficient local concentration on the surface of the molecule the monomers may undergo condensation, as represented in fig. 1.3 (Laugel *et al.*, 2006).
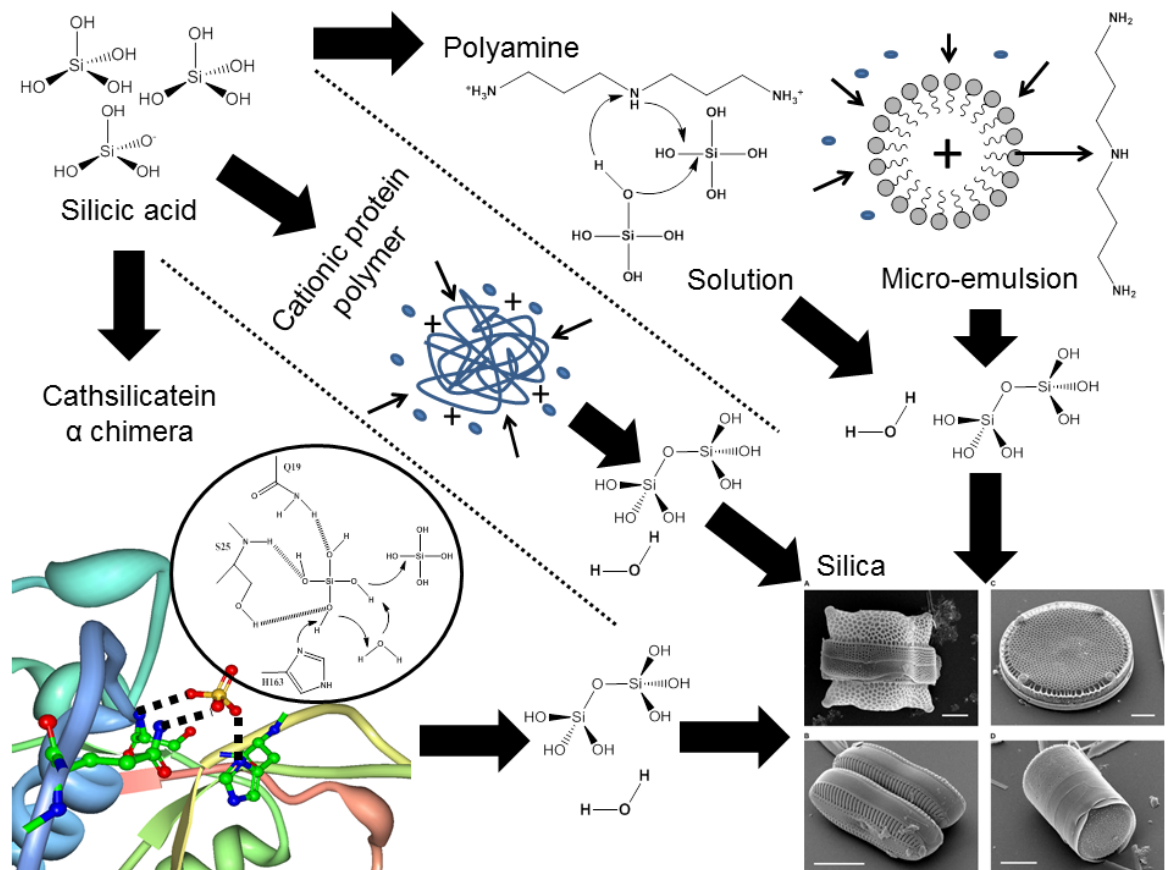
Figure 1.3: Proposed roles and mechanisms of different biomolecules (proteins and polyamines) in silica condensation. The proposed condensation mechanism at the active site of cathsilicatein chimera is shown (Fairhead *et al.*, 2008). The association and

condensation of silicic acid around a cationic protein or polymer is represented (Laugel *et al*, 2006). The condensation and association of silicic acid with polyamines in different states is shown in the upper path (Belton *et al*., 2005; Belton *et al*., 2008). Diatom micrographs adapted from work of M.A Tiffany (San Diego State University) under a Creative Commons Attribution 2.5 Generic license (Bradbury, 2004).

The ability of biomolecules like silicatein α and polyamines to catalyse and control the condensation of silica is of considerable interest for a number of applications, not least in the development of new silica based materials.

1.1.3 Silica in materials chemistry & biomimetics

Sol-gel derived silica is a versatile material that can be used to manufacture a wide range of different materials with varying properties and applications such as chromatography media, desiccants as well as coating and additives for other materials (Kendall, 2000).

In terms of colloidal particles then condensation under alkaline conditions *via* the Stöber method has been widely applied to manufacture mono-disperse non-porous silica particles in the order of several nanometre to several hundred nanometres in diameter (Stöber *et al.,* 1968). This process has been modified to produce a range of particles such as core shell particles with either silica as an interior or exterior (Han & Foulger, 2004; Xu & Perry, 2007). While Stöber particles tend to be non-porous in nature, silica particles with different porosities have been produced, such as for drug delivery (Slowing *et al*., 2008). Alternatively silica particles have acted as additives to other materials or as materials that may be functionalised themselves for further application (Bikram *et al*., 2007; Wang *et al*., 2008).

The ability of biological molecules like proteins and polyamines to influence silica condensation to create complex structures has created a lot of interest in the application of these molecules to replicate the process in the laboratory to produce new materials, namely the field of biomimetics, see fig. 1.3 (Bhushan, 2009). The advantages driving interest in biomimetic processes are that the biological mechanisms of silica processing occur under conditions of neutral pH, ambient temperature and pressure, in comparison to the high temperature, pressure and strong acidic or basic conditions used in conventional industrial

processing, all while organisms have much greater control over the resulting form of the biosilica produced (Patwardhan *et al.*, 2005). By better understanding and applying these mechanisms, more complex silica materials could potentially be created more cheaply and in a much more environmentally friendly and efficient manner.

There are many applications using biomolecules to produce a range of silica based materials in the laboratory through biomimetic approaches illustrated in the literature. For example polyamines like poly(allylamine hydrochloride) or 2-(dimethylamino)ethyl methacrylate have been applied to fabricate silica on glass fibres under ambient conditions (Pogula *et al.*, 2007; Kim *et al.*, 2004). Fine control over the properties (such as hydration state) of the silica product produced through using polyamines like poly(ethylenimine) has been demonstrated (Yuan & Jin, 2005).

The application of silica condensing proteins to materials development has also been achieved by a number of groups developing materials based around silicatein and silaffins (Andre *et al.*, 2012; Rai & Perry, 2010; Rai & Perry, 2012). These biomolecules demonstrate not just the ability to condense silica but enable it to be done in a controlled manner in terms of the properties of the material achieved, such as thickness, roughness and wettability.

Once the principle of using a cationic biomolecule to achieve controlled silica growth had been exploited, the principal could be applied to other proteins and biomolecules which share a similar biochemistry. This being demonstrated using peptides and polyamines that are able to control the shape of the silica particles formed, or thickness of the deposited layer (Tomczak *et al.*, 2005; Rai & Perry, 2009). The properties achieved can often be related back to the chemistry of the biomolecule, for example the number amine groups within the molecule and their spacing (Belton *et al.*, 2005). Finally other proteins with similar physiochemical properties, such as the protein lysozyme or serum albumin may be used to produce biosilica materials with tuneable properties (Rai & Perry, 2009).

1.2 Biomolecules involved in cell-surface interactions

The preceding section demonstrated how biological entities can have considerable influence in materials design. Similarly a wide range of biological processes depend on the interaction with a surface and a wide range of biomolecules are involved in mediating this behaviour both without and within the cell. However, the surface is a difficult region to

study due to its physical constraints but we can define our understanding of the surface and place the activities of biological entities like proteins and cells into this system.

1.2.1 Defining a model of cell-surface interaction

Cell-surface interactions can be difficult to visualise as a complicated three dimensional arrangement of a wide variety of different molecules and structures (both biological and non-biological) operating on a range of different length and temporal scales. Fig. 1.4 attempts to pictorially represent the cells interaction with a surface and some of the processes involved.
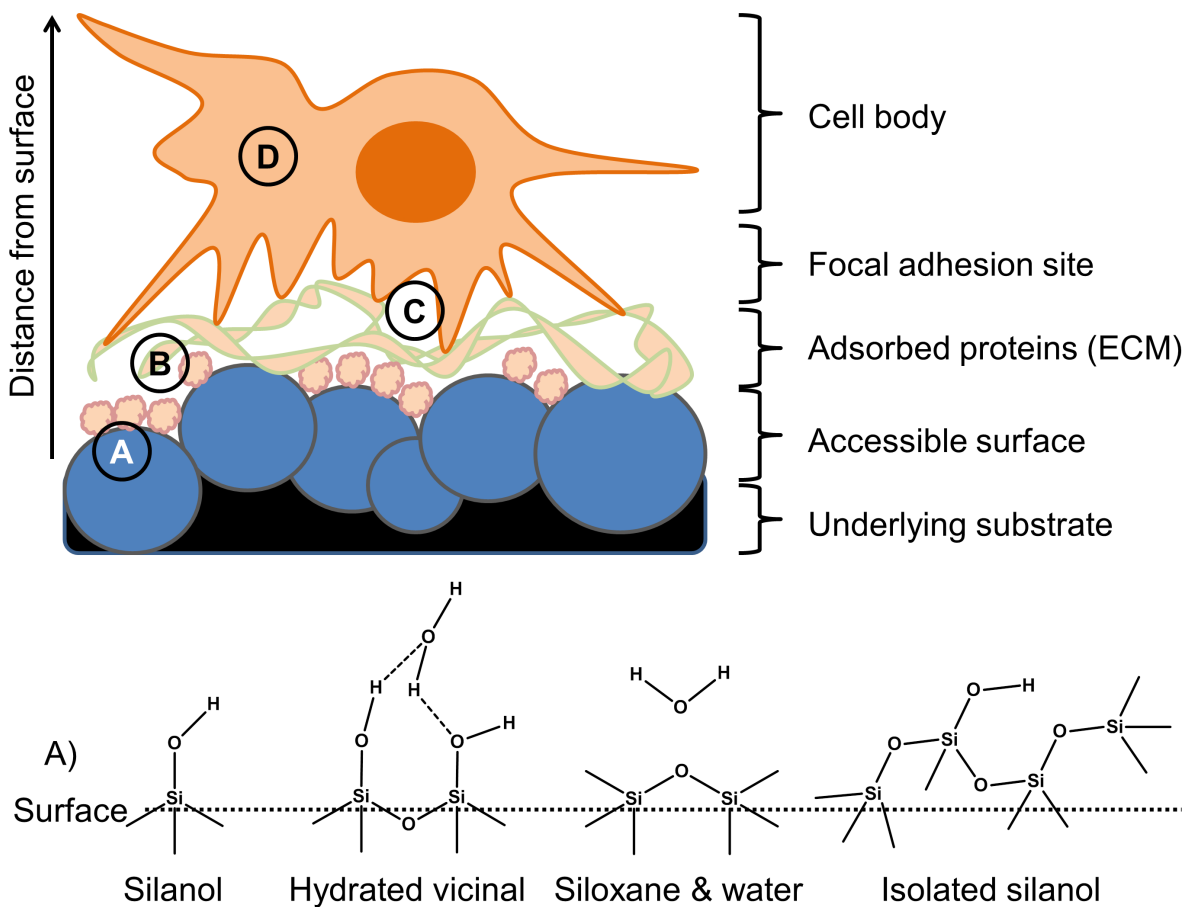
Figure 1.4: Schematic representation of a cell adhering to a surface, highlighting different events at different scales involved in the interaction. A) Represents the chemistry of the surface, common surface chemistries of silica highlighted, B) the proteins adsorbed to the surface, such as the extracellular matrix (ECM). Cell adhesion is represented at C) with focal adhesion to the underlying ECM and D) highlights the cell processes as a consequence of adhesion.

Cell-surface interaction can be divided into a range of different elements from the surface itself to the molecules interacting with this surface at different scales and finally the cell itself. This includes extracellular components which make contact with the surface and the intracellular components which are modified as a result of surface interaction; the cell's response.

It should be noted that events on the surface (such as protein adsorption) will be influenced to a large degree by events in the surrounding environment, for example in the tissue culture context, the surrounding medium and environmental factors (temperature, pressure etc.). Tissue culture media themselves being a complicated composition of salts, metabolites such as glucose and amino acids, vitamins, and potentially buffers, dyes, antibiotics as well as complex mixtures of undefined proteins, metabolites and signalling molecules of biological origin (Eagle, 1955). All of which complicates the study of the surface under realistic conditions.

1.2.2 The surface; between the bulk material & medium

The bottom most layer of the model is the surface itself, which at its simplest it can be described as no more than the top-most layer of accessible atoms, though an exact definition is difficult as it varies between molecules. The covalent radius of a hydrogen atom is ~25 pm but for a sodium atom ~180 pm, (Slater, 1964) the two atoms will describe a given surface differently, this holds true for larger molecules.

Whatever the 'surface' is considered to be, the intra-molecular interactions it permits determines some of the surface properties exhibited. The surface can only be considered in isolation under extreme conditions (high vacuum) and after surface treatment, post-environmental exposure. In reality, the surface is covered with a layer of adsorbed molecules, such as when it is solvated.

In the case of silica (fig. 1.4A) the surface can be expected to comprise of a mixture of condensed siloxane or free silanol groups, the precise composition varying on how the silica was produced and processed (Iler, 1976, Legrand, 1998). Silanol groups will permit hydrogen bonding but a dehydroxylated surface comprised of siloxane groups will not, influencing how aqueous solvents interact with the surface. As such there is the potential of a complicated network of hydrogen-bonding both between neighbouring silanols of silica

itself and between adsorbed species such as water, fig. 1.4A (Iler, 1976; Legrand, 1998). There has been considerable study of the different adsorbed water species both by infra-red and nuclear magnetic resonance spectroscopy (Legrand, 1998).

In addition to atomic composition, surface properties are influenced by the form of the surface, its topology and porosity (degree of voids within the material) will all affect how other molecules interact with the surface. Surface roughness for example can act as a capillary to draw water or as a void to trap air, contributing to surface wetting effects as described by Wenzel (Wenzel R.N, 1936; McHale *et al.*, 2004). As discussed previously silica based sol-gel materials can have a wide variety of forms, chemistries and properties depending on the processing methods used.

Depending on solvent chemistry and surface properties other entities may be present on a surface, such as counter-ions on a charged surface. In the biological context most surfaces adsorb the wide variety of biomolecules such as proteins from a medium.

1.2.3 Extracellular matrix; biological surface modification

An adsorbed layer of biomolecules comprises the next component of the model of cell-surface interaction, fig. 1.4B. Cell-surface interactions being dictated in part by the properties of the surface and in part the ability of the surface to absorb proteins, such as those involved in cell adhesion (Roach *et al.*, 2007). An important aspect of ensuring material biocompatibility is to understand the interactions between the surface of the biomaterial, surrounding cells and the proteins and other macromolecules that adsorb to the surface.

Proteins and other macromolecules are a major constituent of any biological medium and will adsorb to the surface over time, displacing bound solvent molecules like water. This adsorption process starts almost immediately as the material enters the biological environment. (Roach *et al.*, 2007) It is however a dynamic process that is continually remodelled during the time that the material is exposed within the environment (Lutolf, 2009).

The influence of proteins on surface chemistry would be to act as a dynamic layer of surface modification which alters the chemistry and topology at the surface, but also a layer of modification which is influenced by the properties of the surface itself. Studies have shown how variation in the surface such as its topology can alter characteristics of

proteins such as secondary structure conformation; protein orientation and this can vary from protein to protein (Roach *et al.*, 2006).

This dynamic environment is flooded by proteins from the serum and those excreted from the cells themselves, forming what is known as the ECM. The ECM describes the broad range of biomolecules excreted by cells into the surrounding environment. Some of the major constituents include proteoglycans, polysaccharides, fibrous proteins like collagens and adhesion proteins such as fibronectin and vitronectin (Badylak *et al.*, 2009). Physiologically, the ECM occupies the space between cells being the primary constituent of connective tissue and includes the basement membrane (Frantz *et al.*, 2010).

The role of the ECM is as diverse as its constituents and functions include, but are not limited to, acting as a shock absorber, scaffold, store of energy and signalling molecules and finally a site for cell attachment (Frantz *et al.*, 2010). A wide range of ECM constituents are available for tissue culture with variable properties and application depending on composition and manufacture (Badylak *et al.*, 2009).

In tissue culture, the composition of the adsorbed protein will depend not only on the cells culturing upon the surface, but primarily on the composition of the serum used to supplement the growth medium. This is a diverse mixture of proteins, metabolites and other molecules which is poorly defined. Though the majority of the protein components can be attributed to high abundance proteins like serum albumin's and globulin's, there are many orders of magnitude difference in the abundance of different proteins in the serum, (Anderson & Anderson, 2002) it is the lower abundance proteins such as fibronectin and vitronectin that play a major role in cell-surface interactions such as adhesion.

1.2.4 Cellular adhesion

The next component concerns the cells themselves and associated processes that bring cells towards and then maintain them on the surface, cell adhesion. Adhesion itself concerns a range of intra-cellular and extra-cellular molecules, including the ECM, fig. 1.5.
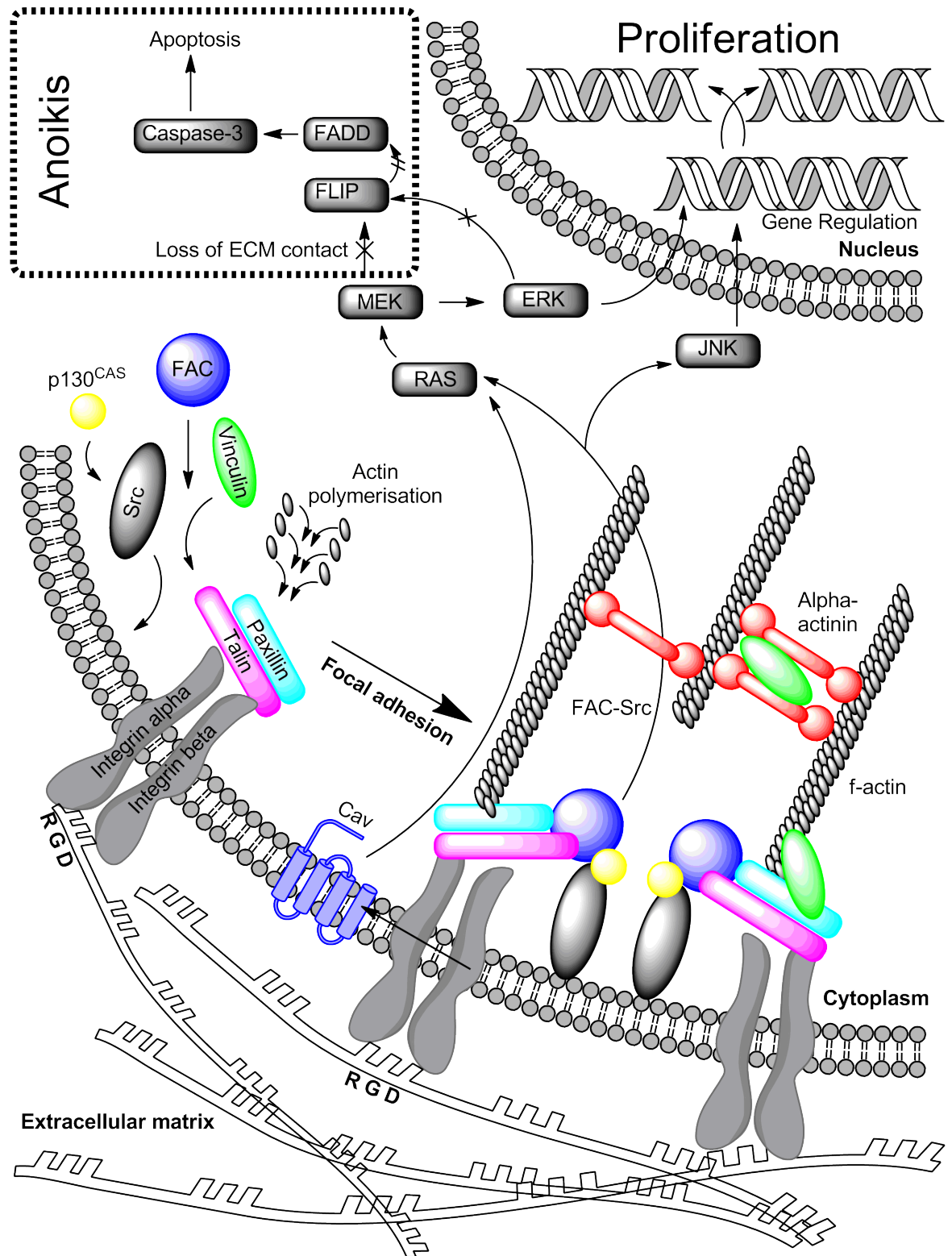
Figure 1.5: Representation of the molecular architecture of a cell adhering to a surface through focal adhesion. Also represented are some of the important signalling pathways involved in mediating the cell response to adhesion such as proliferation and the

programmed death response to a loss of adhesion; anoikis (Chiarugi & Giannoni, 2008; Giancotti & Ruoslahti, 2006; Millard *et al*., 2011).

Protein adsorption is a pre-requisite of cell adhesion with many of the proteins excreted as part of the ECM playing a role in adhesion, such as collagen, vitronectin and fibronectin. Cell adhesion to a surface has long been known to be enhanced through treatment with these ECM proteins (Underwood & Bennett, 1989). Some proteins are more relevant than others however and this seems to vary between cell types, bovine corneal and arterial cells for example are known to be preferential for particular ECM proteins with adhesion and proliferation hindered in cultures lacking vitronectin (Underwood & Bennett, 1989).

This influence is attributed to proteins of the ECM having an abundance of certain amino-acid sequences which have a pro-adhesion effect; one of the best characterised is the Arg-Gly-Asp or RGD sequence which is a ligand for integrin (cell membrane adhesion protein) receptors. The presence of just this sequence on a surface has been shown to enhance the focal adhesion behaviour and induce differentiation of adherent cells such as osteoblasts (Chollet *et al*., 2009; Lee *et al*., 2004). A relationship between adhesion and motility in lymphocytes is another example, with increased adhesion resulting in decreased motility (Bergman & Zygourakis, 1999).

Cell adhesion to surface adsorbed ECM proteins, as in tissue culture, is facilitated by cell adhesion molecules, a number of different types being identified. These primarily concern the class of calcium dependent adhesion molecules, the integrins (Ruosiahti & Pierschbacher, 1987). Though beyond the scope of this work, it should be noted cells are capable of other adhesion processes such as anchoring junctions, tight junctions and gap junctions (Gumbiner, 1996).

The most widely studied role of integrins in cell adhesion is their role at focal adhesion sites, where the cytoskeleton of the cell is anchored through the cell membrane to the ECM, such as at RGD sites (Giancotti & Ruoslahti, 2006). In reality focal adhesions embody a large and dynamic macromolecular assembly which compromises of many individual integrin binding sites and their associated proteins, the general architecture highlighted in fig. 1.5. In addition to cell attachment, focal adhesion sites are implicated in numerous cell processes including signal transduction of the cells surrounding environment to the cytoskeleton, as discussed below.

1.2.5 Attachment as a requirement; intercellular implications of adhesion

Outside of this requirement, but beyond the process of cell adhesion, contact with materials (or rather the proteins that are adsorbed to the materials surface) is believed to have a significant role in a wide range of cell behaviour including motility, morphology, proliferation and differentiation (Wilson *et al.*, 2005).

Motility concerns the cells movement across a surface, often as a response to a stimulus such as a chemo-attractant or as a process in the pathology of a disease (metastasis) (Olson & Sahai, 2009). During the process of motility the cell extends filamentous actin rich filopodia into its environment through extending the f-actin cytoskeleton, these make contact with the underlying ECM and allow formation of new focal adhesion sites. Stress fibres and actomysoin fibres permit the relocation of the cell body while contractile fibres pull in the rear of the cell (Mattila & Lappalainen, 2008).

For anchorage-dependant cell types adhesion it can be a matter of life and death (the general exception being suspension cells such as those found in the circulatory system) as cells unable to attach to the ECM undergo a form of programmed cell death called anoikis (Valentijn & Gilmore, 2004). Without the formation of the cytoskeletal elements associated with ECM adhesion signalling through the death expression pathway induces apoptosis through caspase signal transduction, fig. 1.5 (Sakamoto & Kyprianou, 2010).

Further to this survival requirement, cell attachment is involved in maintaining the cells ability for growth and proliferation, in processes such as cell division. Studies in which the functions of components of focal adhesion sites are compromised such as focal adhesion kinase show decreased DNA synthesis (Gilmore & Romer, 1996). Further work has implicated focal adhesion with a wide range of cell proliferation related pathways such as the MAPK/ERK pathway (Giancotti & Ruoslahti, 2006).

Finally the adhesion of cells to a surface has been demonstrated to play an important role in the fate of cells, modifying the nature of cells capable of undergoing differentiation or maintaining pluripotency (Giancotti & Ruoslahti, 2006; Li *et al.*, 2012). This process has been expanded beyond the act of binding to so-called 'mechanotransduction', the ability to transfer stresses upon the cells cytoskeleton into cell responses (Schwartz & Simone, 2008).

Since the surface which the cell encounters has been shown to have such a significant influence on the cell, understanding the different influences of surface chemistry, protein adsorption and how they influence cell response has been fundamental in the development of tissue culture materials and tissue culture in general.

1.3 Overview of current tissue culture materials

The ability to culture tissues of the body *in vitro* has been fundamental to modern science and is behind many advances in different fields; this ability was first established early in the twentieth century, notably through the work of Harrison R.G. of John Hopkins University and over the following decade's considerable improvements in the culture of tissue has been made (Abercrombie, 1961). From the ability to store tissue for considerable periods using cryogenics, maintaining cultured tissue for extended periods, the discovery and inducement of immortal cell lines, to today where the field of tissue engineering is making considerable progress in the production of artificial tissues and organs from cultured cells *in vitro* (Mazur, 1970; Stepanenko & Kavsan, 2012; Badylak *et al*., 2012). Key to the success of modern tissue culture has been in part the advancement of the tissue culture surface on which adherent cells may grow.

1.3.1 Early materials & tissue culture polystyrene

Silica (at least one form of it - glass) was important in early tissue culture materials which evolved from the glassware used in the laboratory. However, though glass was an adequate vessel for culture, it often required surface modification with a range of different biological polymers like agar, collagen, poly-L-lysine or cellulose applied to permit cell attachment and growth (Hotchin, 1955; Shukla *et al*., 2012; Michalopoulos & Pitot, 1975). This is because, as noted in section 1.2.4, cells require an ECM for adhesion and survival, many common substitutes or analogues being noted in table 1.2 below.

Today, glassware has been largely superseded by plastics which are considerably cheaper and more versatile in form, principal among these is tissue culture polystyrene (TCPS). TCPS differs from conventional polystyrene in that the surface of the polymer is modified to more readily permit cell attachment and proliferation. This is achieved through the incorporation of a range of different chemical functionalities such as carboxyl, hydroxyl, ketone or formyl groups to the surface through treatments like sulphuric acid or oxygen

18.

plasma, of these the loss of the hydroxyl component has been shown to have the most deleterious effect on adhesion (Curtis *et al.*, 1983). Surface treatment is believed to enhance adhesion through the mechanism of enhancing adsorption of ECM adhesion components like fibronectin and vitronectin from the serum and what is produced endogenously by the cells, though vitronectin is believed to be the main contributor to TCPS adhesion (Evans & Steele, 1998; Evans & Steele, 1997; Steele *et al.*, 1995; Curtis *et al.*, 1983).

Table 1.2: Matrix additives for tissue culture

Substrate	Role	Composition	Notes	Manufacturer	Reference
Cellulose	Adherence	β(1-4) linked D-glucose Polysaccharide	-	Various	Hotchin, 1955
Collagen	Adherence, tissue engineering scaffold	Protein family from connective tissue, 28 forms identified	Matrix alternative, the hydrolysate gelatin derives from collagen	Various	Michalopoulos & Pitot, 1975
Entactins	Adherence	Glycoprotein family of the basement membrane	Contains RGD adhesion sequence	Various	Kleinman *et al.*, 1987
Fibronectin	Adherence	~440 kDa ECM glycoprotein	Contains RGD adhesion sequence	Various	Underwood & Bennet, 1989
Foetal calf serum	Proliferation	Complex undefined extract	High intra-batch variability	Various	Eagle, 1955
Laminins	Adherence	Glycoprotein family of the basement membrane	-	Various	Lam & Longaker, 2012
ε-Poly-L-lysine	Adherence	Small (>20 units) natural homo-polypeptide of L-lysine	Bacteria derived, other homo-polypeptides exist	Various	Shukla *et al.*, 2012
Proteoglycans	Adherence	Family of heavily glycosylated ECM proteins	Grouped by glycosaminoglycan e.g. Agrin is a heparan sulphate	Various	Knox & Wells, 1979
Vitronectin	Adherence	~75 kDa ECM glycoprotein	Contains RGD adhesion sequence	Various	Underwood & Bennet, 1989
ECM matrix	ECM forming agent	Mixture of man-made polymers	Sediments ECM in culture	-	Lareu *et al.*, 2007
StemAdhere™ & Vitronectin XF™	Adherence	Recombinant ECM protein	Xenobiotic free	Primorigen Biosciences Inc.	Serra *et al.*, 2012
Matrigel™, Geltrex® & Cultrex®	ECM homologue	Biological extract of proteins with growth factors	Derived from Engelbreth-Holm-Swarm mouse sarcoma cells	BD Bioscience, Trevigen, Invitrogen	Kleinman & Martin, 2005
CELLstart™ & MaxGel™	Defined ECM homologue	Human origin ECM components	Xenobiotic free	Invitrogen & Sigma®	Yang *et al.*, 2012
StemXVivo™ & Synthemax®	Defined ECM homologue	Recombinant ECM proteins	Xenobiotic free	R&D Systems, Corning®	Serra *et al.*, 2012

1.3.2 Diversity of current tissue culture materials

Since the introduction of TCPS a diverse range of tissue culture plastics and treatments have been developed, many of these summarised in table 1.3 below. Advances in surface chemistry have allowed the production of surfaces with well-defined surface chemistries, such as the BD Purecoat™ series which differs from conventional tissue culture plastic in that the surface functionality (be it amino or carboxyl) is of one type and closely controlled (Becton, Dickinson & Company, 2010).

Advances in culture practice (through extensive use of serum in media) and materials, have to some degree eliminated the requirement for pre-treatment with polymers like collagen, though some applications such as difficult to culture cell lines (e.g. culture of primary cell lines and stem cells) still require pre-treatment (Serra *et al*., 2012). As our understanding of the cell adhesion system has become more complete a wider range of proteins for cell culture has become available, either naturally derived or as recombinant proteins.

With the discovery of cell adhesion proteins, surfaces have been developed which incorporate the principals of cell adhesion and the ECM such as the BD PureCoat™ ECM Mimetic & Synthemax™ surfaces. These are functionalised with peptides derived from the active sites of proteins known to be implicated in cell adhesion, such as the RGD sequence (Hersel *et al*., 2003).

Applications such as spheroid formation assays, where the ability of the cell to culture independently of adhesion is tested, low adherence is required for a surface. This may be achieved by passivation of the plastic surface with a hydrophilic, neutrally charged hydro-gel layer that prevents protein uptake, and cell adhesion to the surface, though newer systems permit cell culture without a surface (other than the air/liquid interface formed through surface tension) at all (Low *et al*., 2006; Kelm *et al.,* 2003).

Patterning of the surface through lithography, chemical or mechanical processes have been employed to yield materials better applicable to different roles or better mimic the *in vivo* environment (Kaji *et al*., 2011). An example of this kind of materials would be the Corning® Osteo Assay Surface which has been modified to better resemble the surface of bone for assessing the performance of osteoclast and osteoblast functionality.

Table 1.3: Substrates for tissue culture

Substrate	Role	Chemistry	Notes	Manufacturer	Reference
Glass	Adherent culture	Borosilicate glass	Acid treatment was common	Various	Eagle H, 1955
Agar	Adherent, 3D culture	Agarose and agaropectin polysaccaride	-	Various	Hotchin, 1955
Polystyrene (TCPS)	Adherent culture	Surface treated polystyrene	Single or mixed surfaces chemistry	Various	Curtis *et al*., 1983
Hydroxyapatite	Adherent culture	Calcium phosphate mineral	Indicates bioactivity	Various	Frohbergh *et al*., 2012
BD PureCoat™	Adherent culture	Surface treated polystyrene	Single functionalities	BD Bioscience	Becton, Dickinson & Company, 2010
BD PureCoat™ ECM Mimetic & Synthemax™	Adherent culture	Peptide conjugated polystyrene	Modified with synthetic peptides e.g. fibronectin and collagen I	BD Bioscience, Corning®	Kosovsky, 2012
TCPS low adherence	Low adherence	Hydrophilic, neutral charge	Corning® use hydrogel	Various	Low *et al*., 2006
Perfecta3D® & GravityPLUS™	3D tissue culture	None	Hanging drop for sphere for	3D Biomatrix, InSphero	Kelm *et al.,* 2003
Corning® Osteo Assay Surface	Adherent culture	Patterned tissue culture polystyrene	Assess osteoclast & osteoblast functionality	Corning®	Kartner *et al.*, 2010,
AlgiMatrix®	3D tissue culture	Polysaccharide	Alginate based scaffold	Invitrogen	Rimann & Graf-Hausner, 2012
Alvetex® Scaffold	3D tissue culture	200 µm porous polystyrene membrane	Pore diameter is 40 µm with interconnects of 13µm	Reinnervate	Rimann & Graf-Hausner, 2012
Hyaluronan	3D tissue culture	Polysaccharide of D-glucuronic acid and D-N-acetylglucosamine, >20 million Da	Hydrogels with differing chemistry such as growth factor release	Various	Rimann & Graf-Hausner, 2012
HydroMatrix™	3D tissue culture	Peptide hydrogel	-	Sigma®	Tibbitt & Anseth, 2009
Polycaprolactone	3D tissue culture	Polycaprolactone	Biodegradable	Various	Rimann & Graf-Hausner, 2012
Polyethylene-Glycol, QGel™	3D tissue culture	Polyethylene glycol hydrogel	Differing chemistry such as light sensitivity or biodegradable	Various, QGel	Rimann & Graf-Hausner, 2012

1.3.3 Advanced tissue culture concepts

Building on the principals of using matrix substitutes and advanced surface chemistry in culture has produced a range of advanced tissue culture concepts. One area of interest for applications as diverse as tissue engineering to cancer research has been ensuring that the local tissue culture environment more closely resembles conditions *in vivo* (Hutmacher *et al*., 2010). To this end many advanced tissue culture systems have moved towards the presentation of an artificial extracellular matrix, initially through collection and presentation of biologically derived ECM such as in the Matrigel™ system (Kleinman & Martin, 2005). Later developments built systems that are entirely artificial in nature which have the benefits of being both well defined in nature and free of xeno compounds, better resembling the *in vivo* conditions (Rimann & Graf-Hausner, 2012).

Parallel to the development of xeno free ECM mimics for tissue culture are serum free culture systems (Barnes & Sato, 1980). The problem of serum is that it is poorly defined and variable from batch to batch. While the serum free concept has been around for a long time its implementation has been difficult, some cell lines such as neuronal cells have been adapted to serum free media but the adaptation of other lines remains elusive, due to the complexity of cell requirements (van der Valk *et al*., 2010).

The concept that the culture environment should replicate *in vivo* environments like the ECM has developed the view that the tissue culture surface or scaffold is no longer considered as a flat surface, at the very least it is to be considered as a 2+1D surface in that through topology and roughness it does not purely exist in two dimensions. There has been considerable interest in the development in 3D tissue culture systems, though such materials have existed for some time (e.g. agar) they are becoming more widely employed and investigated (Santos *et al*., 2012).

One form of 3D culture is the use of the hydrogel, that is a polymer network (such as cross-linked poly(ethylene glycol)) with a high water content. Cells have been shown to be able to proliferate and migrate within and atop these materials and they are of particular interest as the gels can be used to approximate biological structures like the ECM. Current hydrogel technologies show smart properties such as responsiveness to physical conditions or 3D processing using light responsive gels. The aim of this work is that through tight control and provision of local cell micro-environments tissues can be engineered within the hydrogel matrix (Lutolf, 2009).

1.3.4 Silica in tissue culture, biomaterials & tissue engineering

Biomaterials may be loosely defined as materials that interact with biological systems to replace or supplement a biological function (Williams, 1988).They can be derived from natural materials, such as silk proteins like fibroin (Vepari & Kaplan, 2007) or synthetics created in the laboratory, such as polymers like polyurethane (Santerre *et al*., 2005). Sol-gel based silica materials have been of growing interest for a range of biological applications, though the response of biological systems to different inorganic materials is poorly studied. Over the last few decades the application of silica materials has moved past the encapsulation of biomolecules to the encapsulation of *Prokaryotic* organisms to surfaces for bioactive materials and tissue culture (Avnir *et al*., 2005).

Encapsulation technology or 'living materials' is well established with the encapsulation of biomolecules like proteins or single cell organisms for biological application, with benefits derived from the encapsulation process including greater enzyme stability (Pierre, 2004). More recent efforts have demonstrated the production of complex high value biological products like monoclonal antibodies from encapsulated *Eukaryotic* hybridoma cells (Desimone *et al*., 2011). Challenges for the area include the inherent issues of long term stability, life-cycle, regeneration and dealing with the stress of encapsulation for biological systems (Blondeau & Coradin, 2012).

Another area of application for silica based materials is in the development of new biomaterials for bone implants such as silica derived glasses and ceramics, in addition to coatings for traditional implants (Verne *et al*., 2009). Of particular interest is the development of bioactive ceramics and glasses. This concept was introduced in the 1960's and involves materials interacting with the biological environment, as opposed to the previous materials which were biologically inert substitutes (Arcos *et al*., 2009). Traditionally important markers of bioactivity are recognised as the formation of hydroxyapatite on the biomaterial under biologically relevant conditions, in addition to protein adsorption (Williams, 2008).

Silica derived glasses and ceramics may be engineered to resemble the structure and physical properties of bone and may permit controlled absorption and release of biologically relevant molecules (Izquierdo-Barba *et al*., 2008). Osteoblasts, fibroblasts and macrophages were found to respond in a similar fashion to biologically active glass 45S5 Bioglass materials both *in vivo* and *in vitro* were unable to activate macrophages (Silver &

Erecinska, 2003). This supports the general belief of non-reactivity for silica based glass and ceramic materials and of the potential for *in vitro* models to determine *in vivo* effects. The interest in stem cells has produced silica materials designed for their application such as hybrid silica alginate matrices with a degree of bioactivity to act as a controlled environment for the delivery of stem cells (Gimeno-Fabra *et al*., 2011).

A wide range of silica based nanoparticle materials have been developed, with application in drug delivery and diagnosis being favoured. Silica nanoparticles functionalised with T-lymphocyte recognising antibodies (anti-CD3 and CD28) were shown to be selectively targeted to and absorbed by lymphocytes with no observed cytotoxic effects (Bottini *et al*., 2007). The study demonstrates the potential application of silica particles as selective transporters within the body, acting as functionalised delivery agents directly to the desired cells.

Finally, the development of new tissue culture surfaces has been considered as an application for sol-gel derived materials. Limited progress has been made in the area, with only a few materials tested, though promising enhancements in tissue culture performance such as enhanced cell growth have been observed (Zolkov *et al*., 2004). It was found that mildly hydrophilic silica culture surfaces with a contact angle of ~70 degrees produced by a sol-gel thin film method were favoured for the culture of buffalo green monkey kidney cells. Surfaces comprised of a methyltriethoxysilane to tetramethoxysilane ratio of between 1:1 and 1:3 permitting improved cell proliferation compared to TCPS (Zolkov *et al*., 2004).

1.4 Current issues in cancer biology

1.4.1 Defining cancer

Cancer is an intractable disease which causes a significant number of deaths each year (over 7.6 million globally in 2008) and is considered a primary global health issue by the World Health Organisation (WHO), cancer being a point of focus for the 2008-2013 action plan in the global strategy for the prevention and control of non-communicable diseases (World Health Organisation, 2005; World Health Organisation, 2008).

The disease is highly complex with multiple forms and causes attributed to it, and difficult to treat, as it can be considered as a dysfunction of the body's own systems. Due to its complexity the disease is difficult to characterise, Hannahan & Weinburg (2000) however proposed a series of generally accepted hallmarks, including:

1. Self-sufficiency in growth signals, through over-expression of receptors like epidermal growth factor receptor (breast, brain and stomach) or production of their own growth factors like tumor growth factor α (Barton *et al.*, 2001).

2. Insensitivity to anti-growth signals and the ability to evade apoptosis through for example disruption of the function of p53, a protein implicated in cell death in many cancers (Chappell *et al.*, 2012).

3. Limitless reproductive potential, the ability to avoid senescence through up-regulation of telomerase (Chmielnicki *et al.*, 2012).

4. Sustained angiogenesis through release of inducers like vascular endothelial growth factor (Lin & Kelly, 2012).

5. Tissue invasion and metastasis, the ability to break away from the primary tumor tissue, enter the circulatory system and initiate tumor growth elsewhere (Petersson *et al.*, 2012).

This initial set of classifiers was published in 2000 and since then understanding of the disease has grown sufficiently that Hannahan & Weinburg published an updated set of properties in 2011. The new list of characteristics incorporated:

1. Deregulated metabolism, such as enzymes involved in androgen metabolism in prostate cancer (Mitsiades *et al.*, 2012).

2. The ability to evade immunosurveillance of the body's defences for tumour like cells, such as the loss of IL-7 to sustain prostate-specific lymphocytes in prostate cancer (Carlo *et al.*, 2009).

3. Recognising that cancer cells are genetically unstable, with increasing numbers of chromosomal artefacts over the course of the disease (Dahiya *et al.*, 1997).

4. Chronic inflammation in tissues afflicted with the disease (Sfanos & De Marzo, 2012).

Through considerable effort has gone into classification of cancer, the field is still some considerable way from being able to reliably relate treatment and prognosis to a specific form of the disease, or identify all possible variants associated with even one aspect of the disease (Manson, 2009). Cancer heterogeneity has long been studied with the aid of immunological techniques such as immunostaining, with different tumour types exhibiting different characteristics such as expressed surface proteins (Broers *et al.*, 1987). Two main types and five sub-groups of breast cancer have been identified based on hormone receptor

expression and tumour origin, a point which conflicts with a stochastic view of cancer formation (Anderson & Matsumo, 2006). Further to this studies based on genomic analysis of 2000 breast cancer patients has been able to identify up to 10 different forms of breast cancer, the authors suggesting that each of these forms can be considered as an individual disease with potentially differing out-come and treatment for the patient (Curtis *et al*., 2012).

This concept of heterogeneity and diversity extends to within the tumour, which can exhibit a variety of cell sub-populations. The existence of these sub-populations has resulted in development of the theories of clonal evolution and of the existence of cancer stem cells (CSC). Clonal evolution explains the heterogeneity of tumours through uncontrolled differentiation, over time the genetically unstable cancer cells accrue mutations, resulting in disease progression, fig. 1.6. CSC theory will be addressed in detail below (Campbell & Polyak, 2007).
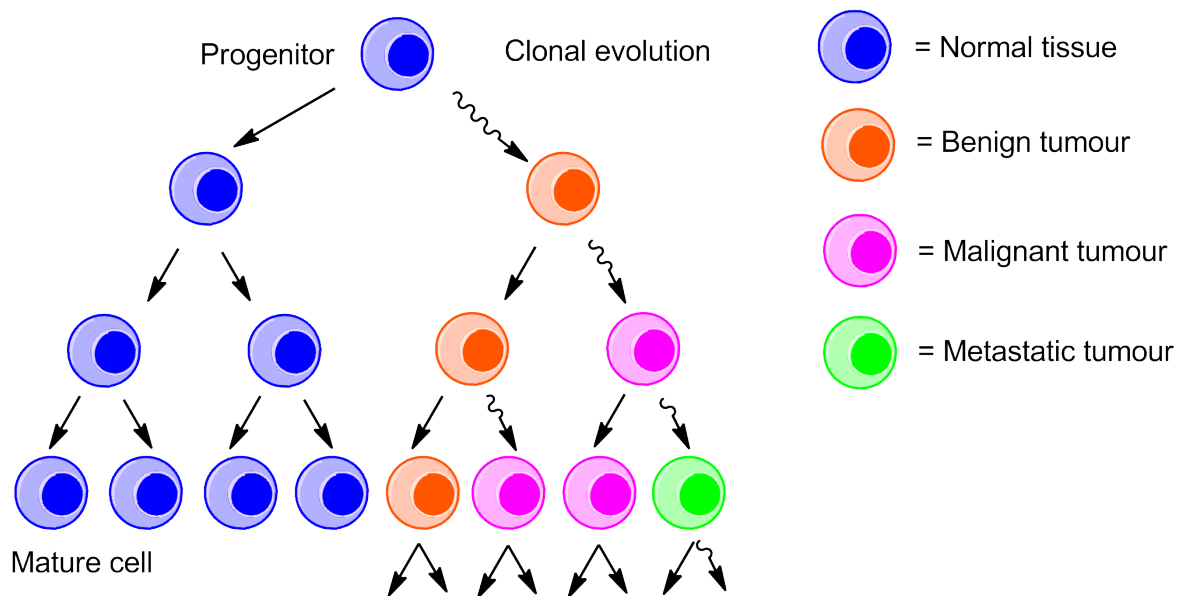
Figure 1.6: The theory of clonal evolution of the tumour, discrete populations of tumour cells deriving from mutations or differentiation during successive rounds of clonal expansion.

1.4.2 Current & prospective treatment strategies

Despite being surmounted with a seemingly ever increasingly complex problem a wide range of treatments are available today based on our current understanding, the WHO considering that 30% of cancers are preventable (World Health Organisation, 2008). Some

notable successes include the identification of viral infections such as the human papilloma virus as being tumour initiating; vaccination against the virus providing protection against cancer (Tay, 2012). Also certain cancers such as the retinoblastomas due to their pathology are almost completely treatable through current therapies (Dimaras *et al.*, 2012).

Traditional therapies for cancer, beyond surgical intervention, include chemotherapy and radiotherapy, both of these techniques relying on the known hallmarks of cancer (Cairncross *et al.*, 2006). These include dosage of the patient with a cytotoxic drug which commonly acts through inhibition of DNA and RNA synthesis, transcription and causes general DNA damage such as the anthracycline class of antibiotics. Since cancers replicate faster than most normal tissues (those of the gut and certain areas of the epithelium being a noted exception) the cytotoxic effect for a given dose is greater on the tumour than the rest of the body, killing the tumour without killing the patient. However numerous side-effects are known and treatment is not suitable in all cases such as the elderly or infirm.

Radiotherapy operates in a similar vein, though instead of a therapeutic drug a dose of ionising radiation is given. This damages DNA in itself and indirectly through the generation of free radical and reactive oxygen species, again since tumour cells are rapidly dividing and have a degraded ability to repair DNA damage the effect is more pronounced on the tumour than surrounding healthy tissue. Today, cancer therapy is often a combinatorial approach; the use of different techniques also limits the chance for the tumour to develop a degree of resistance to one drug for example (Lee *et al.*, 2012).

While chemotherapy and radiotherapy are the mainstays of cancer treatment, a wide range of new and promising treatments are on the horizon which take advantage of the research of the last few decades to improve detection and prognosis of cancer suffers. These new strategies include gene therapy, targeted therapy and immunotherapy.

Virus directed enzyme pro-drug therapy would be an example of gene therapy and involves the selective infection of tumour cells with an oncolytic virus that results in the tumour cells expressing an enzyme (such as nitroreductase) which can produce a cytotoxic drug from a benign pro-drug administered to the patient (Race *et al.*, 2007; Searle *et al.*, 2004). The technique is advantageous over traditional chemotherapy in that only the infected cancerous cells are affected by the cytotoxic drug.

Targeted therapy is so named as it targets specific molecules through drugs or antibodies that the tumour requires to proliferate but unlike chemotherapy or radiotherapy only targets

cancer cells rather than all rapidly dividing cells of the body. An example would be the tyrosine kinase inhibitor Gefitinib (N-(3-chloro-4-fluoro-phenyl)-7-methoxy-6-(3-morpholin-4-ylpropoxy)quinazolin-4-amine) which affects the epidermal growth factor receptor, implicated in the cell cycle and up regulated in among others lung cancer (Sawyers, 2004). A similar strategy is hormone therapy, for example the denial of androgens e.g. testosterone and dihydrotestosterone by either chemical or surgical castration (Damber & Aus, 2008). The targets of this strategy are the result of the greater understanding of the molecular pathology of cancer, though as with all drugs correct clinical trials are essential to fully understand the potential for side effects in the target population.

Immunotherapy is a form of treatment where the patient's own immune system is exploited to combat a disease. This can be in the form of suppression of the immune system for the treatment of allergies (Frew, 2008) or activation of the immune system such as in vaccination (Pawelec & Rees, 2002). Work on the development of cancer vaccines centres on biomarker discover; unique biomolecules present in cancerous tissue to which the immune system may be sensitised against that are not present in healthy tissues. Of the few licensed to date has been Sipuleucel-T a vaccine against hormone refractory prostate cancer with demonstrated patient survival enhancement in phase III clinical trials. Sipuleucel-T targets prostatic acid phosphatase (PAP) through maturing and activating patients antigen presenting cells (APC) in the presence of a PAP derived peptide and APC maturing factor, the product is then infused back to the patient (Kantoff *et al.*, 2010). Despite success these vaccines only provide an extension of life and cannot reverse the progress of the disease but the potential is there and better targets and vaccine strategies such as starting vaccine therapy at a time when the patient's immune system can still combat the disease may improve the performance of the treatment and deal with the escape phase of the cancer (Zhou & Levitsky, 2012; Drake & Antonarakis, 2012).

Adoptive cell transfer therapy (ACTT) is another promising strategy from the field of immunotherapy. ACTT required discovery of a class of cytokines called interleukins (IL). Some such as IL-2, IL-10 and IL-12 are implicated in activation of T-cells and augmentation of the adaptive immune response, anti-tumour effects following interleukin administration being observed (Overwijk *et al.*, 2000). ACTT also relies on the concept of tumour immune-surveillance, that the tumour is detected as abnormal by the body's natural

defences and targeted by cells of the immune system (Swann & Smyth, 2007). ACTT works through isolation by biopsy or from cells cloned *in vitro* of CD8 natural killer T-lymphocytes that demonstrate a strong immune reactivity to the tumour (Dudley *et al.*, 2003; Dudley & Rosenberg, 2007). Isolated cells are sensitised to the tumour through culture in the presence of an activating agent like IL-2 and cancer antigens (Dudley & Rosenberg, 2003). Once cultured in quantity the stimulated cancer specific cells are infused back to the patient, generally after lymphodepletion by chemotherapy to remove non-specific lymphocytes that compete with the infused lymphocytes for growth and activation factors (Aqui, 2008). Clinical trials for the treatment of advanced metastatic melanoma by ACTT when combined with lymphodepletion has shown a rate of tumour regression approaching 50%, significant compared with traditional therapy, early immunotherapy and ACTT or vaccination alone (Fang *et al.*, 2008).

1.4.3 Returning to cancer heterogeneity; stem like cells & their implications

A significant problem identified in the treatment of cancer is the non-heterogeneity of the disease (Fidler, 1978). A considerable concern for modern cancer therapy is evidence that targeting the bulk tumour through treatment by traditional techniques as well as new strategies is not (varying from cancer to cancer and patient to patient) completely effective. That after treatment has finished an element of the tumour can survive to cause re-occurrence (Dalerba *et al.*, 2007). Intrinsic within this observation is that some cells of the tumour can survive, this population being different from the majority of cancer cells, that cancer is not a monolithic entity and has sub-populations with different potential roles within the pathogenesis of the disease.

The concept of the cancer stem cell (CSC) becomes relevant here, originally derived from the model of acute myeloid leukaemia produced by Dick J. *et al.* in 1994 which was hierarchical in nature with a primitive hematopoietic cell with stem cell like properties at the top (Rosen & Jordan, 2009). CSCs may be considered the somatic stem cells tumour equivalent, self-renewing and capable of differentiation into cells which go on to form tumours (Dalerba *et al.*, 2007). The model has gone on to be applied to solid tumours and there is evidence that a percentage of cells within the tumour (though variable from a majority to a fraction of a per cent) can be tumourigenic in immune compromised model

species after injection of only a single cell (Kelly *et al*., 2007). The isolation of CSCs is difficult due to their generally low abundance within the total population, one stem cell for every 10^6 cancer cells screened (Kelly *et al*., 2007).

The theory of a CSC population within the tumour has been the focus of intense interest, though it remains controversial. The CSC definition is disputed and variable both in presence and frequency between different cell lineages, table 1.4 below highlights some of the many markers attributed to the phenotype (Visvader & Lindeman, 2012). Markers determined in solid tumours vary from tumour to tumour and include among others $CD44^+$, $CD24^-$ and $CD133^+$ in breast cancer, EpCAM and $CD133^+$ in colon cancer, $CD44^+$ and $CD24^+$ in pancreatic cancer and $CD133^+$ and integrin $\alpha_2\beta_1$ in prostate cancer (Visvader & Lindeman, 2008; Richardson *et al*., 2004). It can be noted that many of these markers though good at distinguishing populations by flow cytometry they remain ambiguous in terms of their biological relevance to the cancer stem cell (Jaggupilli & Elkord, 2012).

Additionally the CSC is poorly defined in theory, with debate on the nature of cancer stem cells being intrinsic to the tumour (containing a population of classifiable CSCs) or extrinsic in that all tumour cells have that potential but the capability depends on the micro-environment (Rosen & Jordan, 2009; Borovski *et al*., 2011). There is also debate as to CSCs and clonal evolution, though a mixed model of theories may provide a more valid explanation, fig. 1.7 (Visvader & Lindeman, 2008; Clevers, 2011). Though experimental systems show high variability in determining the occurrence of CSCs in different tumours there does appear to be a population of cells capable of acting as tumour initiating cancer stem cells.
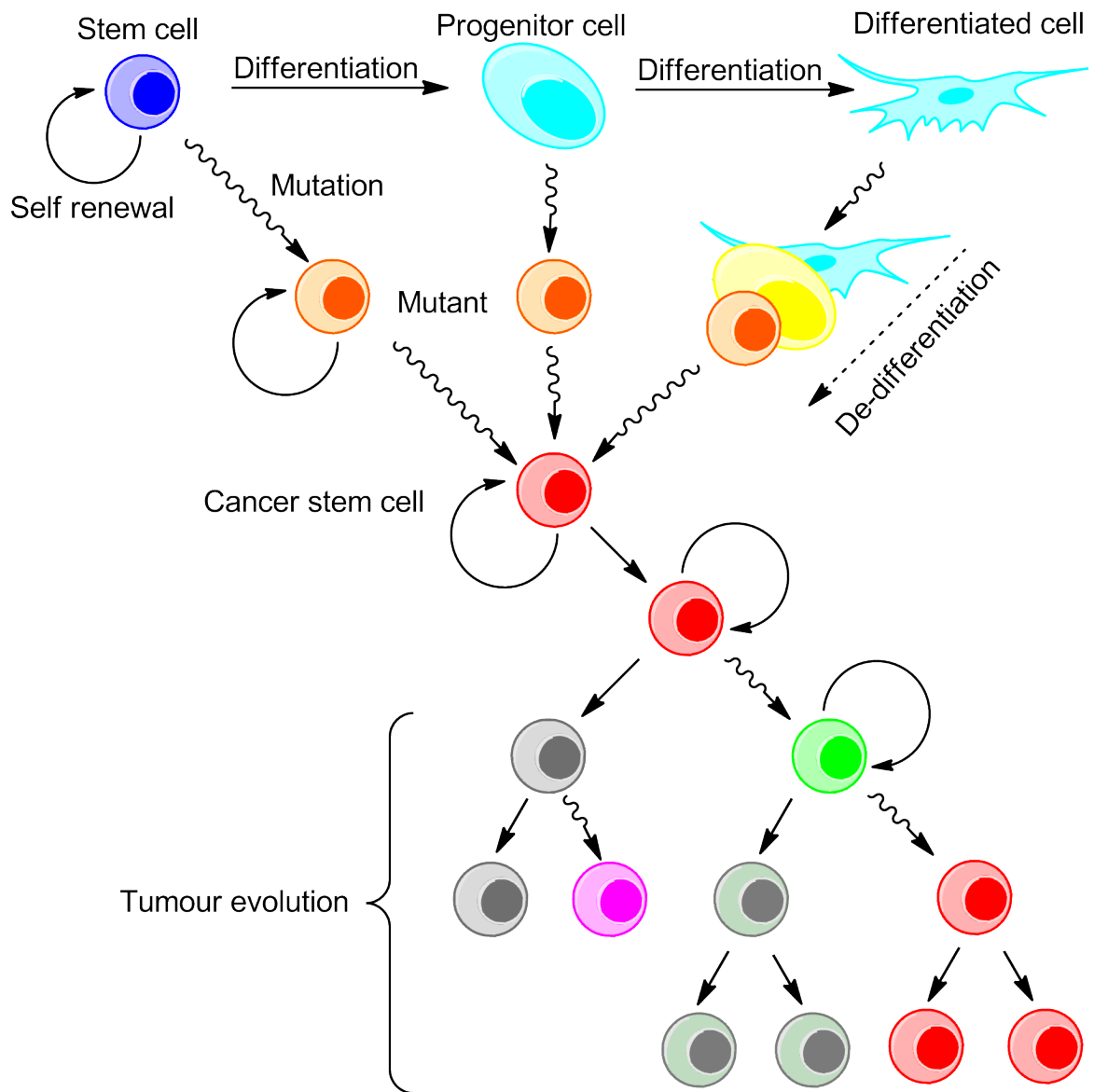
Figure 1.7: Theories concerning the potential origin of CSCs. The latter section concerning tumour evolution reconciles the CSC model to that of clonal evolution (adapted from Clevers, 2011; Goldthwaite, 2011; Visvader & Lindeman, 2012).

Of relevance to cancer therapy is that stem like cells be they CSCs are believed to be resilient to conventional cancer treatment strategies, surviving to cause tumour regression and escape once the initial therapy is complete (Dean *et al*., 2005; Rich, 2007).

Table 1.4: Biomarkers implicated in CSCs & EMT

Phenotype	Type	Marker	Reference
CSC	Surface protein	CD19, CD20, CD24, CD34, CD38 (-), CD44, CD90, CD133, CD326, TACSTD2	Li *et al.*, 2007; Visvader & Lindeman, 2008
	Membrane	CD34 (-), CD133, ABCB5, α2β1 integrin	Richardson *et al.*, 2004; Visvader & Lindeman, 2012
EMT	Surface proteins	E-cadherin (-), ZO-1 (-), N-cadherin, OB-cadherin, α5β1 integrin, αVβ6 integrin, syndecan-1	
	Cytoskeletal	Cytokeratin (-), FSP1, α-SMA, vimentin, β-catenin	Zeisberg & Neilson, 2009
	ECM	Laminin-1 (-), α1(IV) collagen (-), α1(I) collagen, α1(III) collagen, fibronectin, laminin 5	

In an extension of the interest in the role of cells with stem like properties, the phenomenon of epithelial to mesenchymal transition (EMT) and mesenchymal-epithelial transition (MET) has also been of considerable interest, fig. 1.8 (Dunning *et al.*, 2011). It has been observed that populations of cells within the tumour may be transient in nature, able to under the right conditions regain mesenchymal stem cell like properties. This characteristic is much like the proposed extrinsic nature some attribute to the CSC. The parallel here encourages the concept that the CSC may represent part of the EMT population, which in the authors opinion cannot be understated.

Further to this it is believed that these cells after transition may be able to undergo the reverse MET (Thiery & Sleeman, 2006). The relevance of these cells contribute to the progression of the disease is believed to occur after EMT when mesenchymal cells losing cell-cell connections with the primary tumour, migrate as circulatory tumour cells and then undergo MET to initiate metastasis at a new location (Thiery *et al.*, 2009).
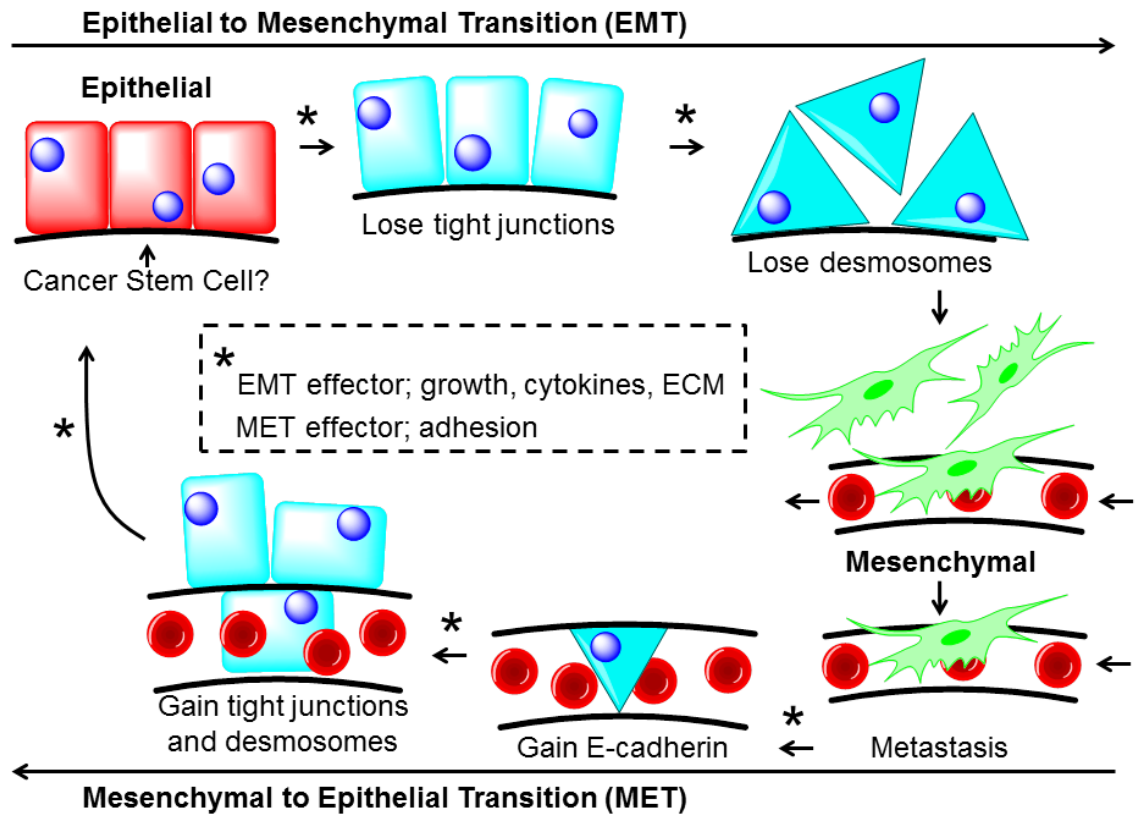
Figure 1.8: The process of EMT, MET and its implication with respect to cancer metastasis. Potential cross over with CSC theory is highlighted (adapted from Thiery & Sleeman, 2006; Sakaki-Yumoto *et al.*, 2013).

Mounting evidence for the presence of CSCs, cells undergoing EMT and the implications this causes for treatment has led to a paradigm shift in the strategy to detect and treat patients with cancer. Conventional therapies target the wrong cell populations of the tumour (Wicha *et al.*, 2006).

1.4.4 Requirement for new targets & new insights

The potential problems identified above can be resolved through greater insights into the nature of cancer and the sub-populations of the tumour involved in the pathology of the disease. With a greater understanding of the disease and the ability to identify and isolate sub-populations of interest like the CSC and cells undergoing EMT the possibility of being able to identify molecular targets for the detection and targeting of these cell sub-populations by next generation therapies like immunotherapy becomes a possibility.

The application of materials and surface chemistry to cancer research has focussed on materials that can assist in the diagnosis or therapy of the disease. For example self-assembling nanoparticles capable of selectively localising to the tumor may assist in diagnosis through imaging *via* delivery of a fluorescent or radioactive label, nuclear magnetic resonance contrast agent or to act as a drug delivery vehicle (Cho *et al*, 2007). Beyond the targeting of inorganic nanoparticles to specific cell types such as cancer through the use of monoclonal antibody conjugated particles (Cortez *et al*, 2006; Kocbek *et al*, 2007), there remains very little research conducted into understanding the interactions between inorganic materials and cancer cells, or other cell lines beyond biomaterial development. It is known that many types of cells such as primary cell lines are very difficult to culture with current systems, new culture materials may expand the range of cell lines available for research and the clinic.

The application of new culture materials such as those based on silica for improving the culture conditions of cancer cells or cancer stem cells, potentially for the selective isolation of cell sub-populations follows as a promising area of research.

1.5 Project aims

This project focusses on the exploitation of silica as a tissue culture surface, as the compound has many characteristics which make silica materials a potentially promising new tissue culture platform. Firstly, silica is generally biocompatible with a known role in nature as a biological scaffold and limited instances of toxicity. Secondly, the chemistry of sol-gel derived silica and its alkoxide precursors is diverse, allowing a wide variety of forms and chemistries to be engineered into the resulting surface. Finally taking advantage of our understanding of silica's biological role the material can be fabricated in a relatively environmentally friendly manner under conditions which do not require extremes of pH, temperature or pressure.

In addition this, study aims to achieve the development of a silica surface suitable for the tissue culture environment using a biomimetic method, building on principals of how biomolecules interact with silica. Then to explore how this surface performs in terms of being able to culture a tumour derived human cell line, to determine if cells will adhere and proliferate on the surface with no adverse toxicity. Once the core process for producing a silica surface for tissue culture has been established the surface properties can be further modified and the new surfaces again trialled in tissue culture. Through this iterative process it can be understood how the different tumour cell lines both individually and in general respond to different surface properties.

Finally the study can use the acquired understanding of how surface property influences cell response to develop materials which should be able to control the cell population in a desired manner. For the purposes of this project and its application to current problems in cancer research, the aim is in the development of materials which can have a selective role in tissue culture. The ability to isolate cell sub-populations relevant to the pathogenesis or treatment of cancer such as cancer stem cells or other therapeutic target cells such as those undergoing EMT would be of considerable benefit to cancer research. In addition to contributing to the fundamental understanding of how cells respond to different materials.

1.6 References

1. Abercrombie M. (1961). Ross Granville Harrison. 1870-1959. *Biogr. Mem. Fellows R. Soc.*, 7:110-6

2. Anderson N.L & Anderson A.G. (2002). The Human Plasma Proteome History, Character, and Diagnostic Prospects. *Mol. Cell. Proteomics*, 29(1):845-67

3. Anderson W.F. & Matsumo R. (2006). Breast Cancer Heterogeneity: A Mixture of At Least Two Main Types? *J. Natl. Cancer Inst.*, 98(14):948-51

4. Andre R, Tahir M.N, Natalio F & Tremel W. (2012). Bioinspired synthesis of multifunctional inorganic and bio-organic hybrid materials. *FEBS J.*, 279(10):1737-49

5. Aqui N.A. (2008). Post-transplant adoptive T-cell immunotherapy. Best *Pract. Res., Clin. Haematol.*, 21(3):503–19

6. Arcos D, Izquierdo-Barba I & Vallet-Regi M. (2009). Promising trends of bioceramics in the biomaterials field. *J. Mater. Sci.: Mater. Med.*, 20(2):447-55

7. Avnir D, Coradin T, Levc O & Livage J. (2005) Recent bio-applications of sol–gel materials. *J. Mater. Chem.*, 16(11):1013-30

8. Badylak S.F, Freytes D.O & Gilbert T.W. (2009). Extracellular matrix as a biological scaffold material: Structure and function. *Acta Biomater.*, 5(1):1-13

9. Badylak S.F, Weiss D.J, Caplan A & Macchiarini P. (2012). Engineered whole organs and complex tissues. *Lancet*, 379(9819):943-52

10. Barnes D. & Sato G. (1980). Serum-free Cell Culture: a Unifying Approach. *Cell*, 22(3):649-55

11. Barton J, Blackledge G & Wakeling A. (2001). Growth factors and their receptors: new targets for prostate cancer therapy. *Urology*, 58(2):114-22

12. Becton, Dickinson & Company. (2010). Defined Cell Culturing Surfaces and Methods of Use. US Patent: US 20100021998A1

13. Belton D.J, Patwardhan S.V & Perry C.C. (2005). Spermine, spermidine and their analogues generate tailored silicas. *J. Mater. Chem.*, 15(43):4629-38

14. Belton D.J, Patwardhan S.V, Annenkov V.V, Danilovtseva E.N, & Perry C.C. (2008). From biosilicification to tailored materials: Optimizing hydrophobic domains and resistance to protonation of polyamines. *Proc. Natl. Acad. Sci. U. S. A.*, 105(16):5963-8

15. Bergman A.J & Zygourakis K. (1999). Migration of lymphocytes on "fibronectin-coated surfaces: temporal evolution of migratory parameters. *Biomaterials*, 20(23-24):2235-44

16. Baeuerlain E. (2000). Biomineralization From Biology to Biotechnology and Medical Application. WILEY-VCH Verlag GmbH, Germany. ISBN: 3-527-29987-4

17. Bhushan B. (2009). Biomimetics: lessons from nature – an overview. *Philos. Trans. R. Soc., A*, 367(1893):1445-86

18. Bikram M, Gobin A.M, Whitmire R.E & West J.L. (2007). Temperature-sensitive hydrogels with SiO2–Au nanoshells for controlled drug delivery. *J. Controlled Release*, 123(3):219-27

19. Blondeau M. & Coradin T. (2012). Living materials from sol–gel chemistry: current challenges and perspectives. *J. Mater. Chem.*, 22(45):22335-43

20. Borovski T, Melo F.D.E, Vermeulen L, & Medema J.P. (2011). Cancer Stem Cell Niche: The Place to Be. *Cancer Res.*, 71(3):634-9

21. Bottini M, D'Annibale F, Magrini A, Cerignoli F, Arimura A, Dawson M.I, Bergamaschi E, Rosato N, Bergamaschi A & Mustelin T. (2007). Quantum dot-doped silica nanoparticles as probes for targeting of T-lymphocytes. *Int. J. Nanomed.*, 2(2):227–33

22. Bradbury J. (2004). Nature's Nanotechnologists: Unveiling the Secrets of Diatoms. *PLoS Biol.*, 2(10): e306

23. Brinker C.J & Scherer G.W. (1998). Sol-Gel Science: The Physics and Chemistry of Sol-Gel Processing. Academic Press, Inc, London. ISBN: 978-0-12-134970-7

24. Broers J.L, Rot M.K, Oostendorp T, Huysmans A, Wagenaar S.S, Wiersma-van Tilburg A.J, Vooijs G.P & Ramaekers F.C. (1987). Immunocytochemical detection of human lung cancer heterogeneity using antibodies to epithelial, neuronal, and neuroendocrine antigens. *Cancer Res.*, 47(12):3225-34

25. Cairncross G, Berkey B, Shaw E, Jenkins R, Scheithauer B, Brachman D, Buckner J, Fink K, Souhami L, Laperierre N, Mehta M & Curran W. (2006). Phase III Trial of Chemotherapy Plus Radiotherapy Compared With Radiotherapy Alone for Pure and Mixed Anaplastic Oligodendroglioma: Intergroup Radiation Therapy Oncology Group Trial 9402. *J. Clin. Oncol.*, 24(18):2707-14

26. Campbell L.L & Polyak K. (2007). Breast Tumor Heterogeneity Cancer Stem Cells or Clonal Evolution? *Cell Cycle*, 6(19):2332-8

27. Carlo E.D, D'Antuono T, Pompa P, Giuliani R, Rosini S, Stuppia L, Musiani P & Sorrentino C. (2009). The Lack of Epithelial Interleukin-7 and BAFF/BLyS Gene Expression in Prostate Cancer as a Possible Mechanism of Tumor Escape from Immunosurveillance. *Clin. Cancer Res.*, 15(9):2979-87

28. Chappell W.H, Lehmann B.D, Terrian D.M, Abrams S.L, Steelman L.S & McCubrey J.A. (2012). p53 expresion controls prostate cancer sensitivity to chemotherapy and the MDM2 inhibitor Nutlin-3. *Cell Cycle*, 11(24):4579-88

29. Chiarugi P & Giannoni E. (2008). Anoikis: A necessary death program for anchorage-dependent cells. *Biochem. Pharmacol.*, 76(11):1352-64

30. Chmielnicki E, Silva K.D, Farrell A, Gershon D & Swami M. (2012). Complex cancer roles for telomerase. *Nat. Med.*, 18(4):507

31. Cho Y.W, Park S.A, Han T.H, Son D.H,c, Park J.S, Oh S.J, Moon D.H, Cho K, Ahn C, Byun Y, Kim I, Kwon I.C & Kim S.Y. (2007). In vivo tumor targeting and radionuclide imaging with self-assembled nanoparticles: Mechanisms, key factors, and their implications. *Biomaterials*, 28(6):1236-47

32. Chollet C, Chanseau C, Remy M, Guignandon A, Bareille R, Labrugere C, Bordenave L, & Durrieu M-C. (2009). The effect of RGD density on osteoblast and endothelial cell behaviour on RGD-grafted polyethylene terephthalate surfaces. *Biomaterials*, 30(5):711-20

33. Clevers H. (2011). The cancer stem cell: premises, promises and challenges. *Nat. Med.*, 17(3):313-9

34. Cortez C, Tomaskovic-Crook E, Johnston A.P.R, Radt B, Cody S.H, Scott A.M, Nice E.C, Heath J.K & Frank Caruso. (2006). Targeting and Uptake of Multilayered Particles to Colorectal Cancer Cells. *Adv. Mater.*, 18(15):1998-2003

35. Currie H.A & Perry C.C. (2007). Silica in Plants: Biological, Biochemical and Chemical Studies. *Ann. Bot.*, 100(7):1383–9

36. Curtis A.S., Forrester J.V., McInnes C & Lawrie F. (1983) Adhesion of cells to polystyrene surfaces. *J. Cell Biol.*, 97(5):1500-6

37. Curtis C, Shah S.P, Chin S, Turashvili G, Rueda O.M, Dunning M.J, Speed D, Lynch A.G, Samarajiwa S, Yuan Y, Gräf S, Ha G, Haffari G, Bashashati A, Russell R, McKinney S, METABRIC Group, Langerød A, Green A,Provenzano E, Wishart G, Pinder S, Watson P, Markowetz F, Murphy L, Ellis I, Purushotham A, Børresen-Dale A-L, Brenton J.D, Tavaré S, Caldas C & Aparicio S. (2012). The genomic and transcriptomic architecture of 2,000 breast tumours reveals novel subgroups. *Nature*, 486(7403):346–52

38. Dahiya R, Lee C, McCarville J, Hu W, Kaur G & Deng G. (1997). High frequency of genetic instability of microsatellites in human prostatic adenocarcinoma. *Int. J. Cancer*, 72(5):762-7

39. Dalerba P, Cho R.W & Clarke M.F. (2007). Cancer Stem Cells: Models and Concepts. *Annu. Rev. Med.*, 58:267-84

40. Damber J-E & Aus G. (2008). Prostate cancer. *Lancet*, 371(9625):17-23

41. Dean M, Fojo T & Bates S. (2005). Tumor stem cells and drug resistance. *Nat. Rev. Cancer*, 5(4):275-84

42. Desimone M.F, De Marzi M.C,Alvarez G.S, Mathov I, Diaz L.A. & Malchiodi E.L. (2011). Production of monoclonal antibodies from hybridoma cells immobilized in 3D sol–gel silica matrices. *J. Mater. Chem.*, 21(36):13865-72

43. Dimaras H, Kimani K, Dimba E.I.O, Gronsdahl P, White A, Chan H.S.L & Gallie B.L. (2012). Retinoblastoma. *Lancet*, 379(9824):1436-46

44. Doi K, Fujino Y, Inagaki F, Kawatsu R, Tahara M, Ohshima T, Okaue Y, Yokoyama T, Iwai S & Ogata S. (2009). Stimulation of Expression of a Silica-Induced Protein (Sip) in *Thermus thermophilus* by Supersaturated Silicic Acid. *Appl. Environ. Microbiol.*, 75(8):2406-13

45. Drake C.G & Antonarakis E.S. (2012). Current status of immunological approaches for the treatment of prostate cancer. *Curr. Opin. Neurol.*, 22(3):197-202

46. Dudley M.E & Rosenberg S.A. (2003). Adoptive-Cell-Transfer Therapy for the Treatment of Patients with Cancer. *Nat. Rev. Cancer*, 3(9):666-75

47. Dudley M.E, Wunderlich J.R, Shelton T.E, Even J & Rosenberg S.A. (2003). Generation of Tumor-Infiltrating Lymphocyte Cultures for Use in Adoptive Transfer Therapy for Melanoma Patients. *J. Immunother.*, 26(4):332-42

48. Dudley M.E & Rosenberg S.A. (2007). Adoptive Cell Transfer Therapy. *Semin. Oncol.*, 34(6):524-31

49. Dunning N.L, Laversin S.A, Miles A.K & Rees R.C. (2011). Immunotherapy of prostate cancer: should we be targeting stem cells and EMT? *Cancer Immunol. Immunother.*, 60(8):1181-93

50. Eagle H. (1955). Nutritional Needs of Mammalian Cells in Tissue Culture. *Science*, 122(3168):501-4

51. Eagle H. (1955). The Specific Amino Acid Requirements of a Mammalian Cell (Strain L) in Tissue Culture. *J. Biol. Chem.*, 214(2)839-52

52. Evans M.D.M. & Steele J.G. (1998). Polymer surface chemistry and a novel attachment mechanism in corneal epithelial cells. *J. Biomed. Mater. Res.*. 40(4):621-30

53. Evans M.D.M & Steele J.G. (1997). Multiple Attachment Mechanisms of Corneal Epithelial Cells to a Polymer—Cells Can Attach in the Absence of Exogenous Adhesion Proteins through a Mechanism That Requires Microtubules. *Exp. Cell Res.*, 233(1):88-98

54. Exley C. (1998). Silicon in life : A bioinorganic solution to bioorganic essentiality. *J. Inorg. Biochem.*, 69(1998):139-44

55. Fairhead M, Kowatz T, McMahon S.A, Carter L.G, Oke M, Johnson K.A, Liu H, Naismith J.H & van der Walle C.F. (2008). Crystal structure and silica condensing activities of silicatein α/cathepsin L chimeras. *Chem. Commun.*, (15):1765-7

56. Fang L, Lonsdorf A.S & Hwang S.T. (2008). Immunotherapy for Advanced Melanoma. *J. Invest. Dermatol.*, 128(11):2596-605

57. Fidalgo A, Rosa M.E & Ilharco L.M. (2003). Chemical Control of Highly Porous Silica Xerogels: Physical Properties and Morphology. *Chem. Mat.*, 15(11):2186-92

58. Fidler I.J. (1978). Tumor Heterogeneity and the Biology of Cancer Invasion and Metastasis. *Cancer Res.*, 38(9):2651-60

59. Frantz C, Stewart K.M & Weaver V.M. (2010). The extracellular matrix at a glance. *J. Cell Sci.*, 123(Pt 24):4195-200

60. Frew A.J. (2008). Sublingual Immunotherapy. *N. Engl. J. Med.*, 358(21):2259-64

61. Frohbergh M. E, Katsman A, Botta G. P, Lazarovici P, Schauer C. L, Wegst U.G.K & Lelkes P.I. (2012). Electrospun hydroxyapatite-containing chitosan nanofibers crosslinked with genipin for bone tissue engineering. *Biomaterials*, 33(36):9176-8

62. Giancotti F.G. & Ruoslahti E. (2006). Integrin Signaling. *Science*, 285(5430):1028-32

63. Gilmore A.P & Romer L.H. (1996). Inhibition of Focal Adhesion Kinase (FAK) Signaling in Focal Adhesions Decreases Cell Motility and Proliferation. *Mol. Biol. Cell, MBoC*, 7(8)1209-24

64. Gimeno-Fabra M, Peroglio M, Eglin D, Alini M & Perry C.C. (2011). Combined release of platelet-rich plasma and 3D-mesenchymal stem cell encapsulation in alginate hydrogels modified by the presence of silica. *J. Mater. Chem.*, 21(12):4086-9

65. Goldthwaite C.A. (2011). Are stem cells involved in cancer? Regenerative Medicine. Chapter 9. Retrieved 04/02/13 http://stemcells.nih.gov/info/Regenerative_Medicine/pages/2006chapter9.aspx

66. Gumbiner B.M. (1996). Cell Adhesion: Review The Molecular Basis of Tissue Architecture and Morphogenesis. *Cell*, 84(3):345-57

67. Hamilton R.F, Thakur S.A & Holian A. (2007). Silica binding and toxicity in alveolar macrophages. *Free Radic. Biol. Med.*, 44(7):1246-58

68. Han M.G & Foulger S.H. (2004). Preparation of poly(3,4-ethylenedioxythiophene) (PEDOT) coated silica core–shell particles and PEDOT hollow particles. *Chem. Commun.*, 2004(19):2154-5

69. Hanahan D. & Weinberg R.A. (2000). The hallmarks of cancer. *Cell*, 100(1):57-70

70. Hanahan D. & Weinberg R.A. (2011). The hallmarks of cancer: the next generation. *Cell*, 144(5):646-74

71. Harrison C.C. (1993). Sol-Gel Chemistry Principles and Applications. Sira Communications, England

72. Hench L.L & West J.K. (1990). The Sol-Gel Process. *Chem. Rev.*, 90(1):33-72

73. Hersel U, Claudia D & Horst K. (2003). RGD modified polymers: biomaterials for stimulated cell adhesion and beyond. *Biomaterials*, 24(24):4385-415

74. Hildebrand M. (2003). Biological processing of nanostructured silica in diatoms. *Prog. Org. Coat.*, 47:256–66

75. Hotchin J.E. (1955). Use of Methyl Cellulose Gel as a Substitute for Agar in Tissue-Culture Overlays. *Nature*, 175(4451):352

76. Hutmacher D.W, Loessner D, Rizzi S, Kaplan D.L, Mooney D.J & Clement J.A. (2010). Can tissue engineering concepts advance tumor biology research? *Trends Biotechnol.*, 28(3):125-33

77. Iler R.K. (1979). The Chemistry of Silica Solubility, Polymerization, Colloid and Surface Properties, and Biochemistry. John Wiley & Sons, New York. ISBN: 0-471-02404-X

78. Izquierdo-Barba I, Arcos D, Sakamoto Y, Terasaki O, Lopez-Noriega A & Vallet-Regı M. (2008). High-Performance Mesoporous Bioceramics Mimicking Bone Mineralization. *Chem. Mat.*, 20(9):3191-8

79. Jaggupilli A & Elkord E. (2012). Significance of CD44 and CD24 as Cancer Stem Cell Markers: An Enduring Ambiguity. *Clin. Dev. Immunol.*, 2012:1-11.

80. Jugdaohsingh R, Calomme M.R, Robinson K, Nielsen F, Anderson S.H.C, D'Haese P, Geusens P, Loveridge N, Thompson R.P.H & Powell J.J. (2008). Increased longitudinal growth in rats on a silicon-depleted diet. *Bone*, 43:596–606

81. Kantoff P.W, Higano C.S, Shore N.D, Berger E.R, Small E.J, Penson D.F, Redfern C.H, Ferrari A.C, Dreicer R, Sims R.B, Xu Y, Frohlich M.W & Schellhammer P.F. (2010). Sipuleucel-T immunotherapy for castration-resistant prostate cancer. *N. Engl. J. Med.*, 363(5):411-22

82. Kartner N, Yao Y, Li K, Crasto G. J, Datti A and Manolson M.F. (2010). Inhibition of Osteoclast Bone Resorption by Disrupting Vacuolar H^+-ATPase a3-B2 Subunit Interaction. *J. Biol. Chem.*, 285(48):37476-90

83. Kaji H, Camci-Unal G, Langer R & Khademhosseini A. (2011). Engineering systems for the generation of patterned co-cultures for controlling cell-cell interactions. *Biochim. Biophys. Acta*, 1810(3):239-50

84. Kelly P.N, Dakic A, Adams J.M, Nutt S.L & Strasser A. (2007). Tumor Growth Need Not Be Driven by Rare Cancer Stem Cells. *Science*, 317(5836):337

85. Kelm J. M., Timmins N. E., Brown C. J., Fussenegger M. & Nielsen L. K. (2003). Method for generation of homogeneous multicellular tumor spheroids applicable to a wide variety of cell types. *Biotechnol. Bioeng.*, 83(2):173-80

86. Kendall T. (2000). Written in sand the world of speciality silica's. *Industrial Minerals*, March: 49-59

87. Kim D.J, Lee K, Chi Y.S, Kim W, Paik H & Choi I.S. (2004). Biomimetic Formation of Silica Thin Films by Surface-Initiated Polymerization of 2-(Dimethylamino)ethyl Methacrylate and Silicic Acid. *Langmuir*, 20(19):7904-6

88. Kleinman H.K, Luckenbill-Edds L, Cannon F.W. & Sephel G.C. (1987). Use of extracellular matrix components for cell culture. *Anal. Biochem.*, 166(1):1-13

89. Kleinman H.K & Martin G.R. (2005). Matrigel: Basement membrane matrix with biological activity. *Semin. Cancer Biol.*, 15(5):378-86

90. Knox P & Wells P. (1979). Cell Adhesion & Proteoglycans. *J. Cell Sci.*, 40:77-88

91. Kocbek P, Obermajer N, Cegnar M, Kos J & Kristl J. (2007). Targeting cancer cells using PLGA nanoparticles surface modified with monoclonal antibody. *J. Control. Release*, 120(1-2):18-26

92. Kosovsky M. (2012). Accelerating R&D of Cell-Based Therapies. *Genet. Eng. Biotechnol. News*,32(17):56-7

93. Krasko A, Lorenz B, Batel R, Schroder H.C, Muller I.M & Muller W.E.G. (2000). Expression of silicatein and collagen genes in the marine sponge *Suberites domuncula* is controlled by silicate and myotrophin. *Eur. J. Biochem.*, 267(15):4878-87

94. Kröger N, Bergsdorf C & Sumper M. (1996). Frustulins: domain conservation in a protein family associated with diatom cell walls. *Eur. J. Biochem.*, 239(2):259-64

95. Kröger N, Deutzmann R & Sumper M. (1999). Polycationic Peptides from Diatom Biosilica That Directs Silica Nanosphere Formation. *Science*, 282(5442):1129-32

96. Lam M.T & Longaker M.T. (2012). Comparison of several attachment methods for human iPS, embryonic and adipose-derived stem cells for tissue engineering. *J. Tissue Eng. Regener. Med.*, DOI: 10.1002/term.1499

97. Lareu R.R, Subramhanya K.H, Peng Y, Benny P, Chen C, Wang Z, Rajagopalan R & Raghunath. (2007). Collagen matrix deposition is dramatically enhanced *in vitro* when crowded with charged macromolecules: The biological relevance of the excluded volume effect. *FEBS Lett.*, 581(14):2709-14

98. Laugel N, Hemmerle J, Porcel C, Voegel J, Schaaf P & Ball V. (2006). Nanocomposite Silica/Polyamine Films Prepared by a Reactive Layer-by-Layer Deposition. *Langmuir,* 23(7):3706-11

99. Lee K.Y, Alsberg E, Hsiong S, Comisar W, Linderman J, Ziff R & Mooney D. (2004). Nanoscale Adhesion Ligand Organization Regulates Osteoblast Proliferation and Differentiation. *Nano Lett.*, 4(8):1501-6

100. Lee C, Raffaghello L & Longo V.D. (2012). Starvation, detoxification, and multidrug resistance in cancer therapy. *Drug Resist. Updates*, 15(1-2):114-22

101. Legrand A.P. (1998). The Surface Properties of Silicas. John Wiley & Sons, Chicester. ISBN: 0-471-95332-6

102. Leung C.C, Yu I.T.S & Chen W. (2012). Silicosis. *Lancet*, 379(9830):2008-18

103. Li C, Heidt D.G, Dalerba P, Burant C.F, Zhang L, Adsay V, Wicha M, Clarke M.F & Simeone D.M. (2007). Identification of Pancreatic Cancer Stem Cells. *Cancer Res.*, 67(3):1030-7

104. Li L, Bennett S.A.L & Wang L. (2012). Role of E-cadherin and other cell adhesion molecules in survival and differentiation of human pluripotent stem cells. *Cell Adh. Migr.*, 6(1):59–70

105. Liang Y, Sun W, Zhu Y & Christie P. (2007). Mechanisms of silicon-mediated alleviation of abiotic stresses in higher plants: A review. *Environ. Pollut.*, 147:422-8

106. Lin J & Kelly W.K. (2012). Targeting angiogenesis as a promising modality for the treatment of prostate cancer. *Urol. Clin. North Am.*, 39(4):547-60

107. Losic D, Mitchell J.G & Voelcker N.H. (2009). Diatomaceous Lessons in Nanotechnology and Advanced Materials. *Adv. Mater.*, 21(29):1-12

108. Low S.P, Williams K.A, Canham L.T & Voelcker N.H. (2006). Evaluation of mammalian cell adhesion on surface-modified porous silicon. *Biomaterials*, 27(26):4538-46

109. Lutolf M.P. (2009). Spotlight on hydrogels. *Nature Mater.*, 8(6):451-3

110. Mason, M. (2009). Management of prostate cancer: future treatment approaches. *Future Prescriber*, 10(3), 9-12

111. Mattila P.K & Lappalainen P. (2008). Filopodia: molecular architecture and cellular functions. *Nat. Rev. Mol. Cell Biol.*, 9(6):447-54

112. Maurel C, Verdoucq L, Luu D-T & Santoni V. (2008). Plant Aquaporins: Membrane Channels with Multiple Integrated Functions. *Annu. Rev. Plant Biol.*, 59:595-624

113. Mazur P. (1970). Cryobiology: The Freezing of Biological Systems. *Science*, 168(3934):939-49

114. McHale G, Shirtcliffe N.J & Newton M.I. (2004). Super-hydrophobic and super-wetting surfaces: Analytical potential? *Analyst*, 129(4):284-7

115. Michalopoulos G. & Pitot H.C. (1975). Primary culture of parenchymal liver cells on collagen membranes: Morphological and biochemical observations. *Exp. Cell. Res.*, 94(1):70-8

116. Mitani N & Ma J.F. (2005). Uptake system of silicon in different plant species. *J. Exp. Bot.*, 56(414):1255–61

117. Mitsiades N, Sung C.C, Schultz N, Danila D.C, He B, Eedunuri V.K, Fleisher M, Sander C, Sawyers C.L & Scher H.I. (2012). Distinct patterns of dysregulated expression of enzymes involved in androgen synthesis and metabolism in metastatic prostate cancer tumors. *Cancer Res.*, 72(23):6142-52

118. Nakata Y, Ueno M, Kihara J, Ichii M, Taketa S & Arase S. (2008). Rice blast disease and susceptibility to pests in a silicon uptake-deficient mutant lsi1 of rice. *Crop Prot.*, 27(3-5):865–868

119. Millard M, Odde S & Neamati N. (2011). Integrin Targeted Therapeutics. *Theranostics*, 1(17):154-88

120. Oberdörster G, Oberdörster E & Oberdörster J. (2005). Nanotoxicology: an emerging discipline evolving from studies of ultrafine particles. *Environ. Health Perspect.*, 113(7):823-39

121. Olson M.F. & Sahai E. (2009). The actin cytoskeleton in cancer cell motility. *Clin. Exp. Metastasis*, 2(4):273-87

122. Overwijk W.W, Theoret M.R & Restifo N.P. (2000). The Future of Interleukin-2: Enhancing Therapeutic Anticancer Vaccines. *Cancer J.*, 6(Suppl. 1):S76-S80

123. Otzen D. (2012). The Role of Proteins in Biosilicification. *Scientifica*, 2012:1-22

124. Patwardhan S.V, Clarson S.J and Perry C.C. (2005). On the role(s) of additives in bioinspired silicification. *Chem. Commun.*, 9:1113-21

125. Pawelec G & Rees R.C. (2002). Cancer vaccination progress. *Trends Mol. Med.*, 8(12):545-6

126. Petersson F, Hui T.S, Loke D & Putti T.C. (2012). Metastasis of Occult Prostatic Carcinoma to the Sphenoid Sinus: Report of a Rare Case and a Review of the Literature. *Head Neck Pathol.*, 6(2):258-63

127. Perry C.C & Lu Y. (1992). Preparation of Silicas from Silicon Complexes: Role of Cellulose in Polymerisation and Aggregation Control. *J. Chem. Soc., Faraday Trans.*, 88(19):2915-21

128. Perry C.C & Keeling-Tucker T. (1998). Aspects of the bioinorganic chemistry of silicon in conjunction with the biometals calcium, iron and aluminium. *J. Inorg. Biochem.*, 69:181-91

129. Perry C.C & Keeling-Tucker T. (2003). Model studies of colloidal silica precipitation using biosilica extracts from Equisetum telmateia. *Colloid Polym. Sci.*, 281:652–64

130. Pierre A.C. (2004). The Sol-Gel Encapsulation of Enzymes. *Biocatal. Biotransform.*, 22(3):145-70

131. Pogula S.D, Patwardhan S.V, Perry C.C, Gillespie J.W, Yarlagadda S & Kiick K.L. (2007). Continuous Silica Coatings on Glass Fibers via Bioinspired Approaches. *Langmuir*, 23(12):6677-83

132. Poulsen N & Kroger N. (2004). Silica Morphogenesis by Alternative Processing of Silaffins in the Diatom *Thalassiosira pseudonana*. *J. Biol. Chem.*, 279(41):42993-9

133. Race P.R, Lovering A.L, White S.A, Grove J.I, Searle P.F, Wrighton C.W & Hyde E.I. (2007). Kinetic and Structural Characterisation of Escherichia coli Nitroreductase Mutants Showing Improved Efficacy for the Prodrug Substrate CB1954. *J. Mol. Biol.*, 368(2):481-92

134. Rai A & Perry C.C. (2009). Fabrication of Tuneable Thickness Silica Films on Solid Surfaces Using Amines and Proteins. *Silicon*, 1(2):91-101

135. Rai A & Perry C.C. (2010). Facile Fabrication of Uniform Silica Films with Tunable Physical Properties Using Silicatein Protein from Sponges. *Langmuir*, 26(6):4152-9

136. Rai A & Perry C.C. (2012). Mussel adhesive protein inspired coatings: a versatile method to fabricate silica films on various surfaces. *J. Mater. Chem.*, 22(11):4790-6

137. Rich J.N. (2007). Cancer Stem Cells in Radiation Resistance. *Cancer Res.*, 67(19):8980-4

138. Richardson G.D, Robson C.N, Lang S.H, Neal D.E, Maitland N.J & Collins A.T. (2004). CD133, a novel marker for human prostatic epithelial stem cells. *J. Cell Sci.*, 117(16):3539-45

139. Rimann M & Graf-Hausner. (2012). Synthetic 3D multicellular systems for drug development. *Curr. Opin. Biotechnol.*, 23(5):1-7

140. Roach P, Farrar D & Perry C.C. (2006). Surface Tailoring for Controlled Protein Adsorption: Effect of Topography at the Nanometer Scale and Chemistry. *J. Am. Chem. Soc.*, 128(12):3939-45

141. Roach P, Eglin D, Rohde K & Perry C.C. (2007). Modern biomaterials: a review—bulk properties and implications of surface modifications. *J. Mater. Sci. Mater. Med.*, 18(7):1263-77

142. Rosen J.M. & Jordan C.T. (2009). The Increasing Complexity of the Cancer Stem Cell Paradigm. *Science*, 324(5935):1670-3

143. Ruoslahti E & Pierschbacher M.D. (1987). New perspectives in cell adhesion: RGD and integrins. *Science*, 238(4826):491-7

144. Sakaki-Yumoto M, Katsuno Y & Derynck R. (2013). TGF-β family signaling in stem cells. *Biochim. Biophys. Acta.*, 1830(2):2280-96

145. Sakamoto S & Kyprianou N. (2010). Targeting Anoikis Resistance in Prostate Cancer Metastasis. *JMAM*, 1(2):205–14

146. Salinas A.J, Vallet-Regí M, Toledo-Fernández J.A, Mendoza-Serna R, Piñero M, Esquivias L, Ramírez-Castellanos R & González-Calbet J.M. (2009). Nanostructure and Bioactivity of Hybrid Aerogels. *Chem. Mater.*, 21(1):41–7

147. Santerre J.P, Woodhouse K, Laroche G & Labow R.S. (2005). Understanding the biodegradation of polyurethanes: From classical implants to tissue engineering materials. *Biomaterials*, 26(35):7457-70

148. Santos E, Harnandez R.M, Pedraz J.L & Orive G. (2012). Novel advances in the design of three-dimensional bio-scaffolds to control cell fate: translation from 2D to 3D. *Curr. Trends Biotechnol.*, 30(6):331-41

149. Schmidt H, Scholze H & Kaiser A. (1984). Principals of hydrolysis and condensation reaction of alkoxysilanes. *J. Non-Cryst. Solids*, 63(1-2):1-11

150. Schmidt H. (1988). Chemistry of material preparation by the sol-gel process. *J. Non-Cryst. Solids*, 100(1-3):51-64

151. Sawyers C. (2004). Targeted cancer therapy. *Nature*, 432(7015):294-7

152. Schwartz M.A & Simone D. (2008). Cell Adhesion Receptors in Mechanotransduction. *Curr. Opin. Cell Biol.*, 20(5):551-6

153. Searle P.F, Chen M, Hu L, Race P.R, Lovering A.L, Grove J.I, Guise C, Jaberipour M, James N.D, Mautner V, Young L.S, Kerr D.J, Mountain A, White S.A & Hyde E.I. (2004). Nitroreductase: A Prodrug-Activating Enzyme for Cancer Gene Therapy. *Clin. Exp. Pharmacol. Physiol.*, 31(11):811-6

154. Serra M, Brito C, Correia C & Alves P.M. (2012). Process engineering of human pluripotent stem cells for clinical application. *Trends Biotechnol.*, 30(6):350-9

155. Sfanos K.S & De Marzo A.M. (2012). Prostate cancer and inflammation: the evidence. *Histopathology*, 60(1):199-215

156. Shimizu K, Cha J, Stucky G.D & Morse D.E. (1998). Silicatein a: Cathepsin L-like protein in sponge biosilica. *Proc. Natl. Acad. Sci. U. S. A.*. 95(11):6234-8

157. Shukla S.C., Singh A, Pandey A.K & Mishra A. (2012). Review on production and medical applications of ε-polylysine. *Biochem. Eng. J.*, 65(15):70-81

158. Silver I.A & Erecinska M. (2004). Interactions of Osteoblastic and Other Cells with Bioactive Glasses and Silica *In Vitro* and *In Vivo*. *Materialwiss. Werkst.*, 34(12):1069-75

159. Slater J.C. (1964). Atomic Radii in Crystals. *J. Chem. Phys.*, 41(10):3199–205

160. Slowing I.S, Vivero-Escoto J.L, Wu C, Lin V.S.-Y. (2008). Mesoporous silica nanoparticles as controlled release drug delivery and gene transfection carriers. *Adv. Drug Delivery Rev.*, 60(11):1278-88

161. Steele J.G, Dalton B.A, Johnson G & Underwood P.A. (1995). Adsorption of fibronectin and vitronectin onto Primaria™ and tissue culture polystyrene and relationship to the mechanism of initial attachment of human vein endothelial cells and BHK-2 1 fibroblasts. *Biomaterials*, 16(14):1057-67

162. Stepanenko A.A & Kavsan V.M. (2012). Immortalization and malignant transformation of Eukaryotic cells. *Cytol. Genet.*, 46(2):96-129

163. Stöber W, Fink A & Bohn E. (1968). Controlled growth of monodisperse silica spheres in the micron size range. *J. Colloid Interface Sci.*, 26(1):62-9

164. Sumper M & Kröger N. (2004). Silica formation in diatoms: the function of long-chain polyamines and silaffins. *J. Mater. Chem.*, 14(14):2059-65

165. Swann J.B & Smyth M.J. (2007). Immune surveillance of tumours. *J. Clin. Invest.*, 17(5):1137-1146

166. Tay. S.K. (2012). Cervical cancer in the human papillomavirus vaccination era. *Curr. Opin. Obstet. Gynecol.*, 24(1):3-7

167. Thiery J.P & Sleeman J.P. (2006). Complex networks orchestrate epithelial–mesenchymal transitions. *Nat. Rev. Mol. Cell Biol.*, 7(2):131-42

168. Thiery J.P, Acloque H, Huang R.Y.J & Nieto M.A. (2009). Epithelial-Mesenchymal Transitions in Development and Disease. *Cell*, 139(5):871-90

169. Tibbitt M.W & Anseth K. S. (2009). Hydrogels as Extracellular Matrix Mimics for 3D Cell Culture. *Biotechnol. Bioeng.*, 103(4):655-63

170. Tomczak M.M, Glawe D.D, Drummy L.F, Lawrence C.G, Stone M.O, Perry C.C, Pochan D.J, Deming T.J & Naik R.R. (2005). Polypeptide-Templated Synthesis of Hexagonal Silica Platelets. *J. Am. Chem. Soc.*, 127(36):12577-82

171. Treguer P, Nelson D.M, Van Bennekom A.J, DeMaster D.J, Leynaert A & Queguiner B. (1995). The Silica Balance in the World Ocean: A Reestimate. *Science*, 268(5209):375-9

172. Underwood P.A & Bennett F.A. (1989). A comparison of the biological activities of the cell-adhesive proteins vitronectin and fibronectin. *J. Cell Sci.*, 93(4):641-9

173. Valentijn A.J & Gilmore A.P. (2004). Anoikis. *Biochem. Soc. Trans.*, 32(3):421-5

174. van der Valk J, Brunner D, De Smet K, Fex Svenningsen A, Honegger P, Knudsen L.E, Lindl T, Noraberg J, Price A, Scarino M.L & Gstraunthaler G. (2010). Optimization of chemically defined cell culture media – Replacing fetal bovine serum in mammalian *in vitro* methods. *Toxicol. In Vitro*, 24(4):1053-63

175. Vepari C & Kaplan D.L. (2007). Silk as a Biomaterial. Progress in Polymer. *Science*, 32(8-9):991–1007

176. Verne E, Bretcanu O, Balagna C, Bianchi C.L, Cannas M, Gatti S & Vitale-Brovarone C. (2009). Early stage reactivity and in vitro behavior of silica-based bioactive glasses and glass-ceramics. *J. Mater. Sci.: Mater. Med.*, 20(1):75-87

177. Visvader J.E & Lindeman G.J. (2008). Cancer stem cells in solid tumours: accumulating evidence and unresolved questions. *Nat. Rev. Cancer*, 8(10):755-68

178. Visvader J.E & Lindeman G.J. (2012). Cancer Stem Cells: Current Status and Evolving Complexities. *Cell Stem Cell*, 10(6):717-28

179. Wang L. Zhao W & Tan W. (2008). Bioconjugated Silica Nanoparticles: Development and Applications. *Nano Res.*, 1(2):99-115

180. Wenzel R.N. (1936). Resistance of solid surfaces to wetting by water. *Ind. Eng. Chem.*, 28(8):988-94

181. Wicha M.S, Liu S & Dontu G. (2006). Cancer Stem Cells: An Old Idea—A Paradigm Shift. *Cancer Res.*, 66(4):1883-90

182. Williams D.F. (1988). Definitions in biomaterials. *J. Polym. Sci., Part C: Polym. Lett.*, 26(9):414

183. Williams D.F. (2008). On the mechanisms of biocompatibility. *Biomaterials*, 29(20):2941-53

184. Wilson C.J, Clegg R.E, Leavesley D.I. & Pearcy M.J. (2005). Mediation of Biomaterial–Cell Interactions by Adsorbed Proteins: A Review. *Tissue Eng.*, 11(1-2):1-18

185. World Health Organisation. (2005). Resolution on cancer control. WHO Document Production Services, WHA58.22

186. World Health Organisation. (2008). 2008-2013 Action Plan for the Global Strategy for the Prevention and Control of Noncommunicable Diseases. WHO Document Production Services, WT500 ISBN:978-92-4-159741-8

187. Xu J & Perry C.C. (2007). A novel approach to Au@SiO2 core-shell spheres. *J. Non-Cryst. Solids*, 353(11-12):1212–5

188. Yamaji N & Ma J.F. (2007). Spatial Distribution and Temporal Variation of the Rice Silicon Transporter Lsi1. *Plant Physiol.*, 143(3):1306–13

189. Yang S, Pilgaard L, Chase L.G, Boucher S, Vemuri M.C, Fink T & Zachar V. (2012). Defined Xenogeneic-Free and Hypoxic Environment Provides Superior Conditions for Long-Term Expansion of Human Adipose-Derived Stem Cells. *Tissue Eng., Part C*, 18(8):593-602

190. Yuan J & Jin R. (2005). Multiply Shaped Silica Mediated by Aggregates of Linear Poly(ethylenemine). *Adv. Mater.*, 17(7):885-8

191. Zeisberg M & Neilson E.G. (2009). Biomarkers for epithelial-mesenchymal transitions. *J. Clin. Invest.*, 119(6):1429-37

192. Zhou Y, Shimizu K, Cha J.N, Stucky G.D and Morse D.E. (1999). Efficient Catalysis of Polysiloxane Synthesis by Silicatein a Requires Specific Hydroxy and Imidazole Functionalities. *Angew. Chem. Int. Ed.*, 38(6):779-82

193. Zhou G & Levitsky H. (2012). Towards Curative Cancer Immunotherapy: Overcoming Posttherapy Tumor Escape. *Clin. Dev. Immunol.*, 2012:1-12

194. Zhuravlev L.T. (2000). The surface chemistry of amorphous silica. Zhuravlev model. *Colloids Surf., A*, 173(1-3):1-38

195. Zolkov C, Avnir D & Armon R. (2004). Tissue-derived cell growth on hybrid sol-gel films. *J. Mater. Chem.*, 14:2200-5

Chapter Two
Experimental Methods

The process of characterising new tissue culture materials and understanding the interaction of these materials with biological systems requires the application of numerous experimental methods. This chapter presents a general overview of these methods in terms of the core principals applied, limitations of these methods and finally the relevance of these methodologies to the experimental work conducted.

2.1 Ultraviolet-visible spectrophotometry, luminometry & fluorometry

2.1.1 Ultraviolet-visible spectrophotometry

Many compounds interact with electromagnetic radiation within the ultraviolet and visible (UV-Vis) wavelength range from around 400-800 nm, fig. 2.1. This interaction can come through attenuation of different wavelengths of the spectrum due to non-bonding electrons, in for example conjugated organic molecules, to the scattering of light in a specific manner due to the physical structure of the sample, as in photonic crystals (John, 1987).

In addition to being able to detect the presence of certain compounds due to their characteristic adsorption spectrum, spectrophotometry is able to directly relate the absorbance of a solution to the concentration of the adsorbing compound in the solution through the Beer-Lambert law (eq. 1)

$$A = \varepsilon c L \qquad\qquad Eq.\ 1$$

The Beer-Lambert law states that a given absorbance (A) is related to the concentration of the compound (c) attenuating the light, for a given path length (L), knowing the extinction coefficient (ε) of the compound. The extinction coefficient represents a measure of how strongly a compound adsorbs light at a specific wavelength for a given amount of compound, can be expressed as $M^{-1}\ cm^{-1}$.
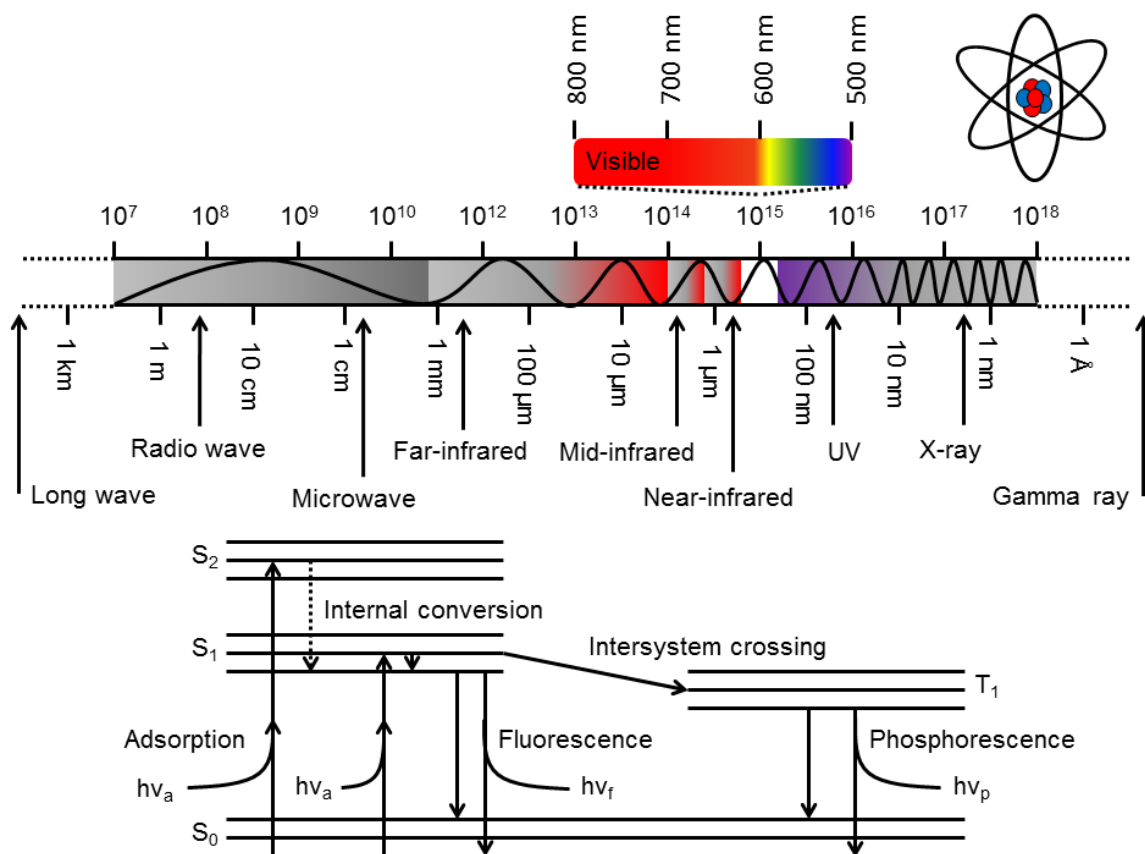
Figure 2.1: Electromagnetic spectrum highlighting position, components and nomenclature used to describe the different bands of the spectrum. A Jablonski diagram representing fluorescence and phosphorescence is shown below the spectrum. Figure adapted from NASA & Lakowicz, 2010.

The detection limit for spectrophotometry depends strongly on the compound and experimental conditions, though limits of detection can extend into the μM range (Demertzis, 2004). In this study spectrophotometry was applied to the characterisation of materials that adsorb UV-Vis wavelengths in addition to the detection of reporter molecules from biochemical assays, such as the detection of protein using the dye 4-amino-5-hydroxy-3-[(4-nitrophenyl)azo]-6-(phenylazo)-2,7-naphthalene disulfonic acid. Measurements were performed using either a Unicam UV2 or Cary® 50 Bio (Agilent, USA) UV-Vis spectrophotometers with a resolution of 0.5 nm for continuous scans or in the 96 well format using an Infinite® M200Pro (Tecan, Switzerland).

2.1.2 Luminometry

Luminescence derives from many sources (but does not concern incandescence), with chemiluminescence or light as the result of a chemical reaction being well-known. A

common example of chemiluminescence from its subdivision bioluminescence concerns the protein luciferase which emits light at the expense of the metabolite adenosine triphosphate (ATP), eq. 2 (Couch *et al*., 1993).

$$ATP + Luciferin + O_2 \xrightarrow{Mg^{2+} + Luciferase} Oxyluciferin + AMP + PP_i + CO_2 + Light \quad Eq. \ 2$$
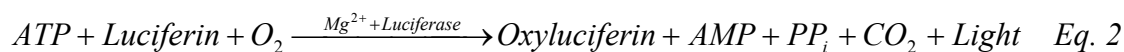
This reaction can be used to monitor the presence of ATP and may be used to monitor other processes by tethering the reaction to another process which generates ATP, eq. 3 (Squirrell *et al*., 2002).

$$Mg^{2+} ADP + ADP \xrightarrow{AdenylateKinase} Mg^{2+} ATP + AMP \qquad Eq. \ 3$$
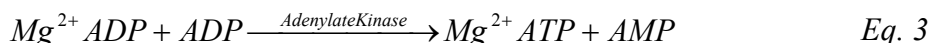
There are many applications that take advantage of luminescence, for this work luminometry was used in combination with the biological assays described above to monitor cell response to different surfaces using a microplate luminometer (Berthold Detection Systems, Germany) with an integration time of one second.

2.1.3 Fluorometry

A further division of luminescence concerns photon emission after excitation following photon adsorption, photoluminescence. This occurs when exited electrons transition from an exited state to a ground state, which occurs very quickly (10^8 sec^{-1} over a 10^{10-9} sec. period) and most commonly results in emission of light at a longer wavelength due to the Stokes shift, fig. 2.1 (Lakowicz, 2010). Relaxation can occur through alternative routes such as dissipation by heat (bond vibration) or phosphorescence which is much slower due to the passage of the electron through 'forbidden' electronic states, fig. 2.1 (Lakowicz, 2010). Fluorescent molecules (fluorophores) are generally aromatic in character and depending on the structure have different excitation and emission wavelengths. Proteins themselves can also have fluorescent characteristics due to specific amino acid residues (primarily tyrosine, tryptophan and phenylalanine) and their derivatives (Lakowicz, 2010). The diverse chemistry of fluorophores makes them suitable for a wide range of applications including but not limited to qualitative and quantitative assays, kinetic experiments, labelling and localisation in fluorescence microscopy and the study of molecular interactions through anisotropy and fluorescence resonance energy transfer. Additionally fluorimetric techniques are highly sensitive, a thousand times more so than absorbance based methods, detection limits in the pM range are readily accomplished (Demertzis, 2004; Lakowicz, 2010). In this work fluorophores were primarily used as indirect labels for visualising other molecules, some of the fluorophores

used in this work are presented in fig. 2.2, associated information in table 2.1 (Lakowicz, 2010).
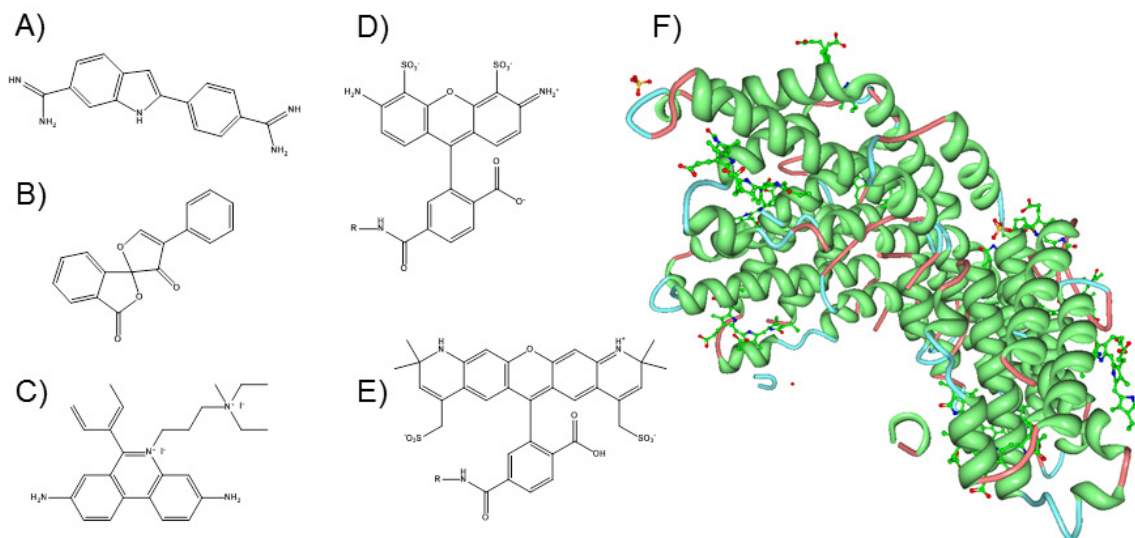
Figure 2.2: Structures of different fluorophores used; A) 4,6-diamidino-2-phenylindole (DAPI), B) fluorescamine, C) propidium iodide, D) Alexa Fluor® 488, E) Alexa Fluor® 568, F) R-phycoerythrin (PE) (Life Technologies & Haugland R.P, 2010; Udenfriend *et al*., 1972; Dengler *et al*., 1995; Panchuk–Voloshina *et al*., 1999; Contreras-Martel *et al*., 2001).

Table 2.1: Fluorophore characteristics

Compound	Colour	λ_{ab}^{max}	λ_{ex}^{max}	Reference
DAPI	Blue	358	461	
Fluorescamine	Yellow	390	475	
Propidium iodide	Red	535	617	Life Technologies & Haugland R.P, 2010
Alexa Fluor 488®	Green	495	519	
Alexa Fluor 568®	Red	578	603	
Alexa Fluor 633®	Far-red	632	647	
LIVE/DEAD®	Blue	416	451	
R-phycoethythin	Yellow	495, 536, 565	576	Lakowicz, 2010

2.2 Induction coupled plasma–optical emission spectroscopy

Induction coupled plasma–optical emission spectroscopy (ICP-OES) can be used to identify quantitatively the presence of different elements. When decomposed and excited by a high temperature Ar plasma generated by a high power radio frequency signal, different atoms emit different characteristic wavelengths of light (atomic spectral lines) as

electrons move from high to low energy states. These emissions are monitored by a monochromator and detector to identify and determine the abundance of specific elements respectively, once a calibration curve for a given element has been produced using standards. Ar and atmospheric elements are not capable of being studied due to their presence in the plasma. Elements which require high energy for excitation are difficult to analyse but most elements can be detected to ppb limits, though actual sensitivity depends from element to element as well as the matrix they are dissolved in prior to excitation in the plasma. In this work an Optima™ 2100 DV ICP-OES (Perkin Elmer®, USA) was applied to the detection of Si (251.611 nm) in complex biological media to assess the stability of the materials produced.

2.3 Fourier transform infra-red spectroscopy

Fourier transform infra-red spectroscopy (FTIR) is the study of the interaction of matter within the infrared (IR) region (14,000-10 cm^{-1}) of the electromagnetic spectrum, fig. 2.1. IR irradiation is absorbed, resulting in atomic bonds vibrating; this vibration depending on the bond type as different bonds attenuate different energies of the IR spectrum. The type and extent of this attenuation at any wavenumber can be determined through interferometry and Fourier transformation of the IR radiation interacting with the sample; considerably faster than monochromatic IR spectroscopy. The infrared spectrum can be split into three regions, near-IR (14,290-4000 cm^{-1}) for overtone and harmonic vibrations, mid-IR (4000-400 cm^{-1}) for fundamental vibrations and far-IR (700-200 cm^{-1}) for studying crystal lattice vibrations for example, fig. 2.1 (Silverstein & Webster, 1998).

FTIR can be used to qualitatively and quantitatively study the chemical groups present, peak assignments for common organic groups are shown in table 2.2. For different vibrations; ν is used to denote stretching vibrations, ν_s for in-phase stretching, ν_a for out-of-phase stretching, δ in-plane bending, γ or τ for out-of-plane bending, ρ for rocking and ω for wagging (Silverstein & Webster, 1998).

While FTIR is a common laboratory technique there are many different sample preparation methods associated with FTIR spectroscopy depending on the sample, be it solid, liquid or gas. Certain sample types, such as films on metals`, can provide an increase in gain provided by a combination of perpendicular polarisation and a specular reflectance system, due to the standing wave electric field at the surface being maximised at the Brewster angle of the surface, which in the case of metal is around 90° (Greenler, 1966).

Table 2.2 FTIR spectral assignments for common organic & silica related peaks (Silverstein & Webster, 1998)

Wavenumber (cm^{-1})	Bond	Group
800-1200, 1500, 1400, 1000	C-C	Alkane
1600, 1400, 1000	C=C	Alkene
2900-3000	C-H	Alkane
1100	C-O	Ether
1400, 1600	C=O	Carboxylic acid
900, 1200, 1600	C-N	Primary amine
2500-3700	O-H	Hydroxyl
1000-1350	Si-O	Siloxane
1300, 1400	Si-C	Methyl silane

The general FTIR technique is transmission of the laser through the sample when suspended within a KBr (largely transparent to mid-IR radiation) disk (fig. 2.3). This technique requires a high pressure press to produce the disk and careful preparation of the KBr matrix and sample to produce good quality spectra, for example avoiding the Cristiansen effect caused by similarities in the optical properties of the sample and matrix particles (Prost, 1973). In this work the main technique used for FTIR is Attenuated Total Reflectance (ATR), using a Spectrum 100 FTIR configured for ATR (Perkin Elmer®, USA). ATR differs from transmission or reflectance spectroscopy in that the sample interacts with the IR laser only through the evanescent wave generated by the laser as it passes through a crystal in contact with the sample (fig. 2.3); surface penetration is in the region of 0.5-2 μm. The technique has advantages in term of the ability to characterise large solid samples with minimal to no sample preparation with a detection limit in the region of μg/cm^2 depending on the sample and the chemistry of interest (Stamm, 2008).
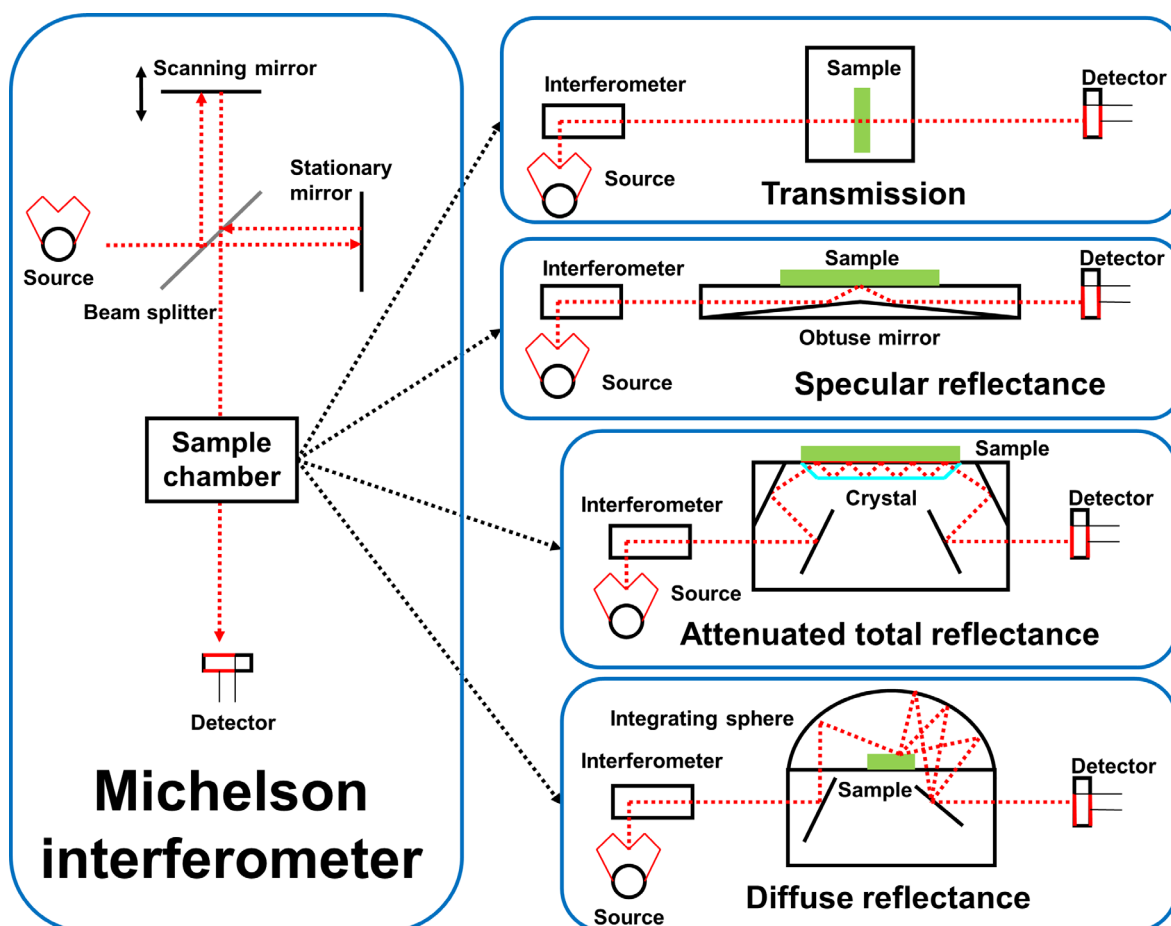
Figure 2.3: Schematic showing the common principal of the FTIR spectrometer and the differences in optics between conventional transmission and other sampling systems such as specular reflectance, ATR and DRIFTS.

Another variant on FTIR, Diffuse Reflectance Infra-red Fourier Transform Spectroscopy (DRIFTS) is especially suited to the study of the surface of small particulate samples (<10 μm) such as a nanomaterial (Fuller & Griffiths, 1978). In DRIFTS an integrating sphere is used to collect the diffusely reflected rather than specular reflected or transmitted light from the surface of the particles (fig. 2.3), this information (normally lost in FTIR) gives a significant increase is gain from the surface of the particle, with a detection limit of at least 625 ppm (Stamm, 2008). The appearance of Restrahlen bands (derivatives of peaks), broader bands and the requirement for Kubelka-Munk correction across the spectrum are complications in using the technique (Fuller & Griffiths, 1978).

Good FTIR spectra require carefully prepared samples and relevant blanks. When appropriate a dry clean purge gas should be continually provided to ensure that variation in atmospheric gasses does not influence the spectra. This is particularly relevant when

looking at bonds that fall into the regions occupied by atmospheric water and CO_2, such as surface water species.

2.4 X-ray photoelectron spectroscopy

X-Ray Photoelectron Spectroscopy (XPS) is used for qualitative and quantitative analysis (including chemical and electronic state) of the elemental composition (with a detection limit in the region of 0.1 atomic %) of materials though detection of emitted photoelectrons (Ratner & Castner, 1997). XPS takes advantage of the photoelectron effect, where photoelectrons are emitted upon bombardment of matter with low energy (1.5 keV) X-rays, fig. 2.4 provides an example XPS spectra and the principle of the method.
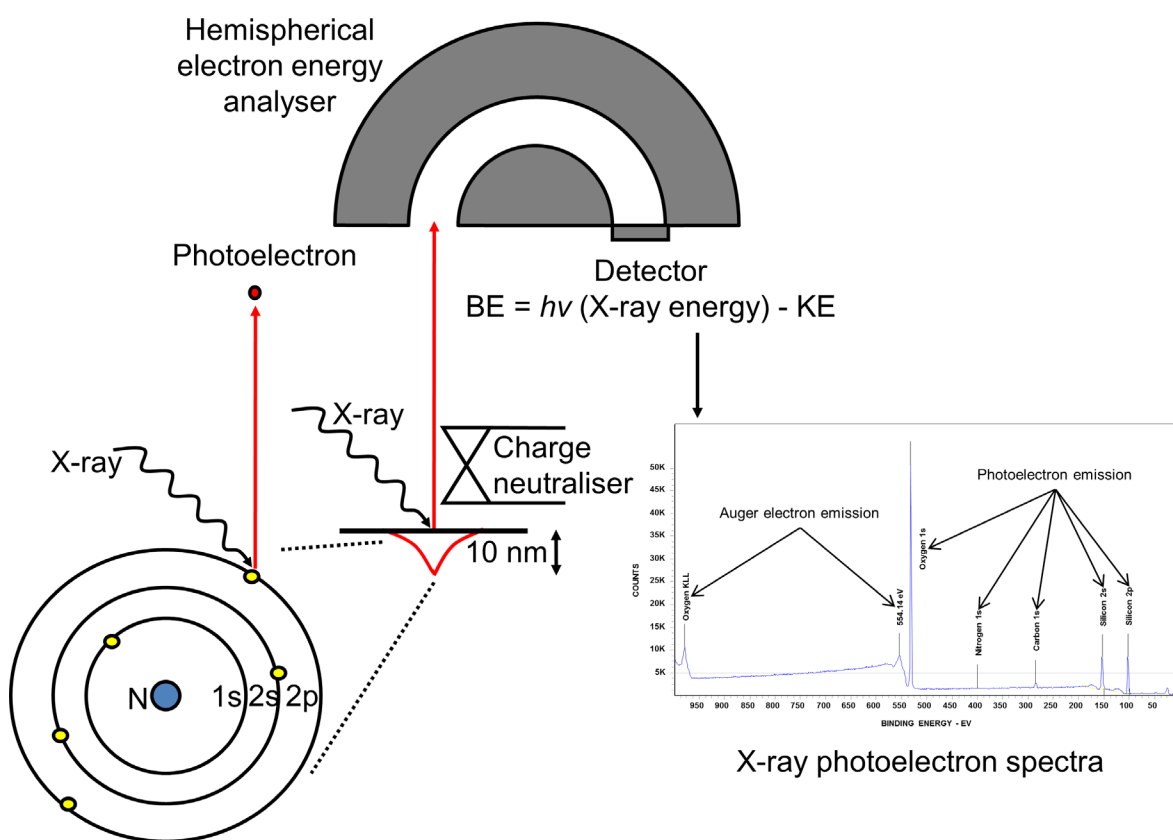
Figure 2.4: Principle of XPS, emission of X-rays to generate photoelectrons, detection and resulting spectra. Figure adapted from Ratner & Castner, 1997.

Since the photoelectrons can only escape from at most the top 10 nm of material the technique is very applicable to surface science and was applied as such in this study (kindly conducted by Mr J. Slocik) using an M-probe XPS spectrometer (Surface Science, USA) with survey scans (1 eV step) and high resolution scans (0.065 eV step) of the Si2p, O1s, C1s and N1s regions (Ratner & Castner, 1997). The measured kinetic energy (KE) of

the electrons is related by the Einstein equation to the binding energy (BE or the difference between initial and final state energies of the atomic system), this binding energy is dependent upon the atom, the orbital the photoelectron originated and its local binding environment.

In XPS C1s ($-CH_3$) is assigned a binding energy of 284.8 eV by convention, but through binding a more electronegative atoms like oxygen this peak can shift to a higher binding energy as electron density is reduced in the valence shell (Ratner & Castner, 1997). Through deconvolution of high resolution scans, the local binding environment can be determined and quantified. A small shift on high resolution scans of non-conductive materials is normally observed due to the use an electron flood gun to neutralise surface charging, corrected relative to the C1s convention.

2.5 Scanning & transmission electron microscopy & energy dispersive X-ray analysis

Since electrons have a shorter wavelength than visible light a microscope using electrons has far greater resolving power (<50 pm). Electron microscopes are normally composed of an electron source (tungsten or LaB_6 crystal filaments), electron accelerating and focussing fields and an electron detector such as a scintillator-photomultiplier or a phosphor screen and charge-coupled detector. There are two principal types of electron microscope, the scanning type scans a focussed electron beam across the sample and detects secondary electrons emitted from the surface which are used to reconstruct a 2D image. Transmission microscopes carry information imparted from the sample as the electron beam passes through the sample, generally as a change in electron beam intensity depending on the depth and composition of the sample through which the beam has passed. Sample preparation differs between SEM and TEM. SEM samples often require coating with a thin layer of another element (generally Au or C) to prevent charging artefacts during imaging, the coating also has the effect of improving the image quality when viewing materials made of lighter elements, the denser nuclei of heavy metals producing more secondary electrons. Sample preparation for TEM however is generally limited to application of the sample to a carbon film coated metal grid, though sectioning samples and preservation of the sample (specifically biological samples) in high power electron beams using cryogenic liquids are more advanced applications of TEM.
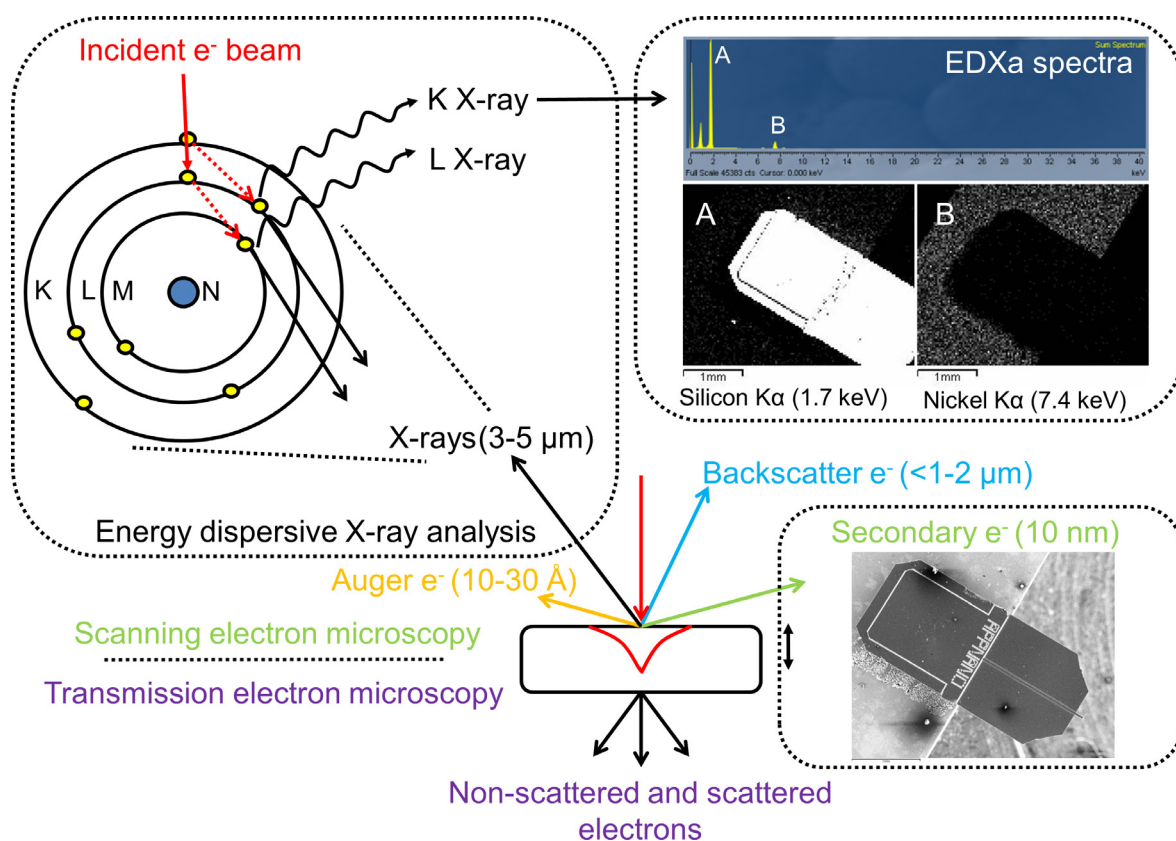
Figure 2.5: Principal of SEM operation and EDXA. Highlighting various emissions as a result of sample irradiation by an electron beam and the depth into the sample at which these emissions can be expected to originate. Figure adapted from Goldstein *et al*., 1997.

One advantage of SEM and TEM is that the requirement to expose the sample to an accelerated electron beam produces X-rays. Similar to XPS the energy of the emitted X-rays is dependent on the element the electron interacted with and as such can be used to qualitatively and quantitatively (to a detection limit of around 0.5 wt%) determine the elemental composition of the sample and the localisation of the elements to areas within the associated electron micrograph (Goldstein *et al*., 1981). This technique is referred to as energy dispersive X-ray analysis (EDXa). A problem with the technique with respect to surface analysis is that the penetration of X-rays is higher than photoelectrons so the depth and speed at which they escape the sample is considerably (>2 µm) greater (fig. 2.5). In this study a JSM-840A SEM (JEOL, Japan) operating in secondary electron mode with an INCAx-sight EDXa system (Oxford Instruments, UK) was applied to characterise the morphology and elemental composition of the surfaces produced.

2.6 Atomic force microscopy

Atomic Force Microscopy (AFM) is one of the scanning probe microscopy techniques which uses the interaction of a probe with a material (probe characteristics being monitored using a laser) to sense the surface and determine its properties. Though generally lower resolution than other techniques like scanning tunnelling microscopy, under optimal conditions sub-atomic resolution can be achieved (Mohn *et al*., 2013).

In this study a Nano-R2 (Pacific Nanotechnology, USA) AFM operating in close contact or 'tapping' mode using P-MAN-SICC-0, U3120A (Agilent, USA) and ACL-10 (AppNano, USA) close contact mounted cantilevers was used to determine topological features of the materials under investigation (fig. 2.6).
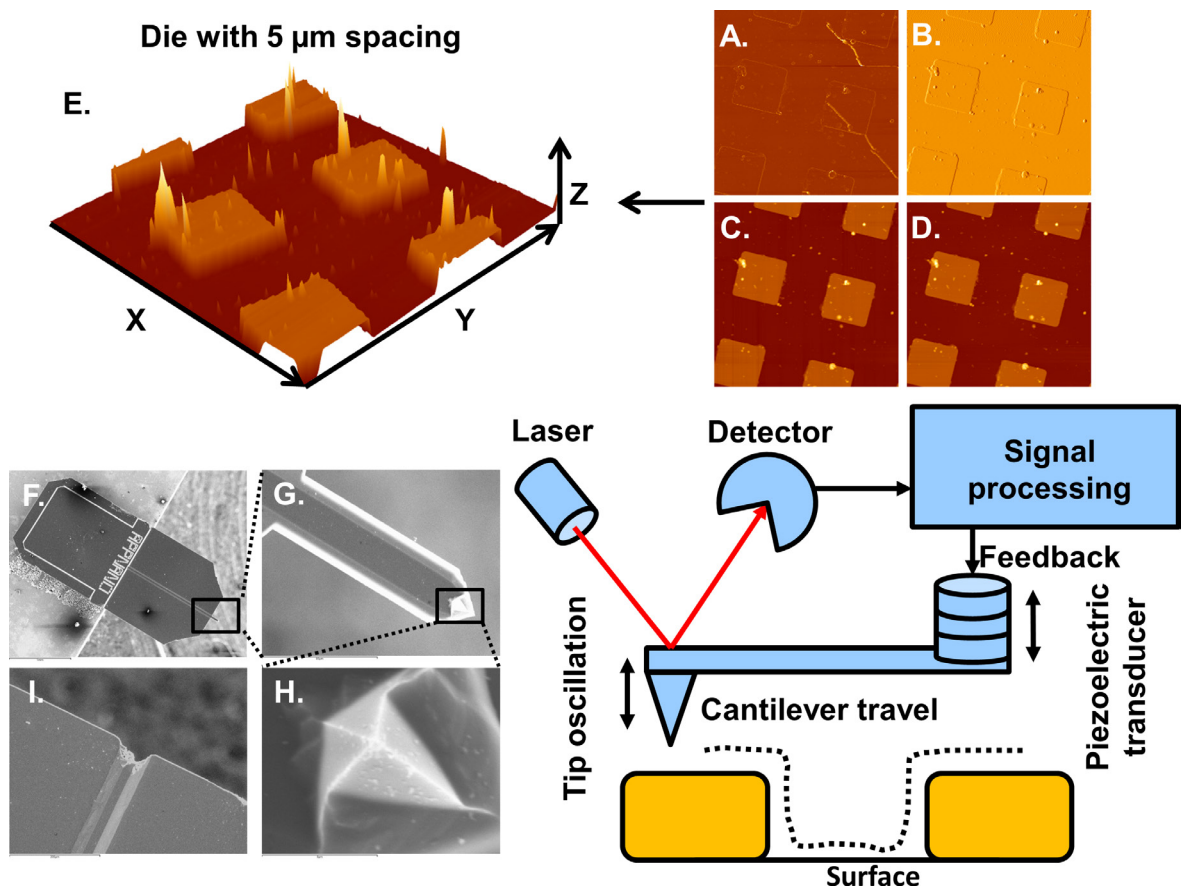
Figure 2.6: Principal of AFM operation in 'tapping' mode, scan of lithography etched surface showing error (A), phase (B), raw scan (C), height (D) data acquisition channels and extracted topological features (E). Electron micrographs of an Agilent U3120A AFM tip (F, G and H) are shown as is a broken tip with cantilever missing (I).

In 'tapping' mode the tip of the cantilever is oscillated at resonant frequency (*ca.* 100-200 kHz), as the tip comes close to the surface of the material under investigation the tip

oscillates at lower amplitude and visa-versa for increasing distances due to intra-molecular forces between the tip and the surface. By maintaining constant amplitude using piezoelectric motors the tip is held a constant distance from the sensed surface. Additional information on the adhesion and viscoelasticity of the surface can be obtained by looking at the phase change in tip oscillation as it passes over different materials (fig. 2.6B) (Leggett, 1997).

With different tips many different properties can be assessed by AFM such as mechanical properties using force distance curves when in contact with the surface but also magnetic and conductive properties. There has been considerable interest in applying AFM to biological samples like the cell, the technique in addition to imaging can also be used to measure cell adhesive properties and with some chemical modification of the tip, antibodies can be scanned across the surface of the cell to detect the presence of specific protein molecules (Roy *et al*., 2010).

Care and careful interpretation must be taken when obtaining scans by AFM, repeating patterns, and mismatch between forward and reverse scans may all indicate imperfections in the tip which introduces artefacts into the data obtained. The shape and size of the actual tip may limit the ability of AFM to sense some topological features. Despite these problems the technique is more versatile than electron microscopy, able to work with wet samples under ambient conditions, has greater resolution (though slower scan times) than confocal microscopy and is readily applicable to the generation of quantitative topological measurements.

2.7 Dynamic light scattering, *zeta* potential & surface *zeta* potential

Dynamic light scattering (DLS) was used for measuring the hydrodynamic radius (from nanometres to several micrometres) of particles in solution (Malvern, 2013). As particles move in solution due to Brownian motion the intensity of light scattered by the particles will vary over time for a given angle, faster (smaller) particles will vary intensity more quickly. A correlation function (C) can be used to analyse variation in intensity (Δk) over time (T), often a decaying exponential where τ represents a time constant, A_0 the baseline and B the intercept of the correlation function (eq. 4) (Malvern, 2013; Schärtl, 2007).

$$C(\Delta k, T) = A_0 \left[1 + B \exp(-2\Gamma\tau) \right] \qquad\qquad \text{Eq. 4}$$

The correlation function can be used to determine a particles diffusion coefficient (D) (eq. 5, 6), where n is the refractive index, λ_0 the laser wavelength and θ the scattering angle (eq. 2.6) (Malvern, 2013).

$$\Gamma = Dq^2 \qquad\qquad \text{Eq. 5}$$

$$q = \left(4\pi n / \lambda_0\right)\sin\left(\theta/2\right) \qquad\qquad \text{Eq. 6}$$

Once this is known the Stokes-Einstein equation can be used to calculate hydrodynamic radius (eq. 7) (Malvern, 2013; Schärtl, 2007). Where k_B is the Boltzmann constant, t represents temperature; η represents viscosity and R_H the hydrodynamic radius. Due to the layers (e.g. Stern layer and slipping plane) of adsorbed solvent on the particle the hydrodynamic radius is slightly larger than the actual radius.

$$R_H = \frac{k_B t}{3\pi\eta D} \qquad\qquad \text{Eq. 7}$$

A variation of DLS can be used to determine the *zeta* potential or electrokinetic potential of a colloid. It may also be described as the difference in potential between the bulk solvent and the slipping plane of the adsorbed solvent layer on the surface of the colloid (fig. 2.7). The *zeta* potential of the colloid can be used as a measure of colloidal stability, colloids with higher *zeta* potential will generally avoid flocculation and the measured potential is influenced by the properties of the colloids surface.
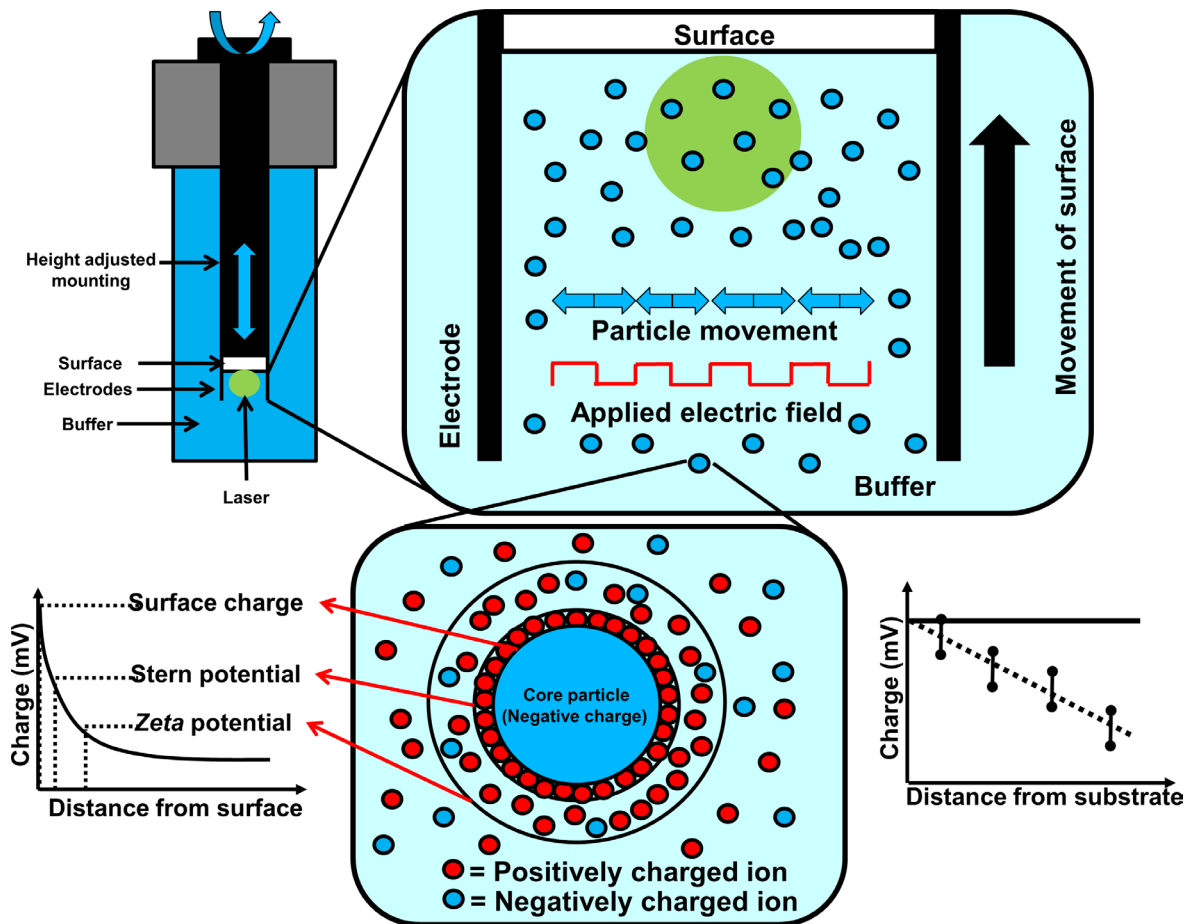
Figure 2.7: Schematic representation of *zeta* potential in a colloidal system and *zeta* potential measurement of a surface using a colloidal system as a 'tracer'.

Determining *zeta* potential is a useful characterisation but due to the nature of the measurement it is normally only applicable to colloids by DLS, until recently *zeta* potential determination for solids required capillary flow techniques like streaming *zeta* potential (Corbett *et al*., 2012). However a recent innovation has allowed DLS to be applied to the measurement of surface *zeta* potential through studying the interaction of 'tracer' particles in solution with a surface, a Nano ZS (Malvern, UK) instrument with surface zeta potential cell (Malvern, UK) was applied in this study (Corbett *et al*., 2012). There is a linear relationship between the charge on the 'tracer' particles, their distance from a surface and the surface *zeta* potential. If the *zeta* potential of the 'tracer' particles is known and the *zeta* potential of the 'tracer' particles is monitored as the surface moves further away from the 'tracer' particles then the *zeta* potential of the surface can be extrapolated from this relationship (fig. 2.7).

It should be noted that surface *zeta* potential is not a direct measure of surface charge but a way to measure *zeta* potential of a surface rather than a colloid. Surface charge can be

estimated from *zeta* potential but requires assumptions, for example on distance of the slipping plane from the particle surface.

2.8 Contact angle and surface free energy

Contact angle measurements of a droplet of liquid on a surface can be used to determine the wetting properties of the material in addition to providing information on the materials surface energy. Both types of measurement were conducted in this study. The method of determining a contact angle (θ) is given by the Young's equation which denotes the relationship between surface tension at the solid-liquid (SL), solid-gas (SG) and gas-liquid (GL) interfaces of the drop (eq. 8 and fig. 2.8) (Kwok *et al.*, 2000). Contact angles less than 90° are considered hydrophilic, those greater hydrophobic, those greater than 120° super-hydrophobic and those <5° super-hydrophilic (Kubo & Tatsuma, 2005).
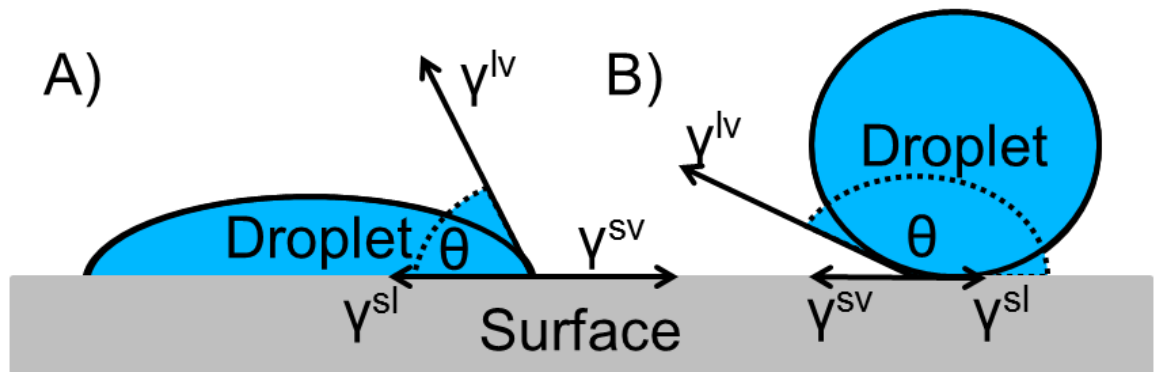
Figure 2.8: Contact angle measurement of hydrophilic (A) and hydrophobic (B) surfaces.

$$\gamma^{sv} = \gamma^{sl} + \gamma^{lv} \cos\theta \qquad\qquad Eq.\ 8$$

The surface free energy of a substance is defined as the measure of excess energy (due to disruption of intermolecular bonds – energetically unfavourable) at the surface of a material in comparison to the bulk material. For a liquid the surface free energy can be readily determined by measuring the surface tension of a sessile (hanging) drop.

For a surface the surface free energy can be determined through measuring the contact angle of a drop in contact with that surface for which the surface energy of the liquid is already known, (eq. 9) once known for a series of liquids the contact angle for any liquid whose surface energy is known can be predicted (Fowkes, 1962). A list of the components used in this study to determine the surface free energy of a surface is given in table 2.3.

$$\gamma_{LS} = \gamma_L + \gamma_S - 2\sqrt{\gamma_L \gamma_S} \qquad\qquad Eq.\ 9$$

Table 2.3: Compounds for surface free energy determination (Attension, 2013)

Compound	γ^{tot}(nN/m)	γ^{d}(nN/m)	γ^{-}(nN/m)	γ^{+}(nN/m)	P (g/cm^3)	η(mPa.s)
ddH$_2$O	72.8	21.8	25.50	25.5	0.998	1.002
Diiodomethane	50.8	50.8	0.0	0.0	3.325	2.8
Ethylene Glycol	48.0	29.0	3.0	30.1	1.1132	16.1
Formamide	58.0	39.0	2.280	39.6	1.133	3.3
Glycerol	64.0	34.0	3.920	57.4	1.261	1412.0

Further information can be extracted from the surface energy value for a liquid or surface if the polar and non-polar components of the total surface free energy are known (eq. 10) (Good & van Oss, 1992).

$$\gamma_L \left(1 + \cos\theta\right) = 2\left[\sqrt{\gamma_L^d \gamma_S^d} + \sqrt{\gamma_L^{acid} \gamma_S^{base}} + \sqrt{\gamma_L^{base} \gamma_S^{acid}}\right] \qquad Eq.\ 10$$

If this is so for the liquids used to probe the surface, then the polar and non-polar components of the surface energy value of the surface can be determined. This makes contact angle a very useful technique for surface science as the liquid will only interact with the very top atomic layers of the material. Information on the materials surface chemistry can be determined through looking at the polar (e.g. silanol groups) and non-polar (e.g. phenyl groups) components of the total surface energy.

A limitation of the technique is that the surface area that is considered is limited by the size of the drop, in this case 5 µL. This is generally on the macroscopic rather than the microscopic scale. Additionally, surface roughness can also influence the wetting properties of the surface; as such the actual chemical properties as determined by surface energy measurement can be difficult to interpret if surface roughness varies dramatically between different samples.

2.9 Immunostaining

Immunostaining is a broadly applied methodology by which an Immunoglobulin (Ig) or antibody is raised against and specific to a target molecule of interest (such as a protein) are applied in the detection of that molecule. These antibodies may be polyclonal, a cocktail of Ig molecules recognising multiple epitopes of the target (more sensitive but

less specific) or polyclonal, derived from one clonal population of cells expressing Ig molecules specific for a single epitope, fig. 2.9.

Immunostaining is applied to many different applications, from probing blots of gel electrophoresis (Western blotting) or an absorbed antigen (enzyme linked immunosorbent assay), staining of cells (immunocytochemistry, immune-electron microscopy and flow cytometry) and tissue sections (immunohistochemistry). In all cases the general methodology involves treating the sample with a primary antibody specific for the target, this may be conjugated with a detection agent directly or a secondary antibody specific for the primary antibody with a conjugated detection agent may be used, fig. 2.9.
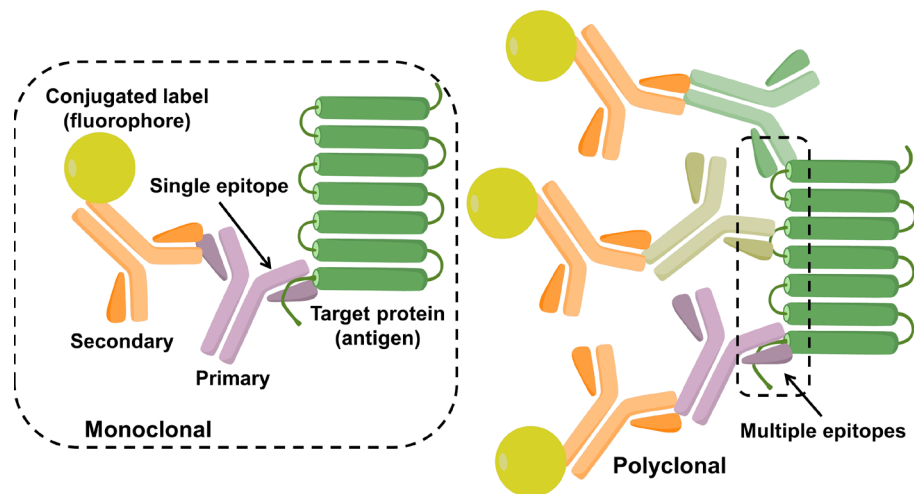
Figure 2.9: Principal of immunostaining for a target protein illustrated for both monoclonal and polyclonal antibodies.

In this study, immunostaining was used for the detection of specific cell markers known to be related to certain cell sub-populations. Care must be taken when selecting antibodies for immunostaining to ensure that there is no risk of unwanted reactivity between the antibodies, other targets or the sample, especially when multiple targets are probed at once (can be avoided using stringent blocking and washing conditions to prevent and remove non-specifically bound antibody). A control to test non-specific background binding is generally used through use of a negative isotype control which should demonstrate minimal binding in the case of a specific antibody.

2.10 Confocal microscopy

Confocal microscopes differ from conventional microscopes in their ability to filter out the majority of light from outside of the focal plane. The confocal technique is

generally performed using a mechanically scanned laser to illuminate only a narrow section of the sample, then removing out of focus light through the use of a pinhole aperture (fig 2.10). Other methods include the use of a spinning disk which contains multiple pinholes to achieve a faster scan than mechanically driven lasers (Pawley, 1995).
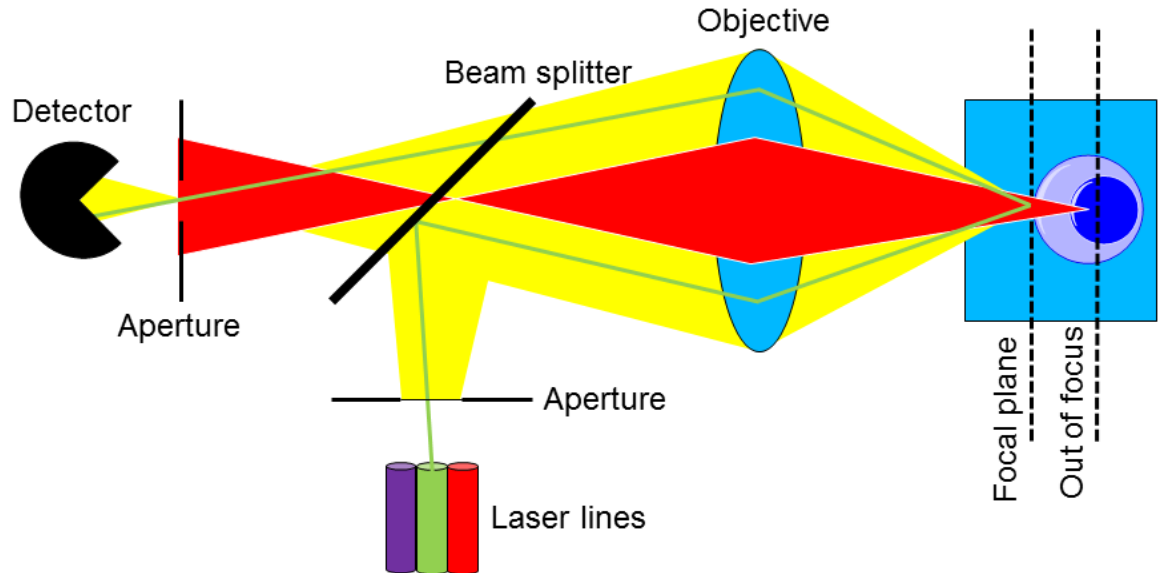
Figure 2.10: Principal of confocal optics, apertures being used to ensure that the majority of out of focus light does not reach the detector, adapted from Lakowicz, 2010.

This ability to remove the out of focus light greatly improves the sharpness and quality of the micrograph achieved. The technique also provides greater optical resolution in the z plane, allowing the localisation of entities like proteins when staining for their presence within cell compartments. In this work a Leica SP5 (Germany) laser scanning confocal microscope was used to visualise and localise the cell cytoskeleton, focal adhesion sites and associated proteins after immunostaining. Opening the aperture increases transmission of light to detect fainter features but allows more out of focus light to reach the detector, decreasing z resolution. Tight control of excitation and emission bands for different fluorophores is required for co-localisation of proteins within the cell, under optimal conditions a resolution of <200 nm in x and y and 500 nm in z can be achieved using a conventional laser scanning confocal microscope (Schermelleh *et al.*, 2010).

2.11 Flow cytometry

Assessing large populations of cells by microscopy is difficult considering the limited field of view and is potentially open to the bias of the experimentalist. Flow

cytometry with its reliance on a similar fluorescent labelling methodology to fluorescence microscopy but with the ability to analyse thousands of cells a second acts as a complimentary technique. This capability was employed using a Gallios™ flow cytometer (Beckman Coulter, UK) to observe changes in the sub-populations of large number of cells through the differential labelling of different protein markers with fluorescent reporters.

Flow cytometry passes suspended labelled cells in a narrow stream which ensures cells pass the excitation optics and detectors one at a time. As the cells individually pass the detector they are excited by the laser and the emission intensity for each cell is recorded, allowing cells to be examined for fluorescent markers, fig. 2.11. Over time (millions of cells can be assessed in a minute) the presence of different sub-populations as a percentage of the total population can be assessed (Hawley & Hawley, 2004).

Additional information is provided by the side and forward scatter of the lasers which provide information on the granularity (uniformity of the surface) and size of the object causing the event respectively. One problem with flow cytometry is that due to the single event nature of the method the cell must be excited with all laser wavelengths nearly simultaneously while being examined for many emission wavelengths at once, causing considerable issues with cross-talk. However with careful compensation for the interference as many as 10 different fluorophores may be used in an experiment at once, permitting observation of multiple populations or metabolic events simultaneously (Hawley & Hawley, 2004). Newer instruments may even image the cell as it passes the detector much like immunofluorescence (Basiji *et al*., 2007).
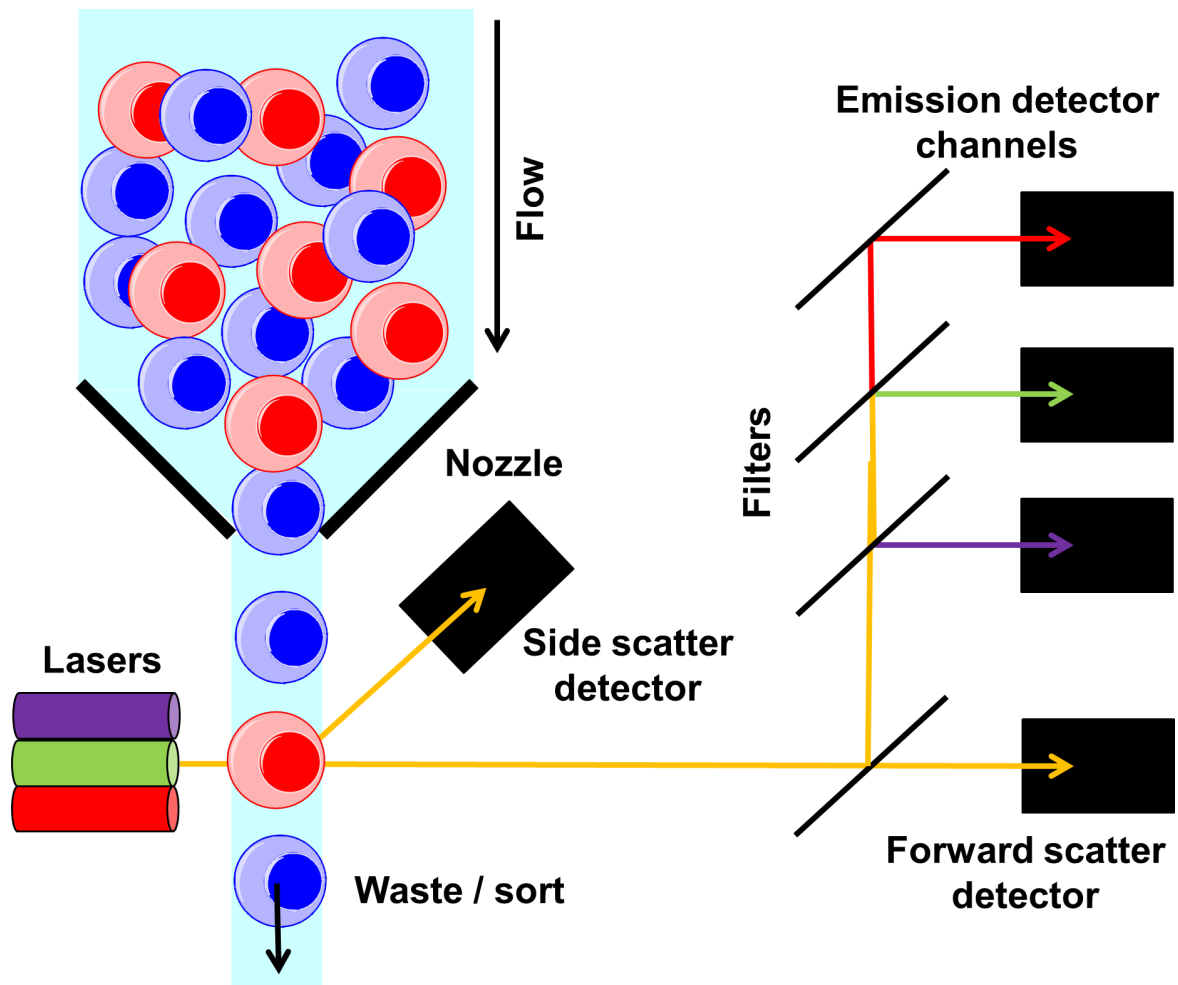
Figure 2.11: Representation of the principal of operation of the flow cytometer, labelled cells travel in a single file stream which passes the excitation and detection optics of the instrument. On passing through the detector individual cells can be assessed to determine the type and extent of the cells labelling.

Finally while during normal flow cytometry experiments the cells are lost to waste, fluorescence activated cell sorting (FACS) allows retention of the populations studied and even separating of sufficiently different populations from one another. This is achieved by ensuring that each cell is not just separated in the stream but separated into its own individual drop. Upon passing the detector and the cells characteristics determined, the drop can be given a charge and then propelled by electric fields to a container for later study or further culture. Through this clones of a specific population can be created, FACS being an invaluable tool for cell selection (Hawley & Hawley, 2004).

2.12 Mass spectrometry

Mass spectrometry (MS) encompasses a variety of techniques which allow the accurate determination of molecular weight (Da), through determining the mass to charge ratio (*m/z*) of ionised species. Initially applied in solving chemical structures the increased capabilities of modern instruments and data processing has seen mass spectrometry become an important tool in biology to study, for example, the proteome of the cell. An overview of mass spectroscopy is presented below, fig. 2.12.
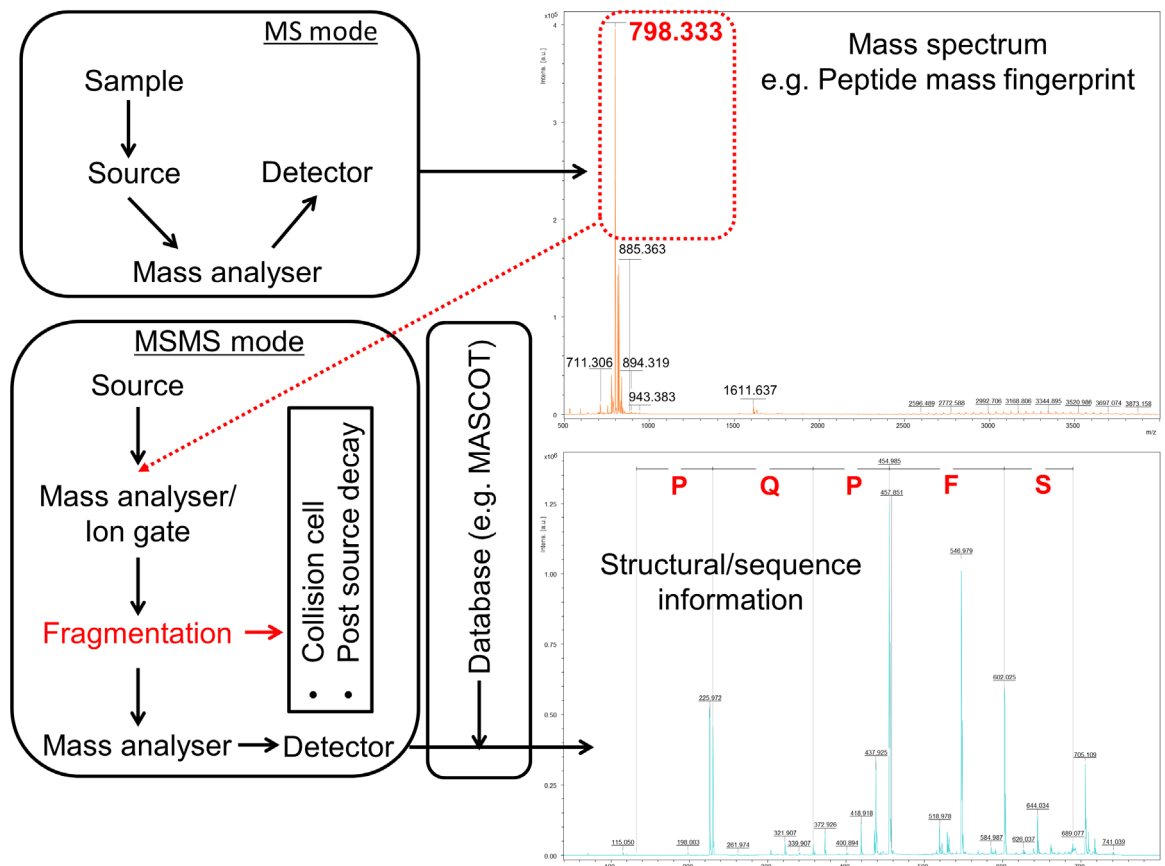
Figure 2.12: Overview of a simple mass spectrometry method, sample (e.g. unknown proteolytically digested protein) is introduced to source, ionised and the resulting ions *m/z* detected as a peptide mass fingerprint MS spectrum. Individual peptide *m/z* (798.333) selected and used to select a precursor ion in the first mass analyser. This precursor is fragmented and the resulting *m/z* products detected after the second mass analyser. Analysis of the fragments by MSMS allows the sequence of precursor peptide to be determined and potentially identification of the digested protein.

In principal, a mass spectrometer can be divided into three components, a method of sample ionisation (source), a mass analyser used to separate ions with different molecular weight and a charged particle detector, the different varieties and combinations of mass spectrometer are discussed in detail in numerous publications and texts and as such will not be discussed in detail here (Hoffmann & Stroobant, 2007).

The ability of mass spectrometry to provide structural information on the analyte is often a necessity as samples are often sufficiently impure or complex and spectrometers have inadequate mass accuracy such that it is impossible to determine the identity of a species based on its parent mass alone, tandem mass spectrometry of a fragmented parent ion is one approach to overcome this, another is to add an additional dimension of separation inside the spectrometer such as ion mobility mass spectrometry which can resolve sequence changes in even short peptides of identical composition (as such *m/z*) through differing ion mobilities.

In addition to the issue of identity the problem of quantification is also a significant problem for mass spectrometry due to the fact that ionisation is not uniform and ion suppression may prevent the ion intensity observed from reflecting the true abundance of the analyte in the sample. A variety of labelling and label free methods are however available for quantification studies and methods to provide quantification of all ion species observed are of considerable interest in modern systems. However validation of mass spectrometry data through complimentary methods such as Western blotting is standard practice.

In this study (kindly performed with the assistance of Prof. M. R. Clench) a MALDI quadrupole time of flight mass spectrometer (Applied Biosystems®, USA) was employed to detect the differential expression of lipids by cells after exposure to different surfaces. Through identification of changes in the cell lipidome, further insights into changes in biological pathways or the appearance of specific cell states (stress etc.) in response to different surfaces may be retrieved.

2.13 References

1. Attension. Surface free energy – theory and calculations. Theory Note 4. http://www.attension.com/file/filarkiv/application-theory-notes/attensiontn4sfe.pdf Last accessed 18th Sept. 2013

2. Basiji D.A, Ortyn W.E, Liang L, Venkatachalam V & Morrissey P. (2007). Cellular Image Analysis and Imaging by Flow Cytometry. *Clin. Lab. Med.*, 27(3):653-viii

3. Contreras-Martel C, Martinez-Oyanedel J, Bunster M, Legrand P, Piras C, Vernede X, Fontecilla-Camps J.C. (2001). Crystallization and 2.2 Å resolution structure of R-phycoerythrin from Gracilaria chilensis: a case of perfect hemihedral twinning. *Acta Crystallogr., Sect. D: Biol. Crystallogr.*, 57(1):52-60

4. Corbett J.C.W, McNeil-Watson F, Jack R.O & Howarth M. (2012). Measuring surface zeta potential using phase analysis light scattering in a simple dip cell arrangement. *Colloids Surf., A*, 396(2012):169-76

5. Crouch S.P.M, Kozlowski R, Slater K.J & Fletcher J. (1993). The use of ATP bioluminescence as a measure of cell proliferation and cytotoxicity. *J. Immunol. Methods*, 160(1):81-88

6. Demertzis M.A. (2004). Low detection limit spectrophotometry. *Anal. Chim. Acta*, 505(1):73-6

7. Dengler W.A, Schulte J, Berger D.P, Mertelsmann R & Flebig H.H. (1995). Development of a propidium iodide fluorescence assay for proliferation and cytotoxicity assays. *Anti-Cancer Drugs*, 6(4):522-32

8. Fowkes F.M. (1962). Determination of interfacial tensions, contact angles and dispersion forces in surfaces by assuming additivity of intermolecular interactions in surfaces. *J. Phys. Chem.*, 66(1962):382

9. Fuller M.P. & Griffiths P.R. (1978). Diffuse Reflectance Measurements by Infrared Fourier Transform Spectrometry. *Anal. Chem.*, 50(13):1906-10

10. Goldstein J.I, Newbury D.E, Echlin P, Joy D.C, Fiori C & Lifshin E. (1981). Scanning electron microscopy and X-ray microanalysis. Plenum press, New York, ISBN 0-306-40768-X

11. Good R.J & van Oss C.J. (1992). The Modern Theory of Contact Angles and the Hydrogen Bond Components of Surface Energies. Modern Approaches to Wettability (Schrader M.E & Loeb G.I), Springer US, New York, ISBN 978-1-4899-1178-0

12. Greenler R.G. (1966). Infrared study of adsorbed molecules on metal surfaces by reflection techniques. *J. Chem. Phys.*, 44(310):1-6

13. Iler R.K. (1979). The Chemistry of Silica Solubility, Polymerization, Colloid and Surface Properties, and Biochemistry. John Wiley & Sons, New York. ISBN: 0-471-02404-X

14. Hawley T.S & Hawley R.G. (2004). Flow Cytometry Protocols. Humana Press. United States of America, 3rd Edition, ISBN 1-58829-234-7

15. Hoffmann E & V Stroobant. (2007). Mass Spectrometry Principals and Applications. John Wiley & Sons, Inc. United States of America, 3rd Edition, ISBN 978-0-470-03311-1

16. John S. (1987). Strong Localization of Photons in Certain Disordered Dielectric Superlattices. *Phys. Rev. Lett.*, 58(23):2486-9

17. Kubo W & Tatsuma T. (2005). Conversion of a solid surface from super-hydrophobic to super-hydrophilic by photocatalytic remote oxidation and photocatalytic lithography. *Appl. Surf. Sci.*, 243(1-4):125-8

18. Kwok D.Y, Ng H & Neumann A.W. (2000). Experimental Study on Contact Angle Patterns: Liquid Surface Tensions Less Than Solid Surface Tensions. *J. Colloid Interface Sci.*, 225(2):323-328

19. Lakowicz J.R. (2010). Principals of Fluorescence Spectrometry. Springer Science & Business Media. United States of America, 3rd Edition, ISBN 978-0-387-31278-1

20. Leggett G.J. (1997). Scanning Tunnelling Microscopy and Atomic Force Microscopy. Surface Analysis the Principal Techniques, 1st Edition, ISBN 0-471-97292, p393-449

21. Life Technologies & Haugland R.P. (2010). The Molecular Probes Handbook: A Guide to Fluorescent Probes and Labelling Technologies. Life Technologies, 11th Edition, ISBN 0982927916

22. Malvern Instruments Ltd. Dynamic Light Scattering: An Introduction in 30 Minutes. DLS technical note, MAK656-01, Last accessed 15th Apr 2013

23. Mohn F, Schuler B, Gross L & Meyer G. (2013). Different tips for high-resolution atomic force microscopy and scanning tunnelling microscopy of single molecules. *Appl. Phys. Lett.*, 102(073109-1-4

24. National Aeronautics and Space Administration (NASA). Electromagnetic Spectrum Diagram. Available: http://mynasadata.larc.nasa.gov/science-processes/electromagnetic-diagram/. Last accessed 12th Apr 2013

25. Panchuk–Voloshina N, Haugland R.P, Bishop–Stewart J, M.K Bhalgat, Millard P.J, Mao F, Leung W-L & Haugland R.P. (1999). Alexa Dyes, a Series of New Fluorescent Dyes that Yield Exceptionally Bright, Photostable Conjugates. *J. Histochem. Cytochem.*, 47(9):1179-1188

26. Pawley J.B. (1995). Handbook of Biological Confocal Microscopy 2nd Edition. Springer Science & Business Media, New York, ISBN 0-306-44826-2

27. Prost R. (1973). The influence of the Christiansen effect on I.R. spectra of powders. *Clays Clay Miner.*, 21(5):363-8

28. Ratner B.D & Castner D.G. (1997). Electron Spectroscopy for Chemical Analysis. Surface Analysis the Principal Techniques, 1st Edition, ISBN 0-471-97292, p43-98

29. Roy S, Kwon S.H, Kwak J & Park J.W. (2010). "Seeing and Counting" Individual Antigens Captured on a Microarrayed Spot with Force-Based Atomic Force Microscopy. *Anal. Chem.*, 82(12):5189-5194

30. Schermelleh L, Heintzmann R & Leonhardt H. (2010). A guide to super-resolution fluorescence microscopy. *J. Cell Biol.*, 190(2):165-75

31. Schartl W. (2007). Light Scattering from Polymer Solutions and Nanoparticle Dispersions. Springer-Verlag, Berlin, ISBN 978-3-540-71950-2

32. Silverstein R.M & Webster F.X. (1998). Spectrometric Identification of Organic Compounds. John Wiley & Sons, Inc. United States of America, 6th Edition, ISBN 0-471-13457-0, p71-143

33. Stamm M. (2008). Polymer Surfaces and Interfaces: Characterization, Modification and Applications. Springer. United States of America, 1st Edition, ISBN 978-3-540-73865-7

34. Squirrell D.J, Prince R.L & Murphy M.J. (2002). Rapid and specific detection of bacteria using bioluminescence. *Anal. Chim. Acta*, 457(1):109-14

35. Udenfriend S, Stein S, Böhlen P, Dairman W, Leimgruber W & Weigele M. (1972). Fluorescamine: a reagent for assay of amino acids, peptides, proteins, and primary amines in the picomole range. *Science*, 178(4063):871-2

Chapter Three

Development of Silica Surfaces for Tissue Culture: Fabrication, Characterisation & Performance in Culture

3.1 Introduction

No commercial silica based tissue culture system (beyond borosilicate glass) exists and few examples are demonstrated within the scientific literature. Of the silica materials currently explored as tissue culture surfaces, the work of Zolkov *et al*. (2004) was the primary contribution. This work explored the influence of increasing methyltriethoxysilane: tetramethoxysilane ratio and poly-L-lysine concentration in the sol composition used to coat the surface, on cell proliferation and adhesion. Both of these variables were found to positively correlate with cell response (Zolkov *et al*., 2004).

Developing silica materials suitable for tissue culture and for determining selective surface properties for the growth of individual tumour sub-populations is a demanding endeavour, as the required properties are unknown. Elucidating selective surface properties would require a family of different silica surfaces to test a range of properties important in influencing cells in culture, such as differing topology and functionality (Huebsch & Mooney, 2009). Whatever these surfaces are, they must be compatible with tissue culture practices and permit cell population expansion.

Numerous tissue culture systems are currently available (table 1.3), however use of these systems in laboratory practice is often minimal e.g. the Google Scholar search 'tissue culture "purecoat"' returned 22 entries in total, 'tissue culture "polystyrene"' returned 3,210 entries for 2013 alone. This disparity can in part be due to the niche application of some of these specialist materials. Another reason may be the fixation of researchers on proliferative performance over other attributes when selecting new culture materials; proliferation alone is a poor attribute, the various grades of tissue culture polystyrene (TCPS) offer excellent performance (adhesion, proliferation) for most cell types. Researchers would be loath to change culture practice for incremental enhancements to proliferation alone. For a new tissue culture system to flourish, it would require a well-defined application that cannot be achieved with TCPS.

As such this initial work explored the development of a material that could be applied to the current TCPS materials, this was deemed advantageous due to the availability, familiarity and economy of the required form factors (24 well, 96 well etc.). A silica film applied to the surface of existing culture vessels was thought to be the solution with most potential, as opposed to a stand-alone silica system, such as an insert. Previous work has demonstrated that growth of silica films can be achieved and controlled *via* a biomimetic method through linking a cationic biomolecule to a surface, fig. 3.1.
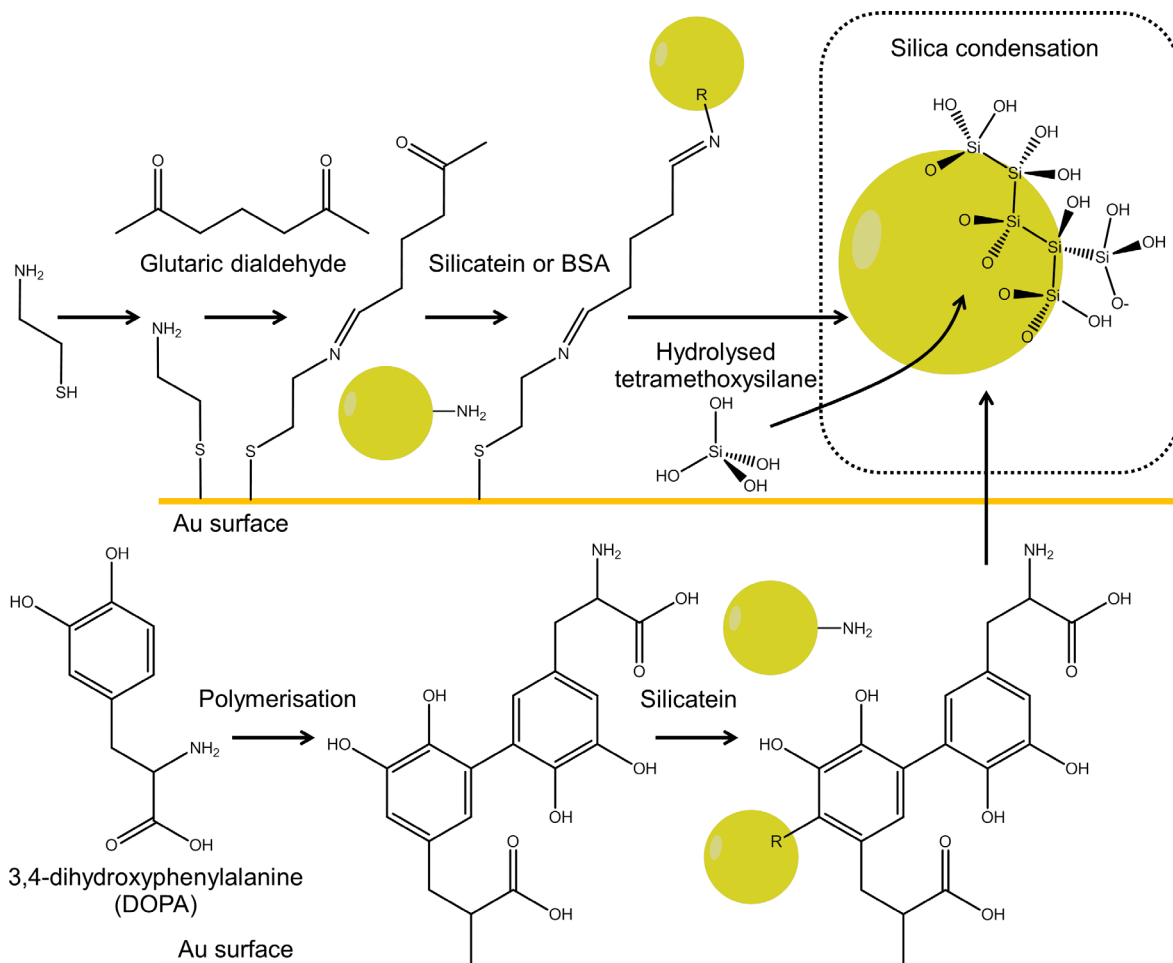
Figure 3.1: Overview of established methods to fabricate silica films *via* a biomimetic method. The basic linker design; surface, linker, biomolecule and silica was to be maintained but adapted for attachment to a polystyrene surface (Rai & Perry, 2009; Rai & Perry, 2010; Rai & Perry, 2012).

Initially this used the marine sponge protein silicatein but cheaper alternatives like bovine serum albumin and lysozyme have been shown to be almost as effective (Rai & Perry, 2009; Rai & Perry, 2010; Rai & Perry, 2012). Adaptation of the linker chemistry for gold surfaces that used disulphide and thiol containing compounds like cysteamine and 3,4-

dihydroxyphenylalanine was necessary for PS surfaces, since thiol chemistry is unsuitable for readily linking to PS surface groups (Rai & Perry, 2010; Rai & Perry, 2012, Karir *et al*., 2006).

Previous studies showed silica condensation conditions as well as post-processing techniques such as the drying method could be used to control the properties of the films created (Rai & Perry, 2010). As such, the characteristics of the silica surfaces produced on PS in terms of roughness and wetting were assessed. Once established and characterised, the performance of the human adherent melanoma FM3 was assessed on the different silica surfaces in terms of adhesion, proliferation and cytotoxicity.

3.2 Materials & methods

3.2.1 Materials

TCPS in 96, 24 and 6 well formats and PS cuvettes were obtained from Sarstedt (UK). Polyaniline hydrochloride, ammonium persulphate, glutaric dialdehyde (GDA), glycerol, naphthol blue black, ethylenediaminetetraacetic acid (EDTA), lysozyme (LYZ), bovine serum albumin (BSA), fibrinogen (Fb), sodium phosphate monobasic, sodium phosphate dibasic, trypan blue solution and tetramethoxysilane (TMOS) were obtained from Sigma-Aldrich® (UK). Ammonium molybdate, plate sealing tape, foetal bovine serum, 1 M hydrochloric acid, sodium hydroxide, 16 M nitric acid, methanol, glacial acetic acid and methylaminophenyl sulphate were obtained from Thermo Fisher Scientific (UK). Silicic acid standard (1000 ppm) was obtained from VWR International (UK). Dulbecco's phosphate buffered saline (DPBS), RPMI-1640 medium; trypsin-versene (EDTA) solution, L-glutamine solution, Toxilight™ Plus and Vialight™ Plus kits were obtained from Lonza BioWhittaker® (UK). The FM3 cell line was originally obtained from Prof. G. Pawelec, University of Tübingen, Germany. Distilled and deionised water (ddH$_2$O) was produced locally by distillation and ion exchange filtration, resulting in a pH of 5.8 and a conductivity of <1 µS/cm^{-1}.

3.2.2 Fabrication of silica films on polystyrene surfaces

Silica films were produced on a polyaniline (PANI), GDA and LYZ intermediate. The PANI surface was prepared by the 14 min polymerisation of 0.25 M aniline hydrochloride in 1 M HCl, activated with 0.08 M ammonium persulphate. The resulting PANI film was functionalised with a solution of 2% (0.21 M) GDA for 2 h at 57°C.

Lysozyme was attached to the GDA functionalised PANI surface by incubating the surface at 4°C overnight with a 1 mg/mL LYZ solution in 0.1 M phosphate buffer at pH 7.2. Pre-hydrolysed (1 mM HCl for 15 min) tetramethoxysilane (TMOS) precursor was used for silica deposition; fig 3.2. A drying control additive of 5% (0.3 M) glycerol was added to some samples. After each stage of the reaction the solution was aspirated and the surface washed with an excess of ddH$_2$O and dried with N$_2$ gas. Silica films were dried under ambient conditions but controlled in terms of duration and humidity depending upon desired film properties.
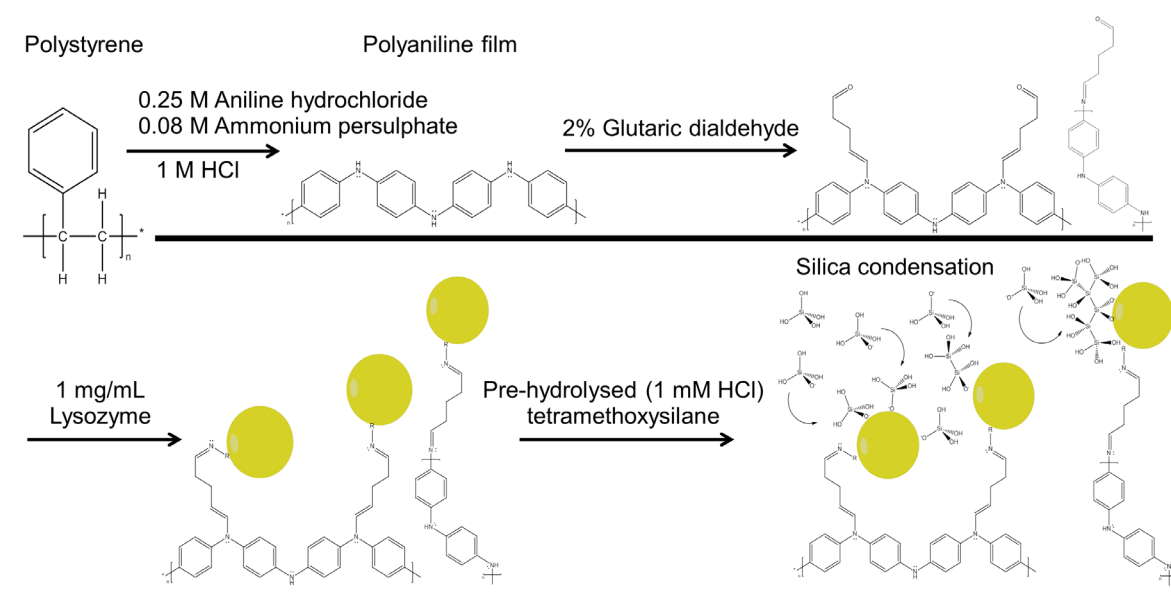
Figure 3.2: Schematic representation of surface fabrication process. Showing PANI deposition, GDA functionalisation of PANI, tethering of lysozyme to the surface before condensation of silica to the lysozyme modified surface.

3.2.3 Ultra-violet visible spectrophotometry

Ultra-violet visible (UV-Vis) spectrophotometry was used to characterise the PANI films, with scans taken using a Cary® 50 Bio UV-Vis spectrometer (Agilent, USA). Spectra were generated between 200-1100 nm at a resolution of 2 nm; PANI was applied directly to a cuvette with unmodified PS used as a blank.

3.2.4 Scanning electron microscopy & energy dispersive X-ray analysis

Scanning electron microscopy (SEM) and energy dispersive X-ray analysis (EDXa) were used to assess surface morphology and elemental composition respectively. A JSM-

840A SEM (JEOL, Japan) operating in the secondary electron mode at an accelerating voltage of 20–25 kV and a working distance between 15 and 35 mm with an integrated INCA X-sight EDXa analysis system (Oxford Instruments, UK) with count rate set to 3 kcounts s^{-1} for all samples. Samples were coated with gold for imaging, and carbon for EDXa analysis using an S150B sputter coater (Edwards, UK).

3.2.5 Atomic force microscopy

Atomic force microscopy (AFM) images were collected using a Nano-R2 atomic force microscope (Pacific Nanotechnology, USA) in close contact mode using either P-MAN-SICC-0 (Pacific Nanotechnology, USA) or ACL-10 (Applied Nanostructures, USA) close contact mounted cantilevers. Nine replicate scans were treated (levelled) before root mean square roughness (RMS) measurements were made using Nanorule software. Line analysis of treated data was used to determine film thickness at each stage of fabrication after a scratch was introduced on the surface in addition to data being collected on silica particle size and distribution.

3.2.6 Fourier transform infra-red attenuated total reflectance spectroscopy

Fourier transfer infra-red-attenuated total reflectance (FTIR-ATR) spectra were collected (32 scans accumulated for each sample) using a Spectrum 100 FTIR spectrometer (Perkin Elmer®, USA) configured for ATR. Spectra between 650 and 4000 cm^{-1} were taken using a diamond ATR crystal with 2 cm^{-1} resolution.

3.2.7 Dynamic light scattering & *zeta* potential

Dynamic light scattering (DLS) and *zeta* potential measurements were taken using a Nano-S Zetasizer (Malvern, UK) using 1 mL disposable and folded capillary cuvettes respectively. Measurements were taken at 25°C using protein as the material (refractive index 1.450, absorbance 0.001) and 0.1 M PBS (pH 7.2) as the dispersant (viscosity 1.0434 cP, refractive index 1.337). In both cases the default measurement duration (with three replicate measurements) and data processing options were used.

3.2.8 Contact angle measurement

Contact angle measurements were taken using a DSA 10 contact angle meter and

analysed using Drop Shape Analysis software (Krüss GmbH, Germany). A 5 μL drop of ddH$_2$O was dispensed onto the surface of the material. Contact angle measurements using three replicate drops across three replicate surfaces were made using 'tangent method 1'. Tangent method 1 calculates the equilibrium contact angle from the advancing and receding contact angle at either side of the drop.

3.2.9 Molybdenum blue assay for determining monosilicic acid

Fabricated silica films were treated with 2 M NaOH for 1 h at 80°C to ensure silica hydrolysis. Silicic acid concentration was estimated using a modification of the molybdenum blue colorimetric method described by Iler (1979). Sample aliquots of 100 μL were added to 15 mL ddH$_2$O and 1.5 mL solution of ammonium molybdate and incubated for 15 min at room temperature. A reducing agent of 8 mL 4-methylaminophenyl sulphate was added and the absorbance of the blue silicomolybdate complex was measured after 2 h at 810 nm using a Unicam UV2 UV-Vis spectrophotometer (Thermo Scientific, USA). The concentration of silicic acid condensed on the different surfaces was calculated from a standard curve of known orthosilicic acid concentrations.

3.2.10 Amido-black protein adsorption assay

Protein adsorption to the different silica films was monitored used the Amido-black assay as described by Roach *et al.* (2006). Surfaces were incubated with 1 mg/mL protein solutions (BSA, Fb) in 0.1 M phosphate buffer (pH 7.2) for a period of 24 h. The protein was then eluted, surface washed twice with ddH$_2$O, stained for 5 min (10% MeOH, 10% glacial acetic acid, 1 wt.% naphthol blue black), washed with an excess ddH$_2$O and three times (38% MeOH, 2% glacial acetic acid) before the dye was detached with 250 μL of eluent (50% EtOH and 50% 0.1 mM EDTA in 50 mM NaOH). A 100 μL aliquot was then analysed by a Spectra Fluor plate reader (Tecan, Switzerland) with a 620 nm incident and 450 nm reference filters, nine replicate surfaces were used.

3.2.11 Tissue culture of the adherent human melanoma FM3

FM3 cell culture conditions were RPMI-1640 growth medium supplemented with 1% L-glutamine and 10% bovine Foetal Calf Serum (FCS). Confluent cultures were passaged or introduced onto culture surfaces by removal of growth media, washing twice with DPBS and then 1x trypsin solution. After 5 min incubation, cells were aspirated and

pelleted by centrifugation (3 min at 400 relative centrifugal force [RCF]), the trypsin solution was removed and the cells suspended in media. Cells (number determined by haemocytometer) were then introduced onto (ultra-violet (UV) sterilised for 15 min) culture surfaces or tissue culture flasks. The incidence of infection was estimated to be between 1-3% of all cultures initiated, this was determined by visually with contaminated cultures eliminated from testing.

3.2.12 Toxilight® adenylate kinase assay

The Toxilight® Plus ATP assay was conducted by reconstituting the lyophilised adenylate kinase detection reagent, allowing all reagents and samples to equilibrate at room temperature. From each sample 20 µL of media was withdrawn and added to 100 µL of reconstituted adenylate kinase detection reagent. After 15 min incubation at room temperature, the RLU intensity was read with a Berthold Detection Systems (Germany) Microplate Luminometer, with integration time 1 s, with three replicates per condition and timepoint.

3.2.13 Vialight® Plus adenosine triphosphate assay

The Vialight® Plus adenosine triphosphate (ATP) assay was conducted by reconstituting the lyophilised ATP monitoring reagent plus, allowing all reagent and samples to equilibrate at room temperature. Cells on each sample plate were lysed (with 2.5 mL of the supplied cell lysis reagent) by incubation at room temperature for 10 min From each sample plate 25 µL of media was withdrawn and added to 100 µL of reconstituted ATP monitoring reagent plus, after 2 min incubation at room temperature the RLU intensity was read in the same manner as the Toxilight® Plus ATP assay.

3.2.14 Cell morphology & proliferation by light microscopy

For cell imaging an Eclipse TS100 light microscope (Nikon, Japan) with 10x0.25 (WD 6.2), 20x0.40 (WD 3.0), 40x0.55 (WD 2.1) lenses was used. Images were digitised with a DN100 Digital Net Camera with 0.7x magnification (Nikon, Japan). Apoptotic cells were stained with 0.4% trypan blue solution in a ratio of one part dye to four parts media. Cells were counted manually from 20x0.25 (WD 6.2) microscope images segregated with a 9x7 grid. Three counts were taken from separate grid sections with total cells determined by multiplication, with three replicate images used per condition and time point.

3.2.15 Centrifugal cell adhesion assay

Cells were plated (*ca.* 25,000 by haemocytometry) onto a 24 well plate and allowed to adhere overnight. Plates were sealed with adhesive tape and centrifuged inverted for 5 min at a rate between 10 to 200 RCF using a 5810R centrifuge with A-2-DWP plate rotor (Eppendorf, Germany). Plates were then imaged with a light microscope 10x0.25 (WD 6.2) to determine the number of cells adhered to the surface after each run; nine replicate surfaces were used for each sample. An initial count was also taken before centrifugation to represent cell adhesion (total population) at zero RCF.

3.2.16 Inductively coupled plasma–optical emission spectroscopy

Silica concentration in the media was quantified by inductively coupled plasma–optical emission spectroscopy (ICP-OES) using an Optima™ 2100 DV optical emission spectrometer with WinLab32 software (Perkin Elmer®, USA). Silicon concentration was determined by measuring signal intensity at 251.611 nm against a standard curve of orthosilicic acid (between 0.01 and 0.75 mg/L^{-1}) with RPMI-1450 medium as the matrix.

3.2.17 Statistical testing

Significant features in the characterisation of the surface and protein adsorption were determined using unpaired two tailed t-tests. For proliferation and toxicity time-course data, in addition to adhesion data, significance was assessed using general linear regression. In both cases the assumptions of normality and constant variance were assessed in the GenStat® 11th Edition software (VSN International Ltd, UK). Error is presented as standard error, unless otherwise stated. The following notation is used to denote significance; (*) P ≤0.05 significant, (**) P ≤0.01, (***) P ≤0.001 and (****) ≤0.0001.

3.3 Results & discussion

3.3.1 Development of suitable linker chemistry for silica film fabrication on polystyrene surfaces

Initial attempts to fabricate silica films on PS were unsuccessful as the type of surface functionality was inadequate to permit biomolecule adsorption directly and thus silica film formation. Polystyrene itself is often chemically treated prior to applications where protein adsorption is required (Meyer-Plath *et al.*, 2003). In order to attach the

biomolecules required to fabricate a silica surface, the PS surface first required modification with an intermediate linker as described in fig. 3.2. Polyaniline (PANI) was selected due to its ability to adhere to PS by hydrophobic interaction on polymerisation and the presence of primary and secondary amines, which provided a basis for further functionalisation (Karir *et al*., 2006). The PANI precursor aniline hydrochloride was polymerised *in situ* (fig. 3.2B, C).
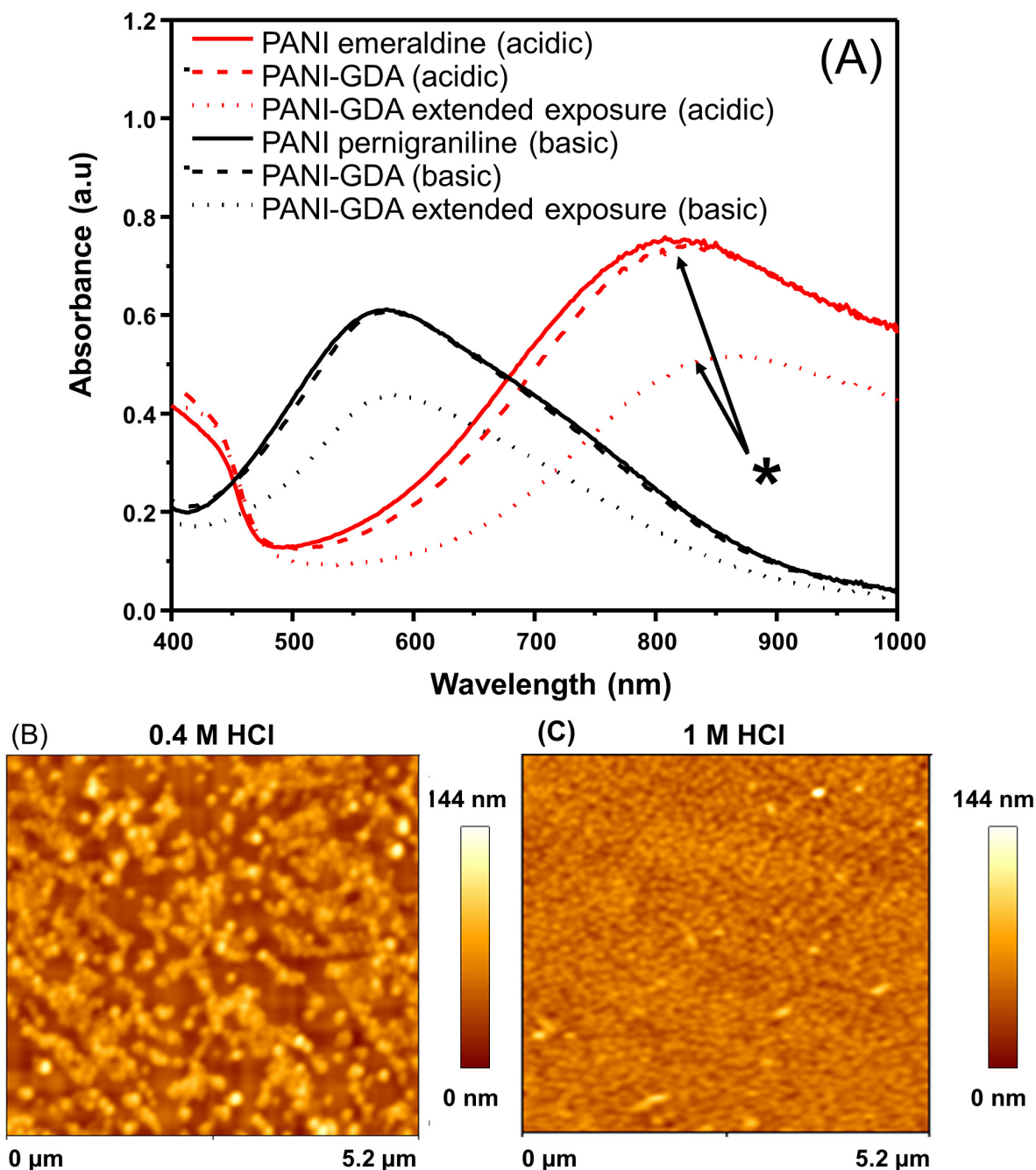
Figure 3.3: Absorbance spectrum (A) of PANI treated PS under acidic and basic conditions and PANI treated PS after exposure for different periods to 2% GDA. An

absorbance shift was seen upon GDA exposure (*). AFM scans B and C show PANI surfaces formed using different concentrations of HCl.

PANI film formation and deposition was immediately apparent through the adsorption band ~830 nm, due to the polaron band transition of PANI in its emeraldine salt form due to the acidic conditions of the reaction, fig. 3.3A, 3.4A (Jang *et al.*, 2006). AFM demonstrated that the uniformity of surface coverage of the films was found to depend on the concentration of HCl; AFM data was used to optimise the surface coverage of the PANI deposition method to 1 M HCl (fig. 3.3B, C).
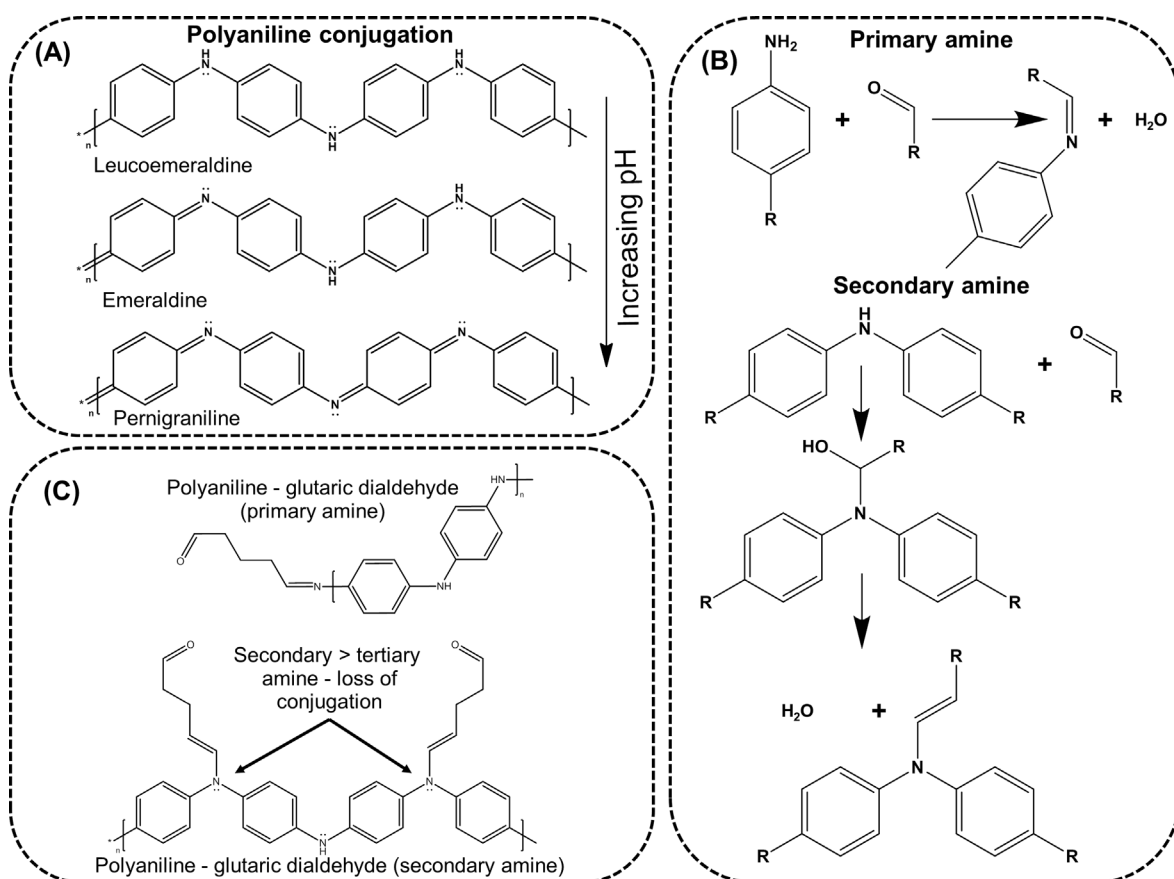
Figure 3.4: Scheme (A), representation of the pH dependant changes in the conjugation system of PANI. Scheme (B), reactions of the primary and secondary amines of PANI with GDA (March, 1977). Scheme (C), outcome of the reactions in scheme (B) highlighting loss of conjugation for secondary amines in PANI after treatment with GDA.

PANI deposited on the surface was modified with GDA and the reaction was believed to occur *via* a nucleophilic addition and elimination mechanism (March, 1977). This involved covalent linking to secondary and primary amines of the PANI film, forming imines and enamines *via* a Schiff base or hemiaminal intermediate while providing a free formyl group

for the attachment of a silica forming biomolecule, fig. 3.4B (Gebert *et al.*, 1989; March, 1977). Changes in UV-Vis absorption maxima under acidic and basic conditions demonstrated that GDA was incorporated into PANI *via* secondary amines in addition to primary amines due to disruption the conjugation system of the polymer (fig. 3.3A*).

Silica films were formed through a bio-inspired route using the protein lysozyme, a ~14.7 kDa enzyme involved in the breakdown of peptidoglycans of the cell walls of gram positive bacteria as a host defence mechanism against bacterium like *Streptococcus* (Karas & Hillenkamp, 1988). Lysozyme is almost ideal for silica formation because of its high reported pI of 11.16 which renders the protein positively charged under most conditions and provides functionality in a manner similar to other silica forming biomolecules like polyamines, silaffins and silicateins (Kuehner *et al.*, 1999). Though in considerable excess as compared to what would be expected on the surface due to instrumental sensitivity limitations, dynamic light scattering (DLS) and *zeta* potential measurements of the protein in the hydrolysis and buffer solutions (25 mg/mL) confirmed the presence of the dispersed protein (and aggregates) with an average size of 4.2 ± 0.05 nm and *zeta* potential of 10 ± 0.8 mV, (appendix A fig. A1 and table A1) as expected from literature values (Czeslik & Winter, 2001; Rabiller-Baudry *et al.*, 2000). Adsorption data for LYZ to PS-PANI and PS-PANI-GDA indicated that GDA treatment increased LYZ adsorption by a factor of 2.5 to ~1.57 ± 0.06 μg/cm^2. The surface was saturated after a period of 1 h, fig. 3.5A. The adsorption of the protein was considered uniform though some aggregate structures were detected on the surface of PS-PANI and PS-PANI-GDA surfaces after LYZ exposure, fig. 3.5B, C.
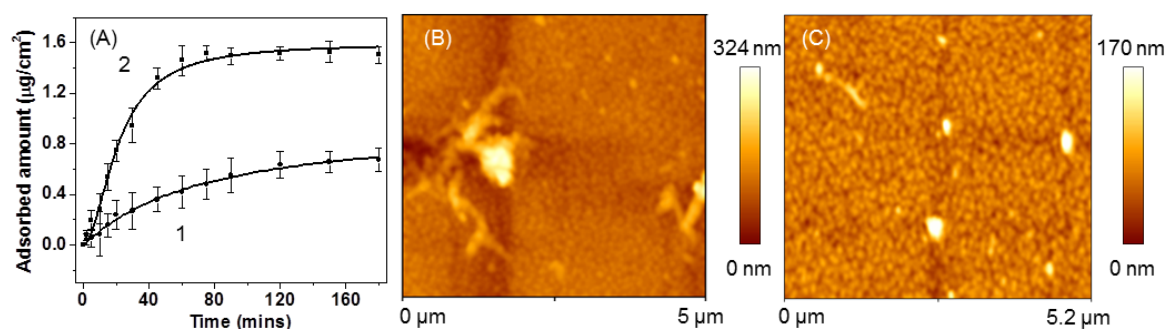
Figure 3.5: Isotherms demonstrating the differential adsorption of LYZ to PANI (A1) and PANI-GDA (A2) surfaces. AFM scans of PANI (B) and PANI-GDA (C) after LYZ adsorption.

FTIR-ATR spectra taken at each stage of the surface treatment process were able to identify the different chemical modifications present on the surface, fig. 3.6. Absorbance peaks characteristic of PS were detected at ~2800-3000 cm^{-1} corresponding to $v_{as}CH_2$ and v_sCH_2 of the polymer backbone and vCH of the aromatic rings, at ~1400-2000 cm^{-1} corresponding to the vCC bonds of the aromatic rings and alkane backbone (Silverstein & Webster, 1998). After treatment with PANI broad peaks ~2000-3600 cm^{-1} and peak broadening ~1600 cm^{-1} representing the introduction of primary and secondary aromatic NH bonds and salts were detected which was supported with the appearance of a peak ~1250 cm^{-1} representing vCN for primary and secondary aromatic amines (Silverstein & Webster, 1998). After treatment with GDA this peak was reinforced at wavenumbers above 3000 cm^{-1} suggesting formation of tertiary aromatic amines, free aldehyde groups with enhanced peaks at 2720 cm^{-1} and 1740 cm^{-1} also suggesting the presence of aldehyde functionality (Silverstein & Webster, 1998). Further growth of signals in the amide I region around 1650 cm^{-1} and other amine regions suggested incorporation of protein (Silverstein & Webster, 1998).
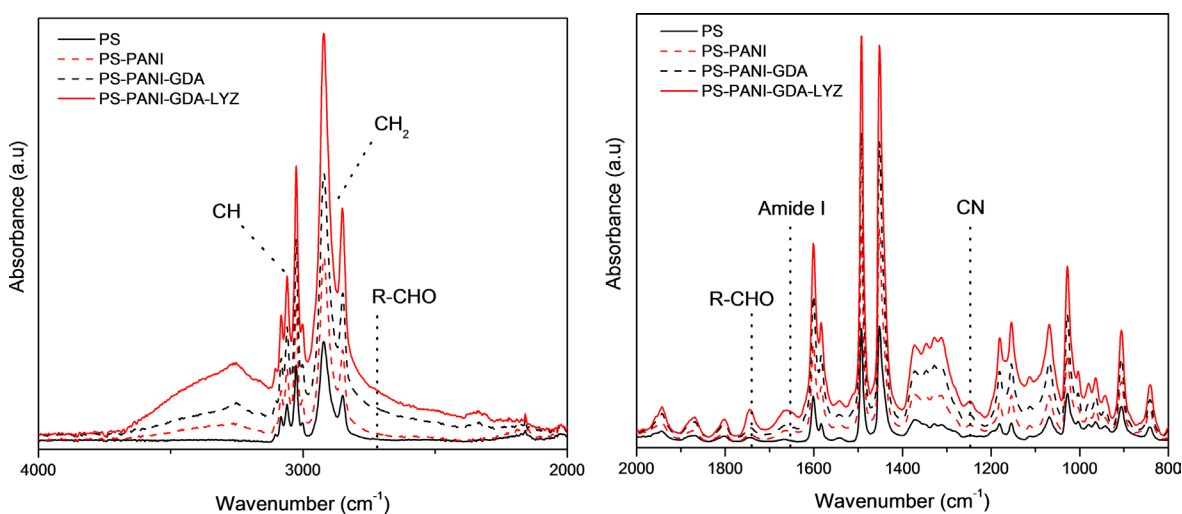
Figure 3.6: Representative FTIR-ATR spectra of PS, PS-PANI, PS-PANI-GDA, PS-PANI-GDA-LYZ films.

The silica condensation system was 0.5 M pre-hydrolysed (1 mM HCl) TMOS which is converted to an active form through acid hydrolysis of the methoxy groups to render methanol and silicic acid which provides free silanols for condensation to silica (fig. 1.1A) (Rai & Perry, 2009; Rai & Perry, 2010). That silica formed on the surface was demonstrated using EDXa in addition to SEM (fig. 3.7), AFM (fig. 3.8, fig. 3.11, and fig.

3.12), ATR-FTIR (fig. 3.9) and the molybdenum blue assay, which indicated 2.45 ± 0.70 mM or 0.04 mg cm^2.
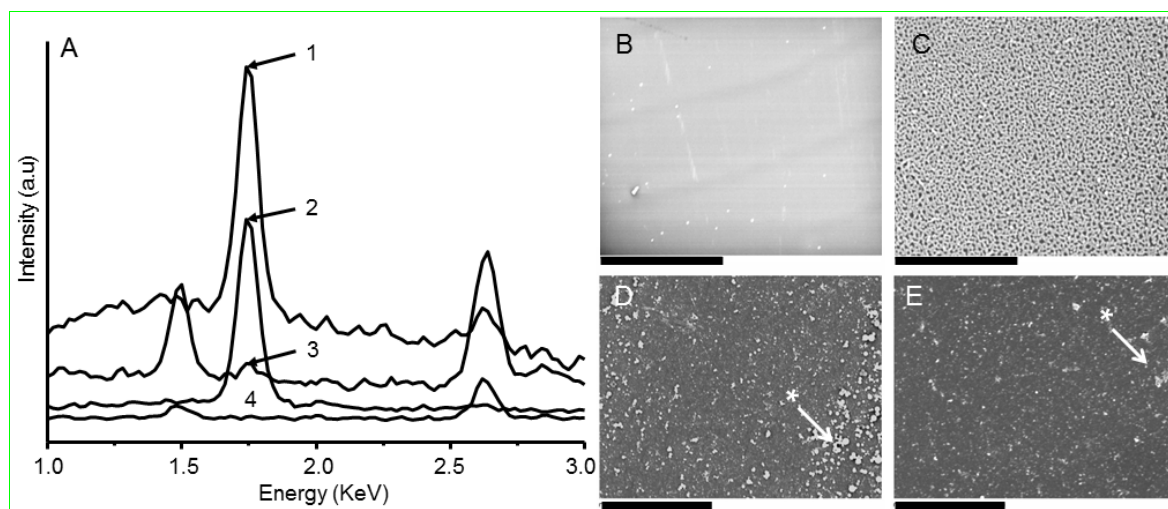
Figure 3.7: Representative EDXa spectra (A) of PS-PANI-GDA-LYZ-SiH (1), PS-PANI-GDA-LYZ-SiG (2), PS-PANI (3) and PS-PANI-GDA-Si (4) surfaces. SEM micrographs of PS (B), PS-PANI (C), SiH (D) and SiG (E) are represented with the scale representing 50, 5, 30 and 30 μm respectively. Surface features formed after silica deposition are highlighted (*) in SEM micrographs D, E.

EDXa demonstrates a silicon specific Kα X-ray emission peak at 1.74 KeV for PS-PANI-GDA-LYZ-SiH and SiG films after treatment with hydrolysed TMOS; the peak was not present for the original PS-PANI or PS-PANI-GDA surface after treatment with hydrolysed TMOS. This highlights the importance of the lysozyme in the formation of the silica film. The SiG and SiH terminology relates to the different drying controls used to prevent film cracking, a significant problem for sol-gel derived films, SiG incorporates 5% glycerol as a drying control chemical additive (appendix A, fig. A2) (Rao & Rao, 2002). SiH incorporates no additive but used an extended 48 h drying period; neither SiH nor SiG demonstrated significant surface defects, fig. 3.7D, E due to uncontrolled drying effects. SEM micrographs show changes in the morphology of the surface as major layers are deposited. The TMOS treated surfaces were covered in a range of differently sized and interconnected particle structures not seen for previous layers, fig. 3.7C, D*, E*.

Analysis of the distribution in size of these structures was conducted by AFM (fig. 3.8) in addition to being a complimentary imaging technique, AFM also allowed qualitative information on film roughness to be gathered, table 3.1.
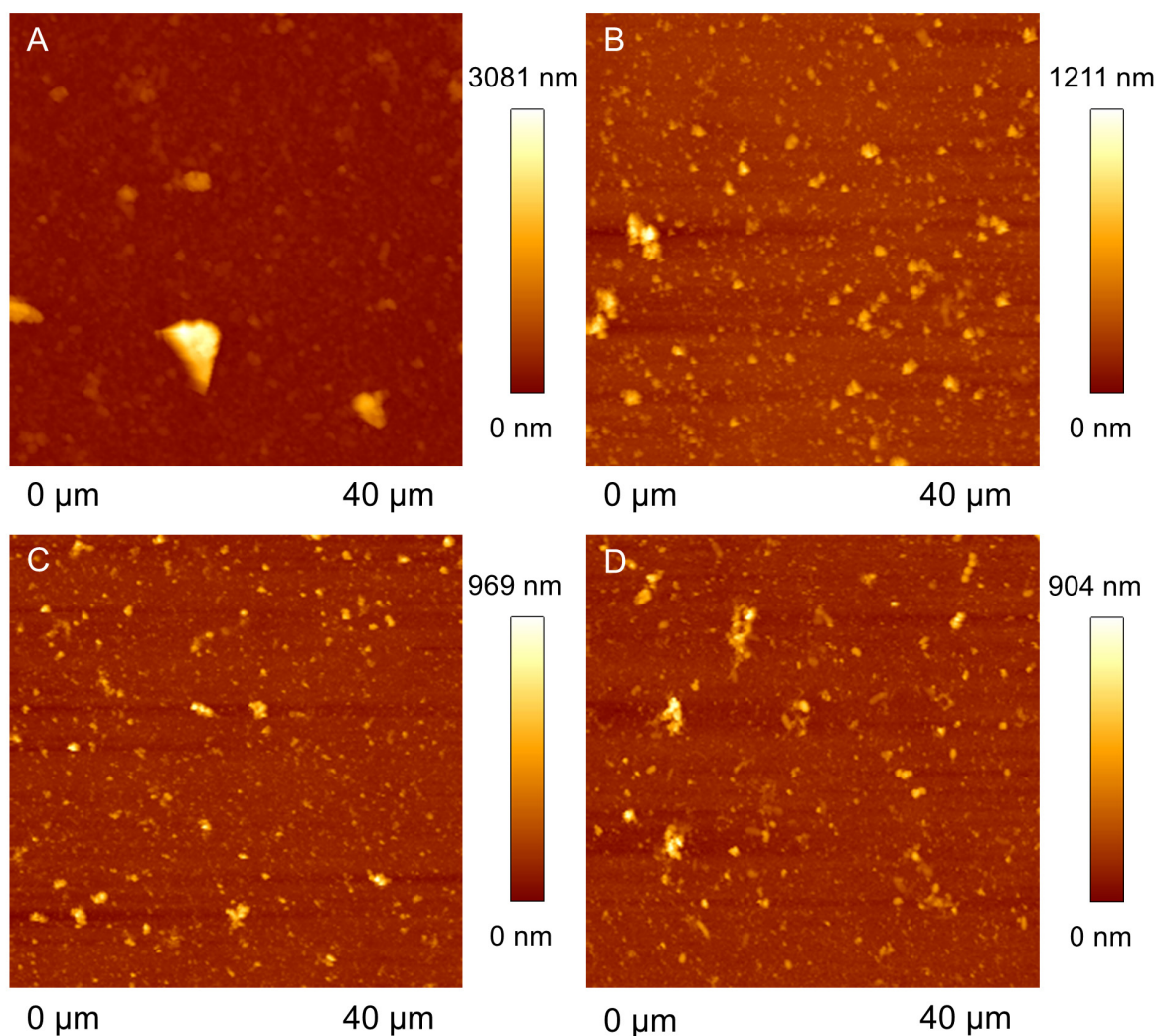
Figure 3.8: Representative AFM topological scans of PS-PANI-GDA-LYZ-SiH (A) and SiG (B) films. These films are also represented after treatment with FCS, (C) and (D) respectively.

Table 3.1: AFM analysis of SiH & SiG surfaces

Surface	SiH	SiG
Particle size (µm)	1.442 ± 0.109	1.054 ± 0.057
Particle frequency (particles/nm^2)	~1.5	~1.2
RMD roughness (nm)	75.17 ± 1.6	61.1 ± 3.3

The structures on the SiH surface were found to be significantly ($p < 0.05$, $n = 140$) larger than those on the SiG surface. After exposure to hydrolysed TMOS the increase in absorbance at ~1075 cm^{-1} provided evidence for the formation of siloxane bonds formed as a result of the formation of silica from silicic acid, fig. 3.9. This characteristic absorbance

was not found for the untreated PS-PANI-GDA-LYZ surface (Silverstein & Webster, 1998), fig. 3.9.
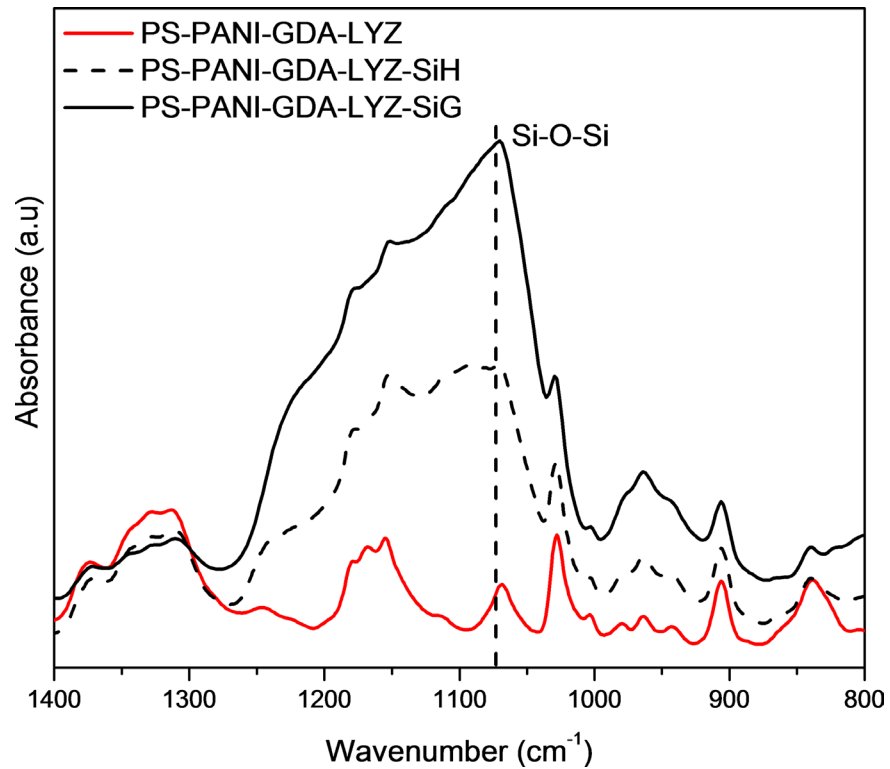
Figure 3.9: Representative FTIR-ATR spectra of PS-PANI-GDA-LYZ, PS-PANI-GDA-LYZ-SiH and SiG films; peaks noted demonstrate evidence of silica deposition.

The properties of the silica layer, such as root mean square (RMS) roughness and thickness by AFM and wetting properties by contact angle measurement were assessed; this data being compared to the underlying layers at each stage, fig. 3.10.
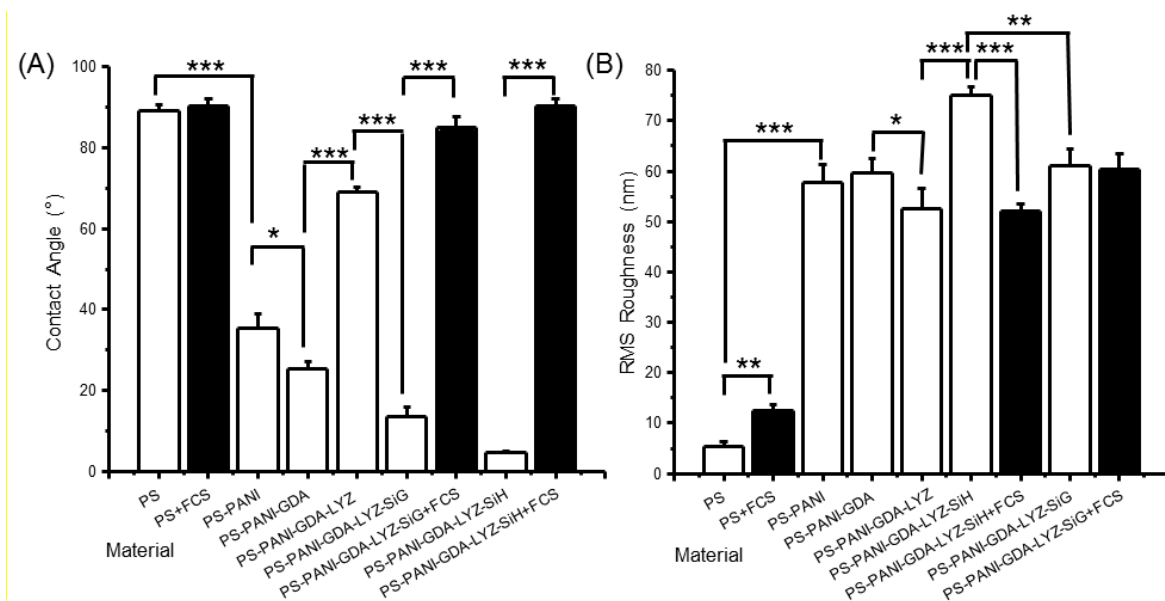
Figure 3.10: Contact angle (A) and root mean square (RMS) roughness (B) measurements after different stages of films fabrication and select materials after treatment with foetal calf serum (FCS) under culture conditions (n = 9).

The addition of PANI to the PS surface was seen to reduce the contact angle compared to the PS surface due to the increased potential for hydrogen bonding between water and the primary and secondary amines of the polymer chains; roughness being increased due to polymer aggregation on the moulded PS surface. GDA treatment continues the above wetting trend due to introduction of carbonyl groups and the addition of another layer of material, however the trend for surface roughness was not deemed significant due to the small size of the shift. Lysozyme treatment resulted in an intermediate hydrophobic contact angle as like many globular proteins it contains both hydrophilic and hydrophobic regions accessible to solvent (grade average of hydropathicity: -0.150, ProtParam ExPASy, Uniprot sequence P00698), unexpectedly roughness decreased suggesting the protein acts as a molecular 'filler' across the topology of the surface, a phenomena observed by others (Scopelliti *et al.*, 2010). Finally silica deposition resulted in a significant increase in roughness as silica structures form across the surface and a significant decrease in contact angle due to the abundance of silanol groups on the surface, which are readily amenable to hydrogen bonding. In the case of the SiH film this decrease was to the point of super-hydrophilicity, the surface exhibiting an average water contact angle of <5°. AFM measurements were also used to estimate the thickness of a deposited layer, through a

scratch test. After each successive layer the height of the film on the surface was measured after inducing a scratch through all the layers, fig. 3.12.

Table 3.2: Film thickness at each stage of fabrication.	
Material	Thickness (nm)
PS-PANI	119.5 ± 4.4
PS-PANI-GDA	114.4 ± 3.8
PS-PANI-GDA-LYZ	138.3 ± 11.0
PS-PANI-GDA-LYZ-SiH	213.7 ± 20.4
PS-PANI-GDA-LYZ-SiG	192.9 ± 37.9
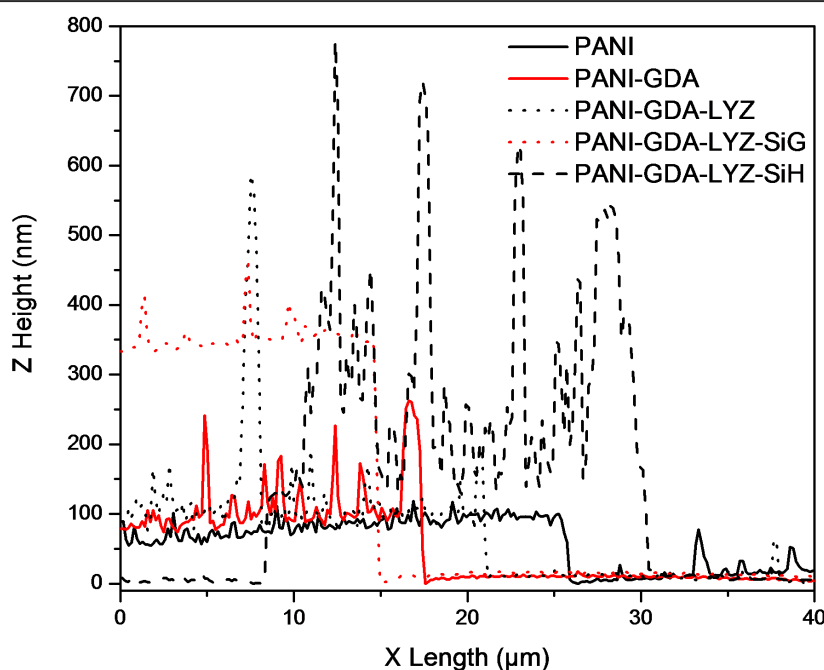
Figure 3.11: Representative thickness profiles obtained from AFM topological scans of induced scratches at different stages of surface fabrication. Table 3.2 provides quantification of the different thickness measurements (n = 6).

Surface thickness was shown to generally increase and become more variable with the sequential deposition of the different surface layers. However after the initial increase in thickness with the deposition in PANI, no significant increase in thickness was detected on addition of GDA, as with RMS measurement (fig. 3.10) this suggests no multilayer deposition of material occurs during GDA functionalisation of the polymer. A thickness increase was detected with the addition of LYZ, which considering the size of LYZ to be 45x35x35 Å suggests a multilayer on the surface (Czeslik & Winter, 2001), this would

correlate with the adsorbed amount of LYZ assayed (fig. 3.5A). The largest contribution in film thickness after PANI comes from the deposition of silica on the surface.

The materials fabricated here are considerably more hydrophilic than those presented previously (Rai & Perry, 2009; Rai & Perry, 2010; Rai & Perry, 2012). This surface property likely arises due to the presence of both an appropriate surface chemistry for a hydrophilic surface in addition to the higher surface roughness exhibited by these surfaces in comparison to those achieved on the smoother Au treated glass slides using thiol and disulphide linkers (Bico *et al.*, 2002). It should also be noted that the measurement's for surface wetting for the SiH surface presented above were taken after two months of storage, demonstrating that the surface properties achieved are sustained over time.

3.3.2 Proliferative and cytotoxicity response of melanoma to silica surfaces

Several methods were used to assess cell response to hydrophilic (SiG) and super-hydrophilic (SiH) silica functionalised PS in the context of the adherent human melanoma cell line FM3. Experiments were performed in the presence and absence of foetal calf serum (FCS). The response of 250,000 cells (determined by haemocytometer on day zero) in response to different culture surfaces was assessed. From previous studies and the known properties of these surfaces a negative influence on cells in comparison to the TCPS control was expected (Zolkov *et al.*, 2007; Saltzman & Kyriakides, 2007).

A day after plating, cells on all surfaces exhibited the morphological changes characteristic of the spreading seen after cell adhesion; cells were not inhibited from attachment to the silica surfaces. Over the next three to four days the cells were monitored as they progressed to confluence, fig. 3.14. Contrary to expectation, the hydrophilic and super-hydrophilic nature of the silica surfaces did not appear to prevent cell growth or promote increased cell death. These observations were supported by an analysis of the cell numbers observed over time in addition to the monitoring of cell proliferation by ATP assay and cell death through an adenylate kinase release assay, fig. 3.15.
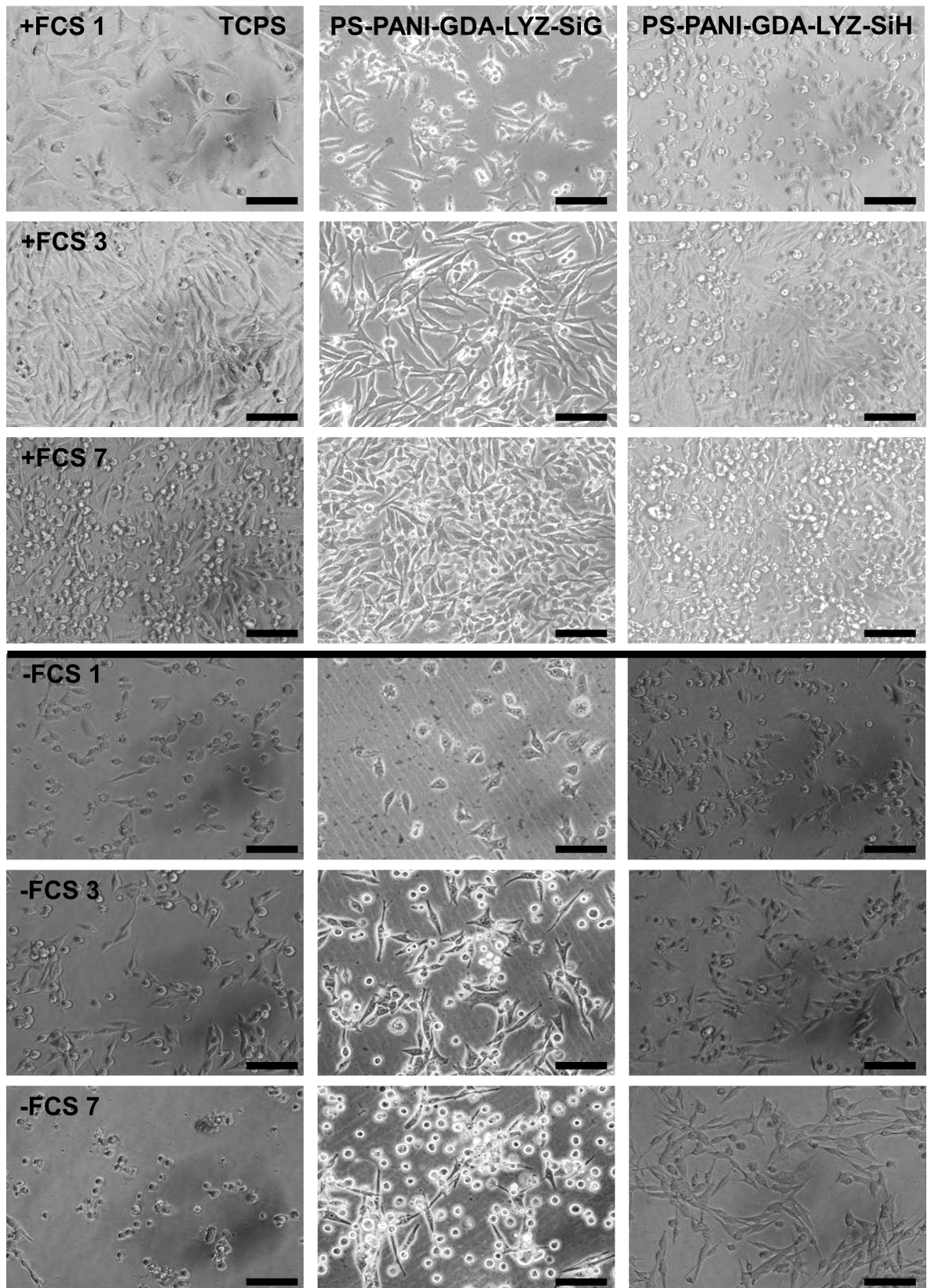
Figure 3.12: Representative light micrographs taken of FM3 cells cultured on TCPS, SiH and SiG surfaces in the presence and absence of FCS over a seven day period. Scale bar represents 100 µm.

Over the seven days of the experiment, cells grown in the presence of FCS progressed to confluence by day four, after which the rate of growth significantly slowed (though considering a duplication rate of 26.4 h the rate would have slowed after the second day), with a significant change in cell numbers over time ($F_{(1,819)}$ 85.98, $P < 0.001$, R^2 0.05) (fig. 3.9 A, D). No significant difference was determined between TCPS and either of the silica surfaces. Cells grown without FCS (though not serum starved) over this period also showed no significant difference in cell proliferation between surfaces, with population growth static over the seven days and no significant increase in cell numbers. This result was expected as without FCS to supply the necessary growth factors required, cells are generally believed to arrest in the G1 or G0 phase of the cell cycle (Cooper, 2003).

Cellular ATP showed a significant ($F_{(1,388)}$ 41.8, $P < 0.001$, R^2 0.09) difference over time between cells grown with FCS (fig. 3.9 C, F) and those without FCS, again suggestive of a static population. A significant difference between the silica surfaces and TCPS was detected for both SiH ($F_{(1,116)}$ 119.2, P 0.044, R^2 0.40) and SiG surfaces ($F_{(1,128)}$ 52.8, P 0.012, R^2 0.26), though no significant difference was determined between the two silica surfaces themselves. This data suggests that although both silica surfaces permit cell growth, a higher rate of growth was observed on TCPS over this period. The discrepancy between the two proliferation assays can perhaps be explained by the higher sensitivity of the biochemical assay technique in assessing large cell populations, as compared to a microscopy based method.
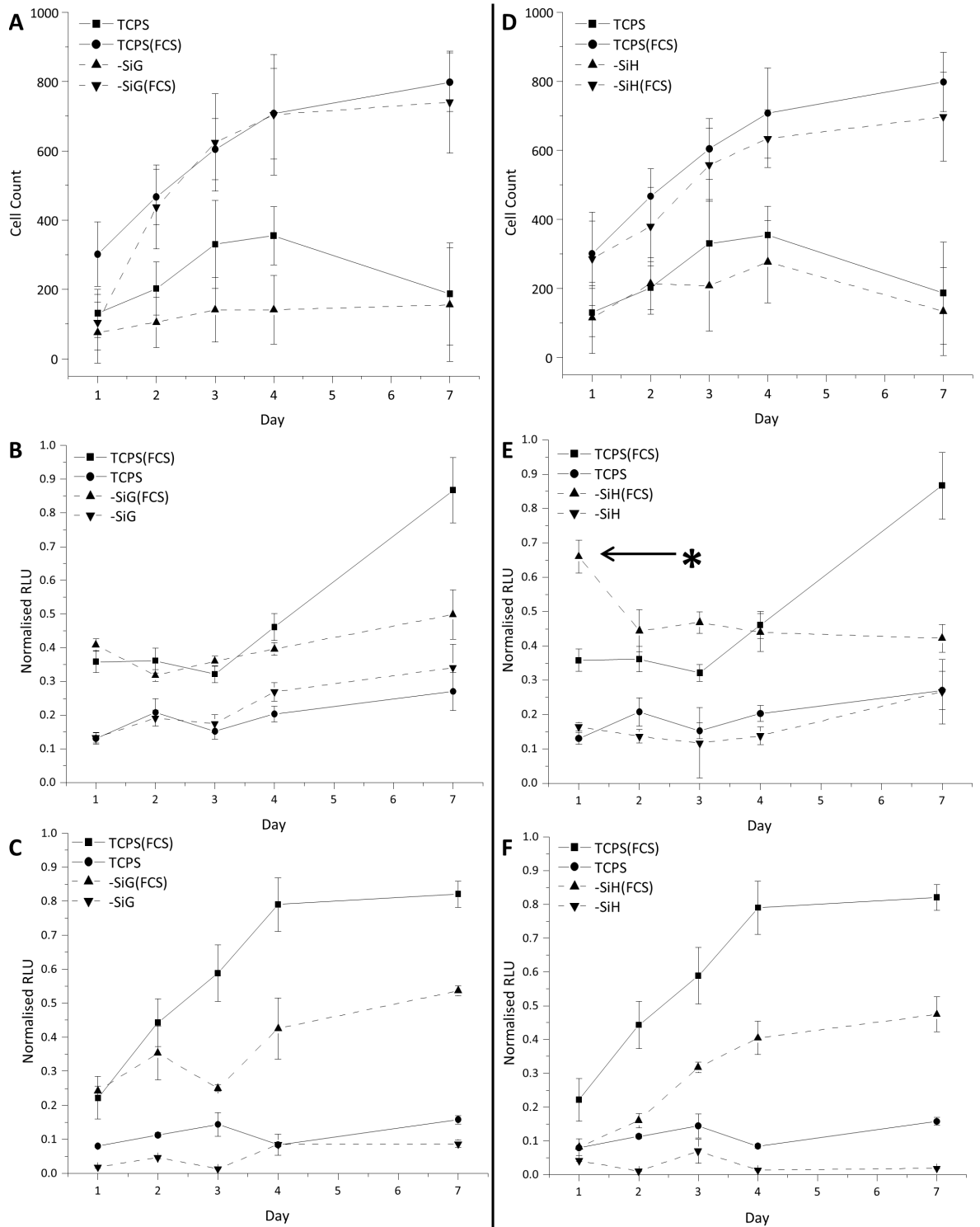
Figure 3.13: FM3 cell response to hydrophilic (SiG) (A, C, E) and super-hydrophilic (SiH) (B, D, F) silica functionalised PS in terms of proliferation (A, B), adenylate kinase release (B, E) and cellular ATP (C, F). Data highlighted (*) in E, shows higher initial cell death for SiH surface with FCS.

Adenylate kinase assays showed a significantly higher level of adenylate kinase release for cells grown with FCS than those without, (fig. 3.9 B, E) likely due to the higher level of cell turnover in these cultures ($F_{(1,738)}$ 326.7, $P < 0.001$, R^2 0.44). There was a significant difference in cell death between TCPS and SiG ($F_{(1,128)}$ 15.3, $P < 0.001$, R^2 0.08) and SiH ($F_{(1,131)}$ 41.3, $P < 0.001$, R^2 0.21) surfaces with FCS. There was no significant difference in cell death over time between polystyrene or silica cultures without FCS. For the TCPS surfaces with FCS, a significantly higher rate of cell death was observed over time, indicative of a higher turnover of cells on this surface though the potential difference in cell numbers towards the end of the assay as determined by the ATP assay may also explain this trend.

While most assay responses were found to follow a similar trend with time, an anomaly was noted for the adenylate kinase assay for the SiH surface with FCS (fig. 3.9E*). The initially higher level of cell death noted indicates an initially higher rate of cell death on the first day which drops back into agreement with the TCPS control by day two. This indicates that at least initially the SiH surface presented a more toxic surface to the culture; this could potentially be explained by a delay in a biological process such as adaptation of the cell to the culture conditions or delay in sufficient adsorption of proteins to the surface to occur inhibiting cell attachment and survival.

In addition to proliferation, adhesion is an important characteristic of a cells interaction with the surface. Cell adhesion was assessed by a modified centrifugal adhesion assay (fig. 3.10A) (Reyes & Garcia, 2003). After a 24 h culture period SiH and SiG silica, in comparison with TCPS were examined.
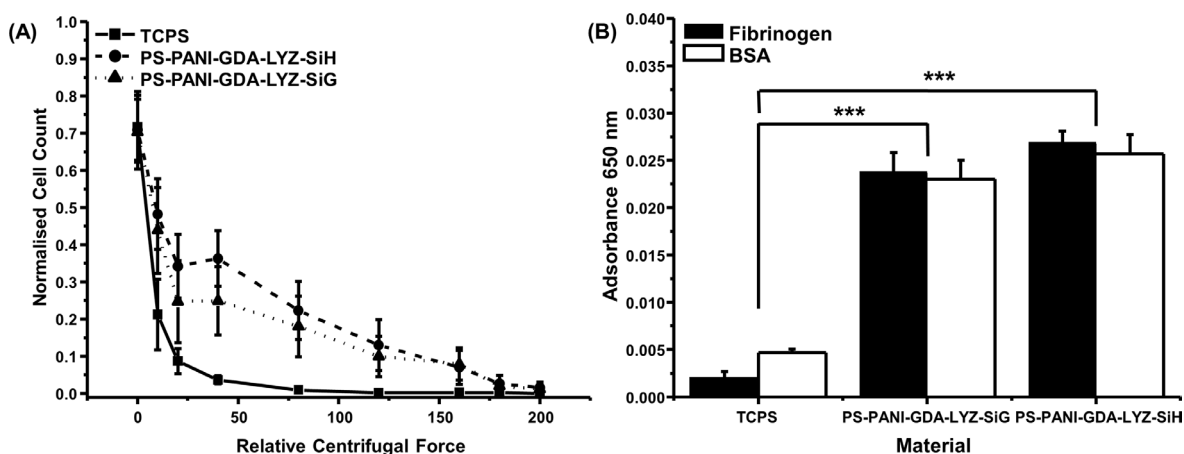
Figure 3.14: Cell adhesion (A) as measured by centrifugal adhesion assay (n = 9) and measured adsorption of fibrinogen and BSA (B) to the same surfaces by the Amido-black assay (n = 9).

Cells cultured on the different surfaces exhibited significantly different adherence responses, fig. 3.16A. FM3 cells showed significantly enhanced adhesion for SiH ($F_{(1,277)}$ 88.14, $P < 0.001$, R^2 0.32) and SiG ($F_{(1,247)}$ 103.5, $P < 0.001$, R^2 0.41) surfaces in comparison to TCPS, though no difference was detected between the silica surfaces. Cells resisted centrifugal forces two to three times higher on SiH and SiG surfaces than polystyrene before 50% detachment and increased the RCF at which the population could adhere to 160 RCF. The SiH and SiG surfaces were also shown by the Amido-black assay to significantly enhance the uptake of protein from the media, in this case fibrinogen (Fb) and bovine serum albumin (BSA) in comparison to TCPS, fig. 3.16B.

The stability of the surfaces was a consideration as silica leaching into the media could potentially influence cell response. Inductively coupled plasma-optical emission spectroscopy (ICP-OES) was performed on media after seven days of surface exposure under culture conditions. The amount of leached silica was determined to be 0.096 ± 0.020 mg L^{-1}, 0.026 ± 0.021 mg L^{-1} and less than 0.01 mg L^{-1} respectively for the SiH, SiG and TCPS surfaces. All samples demonstrated considerably lower silicon content than most tap waters at ~10 to 20 ppm, suggesting the surfaces are stable under the culture conditions and exposure time used and that the concentration of soluble silicon species was unlikely to be a major factor in the cell response observed over the culture period used (McNaughton *et al*., 2005).

In summary the hydrophilic and super-hydrophilic silica surfaces were shown to permit the adhesion and proliferation of cells in a comparable manner to a traditional cell proliferation surface. Additionally the surfaces demonstrated enhancement of some cell response characteristics such as cell and protein adhesion. The protein adsorption data provides a potential mechanism for this biocompatibility; enhancing adsorption of protein to the silica surfaces. Both topology and functionality are known to influence protein adsorption, itself a prerequisite for cell adhesion and proliferation (Jeong *et al*., 2000; Roach *et al*., 2006; Roach *et al*., 2007). It is hypothesised that rather than a direct influence on cell adhesion, the silica surfaces provide an appropriate surface topology and surface chemistry to facilitate the adhesion and proliferation of cells in the presence of FCS through the enhanced adsorption of extracellular matrix and adhesion proteins from the media to the surface (Ingber, 2005; Huang & Ingber, 1999). This in turn enhances adhesion and facilitates proliferation; the lag in required protein adsorption may explain the initial cell toxicity for the SiH surface. Contact angle measurements of silica films after exposure to serum support this with the measured contact angle increasing to a value comparable to

untreated PS while surface roughness decreased (fig. 3.7A, B). Though the influence of UV sterilisation was not considered the alteration of the contact angle and topology of the culture surface through the physical adsorption of proteins at the surface is likely what renders the surfaces comparable and compatible for cell culture.

The results are in general agreement with established thought in that intermediate surface wetting angles favour cell culture (Zolkov *et al.*, 2007; Saltzman & Kyriakides, 2007). What has been established is that the boundary of initial surface wettability of a surface for the successful adhesion and proliferation of cells in serum can be as low as 5° without compromising the ability of cells to proliferate, at least for the adherent melanoma cell line FM3 in the presence of serum. The incorporation of a normal human cell line into the study would have improved the relevance of these conclusions to fields such as biomaterials design but are outside the scope of the cancer sub-population centred aims of the study. However, this work challenges the idea that the surface must conform to a specific initial characteristic if it is to perform as a culture surface (at least for global adhesion and proliferation) when a form of post-fabrication modification, like serum, is used in culture. However, a detailed understanding at the molecular level of how silica surfaces exert effects on cell adhesion and proliferation in combination with adsorbed serum proteins is missing.

3.4 Conclusions

Investigations into cell-surface interactions with the aim of developing selective culture surfaces would require a library of well-defined materials of varying chemical and physical properties to be generated. This work demonstrated the adaptation of an existing methodology for the fabrication of silica films to polystyrene using a PANI and GDA linker as a means of generating these surfaces. The films, as with those fabricated previously, were demonstrated to have the potential for exhibiting a variety of wetting properties depending on the fabrication method, in this case incorporation of a small organic molecule into the condensation system.

The surfaces were demonstrated to be applicable to tissue culture with UV treatment and could be scaled down without significantly altering surface properties. Preliminary tissue culture compatibility studies using the adherent human melanoma cell line FM3 demonstrated that cells could adhere and proliferate on the silica surfaces in a comparable fashion to tissue culture polystyrene. Considering the extremely hydrophilic nature of the

surfaces this response was somewhat controversial. However a mechanism for understanding why the surfaces were able to perform in the manner observed may come from the significant increase in protein uptake, the surface chemistry being remodelled in the culture environment to a more cell compatible chemistry, highlighting the importance of the protein aspect of cell-surface interactions.

The method demonstrated provides a basis for the establishment of a library of materials from which to assess surface-protein-cell interactions and determine properties which could be useful to the development of a selective surface, as the next chapter looking at the development of this library and the associated cell responses addresses.

3.5 References

1. Bico J, Thiele U & Quere D. (2002). Wetting of textured surfaces. *Colloids Surf., A*, 206(1-3):41-6

2. Cooper S. (2003). Reappraisal of serum starvation, the restriction point, G0, and G1 phase arrest points. *FASEB J.*, 17(3):333-340

3. Czeslik C & Winter R. (2001). Effect of temperature on the conformation of lysozyme adsorbed to silica particles. *Phys. Chem. Chem. Phys.*, 2001(3):235-239

4. Gebert P.H, Batich C.D, Tanner D.B & Herr S.L.(1989). Polyaniline *via* Schiff Base Chemistry. *Synth. Met.*, 29:E371-E376

5. Huang S & Ingber D.E. (1999). The structural and mechanical complexity of cell-growth control. *Nat. Cell Biol.*, 1:E131-8

6. Huebsch N. & Mooney D.J. (2009). Inspiration and application in the evolution of biomaterials. *Nature*, 462(7272):426-432

7. Ingber D.E. (2005). Mechanical control of tissue growth: function follows form. *Proc. Natl. Acad. Sci. U. S. A.*, 102(33):11571-2

8. Jang J, Ha J & Lim B. (2006). Synthesis and characterization of monodisperse silica–polyaniline core–shell nanoparticles. *Chem. Commun.*, 2006(15):1622-1624

9. Jeong J.H, Lim D.W, Han D.K & Park T.G. (2000). Synthesis, characterization and protein adsorption behaviours of PLGA/PEG di-block co-polymer blend films. *Colloids Surf., B*, 18(3-4):371-9

10. Karir T, Hassan P.A, Kulshreshtha S.K, Samuel G, Sivaprasad N & Meera V. (2006). Surface Modification of Polystyrene Using Polyaniline Nanostructures for Biomolecule Adhesion in Radioimmunoassays. *Anal. Chem.*, 78(11):3577-3582

11. Karas M & Hillenkamp F. (1988). Laser Desorption Ionization of Proteins with Molecular Masses Exceeding 10 000 Daltons. *Anal. Chem.*, 60(20):2299-2301

12. Kuehner D.E, Engmann J, Fergg F, Wernick M, Blanch H.W & Prausnitz J.M. (1999). Lysozyme Net Charge and Ion Binding in Concentrated Aqueous Electrolyte Solutions. *J. Phys. Chem. B*, 103(8):1368-1374

13. March J. (1977). Advanced organic Chemistry: Reactions, Mechanisms, and Structure. McGraw-Hill Kogakusha, Japan, 2nd Ed., ISBN 0-07-040247-7

14. McNaughton S.A, Bolton-Smith C, Mishra G.D, Jugdaohsingh R, Powell J.J. (2005). Dietary silicon intake in post-menopausal women. *Br. J. Nutr.*, 94(5):813-7

15. Meyer-Plath A.A, Schröder K, Finke B & Ohl A. (2003). Current trends in biomaterial surface functionalization—nitrogen-containing plasma assisted processes with enhanced selectivity. *Vacuum*, 71(3):391-406

16. Rabiller-Baudry M, Chaufer B, Aimar P, Bariou B & Lucas D. (2000). Application of a convection–diffusion–electrophoretic migration model to ultrafiltration of lysozyme at different pH values and ionic strengths. *J. Membr. Sci.*, 179(1-2):163–174

17. Rai A & Perry C.C. (2009). Fabrication of Tuneable Thickness Silica Films on Solid Surfaces Using Amines and Proteins. *Silicon*, 1(2):91-101

18. Rai A & Perry C.C. (2010). Facile Fabrication of Uniform Silica Films with Tunable Physical Properties Using Silicatein Protein from Sponges. *Langmuir*, 26(6):4152-4159

19. Rai A & Perry C.C. (2012). Mussel adhesive protein inspired coatings: a versatile method to fabricate silica films on various surfaces. *J. Mater. Chem.*, 22(11):4790-4796

20. Rao A.P & Rao A.V. (2002). Study the influence of drying control chemical additives on the physical and optical properties of nanocrystalline cadmium sulphide-doped tetraethylorpthosilicate silica xerogels. *J. Mater. Synth. Process.*, 10(1):7-16

21. Reyes C.D. & García A.J. (2003). A centrifugation cell adhesion assay for high-throughput screening of biomaterial surfaces. *J. Biomed. Mater. Res., Part A*, 67A(1):328–333

22. Roach P, Eglin D, Rohde K & Perry C.C. (2007). Modern biomaterials: a review - bulk properties and implications of surface modifications. *J. Mater. Sci. Mater. Med.*, 18(7):1263-77

23. Roach P, Shortcliffe N.J, Farrar D & Perry C.C. (2006). Quantification of surface-bound proteins by fluorimetric assay: comparison with quartz crystal microbalance and Amido Black assay. *J. Phys. Chem. B*, 110(41):20572-20579

24. Roach P, Farrar D & Perry C.C. (2006). Surface Tailoring for Controlled Protein Adsorption: Effect of Topography at the Nanometer Scale and Chemistry. *J. Am. Chem. Soc.*. 128(12)3939–45

25. Saltzman W.M & Kyriakides T.R. (2007). Principles Tissue Engineering. Academic Press, 3rd Ed., p. 279 ISBN 978-0-12-370615-7

26. Scopelliti P.E, Borgonovo A, Indrieri M, Giorgetti L, Bongiorno G, Carbone R, Podesta A & Milani P. (2010). The Effect of Surface Nanometre-Scale Morphology on Protein Adsorption. *PLos One*, 5(7)e11862:1-9

27. Silverstein R.M & Webster F.X. (1998). Spectrometric Identification of Organic Compounds. John Wiley & Sons, Inc. United States of America, 6th Edition, ISBN 0-471-13457-0, p71-143

28. Zolkov C, Avnir D & Armon R. (2004). Tissue-derived cell growth on hybrid sol-gel films. *J. Mater. Chem.*, 14:2200-2205

Chapter Four

Response of Tumour Cell Lines to Silica Materials of Varying Chemical Properties

4.1 Introduction

The previous chapter established a system of chemistry by which a silica film could be fabricated on polystyrene; this was demonstrated to be capable of supporting the adhesion and proliferation of an adherent human melanoma cell line. To convert this into a tissue culture system capable of screening for selective properties, a range of surfaces with different chemistries needed to be developed and the biological response to these chemistries assessed. Once a variety of cell responses had been established, specific functionalities could be selected to trial potential selective effects.

There are many different surface properties considered important in biomaterial design. They include but are not limited to surface topology, functionality, porosity and mechanical properties (Huebsch & Mooney, 2009). In this study surface functionality was varied through the use of different alkylsilanes, since changing surface functionality of the base SiH surface demonstrated in the previous chapter would be the simplest method for the creation of a variety of distinct surfaces.

The cell line FM3, while included within this study as a reference to the previous work (chapter three), is not a suitable candidate for cell enrichment studies as it is not commonly associated with known cancer sub-populations. Cell lines introduced in this component of the study included P4E6 a prostate cancer cell line which has been reported to contain a population of stem like cells believed by the author of that study to be cancer stem cells (Maitland *et al.*, 2001). Also included is the cell line OPCT1, a purported prostatic adenocarcinoma cell line that has been used in the study of the epithelial-mesenchymal transition and contains cell sub-populations related to these phenotypes (Palazzolo, 2005; Dunning-Foreman, 2012). These cell lines were used as candidates for assessing cell response and the potential for cell sub-population enrichment and selection.

4.2 Materials & methods

4.2.1 Materials

Tissue culture polystyrene plates in 96, 24 and 6 well formats were obtained from Sarstedt (UK). Optilux™ 96-well black flat bottom imaging plates were obtained from BD (UK). Polyaniline hydrochloride, ammonium persulphate, glutaric dialdehyde, diiodomethane, formamide, glycerol, ethylene glycol, naphthol blue black, ethylenediaminetetraacetic acid (EDTA), lysozyme (LYZ), bovine serum albumin (BSA), fibrinogen (Fb), TWEEN® 20, sodium phosphate monobasic, sodium phosphate dibasic, Trizma® hydrochloride, paraformaldehyde, 3-amino-7-dimethylamino-2-methylphenazine hydrochloride (neutral red dye), mouse polyclonal anti-human fibronectin antiserum, mouse anti-human vinculin monoclonal (clone hVIN-1) from ascites fluid, phenyltriethoxysilane (PTEOS), 3-aminopropyltriethoxysilane (APTEOS) and tetramethoxysilane (TMOS) were obtained from Sigma-Aldrich® (UK). Methyltriethoxysilane (MTEOS) was obtained from Alfa Aesar (UK). Bovine foetal calf serum (FCS), plate sealing films, 1 M hydrochloric acid, sulphuric acid, sodium hydroxide, nitric acid, methanol, cover slips, glass slides (Menzel-Gläser) and glacial acetic acid were obtained from Thermo Fisher Scientific (USA). EtOH was supplied by Hayman Speciality Products (UK). Calbiochem® BSA fraction IV was supplied by EMD Millipore (USA). R&D Systems® (UK) supplied streptavidin conjugated horseradish peroxidase and the substrate reagent used for the ELISA. Goat anti-rabbit IgG conjugated to biotin was supplied by Dako (UK). Dulbecco's phosphate buffered saline (DPBS), RPMI-1640 medium, trypsin-versene (EDTA) solution, L-glutamine solution was obtained from Lonza BioWhittaker™ (UK). Keratinocyte serum free medium (KSFM) with L-glutamine and TrypLE™ Express were obtained from Gibco®, Life Technologies™ (UK). Rabbit polyclonal anti-human vimentin was supplied by abcam® (UK). Alexa Fluor® 568 conjugated phalloidin, Alexa Fluor® 488 conjugated goat anti-mouse IgG, Alexa Fluor® 488 conjugated goat anti-rabbit IgG, Alexa Fluor® 633 conjugated goat anti-mouse IgG, rabbit IgG isotype control and rabbit IgG isotype controls were supplied by Invitrogen®, Life Technologies™ (UK). VECTASHIELD® mounting medium with 4', 6-diamidino-2-phenylindole (DAPI) was obtained from Vector Laboratories (UK). The FM3 cell line was originally obtained from Prof. G. Pawelec, University of Tübingen, Germany. The OPCT1 cell line was originally obtained from Onyvax, UK. The P4E6 cell line was originally obtained from Prof. N.J Maitland, University of York, UK. Distilled and deionised water

(ddH$_2$O) was produced locally by distillation and ion exchange filtration, resulting in a pH of 5.8 and a conductivity of <1 µS/cm^{-1}.

4.2.2 Silica film functionalisation

Films (SiH) fabricated as per method 3.2.1 were functionalised with 0.5 M alkylsilane precursor solution containing one –R group substituted with either methyl, phenyl or 3-aminopropyl functionalities. The precursors were hydrolysed with 1 mM HCl for 15 min before being exposed to the surface for up to 18 h, methyl and phenyl substituted precursors incorporated 70% EtOH to prevent phase separation; 3-aminipropyl incorporated an equimolar concentration of HCl. After this period the solution was aspirated and the surface washed with an excess of ddH$_2$O with drying under ambient conditions.

4.2.3 Atomic force microscopy

Atomic force microscopy was performed as described in section 3.2.4.

4.2.4 X-ray photoelectron spectroscopy

X-Ray photoelectron spectroscopy spectra were obtained using a Surface Science M-probe XPS spectrometer with survey scans (1 eV step) and high resolution scans (0.065 eV step) of the Si2p, O1s, C1s and N1s regions taken for each sample. XPS sample analysis was kindly conducted by J. Slocik.

4.2.5 Contact angle & surface free energy measurement

Contact angle measurements were taken using a DSA 10 contact angle meter and analysed using the Drop Shape Analysis software (Krüss GmbH, Germany). A 5 µL drop of ddH$_2$O was dispensed onto the surface of the material. Contact angle measurements using three replicate drops across three replicate surfaces were made using 'tangent method 1'. Surface energy measurements were taken using an Attension Theta optical tensiometer (Biolinscientific, Sweden). A 5 µL drop of water, diiodomethane and formamide was applied to the surface and the static contact angle measured by the Young-Lapace method. After three replicate measurements across three replicate surfaces using all the liquids, surface energy was determined by the acid-base method in the surface free energy calculator of the OneAttension (v1.7) software (Biolinscientific, Sweden).

4.2.6 Amido-black protein adsorption assay

The protein adsorption assay was conducted as described in section 3.2.9.

4.2.7 Enzyme-linked immunosorbent assay

The indirect enzyme-linked immunosorbent assay (ELISA) was used to quantify fibronectin adsorption, using a polyclonal rabbit anti-fibronectin antiserum as a detection antibody, the surface acted as a capture antibody. After exposing surfaces to RPMI-1640 medium containing 10% FCS the surfaces were washed with 400 µL of wash buffer (0.05% TWEEN-20 in TBS [50 mM Tris-HCl, 150 mM NaCl], pH 7.4) and blotted dry. The surfaces were then incubated with 100 µL of 100 ng/mL (determined by titration) anti-fibronectin antiserum (TBS 2% BSA) for 2 h at room temperature. After washing and blotting, surfaces were incubated with 100 µL of 50 ng/mL (determined by titration) biotinylated polyclonal goat anti-rabbit IgG detection antiserum in TBS (2% BSA) for 2 h at room temperature before washing and blotting. Streptavidin-horse radish peroxidase (100 µL) at a dilution of 1:200 in TBS (2% BSA) was added to each well and incubated at room temperature for 20 min while protected from light. Substrate solution (100 µL) was added to each well and incubated at room temperature for 20-30 min while protected from light before 50 µL of stop solution (H_2SO_4) was added. Aliquots of 100 µL were transferred to a new 96 well plate and absorbance measured at 450 nm with a 570 nm reference filter.

4.2.8 Tissue culture of adherent human cell lines

FM3 culture conditions were RPMI-1640 growth medium supplemented with 1% L-glutamine and 10% FCS extract. Confluent cultures were passaged or introduced onto culture surfaces by removal of growth media, washing twice with DPBS and then 1x trypsin solution. After 5 min incubation, cells were aspirated and pelleted by centrifugation (3 min at 400 RCF), the trypsin solution was removed and the cells suspended in media. Cells (number determined by haemocytometer) were then introduced onto (ultra-violet (UV) sterilised for 15 min) culture surfaces or tissue culture flasks. OPCT1 culture conditions were KFSM medium supplemented with 1% L-glutamine and 2% bovine (FCS) extract. During passage, cells were treated with 1x TrypLE™ Express trypsin substitute but otherwise treated the same as FM3. P4E6 culture and passage conditions were identical to OPCT1.

4.2.9 Neutral red proliferation/viability assay

Cells were seeded onto a 96 well plate at a density of 5,000 cells per well as determined by haemocytometer and cultured over a period of 7 days. After the culture period cell number was assessed using the neutral red assay as described by Repetto *et al.*, 2008. The assay comprised nine replicate surfaces and was repeated across four passages.

4.2.10 Centrifugal cell adhesion assay

The cell adhesion assay was performed as described in section 3.2.15. To obtain additional information from the data series, data was fitted to a single phase decay curve, the various components (fig. 4.1) of which could be tested for significance with additional post-test analysis individually as opposed to simply determining if the fitted general linear regression line differed between treatments.
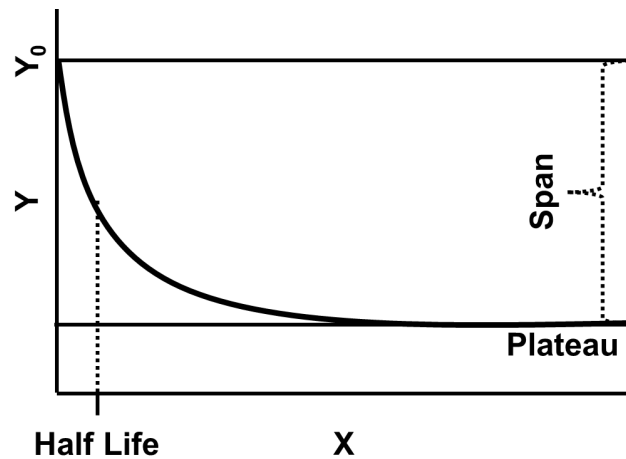
$$Y = \left(Y^0 - Plateau\right) * exp(-k * X) + Plateau$$

Figure 4.1: Single phase decay model fitted to cell adhesion data, figure shows the various attributes of the model in relation to Y (cell number) and X (applied centrifugal force, RCF) and the fitted equation.

4.2.11 Visualisation by immunofluorescence & confocal microscopy

Cells were cultured from an initial density of 5,000 cells per well on a florescence compatible 96 well plate for 2 days prior to fixing and staining. The fixing and staining procedure below states the protocol for a 24 well plate, for a 96 well plate volumes are reduced by a factor of six. Medium was aspirated and cells washed twice with PBS before fixing with 500 µL of 4% paraformaldehyde for 30 min. The fixative was aspirated and the cells washed twice with PBS before exposure to 500 µL blocking solution (10% BSA with

0.1% TWEEN-20 in PBS for cell permeabilisation) for 1 h with agitation. The blocking solution was aspirated and 200 µL of primary antibody diluted in blocking solution (table 4.1) was added and incubated for one h at RT. The primary antibody was aspirated and the cells washed with 0.1% TWEEN-20 in PBS for three 10 min washes. The secondary antibody diluted in blocking solution (table 4.1) was added at RT for a 1 h incubation before aspiration and three 10 min washes with 0.1% TWEEN-20 in PBS. Slips were then placed face down on a slide with one drop (5 µL) of vector shield (1 µL for plates with 50 µL 1:1 glycerol: ddH$_2$O to raise meniscus) and imaged using an SP5 confocal microscope (Leica, Germany).

Table 4.1: Antibodies and conditions for immunostaining

Antibody	Dilution
Mouse anti-human vinculin	1:1000
Goat anti-Mouse Alexa Flour® 488 secondary	1:1500

4.2.12 Cell light microscopy

Microscopy imaging was conducted using an Olympus BX51 microscope using 10x, 20x and 40x objectives and a DF71 camera controlled through CellF software (Olympus, Japan).

4.2.13 Imaging of live cells

Cells were seeded to surface modified BD Optilux™ 96-well flat bottom imaging plates, black with clear bottoms, at a density of 15,000 cells per well. Cells were imaged over a 12 h period with an interval of 5 min using an SP5 confocal microscope using differential interference contrast (DIC) and a HC PL FLUOTAR 20.x0.50 dry objective to image cell activity at 1024x1024 resolution (Leica, Germany). Focal plane and well location (central locations were selected) were set initially and the stage automatically driven during the experiment. During the assay period cells were maintained at 37°C using a temperature controlled chamber (life imaging services, Switzerland); CO$_2$ was maintained at ambient conditions.

4.2.14 Statistical testing

Statistical testing was conducted using the GraphPad Prism 6 (v.6.01) software package

(GraphPad Software, USA). Significant features in the material characterisation, proliferation, adhesion, cell motility and protein adsorption data was determined using either one or two way ANOVA with Tukey's multiple comparisons post-test. In all cases the assumptions of normality and constant variance were assessed. In the following work all error unless otherwise stated is presented as standard error of the mean. The following notation is used to denote significance; (*) P $\leq$0.05 significant, (**) P $\leq$0.01, (***) P $\leq$0.001 and (****) $\leq$0.0001.

4.3 Results & Discussion

4.3.1 Development & characterisation of silica films of varying functionality

Once silica is present on a surface, surface silanols may facilitate further condensation of hydrolysed silane precursors to the surface. If the precursor is varied from the original silicon alkoxide to an organosilicon alkylsilane compound, then functionality can be introduced to the silica polymer network through the condensation process. A wide range of different organosilanes are available through substitution of one or more Si-O bonds with a Si-R group. Silica films as produced in chapter three were treated for 18 h with methyl, phenyl or 3-aminopropyltriethoxysilane, the treatment time was extended as the substitution of Si-O to Si-R is known to slow the rate of condensation (Osterholtz & Pohl, 1992). The surface groups selected (methyl (SiH-M), phenyl (SiH-P), 3-aminopropyl (SiH-3AP)) were chosen due to their fundamental nature, divergent properties expected and occurrence in natural building blocks like amino acids, such that they are found on naturally occurring surfaces like cell membrane proteins. After condensation the surface topology and chemistry were assessed to determine the influence of alkylsilane incorporation on surface characteristics. Surface topology and film thickness were assessed by AFM, fig. 4.2, fig. 4.3 and table 4.2.
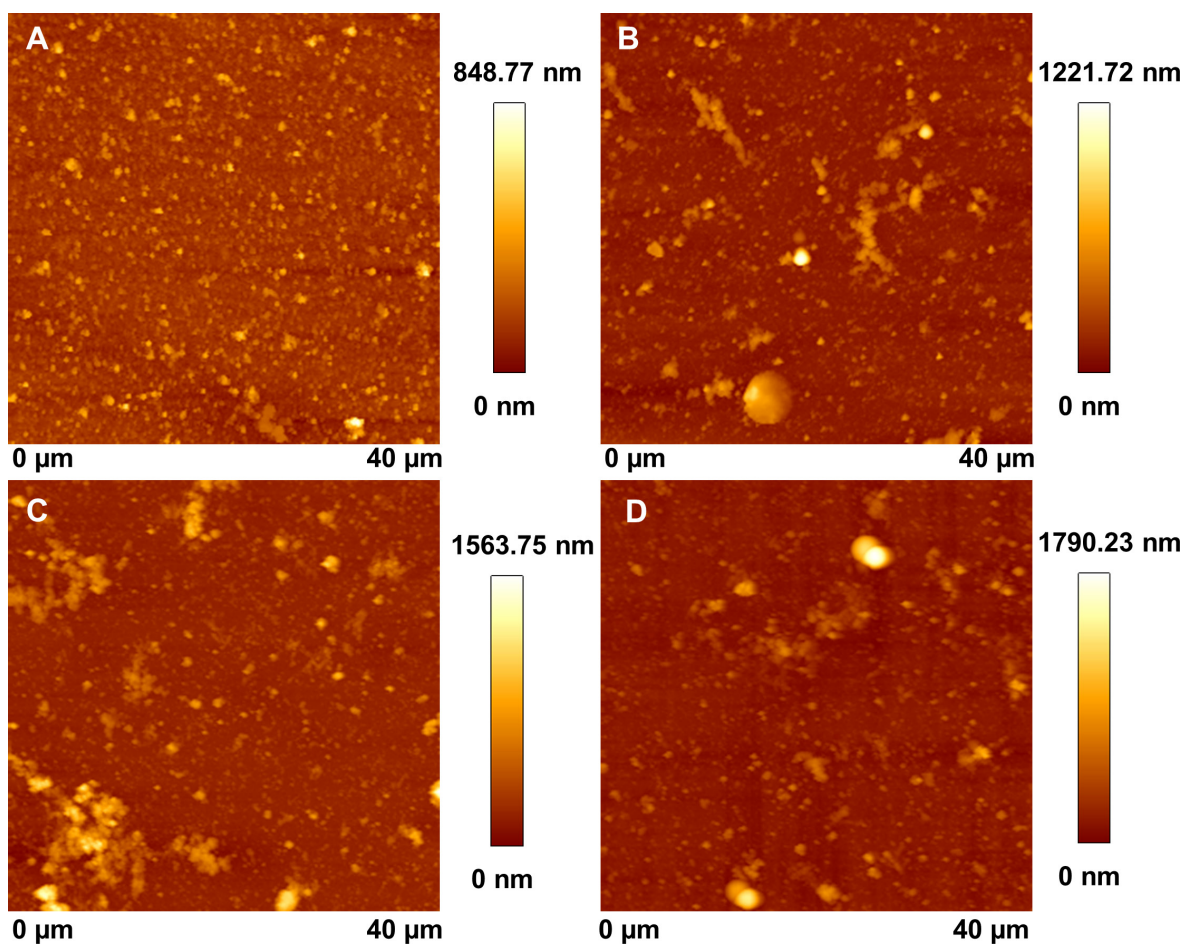
Figure 4.2: Representative AFM scans showing surface topology of unmodified SiH (A), SiH-Methyl (B), SiH-Phenyl (C) and SiH-3-aminopropyl (D) films (n = 9).

Post functionalisation it was shown that film roughness was largely uniform and no significant variation from the unmodified SiH surface was observed, fig. 4.2 and table 4.2. This would suggest that the alkylsilanes are incorporated on free silanol groups with the base surface as a template, with limited formation of new topological structures as a result of alkylsilane condensation.
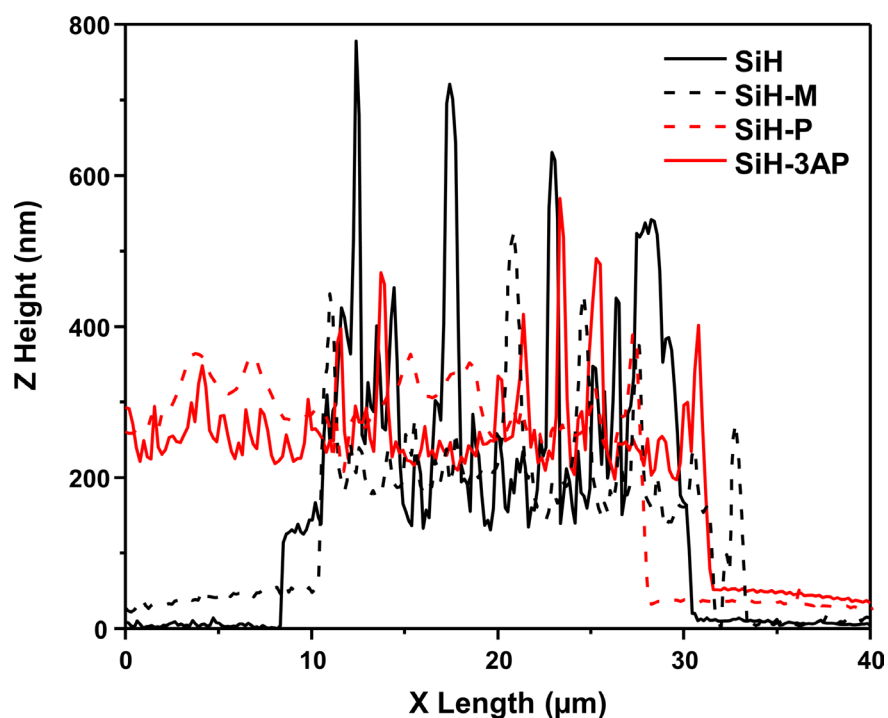
Figure 4.3: Representative cross sections through differently functionalised silica surfaces, produced from topological scans measured by AFM (n = 6). Cross sections illustrate measured film thickness between the surfaces.

Table 4.2: Roughness & thickness of functionalised silica surfaces

Material	RMS roughness (nm)	Thickness (nm)
PS-PANI-GDA-LYZ-SiH	75.17 ± 1.56	213.79 ± 20.45
PS-PANI-GDA-LYZ-SiH-M	76.84 ± 3.59	180.36 ± 9.63
PS-PANI-GDA-LYZ-SiH-P	78.98 ± 3.36	203.61 ± 15.51
PS-PANI-GDA-LYZ-SiH-3AP	71.62 ± 3.70	176.29 ± 7.98

As expected from the roughness data there was no major change in surface thickness for the modified films, fig. 4.3 and table 4.2. This suggests that the alkylsilanes are incorporated on free silanol groups, with the surface acting as a template. The ability to modify surface functionality without significantly altering surface topology is useful as only one variable (functionality) will be changing significantly during the biological studies.

Observations by EDXa were not attempted as the high surface penetration of this technique (1-2 μm) would limit the sensitivity to supposed small surface changes, additionally all elements which could be detected (C, N, O, Si) already exist. Attempts to characterise

surface functionality by ATR-FTIR were also unsuccessful, likely due to the combination of the small amount of functionalisation present and the ~0.5-2 μm depth penetration of the technique resulting in considerable background from the underlying and chemically diverse (through indistinct from the functionality incorporated) layers. Evidence for the functionality of the films was provided initially by measurement of the surface wettability by contact angle measurement, which as a true surface technique is not limited by spectral noise from underlying chemical layers, fig. 4.4 and table 4.3.
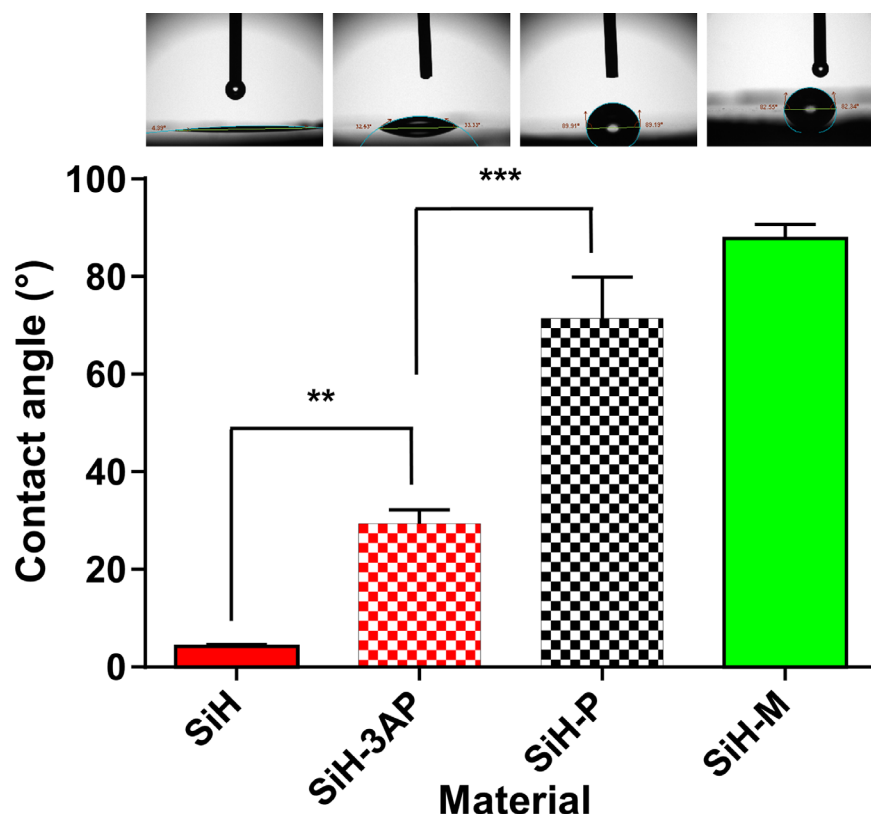
Figure 4.4: Average water contact angles of silica films after treatment with differently substituted alkylsilanes (n = 9). Representative images of the typical water contact angles obtained also are displayed.

As determined previously the base SiH surface was super-hydrophilic in character, upon treatment with different alkylsilanes this contact angle increased significantly from the base surface. The most hydrophobic surfaces being achieved with methyl and phenyl substituted alkylsilanes, these were significantly more hydrophobic that the intermediate wetting achieved with the 3-aminopropyl substituted alkylsilane. In an extension of the standard contact angle measurement, when assessed with a range of different liquids, contact angle may be used to assess the surface free energy of the surfaces, fig. 4.4 table 4.3.
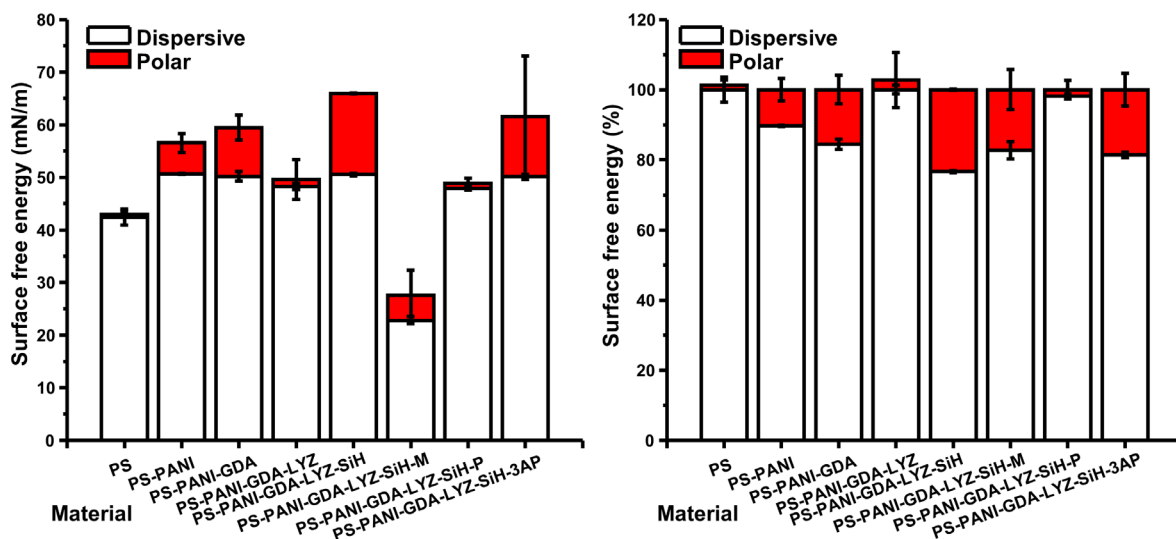
Figure 4.5: Total surface free energy (γ^{tot}) of the fabricated films measured at different stages of fabrication and after treatment with different alkylsilanes (A), highlighting the contributing polar and dispersive forces. The polar (γ^{p}) and dispersive (γ^{d}) components are also plotted as a percentage of γ^{tot} (B).

Table 4.3: Surface free energy of inorganic films on polymer surfaces

Sample	θ (°)	γ^{tot} [mN/m]	γ^{d} [mN/m]	γ^{p} [mN/m]	γ^{+} [mN/m]	γ^{-} [mN/m]
TCPS	89.75 ± 4.4	41.87 ± 0.9	42.44 ± 1.5	-0.57 ± 0.6	-0.08 ± 0.3	1.29 ± 0.8
PS-PANI	44.16 ± 5.7	56.51 ± 1.9	50.65 ± 0.1	5.87 ± 1.8	0.56 ± 0.2	5.22 ± 0.3
PS-PANI-GDA	35.29 ± 4.6	59.45 ± 2.8	50.18 ± 0.9	9.28 ± 2.4	0.84 ± 0.3	5.69 ± 0.6
PS-PANI-GDA-LYZ	52.48 ± 4.8	46.92 ± 3.4	48.26 ± 0.6	-1.34 ± 3.8	-0.11 ± 0.4	5.28 ± 0.3
PS-PANI-GDA-LYZ-SiH	4.17 ± 1.3	65.94 ± 0.03	50.53 ± 0.2	15.41 ± 0.1	1.56 ± 0.01	6.67 ± 0.01
SiH-M	87.76 ± 2.9	27.58 ± 1.5	22.82 ± 0.7	4.76 ± 1.6	1.63 ± 0.35	1.44 ± 0.43
SiH-P	82.31 ± 15.1	48.89 ± 1.6	47.95 ± 0.7	0.94 ± 2.3	1.21 ± 0.5	0.57 ± 0.9
SiH-3AP	30.71 ± 8.1	61.58 ± 4.7	50.1 ± 0.8	11.48 ± 5.0	1.02 ± 0.5	5.8 ± 0.6

The initial TCPS material is at the intersection between a hydrophobic and hydrophilic material and the measured surface free energy matches well with literature values and was comprised primarily of dispersive forces (Harnett *et al*., 2007). On treatment with PANI the contact angle drops significantly, though the γ^{tot} rises and gains a greater contribution from polar groups that are basic in nature (primary and secondary amines within the polymer). These trends continue as the PANI film was further functionalised with GDA. On treatment with lysozyme however contact angle rises and the films show a lower γ^{tot} with a lower polar component, though still predominately basic in nature. The value

achieved approximates the theoretical limit achievable with a protein treated surface; 45 mN/m (Harnett *et al*., 2007). The super-hydrophilic silica surface demonstrated the highest surface free energy of all the materials tested and the lowest water contact angle; this surface had the highest polar contribution and was still predominately basic in nature, though showing a more acidic character.

On functionalisation, the contact angle and surface energy of the films changed from the super-hydrophilic, high surface energy base material. On treatment with PTEOS the surface became more hydrophobic (almost to the point of the original TCPS) and surface energy dropped as the surface was likely passivated by surface phenyl groups with surface energy being almost entirely derived from the dispersive component. A similar alteration was also noted for the methyl modified surface. For the APTEOS treated surfaces, though significantly increasing the water contact angle, similar values for surface energy were maintained, likely due to the introduction of the polar amine group in addition to the propyl chain. The polar component of the surface was also determined to be primarily basic in nature. The measured surface energy and wettability of the films suggested that the modification expected had occurred to some degree.

XPS was used to characterise the chemical composition of the surfaces, data is shown in table 4.4 and fig. 4.2. Since XPS offers lower surface penetration ~10 nm and good sensitivity for detection of unique functional groups it is more suitable for this type of surface analysis and complex samples than EDXa and ATR-FTIR.

Table 4.4: XPS of inorganic films on polymer surfaces

					Elemental composition (Atomic %)	
Sample	Si2p	O1s	C1s	N1s	O:Si	N:C
PS-PANI-GDA-LYZ	-	7.21	88.80	3.99	-	01:23.81
PS-PANI-GDA-LYZ-SiH	9.93	20.16	68.68	1.23	2.03:1	01:55.83
PS-PANI-GDA-LYZ-SiH-M	22.59	43.23	32.43	1.75	1.91:1	01:18.53
PS-PANI-GDA-LYZ-SiH-P	5.16	9.58	85.26	-	1.85:1	-
PS-PANI-GDA-LYZ-SiH-3AP	7.45	16.68	73.94	1.93	2.23:1	01:38.31
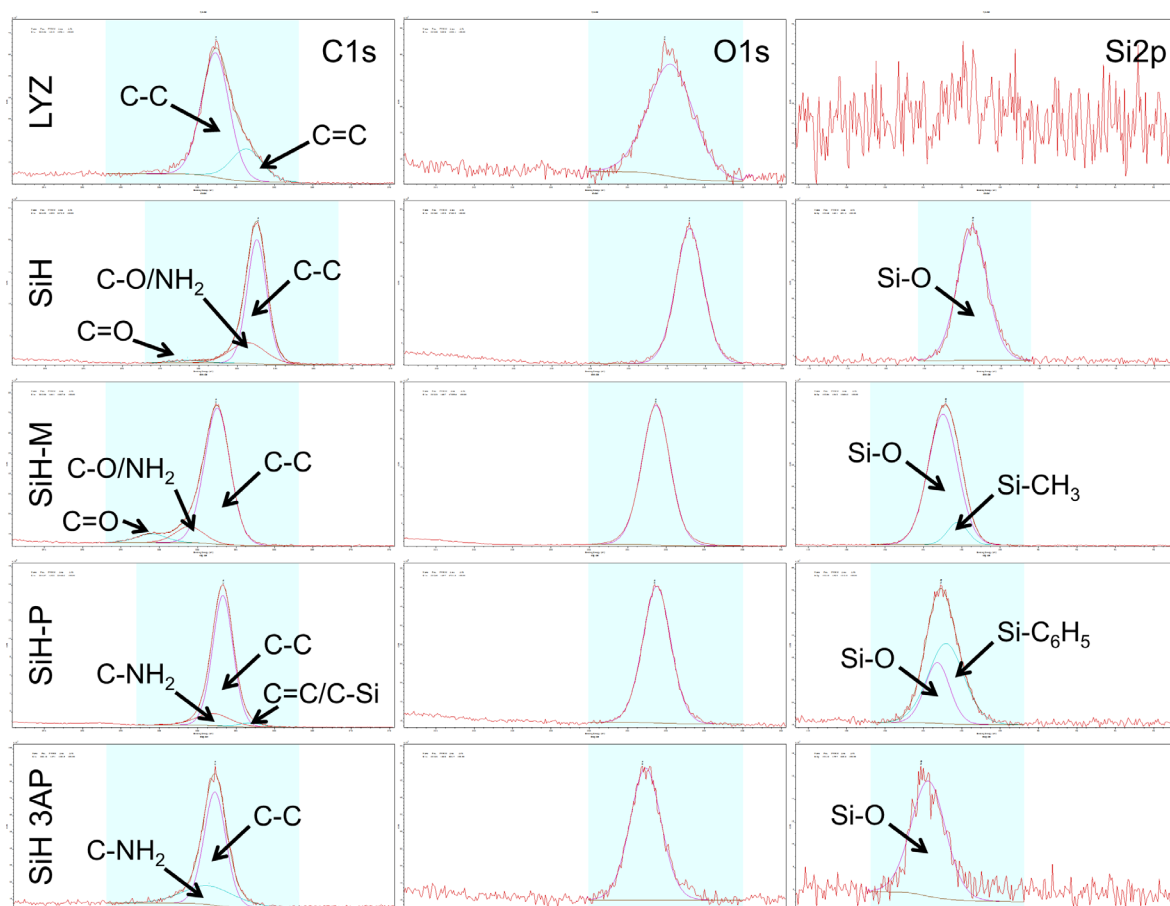
Figure: 4.6: High resolution XPS taken of Si2p, O1s, C1s and N1s peaks for differently functionalised silica surfaces. Deconvolution of the peaks shows information on the contributing functional groups (NIST, 2012).

The untreated PS-PANI-GDA-LYZ surface demonstrated oxygen, carbon and nitrogen with no silicon presence. The composition of the surface differed from the theoretical value derived from the sequence of lysozyme which was estimated to be 62.11, 18.85 and 17.97 atomic % respectively for C, N and O. The abundance of carbon and oxygen suggests that the underlying GDA linker is exposed and that protein surface coverage may be less than total. The high resolution O1s peak maximum was ~131.8 eV, this could be attributed to carbonyl containing groups (Gerenser, 2012). Upon exposure to the hydrolysis solution silicon was deposited on the PS-PANI-GDA-LYZ surface. An O:Si ratio of almost 2:1 would agree with the chemical formula of SiO_2 and would suggest the surface was ~30 atomic % silica, residual carbon and nitrogen may be attributed to exposed underlying polymer. This conclusion is supported by O1s and Si2p peaks ~532.7 and ~103.2 eV which is characteristic of silica (Guittet *et al*., 2001). The SiH methyl surface demonstrated higher silica coverage, ~65 atomic % of the surface. Deconvolution of the C1s peak resolved a

peak ~102.21 eV which may be attributed to $SiCH_3$ and constituted 10.78% of the Si2p signal, which would suggest a surface composition of 9.74 atomic % (Inoue & Takai, 1996). In comparison for the SiH phenyl surface, silica coverage was lower, ~15 atomic % of the surface. Deconvolution of the C1s peak resolved a peak ~102.82 eV which may be attributed to SiC_6H_5 and constituted 65.36% of the Si2p signal, which would suggest a surface composition of ~26.98 atomic % (Stobie *et al.*, 2007). Analysis of the 3-aminopropyl treated surface would suggest ~15 atomic % of silica on the surface, though with no more than 1.93 atomic % attributed to the N1s signal, at most only 1.93 atomic % of the Si2p signal could be attributed to APTEOS or at most ~14 atomic % of the surface if the contribution of the propyl chain and siloxane groups is considered.

Overall it can be noted from the XPS analysis that surface coverage was unlikely to be complete for any functionality or deposited compound, the materials produced probably exhibit multiple functionalities in culture. Limitations of this analysis include the problem of surface inhomogeneity or contamination, which may distort the results of the analysis for these surfaces. It can be noted that the amount of functionality on the surface was variable, being between ~10-25 atomic % at most depending on the functionality (variability is not unexpected as the fabrication procedure treats each precursor similarly without individual optimisation).

Despite the difficulty in characterising the surfaces by an available spectroscopy based technique, surface energy measurements demonstrate that the functionality induced was sufficient to generate materials with distinct chemical characters, the question posed with respect to this information is 'how much functionality is required to modify the characteristics of a surface to a desired level' and 'can modest changes to surface chemistry influence the response of cells in culture'?

4.3.2 Proliferative response to silica surfaces of varying functionality

With the development of materials exhibiting a range of different chemical properties, the influence of these new materials on cell growth was assessed. With many cell lines, surfaces and conditions to examine, the selection of a simple, arrayed and inexpensive assay was desirable. In this respect cell response was measured through a proliferation and cytotoxicity assay based on the vital stain, neutral red (Repetto *et al.*, 2008).

The neutral red assay monitors the uptake of the vital stain 3-amino-7-dimethylamino-2-methylphenazine which is neutral at physiological pH and passively diffuses into the cell. In viable cells (which produce ATP) pH gradients are maintained in cell compartments such as the lysosome, here the dye accumulates through electrostatic interactions with anionic and phosphate groups of the lysosome matrix due to its charge under acidic conditions (Repetto *et al*., 2008). Retained dye can be liberated and used as a measure of cell proliferation and cytotoxicity. The assay looked at the response of 5^x10^3 cells over a seven day culture period, with and without serum (though cells were not serum starved beforehand), fig. 4.7. To give an indication of the numbers of cells involved FM3, OPCT1 and P4E6 have a duplication rate of 26.4, 34 and 38.4 h respectively.
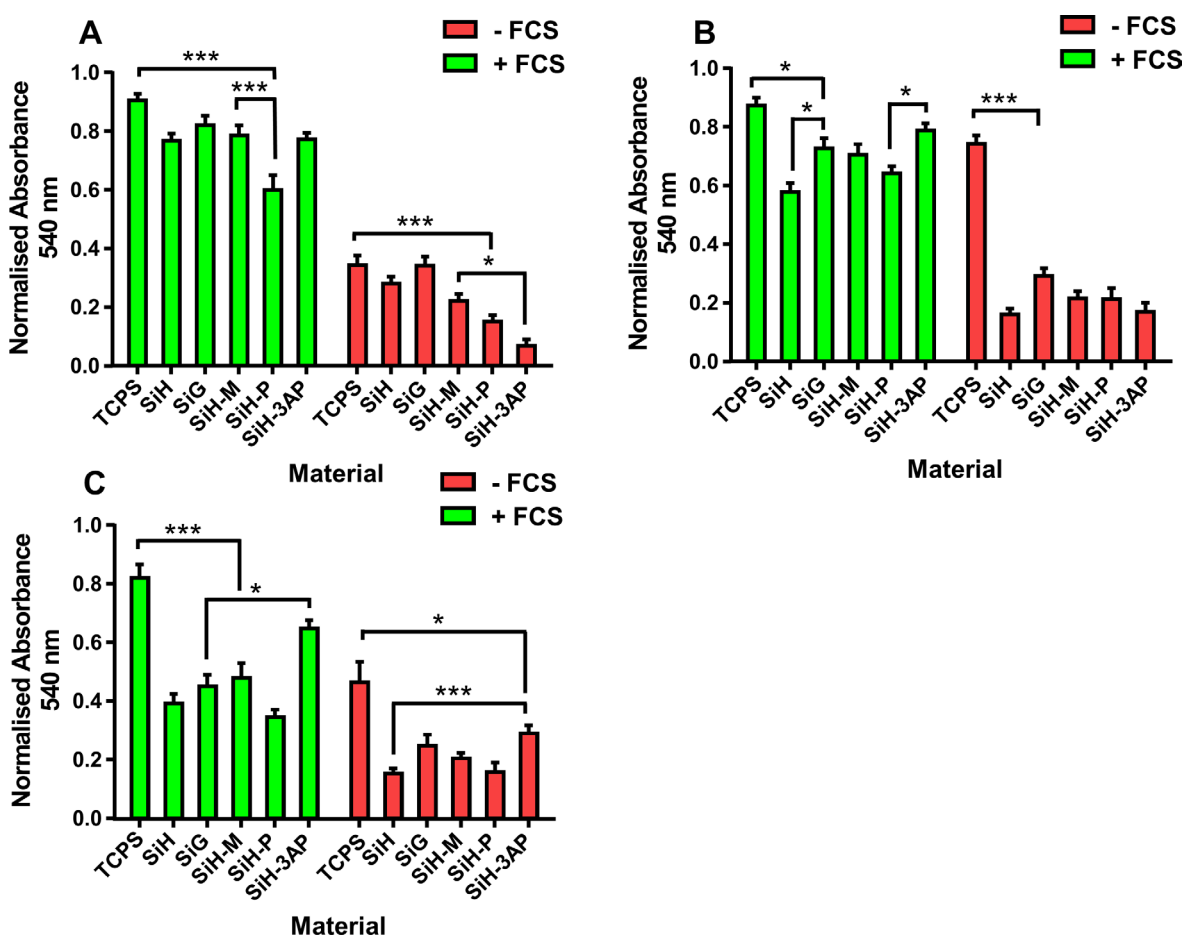
Figure: 4.7: Neutral red proliferation/cytotoxicity assay of FM3 (A), OPCT1 (B) and P4E6 (C) cell lines after a seven day culture period on differently functionalised silica surfaces and TCPS in the presence and absence of FCS (n = 36).

The outcome of the neutral red assay for the FM3 cell line (fig. 4.7A) matched the expected result from the outcome of the proliferative and cytotoxicity assays performed in the previous chapter in that there was no significant variation between TCPS and the SiH

and SiG surfaces. In summary the influence of surface and serum were highly significant factors influencing cell proliferation ($F_{(5, 132)}$ = 20.68 P <0.0001, $F_{(1, 132)}$ = 1028 P <0.0001 respectively). An interaction between serum and surface was also observed ($F_{(5, 132)}$ = 5.033, P = 0.0003), indicating that some surfaces are influenced more greatly by the loss of serum than others, this interaction can likely be attributed as the response to the protective effect of serum in culture (Wasil *et al*., 1987; Kunas *et al*., 1990). *Ad hoc* testing by Tukey's test between the different surfaces showed a highly significant decrease in proliferation on SiH-P surfaces with respect to the other surfaces in the presence of FCS. In the absence of FCS the SiH-P surfaces also performed significantly worse than surfaces other than TCPS, SiH and SiH-M, where no significant variation was observed. However SiH-3AP became the worst performer with significantly worse performance against all other surfaces except SiH-P, where no significant difference was observed.

The OPCT1 cell line (fig. 4.7B) showed similar responses with respect to FM3 in that both serum and surface were demonstrated as significant factors influencing cell proliferation ($F_{(1, 179)}$ = 625.7 P <0.0001, $F_{(5, 179)}$ = 55.11 P <0.0001 respectively) and an interaction was observed ($F_{(5, 179)}$ = 15.05 P <0.0001). In the case of OPCT1 Tukey's test for TCPS showed significantly higher proliferation for all but SiH-3AP, the worst performing surface being SiH, though this was insignificant in comparison to SiH-M and SiH-P. OPCT1 in the presence of serum appears to favour the SiG and SiH-3AP surfaces though no significant difference between this surface and SiH-M and SiH-3AP was observed. In the case of serum withdrawal there was no difference between the surfaces except TCPS showed significantly higher proliferation than all other surfaces, proliferation was actually insignificant in comparison to growth on TCPS with serum. Considering the serum dependency of the cell lines, this tolerance to serum loss over the culture period observed for TCPS was unusual; this may be attributed to the point that cells were serum withdrawn and not serum starved. A reservoir of serum may still have been present in culture which on a favourable surface like TCPS facilitated growth, serum starvation may well have eliminated this effect and synchronised the cell cycle in the assays, ensuring greater uniformity in the cell population response. It is also noted that certain tumour cell lines are less serum dependant than normal or other tumour cell lines for proliferation (Sobel & Sadar, 2005).

The P4E6 cell line (fig. 4.7C) showed similar responses in overview to FM3 and OPCT1 as both serum and surface were demonstrated as significant factors influencing cell proliferation ($F_{(1, 152)}$ = 149.2 P <0.0001, $F_{(5, 152)}$ = 28.64 P <0.0001 respectively). In this

case the interaction was not significant. As with OPCT1 Tukey's test for TCPS showed significantly higher proliferation for all but SiH-3AP, the worst performing surface being SiH-P, though this was insignificant in comparison to all other surfaces but SiH-3AP. SiH-3AP showing significantly higher proliferation/lower cytotoxicity than all surfaces but SiH-M (where the difference was insignificant) and TCPS.

Others have reported a beneficial proliferative effect comparable to TCPS for amino surfaces in the presence of FCS for modified Ti and polymer surfaces (Cai *et al*., 2006; Lee *et al*., 1994). Though the loss or reverse of this effect for FM3 and OPCT1 in the absence of serum suggests the surface is actually hostile and the uptake of serum is what permits biocompatibility and cell proliferation as concluded in chapter three.

The assay demonstrated that the proliferative/cytotoxicity response of a cell line is dependent on the surface used in culture as could be expected, but also that the response is cell line dependant. Though there are some conserved responses (general compatibility of TCPS), unique preferences of certain cell lines for some surfaces is apparent, for example the varying tolerance to the SiH-3AP surface. The protective influence of serum mitigates the influence of the surface for certain cell lines, with greater loss of tolerance without serum than with serum, such as the response for SiH-3AP for FM3 and OPCT1.

The potential of these observations in the development of surfaces for cell selection or enrichment is that surfaces favouring or acting to restrict the proliferation of certain cell types may be used to isolate or remove that cell type from culture. Similarly surfaces with a cytotoxic effect against a particular cell line or sub-population could be used to select against them in culture.

4.3.3 Influence of differently functionalised silica surfaces on cell adhesion

An additional parameter by which one can assess how cells respond to different surfaces was through observing cell adhesion. This was performed through a modified centrifugal adhesion assay as shown in fig. 4.8 (Reyes & Garcia, 2003).

The FM3 cell line was the least adherent of all the cell lines tested, being the only cell line which was consistently depleted from the surface across all surfaces for the range of RCF examined, fig. 4.8A. The surface was found to be highly significant with respect to explaining cell count both in terms of the rate of loss of cells with respect to RCF (K) and cell number at 200 RCF (plateau) ($F_{(10, 846)}$ = 8.883, P <0.0001, R^2 = 0.7203). The rate of

cell loss (K) was separately determined to vary significantly between the different surfaces ($F_{(4, 1467)} = 13.87$, P <0.0001). A *post hoc* Turkey's test determined that K was significantly different between SiH than TCPS (P <0.0001). K was also significantly different between SiH and SiH methyl, the next most adherent surface (P 0.0393) and SiH 3-aminopropyl (P 0.0044). There was no difference in K between the other surfaces, or between the surfaces in terms of the plateau. The difference between SiH and the other surfaces relates to the slower rate of cell loss with RCF, suggesting cells were most adherent on this surface (as determined previously) followed by SiH methyl and then the other surfaces.
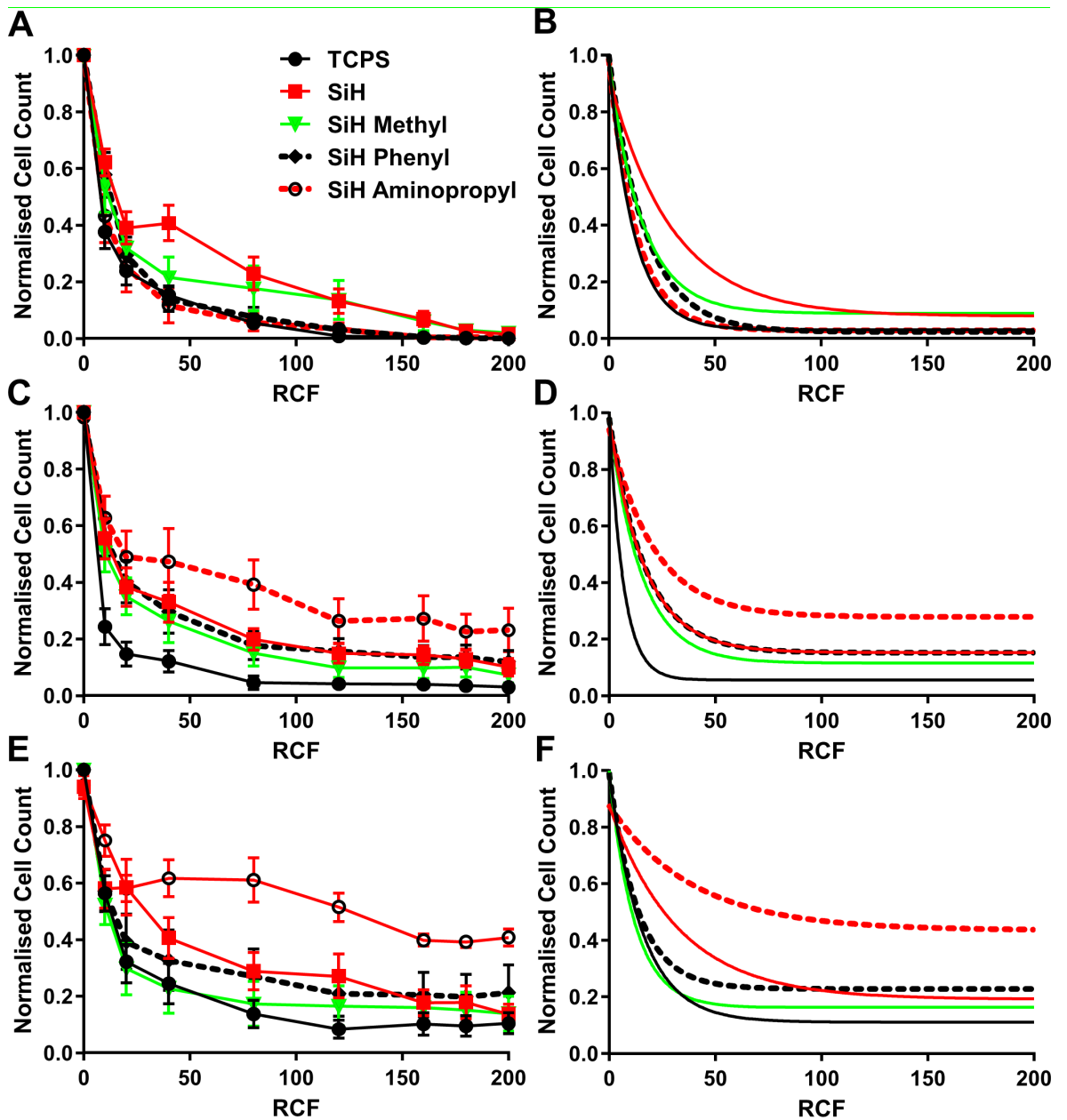
Figure: 4.8: Centrifugal adhesion assay of FM3 (A, B), OPCT1 (C, D) and P4E6 (E, F) cell lines after culture over a seven day period for differently functionalised silica surfaces

and TCPS. Both the cell counts (A, C, E) and fitted one phase exponential decay curves (B, D, F) are represented for each data set (n = 6).

The OPCT1 line (fig. 4.8B) also showed a varying level of adhesion between the differently functionalised materials ($F_{(8, 345)}$ = 11.94, P <0.0001, R^2 = 0.7128), though this cell line exhibited a response where at 200 RCF cells were still attached to some of the surfaces. Turkey's testing determined OPCT1 like FM3 showed a slower rate of loss for SiH (P <0.0001), SiH methyl (P <0.0001), SiH phenyl (P <0.0001) surfaces in comparison to TCPS, with the SiH 3-aminopropyl (P <0.0001) surface demonstrating the greatest retention of cells over time. Additionally OPCT1 also demonstrated significant differences by Turkey's *post hoc* testing in the final adherent cell number with the SiH 3-aminopropyl surface having significantly greater cell numbers adherent at the end of the assay in comparison to TCPS (P <0.0001, d.f. = 1467), SiH methyl (P 0.0006), SiH (P 0.0189) and SiH phenyl (P 0.0171) surfaces. Overall the plateau was considered significantly different between the different surfaces ($F_{(4, 1467)}$ = 17.94, P <0.0001).

The P4E6 response (fig. 4.8C) closely matched OPCT1 in that the amino functionalised material was the most adhesive and the surface was a significant factor with regards to adherent cell number ($F_{(8, 336)}$ = 14.15, P <0.0001, R^2 = 0.5537). Turkey's testing determined P4E6 demonstrated a slower rate of loss for SiH *versus* SiH methyl (P <0.0045) and SiH phenyl (P <0.0326) surfaces. SiH 3-aminopropyl surface also had a slower rate of loss than SiH methyl (P <0.0030) and SiH phenyl (P 0.0212) surfaces. P4E6 by Turkey's *post hoc* testing also determined demonstrated significant differences in the final adherent cell number with the SiH 3-aminopropyl surface having significantly greater cell numbers adherent at the end of the assay in comparison to TCPS (P <0.0001) and the SiH methyl (P <0.0001), SiH (P <0.0001) and SiH phenyl (P <0.0001) surfaces.

The RCF at which fifty per cent of cell loss from the surface occurs (RCF_{50}) provides another measure of assessing cell adhesion to the surface, table 4.5. It can be noted that this value is higher for the 3-aminopropyl modified surface for OPCT1 and P4E6 in comparison to FM3 suggesting stronger adhesion to this surface, while for FM3 the bare silica surfaces have the greatest RCF_{50}. Table 4.5 also records the average number of remaining cells (RC) adherent at an RCF of 200. While for FM3 few cells to none remain for most surfaces, for OPCT1 and P4E6 larger numbers of cell remained at the end of the assay with a preference for the amino modified silica surface and disfavouring of the TCPS surface.

Table 4.5: RCF$_{50}$ and RC of different cell lines for different surfaces

Cell line	TCPS	SiH	SiH-M	SiH-P	SiH-3AP
FM3	8.08	20.44	15.46	10.78	11.81
95% CI	7.049-9.473	16.31-27.36	8.219-15.66	9.949-14.54	7.177-11.81
RC	0 ± 0	3 ± 2	3 ± 2	0 ± 0	1 ± 1
OPCT1	4.62	11.62	10.49	11.60	14.45
95% CI	3.82-5.842	9.091-16.09	8.272-14.34	8.955-16.60	9.179-33.97
RC	2 ± 1	8 ± 3	10 ± 5	15 ± 6	19 ± 6
P4E6	10.72	22.40	8.18	9.36	26.95
95% CI	8.496-14.52	15.09-43.47	5.864-13.52	6.194-19.12	16.38-76.11
RC	18 ± 8	16 ± 4	11 ± 4	19 ± 6	39 ± 4

In summary adhesion trends are as follows; PS < SH-M = SH-P < SH < SH-AP though a different response was observed between the melanoma FM3 and the prostatic epithelial adenocarcinoma cell lines OPCT1 and P4E6, with FM3 having lower adherence and favouring the bare silica surface while OPCT1 and P4E6 favoured the 3-aminopropyl modified silica. This observation further demonstrates the selective preferences for different surfaces between broadly different cell types. The potential of these observations to a selective method based on cell adhesion could be directly applicable.

Studies by others have shown similar cell adhesion responses to similar surface chemistries, Keselowsky *et al.*, using self-assembled monolayers (SAM) of alkanethiols reported hydroxyl functionalities having the greatest adhesion for the mouse osteoblast precursor cell line MC3T3 (Keselowsky *et al.*, 2003). Higher adhesion to amino and carboxyl surfaces as opposed to a methyl functionality was also demonstrated, these trends are in general agreement with the observations reported here. The mechanism reported for differential adhesion is surface dependant changes in fibronectin adsorption and conformation influencing integrin $\alpha_5\beta_1$ binding (Keselowsky *et al.*, 2003). These reports were in agreement with older reports for carboxyl and methyl SAM with Swiss 3T3 fibroblasts (McClary *et al.*, 2000). Furthermore the modified integrin binding was shown to enhance osteoblast differentiation on amino and hydroxyl terminated SAM (Keselowsky *et al.*, 2003). That adhesion can be correlated with protein adsorption and cell differentiation offers another route and mechanism for the development of a selective surface.

4.3.4 Morphology of tumour cells cultured on differently functionalised silica surfaces

When observed that tumour cells adhere significantly differently to different surfaces, the influence of the surface on the cells cytoskeleton through which it interacts with the surface was studied. Immunofluorescence confocal microscopy was used for the observation of f-actin which forms the stress fibres of the cytoskeleton and vinculin which acts as a component of focal adhesion sites after two days of culture on the differently functionalised surfaces, fig. 4.9. Isotype controls for non-specific secondary background staining can be found in appendix B (fig. B1). Representative micrographs (maximal projections) of the staining of the melanoma FM3 are shown in fig. 4.9; micrographs for the staining of OPCT1 in fig. 4.10 and micrographs for the staining of P4E6 in fig. 4.11.

Overall no significant variations were noted for FM3 morphology between the different surfaces, all surfaces demonstrating cells whose morphology was characteristic of cells that had adhered and spread on the surfaces. FM3 cells were observed with f-actin outlining the characteristically polygonal arrangement of stress fibres seen for fibroblastoid cells (Li et al., 2005). Vinculin was expressed at the cell membrane and in the cytoplasm a high and low population were observed

As with FM3 no major variation was seen for OPCT1. Cells were noted to have the characteristics associated with adhesion, cell spreading and exhibiting a normal morphology. The overall morphology was distinct from FM3 with cell-cell contact more strongly represented, indicative of the lineage of OPCT1 epithelial cells compared to the fibroblasts of the FM3 cell line. Vinculin was localised on the membrane, cytoplasm and was also localised at the nucleus for some cells, refer to highlighted cells in fig. 4.10.

As with the preceding cell lines, P4E6 cells were noted to have characteristics associated with adhesion, spreading and of normal morphology and no major variations were noted between surfaces. The overall morphology was shared with OPCT1 as opposed to FM3 with cell-cell contact well represented, again indicative of the epithelial lineage. Vinculin, as for FM3 was localised on the membrane and cytoplasm but not with the nucleus, unlike OPCT1. Two clear phenotypes were seen in P4E6 for vinculin expression; high and low, as with FM3. Overexpression of vinculin is associated with cancer progression and proliferation, highlighting the clinical relevance of the observation of such cell sub-populations and the heterogeneity of even established tumour cell lines (Ruiz et al., 2010).
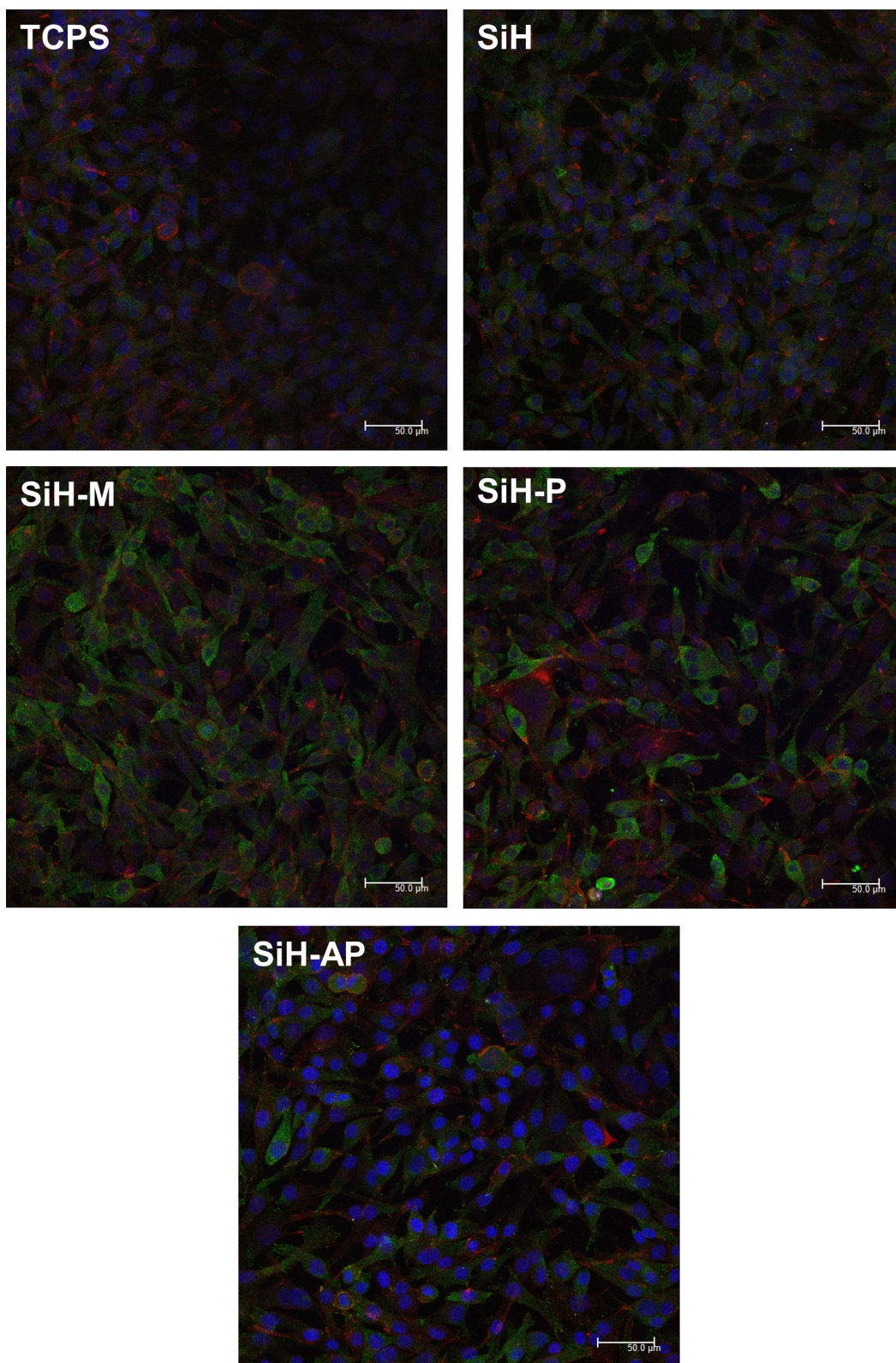
Figure: 4.9: Representative confocal micrographs (maximal projections) of FM3 after culture over a two day period for differently functionalised silica surfaces and TCPS. The micrograph represents fluorophore intensity of the nucleus, vinculin and f-actin by the respective emission wavelength (blue, green and red).
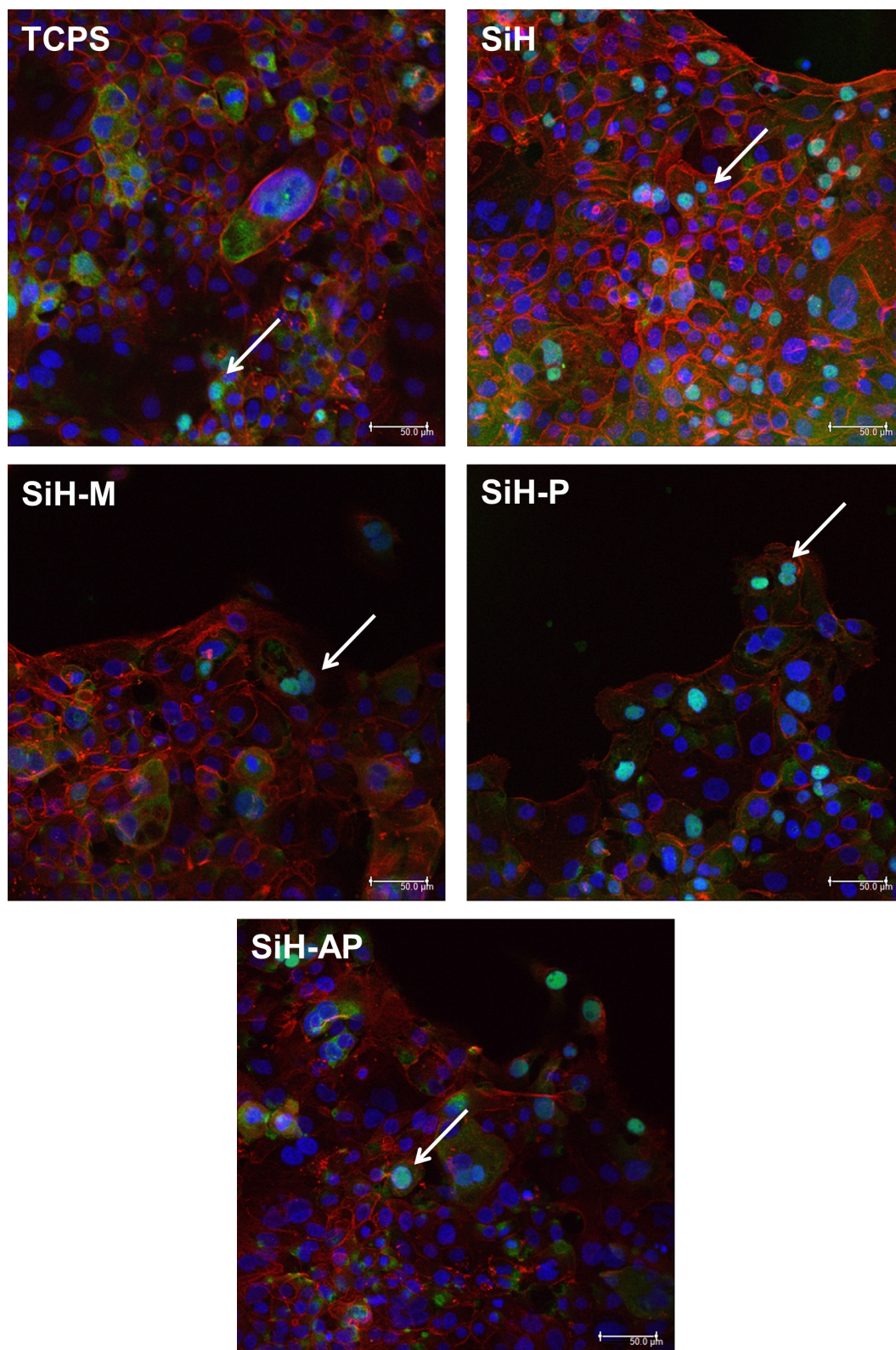
Figure: 4.10: Representative confocal micrographs (maximal projections) of OPCT1 after culture over a two day period for differently functionalised silica surfaces and TCPS. The micrograph represents fluorophore intensity of the nucleus, vinculin and f-actin by the respective emission wavelength (blue, green and red). Arrows highlight examples where

vinculin and DAPI co-localisation have occurred. Arrows denote representative cells where localisation of DAPI and vinculin has occurred.
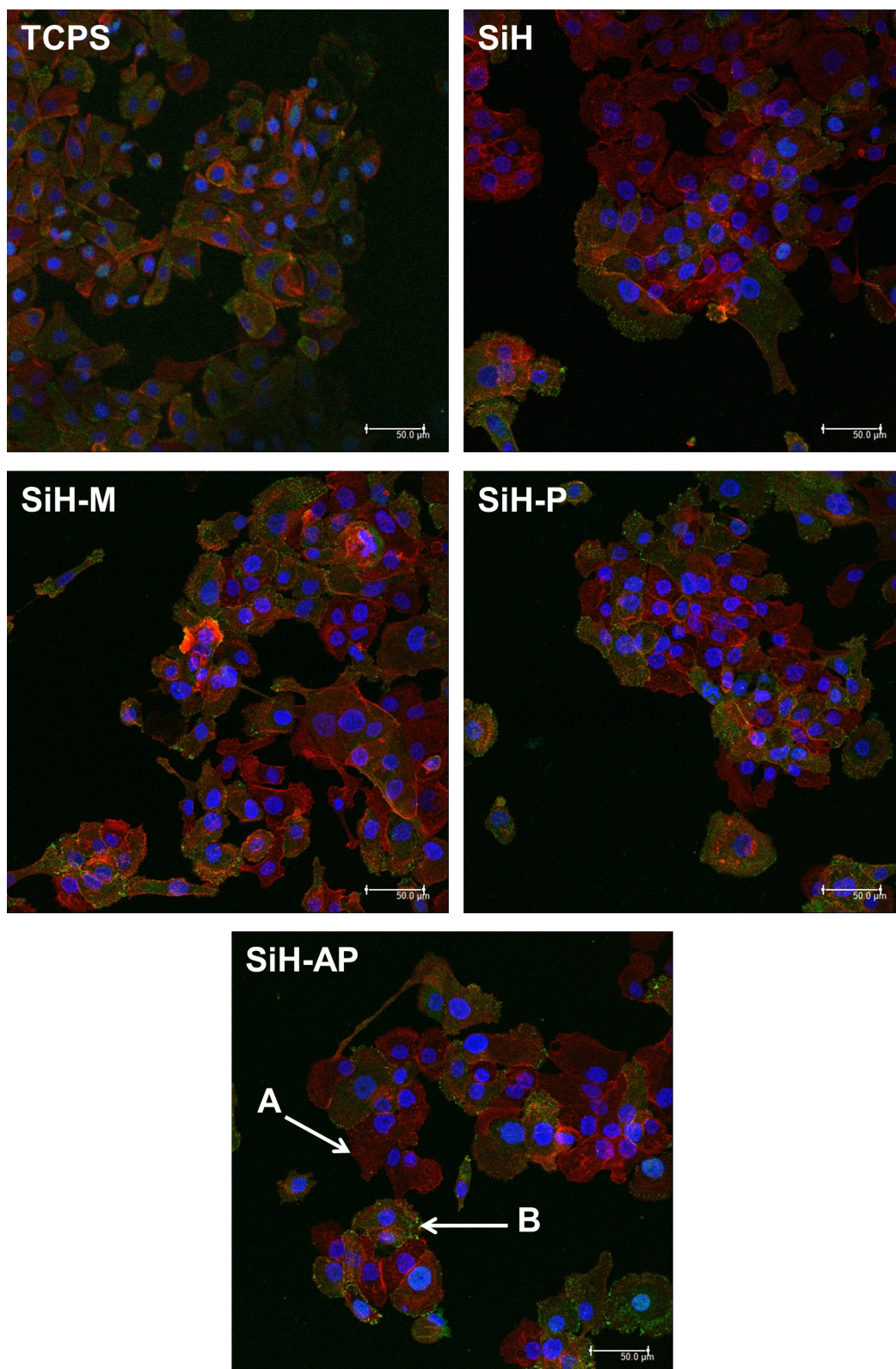
Figure: 4.11: Representative confocal micrographs (maximal projections) of P4E6 after culture over a two day period for differently functionalised silica surfaces and TCPS. The micrograph represents fluorophore intensity of the nucleus, vinculin and f-actin by the

respective emission wavelength (blue, green and red). Representatives of vinculin low and high expressing populations are highlighted for SiH-AP as populations A and B respectively.

That cell lines showing significant differences in their proliferative and adhesive performance were found to have conserved morphologies was unexpected. However, it has been noted by others that major morphological changes in cells may not be seen despite very divergent effects in cell response to specific surfaces (Kilian & Mrksich, 2012). It may be that the cytoskeletal changes are too subtle in these matters to be detected by IF staining (at last at the resolution used) and that perhaps quantifying the expression of known adhesion molecules by quantitative polymerase chain reaction or transcription microarrays would be a more sensitive approach. However the ready ability to identify different cell populations using IF staining by known markers was a promising result for later studies into cell sub-populations.

4.3.5 Cell response in real time through live cell imaging

An important focus of study when considering cell protein surface interactions is to consider the rate at which events happen on the surface, such as initial adhesion and subsequent motility. While protein adsorption will start immediately, cellular events take minutes to occur. Imaging of fixed and stained cells can often lead to an impression of a static and permanent character. However this is far from the reality, the cell is a dynamic and highly motile entity, well-illustrated by visualisation of cells in real time, fig. 4.12.

Live cell imaging was applied (as a complementary study to the adhesion and cytoskeletal studies) to the OPCT1 and FM3 cell lines during the initial 12 h of contact with the surface, after a period of four h to allow for cell settling from suspension and surface attachment. Extraction of cell velocity and the distance travelled during this period was obtained, fig. 4.12A, B.
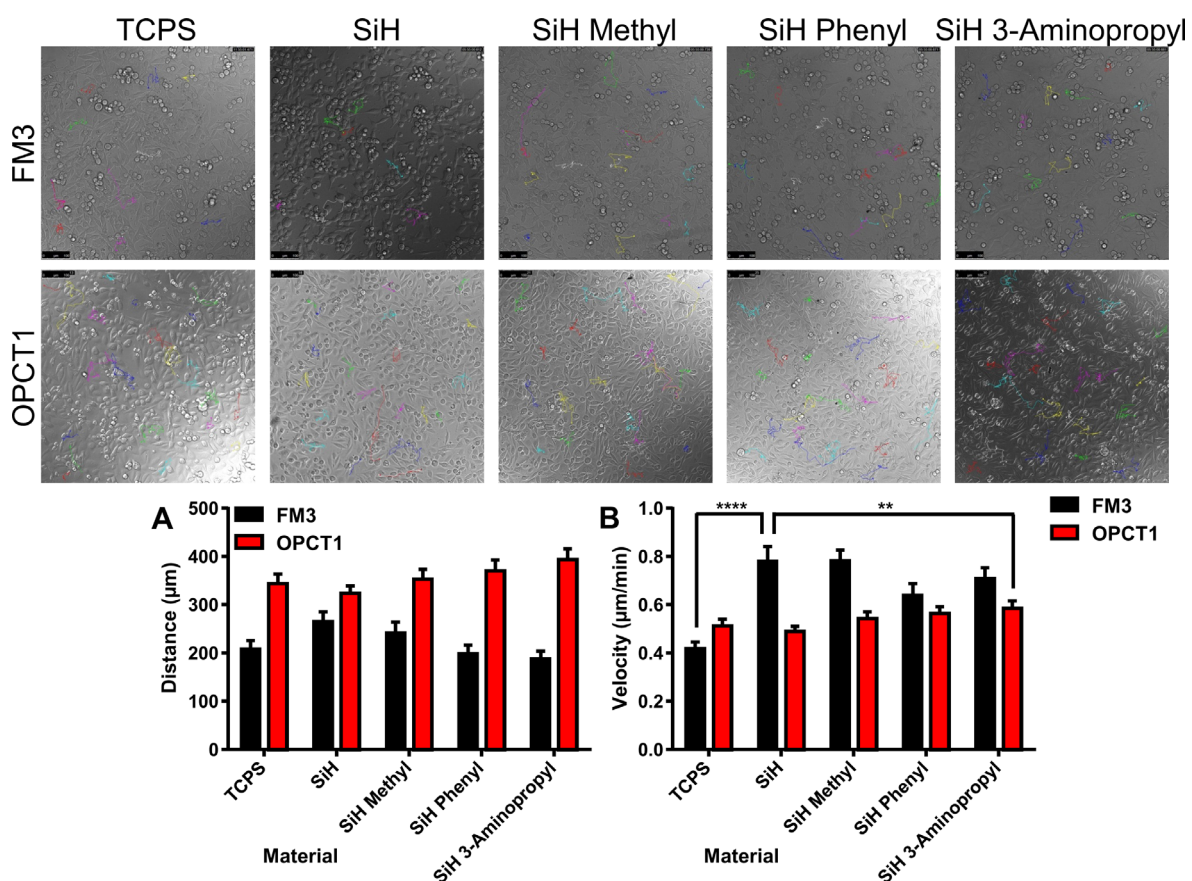
Figure: 4.12: Tracks of OPCT1 and FM3 cells on TCPS, silica (SiH), SiH methyl, SiH phenyl and 3-aminopropyl modified SiH surfaces. Graph (A); extracted distance and velocity (B) achieved by FM3 (n = 50) and OPCT1 cells (n = 100) for these tracks.

The distance travelled by the cells on different surfaces was found to be insignificant, though the difference between distance travelled between OPCT1 and FM3 was significant ($F_{(1, 746)}$ = 94.96, P <0.0001). However this should be treated with caution as FM3 was noted to be highly synchronised in its cell division, with many cell tracks aborted before the complete 12 h observation period due to cells leaving the surface to undergo division.

The velocity at which the cells travelled across the surfaces was also significantly different between the two cell lines ($F_{(1, 745)}$ = 32.02, P <0.0001), with FM3 generally moving faster than OPCT1. The surface was determined to a significant factor in determining cell velocity ($F_{(4, 745)}$ = 10.14, P <0.0001), there was also a significant interaction ($F_{(4, 745)}$ = 9.098, P <0.0001) suggesting that different cell lines travelled at different velocities for a given surface. A *post hoc* Turkey's test determined the significance of differences between the different surface treatments, fig. 4.12B. FM3 adhered to TCPS demonstrating the lowest motility, those on silica and methyl modified silica the highest, no significant differences were determined between the surfaces for OPCT1.

The link between cell motility and adhesion is difficult to interpret with this limited data-set; however where differences could be resolved for FM3, higher adherence appears to correlate with higher motility. Interestingly the 3-aminopropyl surface demonstrated the highest mean velocity for OPCT1, though comparison to other observations showed this to be insignificant. However OPCT1, despite higher adherence than FM3, demonstrated lower levels of motility, though it may be difficult to draw comparisons this broadly as FM3 and OPCT1 are divergent cell types.

Others that have studied cell motility for topologically distinct surfaces have shown that mouse endothelial and rat mesenchymal cells showed higher motility for smaller surface features on differently sized (15 nm *vs.* 100 nm) TiO_2 nanotubes (Park *et al.*, 2009). Tan & Saltzman found that for polyimide surfaces treated with an 'inert' Au-Pd alloy, no influence on motility was observed for neutrophils (Tan & Saltzman, 2002). However with MC3T3-E1 osteoblast-like cells a difference in motility was shown with a wider range of surface chemistries, though incomparable due to the thiol and quaternary amine functionalities selected (Webb *et al.*, 2000). Overall studies on motility focus on patterning on the micron scale, the random nature of the topology on the silica surfaces used in this study would not be expected to direct cell orientation (which was not seen), however little work has looked at the influence of functionality.

The study of motility in this manner is an interesting endeavour as it is a study of the cell response in real time, even though it suffers from considerable problems in terms of data analysis and literature depth. The provision of software capable of accomplishing accurate cell tracking in an automated fashion with larger cohorts of cells or specialist microscopy techniques such as surface plasmon resonance microscopy, could greatly improve the application of the technique and the quality of data and thus conclusions drawn (Giebel *et al.*, 1999). A surface dependant influence on motility appears to exist, at least for some cell lines, in this case FM3.

4.3.6 Adsorption of proteins to differently functionalised silica surfaces

In the previous chapter, cell response was attributed in part to the adsorption of serum proteins from the medium. The adsorption of serum proteins such as serum albumin, fibronectin and FCS was also studied in relation to the differently functionalised silica surfaces, applying the Amido-black protein assay, fig. 4.13.
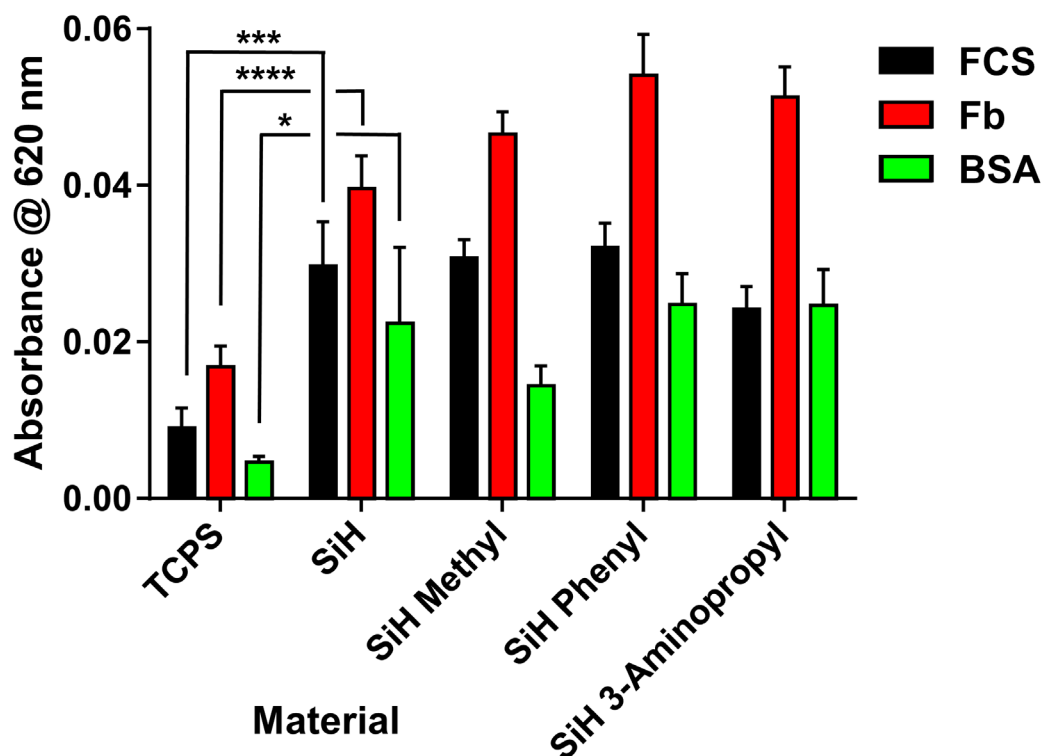
Figure: 4.13: Adsorption of (A) FCS (5% in RPMI-1640 media), in addition to 15 mM (1 mg/mL) (B) BSA and (C) Fb to differently functionalised silica surfaces (n = 36).

Overall, the amount of protein adsorbed was found to vary significantly ($F_{(8, 186)}$ = 62.12 P <0.0001) between the surfaces. The absorbance was also found to vary significantly between different proteins but this may be attributed to the differing Amido-black response, since no normalisation for this effect was performed in this study as opposed to the study of Roach *et al.* (Roach *et al.*, 2006). However, protein adsorption, while significantly different between proteins, was also found to be significantly different ($F_{(8, 186)}$ = 2.617 P = 0.0098) between surfaces, this interaction or uniformity in response is difficult to explain in terms of differential dye uptake between proteins alone and suggests that the proteins respond differently depending on the surface, much like the response seen for the cell lines noted above.

In a similar manner to the study previously conducted, BSA and Fb were found to adsorb in significantly higher quantities to the modified surfaces in comparison to TCPS. This study showed that FCS followed the same pattern. This should be unsurprising as FCS primarily constitutes BSA (estimated concentration 237.9 mM, appendix B (table B1)) but suggests that the trends observed for model proteins in PBS would be comparable to what is seen for *in vitro* conditions. Of the differences observed between the surfaces, not all

surfaces varied significantly differently from TCPS. The adsorption of FCS to the 3-aminopropyl silica surface did not vary significantly, nor the adsorption of BSA to the methyl modified silica surface. Beyond this, though statistical means varied between the surfaces, it was not possible to resolve these differences as significant.

Topology is also well known to influence protein adsorption (Roach *et al*., 2006). For surfaces an increase in surface roughness has been found to increase protein (fibrinogen) adsorption (Rechendorff *et al*., 2006), which supports the findings of this study where higher protein adsorption for methyl and phenyl functionalised silica in comparison to the functionally similar but much smoother TCPS was found. Adsorption of fibrinogen was also found to be comparable between functionally modified (methyl, hydroxyl and carboxyl) surfaces (Tegoulia & Cooper, 2000).

Albumin adsorption has been shown to be reduced by increasing surface roughness for Ti surfaces; this is contrary to the findings of this study, though chemistry was unconsidered in the study of Deligianni *et al*., which may be playing a more significant role in the adsorption of this protein, compared to topology (Deligianni *et al*., 2001). Others have refuted adsorption changes with roughness for BSA or fibrinogen (Cai *et al*., 2006). More recent studies using microarrays rather than isotope labelling or bicinchoninic acid assay have reported increased uptake of albumin, fibrinogen and lysozyme to rougher (>30 nm) materials, which is in agreement with this work (Scopelliti *et al*., 2010). Deligianni *et al*. showed that there was a differential adsorption between BSA and fibronectin which they attributed as a mechanism for the enhanced adhesion and proliferation seen on the rougher surfaces (Deligianni *et al*., 2001).

The influence of surface topology or functionality may act to change the conformation or packing of proteins on the surface, this in turn may be responsible for some of the differences observed in protein adsorption between the different surfaces used in this study. Further experimental evidence would be required to demonstrate this hypothesis for these surfaces, such as application of FTIR or antibodies specific to certain epitopes to show conformational changes in proteins and measuring absolute protein concentration on the surface by protein assay or other methods like quartz crystal microbalance (Roach *et al*., 2006; Roach *et al*., 2006; Keselowsky *et al*., 2005). Though the concept that surfaces can induce specific changes in protein confirmation and packing has already been demonstrated (Roach *et al*., 2006; Keselowsky *et al*., 2005), understanding the process for these surfaces may provide further insight into the mechanism of any selective surface

produced and potentially the ability to tune the surface properties by modulating the extent of the protein surface interaction.

4.3.7 ELISA for fibronectin adsorption to the functionalised silica surfaces.

Having noted differences in the adsorption of model proteins, indirect enzyme-linked immunosorbent assay (ELISA) offered the opportunity to quantify the specific adsorption of proteins of interest to the surfaces. In this case, due to its acknowledged role in adhesion and differentiation (Keselowsky *et al*., 2003), the extracellular matrix protein fibronectin was selected for study by ELISA to determine the amount of this protein adsorbed by the differently functionalised surfaces, fig. 4.14.
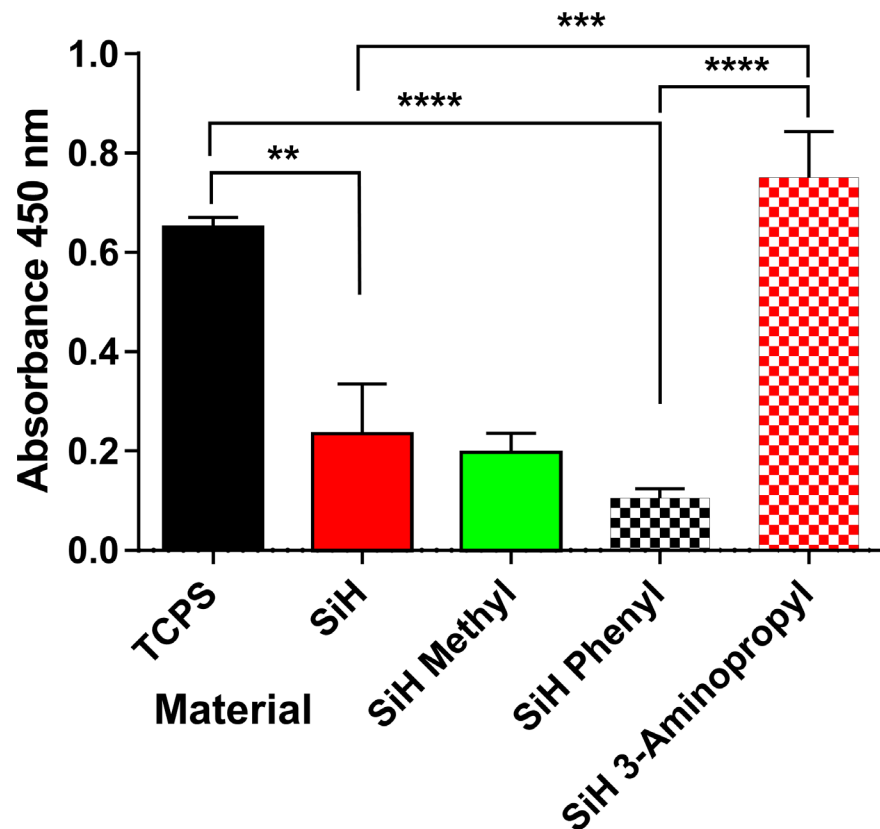
Figure: 4.14: Adsorption of fibronectin to differently functionalised silica surfaces and TCPS as measured by ELISA (n = 9).

Fibronectin (FN) has previously been measured in FCS at a concentration of between 25-30 µg/mL (Hayman & Ruoslahti, 1979). After exposure surfaces were found to adsorb FN significantly differently ($F_{(6, 57)}$ = 16.24, P<0.0001) depending on the surface. The highest FN absorbers were TCPS and the 3-aminopropyl modified silica surface, no significant

difference was detected between these surfaces, fig. 4.14. Silica, methyl and phenyl modified silica all adsorbed significantly less FN than TCPS and 3-aminopropyl modified silica, there was no significant differences between these surfaces directly, though the difference between TCPS and 3-aminopropyl modified silica was greater for phenyl modified silica than silica or methyl modified silica.

Since fibronectin (*Bos taurus*) has a theoretical pI of 5.32 and hydropathicity of -0.496 (ProtParam ExPASy, Uniprot sequence P07589), FN can be described as a negatively charged, hydrophilic protein under culture conditions (appendix B, table B2); this would explain the favouring of positively charged high energy surfaces over low energy surfaces or negatively charged high energy surfaces. This suggests that the interaction mechanism is more strongly influenced by electrostatic forces, a mechanism favoured in fundamental studies on the forces governing peptide-surface interaction (Tomczak *et al*., 2005).

The positive response of TCPS to FN uptake is notable as total protein adsorption was found to be lower than all other surfaces, also that the surface chemistry of this surface is believed to be predominately methyl groups (60.3%), with hydroxyl (21.2%) and carboxyl (16.8%) groups (Battison *et al*., 2012). However it underlines the observation of the prior Amido-black study which suggested that individual proteins respond differently to different surfaces.

Elipsometry studies by others have shown FN adsorbs at higher concentrations on hydrophobic silica as opposed to hydrophilic surfaces, though the statistic validity of the results were not tested (Jönsson *et al*., 1982). Evans & Steele showed by ELISA that for polymer surfaces FN uptake was enhanced for hydrophilic *vs*. hydrophobic surfaces (Evans & Steele, 1998). More recent studies have shown increased FN uptake on amine enriched culture surfaces like Primaria™ (Steele *et al*., 1995; Petit *et al*., 2011).

In the context of proliferation and adhesion, FN adsorption correlates well with previous studies (higher adhesion and proliferation generally correlates with greater FN adsorption), though TCPS adhesion would be expected to be higher for all cell lines, as would FM3 adhesion to the 3-aminopropyl surface. The latter at least may be due to the toxicity seen in the case of FM3 on the 3-aminopropyl surface due to the short period in culture prior to testing. In terms of motility a weak correlation (3-aminorpropyl surface as an outlier) with low FN adsorption and high motility may be discerned for FM3, which correlates with observations of motility of L929 fibroblasts on polyethylene glycol induced FN gradients (Tziampazis *et al*., 2000).

The ability to selectively tailor protein adsorption through controlled changes in surface chemistry in complex protein mixtures; perhaps acting through the 'Vroman effect' (Steele *et al.*, 1995; Curtis & Forrester, 1984), is well established and could be an important mechanism for both understanding and directing the development of selective surfaces.

4.4 Conclusions

The generation of differently functionalised silica materials was possible using alkylsilanes and the existing silica surface as a template. These materials exhibited varying properties in terms of wettability (<5° - ~90°) and a varying surface free energy (28 – 66 mN/m), which correlated with the supposed functionality introduced. The surface roughness, thickness and topology were conserved after modification. An outstanding question relates to what extent functionalisation has occurred, the identity and abundance of alternative functionalities on the surfaces requires further exploration.

Different cell lines responded significantly differently to the different surfaces in terms of adhesion and proliferation and these observations correlate with known studies for similar functionalities. In general TCPS and SiH-3AP were the favoured growth surfaces, with SiH-P the least favoured though this response was dependent on the cell line and serum conditions. The SiH-3AP surface also permitted significantly higher adhesion than all other surfaces, TCPS demonstrating the lowest adhesion performance. Proteins were also shown to interact differently with the surfaces; TCPS performed worst in term of general protein adsorption but along with the SiH-3AP surface TCPS was demonstrated to selectively adsorb FN. The interaction of proteins with the surfaces correlates with cell response and can to some extent guide the interpretation of the cell response to the surfaces.

These observations lay the foundation for a selective surface as the different responses observed can be exploited to select for a specific population of cells in co-culture. They also provide a mechanism by which selection may occur; the intermediate protein layer. As chapter three illustrated how the protein coating influences surface properties, so this chapter illustrates that surface properties may influence protein adsorption. This in turn may be applied to influence the cell, as will be examined in chapter five.

4.5 References

1. Battiston K.G, McBane J.E, Labow R.S & Santerre J.P. (2012). Differences in protein binding and cytokine release from monocytes on commercially sourced tissue culture polystyrene. *Acta Biomater.*, 8(1):89-98

2. Cai K, Frant M, Bossert J, Hildebrand G, Liefeith K & Jandt K.D. (2006). Surface functionalized titanium thin films: Zeta-potential, protein adsorption and cell proliferation. *Colloids Surf., B*, 50(1):1-8

3. Cai K, Bossert J & Jandt K.D. (2006). Does the nanometre scale topography of titanium influence protein adsorption and cell proliferation? *Biomaterials*, 49(2):136-44

4. Curtis A.S.G & Forrester J.V. (1984). The competitive effects of serum proteins on cell adhesion. *J. Cell Sci.*, 71:17-35

5. Deligianni D.D, Katsala N, Ladas S, Sotiropoulou D, Amedee J & Missirlis Y.F. (2001). Effect of surface roughness of the titanium alloy Ti-6Al-4V on human bone marrow cell response and on protein adsorption. *Biomaterials*, 22(11)1241-51

6. Dunning-Foreman N.L. (2012). Investigating the properties of cancer stem cells and epithelial to mesenchymal transition in human prostate cancer. PhD. Nottingham Trent University

7. Evans M.D.M. & Steele J.G. (1998). Polymer surface chemistry and a novel attachment mechanism in corneal epithelial cells. *J. Biomed. Mater. Res.*, 40(4):621-630

8. Gerenser L.J. (2012). XPS studies of in situ plasma-modified polymer surfaces. *J. Adhes. Sci. Technol.*, 7(10):1019-40

9. Giebel K, Bechinger C, Herminghaus S, Riedel M, Leiderer P, Weiland U & Bastmeyer M. (1999). Imaging of cell/substrate contacts of living cells with surface plasmon resonance microscopy. *Biophys. J.*, 76(1 Pt. 1): 509–16

10. Guittet M.J, Crocombette J.P & Gautier-Soyer M. (2001). Bonding and XPS chemical shifts in $ZrSiO_4$ versus SiO_2 and ZrO_2: Charge transfer and electrostatic effects. *Phys. Rev. B*, 63(12):63-70

11. Harnett E.M, Alderman J & Wood T. (2007). The surface energy of various biomaterials coated with adhesion molecules used in cell culture. *Colloids Surf., B*, 55(1):90–97

12. Hayman E.G & Ruoslahti E. (1979). Distribution of fetal bovine serum fibronectin and endogenous rat cell fibronectin in extracellular matrix. *J. Cell Biol.*, 83(1):255-9

13. Huebsch N. & Mooney D.J. (2009). Inspiration and application in the evolution of biomaterials. *Nature*, 462(7272):426-432

14. Inoue Y & Takai O. (1996). Spectroscopic studies on preparation of silicon oxide films by PECVD using organosilicon compounds. *Plasma Sources Sci. Technol.*, 5(2):339-43

15. Jönsson U, Ivarsson B, Lundström I & Berghem L. (2012). Adsorption behaviour of fibronectin on well-characterized silica surfaces. *J. Colloid Interface Sci.*, 90(1):148-63

16. Keselowsky G.K, Collard D.M, García A.J. (2003). Surface chemistry modulates fibronectin conformation and directs integrin binding and specificity to control cell adhesion. *J. Biomed. Mater. Res., Part A*, 66(2):247-59

17. Keselowsky B.G, Collard D.M & García A.J. (2005). Integrin binding specificity regulates biomaterial surface chemistry effects on cell differentiation. *Proc. Natl. Acad. Sci. U. S. A.*, 102(17):5953-5957

18. Kilian K.A & Mrksich M. (2012). Directing Stem Cell Fate by Controlling the Affinity and Density of Ligand–Receptor Interactions at the Biomaterials Interface. *Angew. Chem. Int. Ed.*, 51(20):4891-5

19. Kunas K.T & Papoutsakis E.T. (1990). The protective effect of serum against hydrodynamic damage of hybridoma cells in agitated and surface-aerated bioreactors. *J. Biotechnol.*, 15(1-2):57-70

20. Lee J.H, Jung H.W, Kang I & Lee H.B. (1994). Cell behaviour on polymer surfaces with different functional groups. *Biomaterials*, 15(9):705-11

21. Li M, Mondrinos M.J, Gandhi M.R, Ko F.K, Weiss A.S, Lelkes P.I. (2005). Electrospun protein fibers as matrices for tissue engineering. *Biomaterials*, 26(30):5999-6008

22. Maitland N.J, Macintosh C.A, Hall J, Sharrard M, Quinn G & Lang S. (2001). *In vitro* models to study cellular differentiation and function in human prostate cancers. *Radiat. Res.*, 155(1):133-142

23. McClary K.B, Ugarova T & Grainger D.W. (2000). Modulating fibroblast adhesion, spreading, and proliferation using self-assembled monolayer films of alkylthiolates on gold. *J. Biomed. Mater. Res.*, 50(3):428-39

24. NIST X-ray Photoelectron Spectroscopy Database, Version 4.1 (National Institute of Standards and Technology, Gaithersburg, 2012); http://srdata.nist.gov/xps/.

25. Osterholtz F.D. & Pohl E.R. (2012). Kinetics of the hydrolysis and condensation of organofunctional alkoxysilanes: a review. *J. Adhes. Sci. Technol.*, 6(1):127-49

26. Palazzolo B, Heng H, Mohammad R, Theocharous P & Eliason J.F. (2005). Characterization of three pairs of prostate cells lines derived from tumour and adjacent normal tissues. *AACR Meet. Abstr.*, 2005:462

27. Park J, Bauer S, Schmuki P & von der Mark K. (2009). Narrow Window in Nanoscale Dependent Activation of Endothelial Cell Growth and Differentiation on TiO2 Nanotube Surfaces. *Nano Lett.*, 9(9):3157-64

28. Petit A, Demers C.N, Girard-Lauriault P.L, Stachura D, Wertheimer M.R, Antoniou J & Mwale F. (2011). Effect of nitrogen-rich cell culture surfaces on type X collagen expression by bovine growth plate chondrocytes. *Biomed. Eng.* Online. 10(4) doi: 10.1186/1475-925X-10-4

29. Rechendorff K, Hovgaard M.B, Foss M, Zhdanov V.P & Besenbacher F. (2006). Enhancement of Protein Adsorption Induced by Surface Roughness. *Langmuir*, 22(26):10885-8

30. Repetto G, del Peso A & Zurita J.L. (2008). Neutral red uptake assay for the estimation of cell viability/cytotoxicity. *Nat. Protoc.*, 3(7):1125-1131

31. Reyes C.D. & García A.J. (2003). A centrifugation cell adhesion assay for high-throughput screening of biomaterial surfaces. *J. Biomed. Mater. Res., Part A*, 67A(1):328–333

32. Roach P, Shirtcliffe N.J, Farrar D & Perry C.C. (2006). Quantification of surface-bound proteins by fluorimetric assay: comparison with quartz crystal microbalance and Amido Black assay. *J. Phys. Chem. B*, 110(41):20572-20579

33. Roach P, Farrar D & Perry C.C. (2006). Surface Tailoring for Controlled Protein Adsorption: Effect of Topography at the Nanometer Scale and Chemistry. *J. Am. Chem. Soc.*, 128(12):3939-45

34. Ruiz C, Holz D.R, Oeggerli M, Schneider S, Gonzales I.M, Kiefer J.M, Zellweger T, Bachmann A, Koivisto P.A, Helin H.J, Mousses S, Barrett M.T, Azorsa D.O & Bubendorf L. (2010). Amplification and overexpression of vinculin are associated with increased tumour cell proliferation and progression in advanced prostate cancer. *J. Pathol.*, 223(4):543-52

35. Scopelliti P.E, Borgonovo A, Indrieri M, Giorgetti L, Bongiorno G, Carbone R, Podesta A & Milani P. (2010). The Effect of Surface Nanometre-Scale Morphology on Protein Adsorption. *PLos One*, 5(7):e11862

36. Sobel R.E & Sadar M.D. (2005). Cell lines used in prostate cancer research: A compendium of old and new lines - Part 1. *J. Urol.*, 173(2):342-59

37. Steele J.G, Dalton B.A, Johnson G & Underwood P.A. (1995). Adsorption of fibronectin and vitronectin onto Primaria™ and tissue culture polystyrene and relationship to the mechanism of initial attachment of human vein endothelial cells and BHK-2 1 fibroblasts. *Biomaterials*, 16(14):1057-1067

38. Stobie N, Duffy B, McCormack D.E, Colreavy J, Hidalgo M, McHale P & Hinder S.J. (2007). Prevention of Staphylococcus epidermidis biofilm formation using a low-temperature processed silver-doped phenyltriethoxysilane sol-gel coating. *Biomaterials*, 29(8):963-9.

39. Tan J & Saltzman W.M. (2002). Topographical control of human neutrophil motility on micropatterned materials with various surface chemistry. *Biomaterials*, 23(15):3215-25

40. Tegoulia V.A & Cooper S.L. (2000). Leukocyte adhesion on model surfaces under flow: Effects of surface chemistry, protein adsorption, and shear rate. *J. Biomed. Mater. Res.*, 50(3):291-301

41. Tomczak M.M, Glawe D.D, Drummy L.F, Lawrence C.G, Stone M.O, Perry C.C, Pochan D.J, Deming T.J & Naik R.R. (2005). Polypeptide-templated synthesis of hexagonal silica platelets. *J. Am. Chem. Soc.*, 127(36):12577-82

42. Tziampazis E, Kohn J & Moghe P.V. (2000). PEG-variant biomaterials as selectively adhesive protein templates: model surfaces for controlled cell adhesion and migration. *Biomaterials*, 21(5):511-20

43. Wasil M, Halliwell B, Hutchison D.C.S & Baum H. (1987). The antioxidant action of human extracellular fluids. *Arch. Biochem. Biophys.*, 280(1):1-8

44. Webb K, Hlady V & Tresco P.A. (2000). Relationships among cell attachment, spreading, cytoskeletal organization, and migration rate for anchorage-dependent cells on model surfaces. *J. Biomed. Mater. Res.*, 49(3):362-8

Chapter Five

Applying Cell Response to Inorganic Materials: Developing a Selective Surface

5.1 Introduction

Selection or enrichment of cell sub-populations is achieved today primarily through the application of bio-conjugate chemistry and immunological mechanisms. Foremost in this is the fluorescence activated cell sorter (FACS) where the combination of immunofluorescence labelling, fluorometry and electrostatic deflection as described in section 2.14 permits the sorting of multiple cell populations with differential immunofluorescence labelling (Hawley & Hawley, 2004). Selective columns (such as magnetically assisted cell sorting [MACS] columns) have also been available for some time, which again use the affinity of a biomolecule to a cell specific molecule such as a surface glycoprotein to capture sub-populations of cells from mixed populations, in the case of MACS the separation is achieved by a magnetic bead system (Miltenyi *et al*., 1990). These techniques are becoming ever more advanced, with emerging concepts being the miniaturisation of systems like flow cytometry to 'lab-on-a-chip' formats, integrated sample preparation and movement away from fluorescence to magnetic or isotopic separation to permit greater labelling combinations (Helou *et al*., 2013).

Limitations of all these techniques include:

- Limited to the requirement of differential immunostaining. If no antibody or well defined target is available or the target is internal then these methods are not generally applicable.

- Heavily pre-disposed to non-adherent cell lines, since cell-cell adhesion is undesirable due to the potential that two different cells types could be sorted together by attachment to one another.

- Cell surface proteins are attacked by the proteases required to remove adherent cells from the culture system, potentially altering observed marker expression.

- Expensive in terms of the reagents and technical expertise required.

- Finally while they are able to sort they are unable to maintain a transient cell sub-population post-sort as the selective pressure is limited in duration to the point of sorting.

The response of a cell sub-population to a culture surface of defined properties holds considerable potential in the field of cell selection and enrichment, not least because the majority of the criticisms surrounding the above techniques are not applicable. The caveat to this approach however is that a suitable mechanism and surface for the cell response required (e.g. differentiate from phenotype A to B and maintain B) must be defined. As demonstrated in the previous chapter different cell lines respond differently to surfaces with different surface properties. With differing responses, proliferation, adhesion or motility the potential for the development of a selective surface by one of these mechanisms becomes possible if a suitable model is available (fig. 5.1).
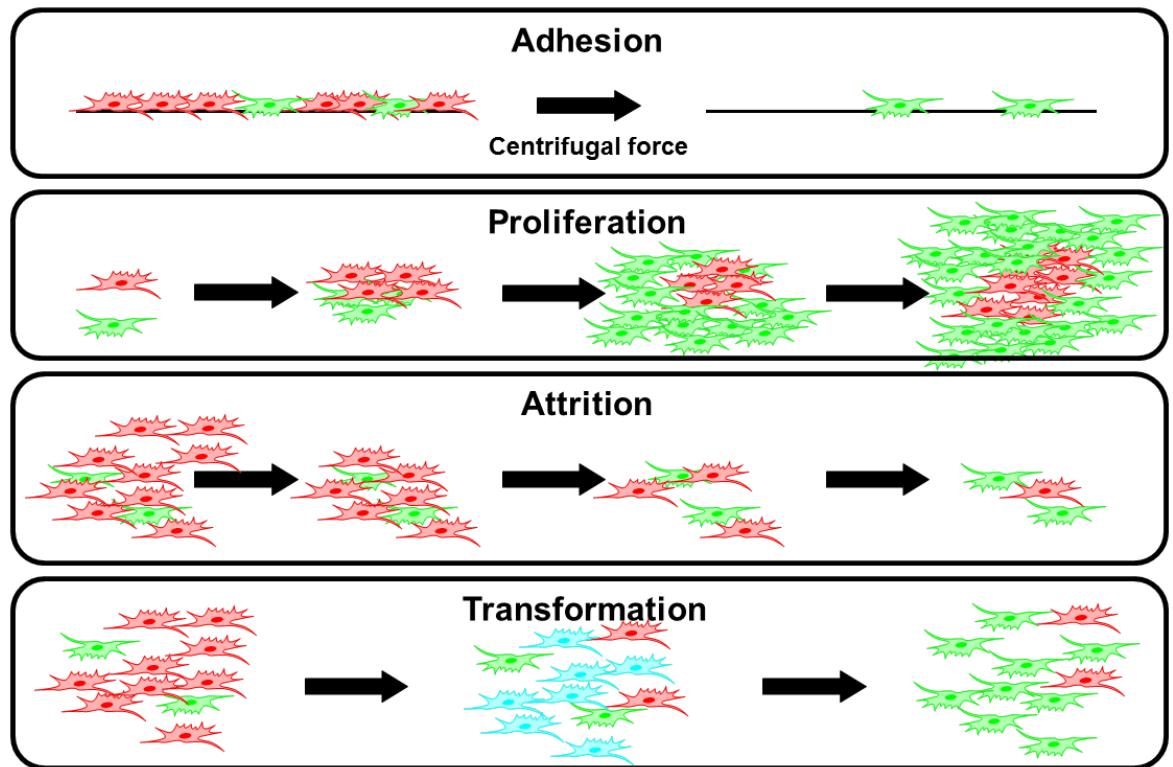
Figure: 5.1: Different mechanisms (adhesion, proliferation, attrition and transformation) of selection that could potentially be applied using material surface properties to guide the cell response.

The first strategy 'adhesion' builds on the understanding that cells adhere differently to different materials as demonstrated in the previous chapter (4.3.3), if a surface could be engineered on which a cell type is more adherent then selection would be achieved. The

'proliferation' and 'adhesion' strategies build on the observation that cells are selectively tolerant to different materials (4.3.2), these strategies represent two sides of the same effect in that for a particular surface in which only one cell type is tolerant then one population will survive and be relatively enriched compared to the intolerant cell type. The final strategy operates on the understanding that the cell receives cues from its environment (1.2.5), cells with the potential to differentiate may be directed by the cues they receive from their environment to transform to the desired phenotype in a controlled manner.

Application of these strategies requires an understanding of cell-surface response which is currently incomplete or unavailable. However, many studies have demonstrated that different surface properties like topology and functionality influence the proliferation, adhesion and morphology of cells in culture and work continues to catalogue the bulk population responses of different cell lines to different materials (Lee *et al.*, 1993; da Costa *et al.*, 2011; Ni *et al.*, 2012). Others have demonstrated that the role of the tissue culture surface in influencing the culture can be more than just the ability to modify bulk effects in the culture but to specifically control cell fate. For example it has been demonstrated that through control of the density of the well-known cell adhesion ligand, the RGD peptide, the fate of mesenchymal stem cells can be regulated (Killian & Mrksich, 2012).

Further to this it has been demonstrated that the surface itself (opposed to the linking of biological entities with known bioactivity) through exhibited properties like topology can direct cell fate (Connelly *et al.*, 2010). The use of materials with defined surface properties to control the fate of the culture is an emerging area; another study has shown how patterning a surface on the nano-scale can produce a surface on which mesenchymal cells can be maintained for extended periods in absence of differentiation (McMurray *et al.*, 2011). Through being able to modify surface properties and understand the impact on cell response, the potential of a new generation of bioactive materials for biomaterials application and for use *in vitro* become possible.

To investigate material selectivity, prior understanding of cell responses for two different cell lines (FM3 & OPCT1) was applied. In a manner inspired by the crude selective strategy using surfaces applied to the isolation of different types of white blood cell from PBMC (Sallusto & Lanzavecchia, 1994), OPCT1 cells with their greater adhesive strength for a given material would be isolated from co-culture with FM3.

5.2 Materials & Methods

5.2.1 Materials

Tissue culture polystyrene in 96 and 24 well formats were obtained from Sarstedt (Germany). Polyaniline hydrochloride, ammonium persulphate, glutaric dialdehyde, lysozyme, TWEEN® 20, sodium phosphate monobasic, sodium phosphate dibasic, paraformaldehyde, 3-amino-7-dimethylamino-2-methylphenazine hydrochloride (Neutral Red dye), 0.4% trypan blue solution, 3-aminopropyltriethoxysilane (APTEOS) and tetramethoxysilane (TMOS) were obtained from Sigma-Aldrich® (UK). Bovine foetal calf serum (FCS), 1 M hydrochloric acid, methanol, cover slips, glass slides (Menzel-Gläser) and glacial acetic acid were obtained from Thermo Fisher Scientific (UK). EtOH was supplied by Hayman Speciality Products (UK). Calbiochem® BSA fraction IV was supplied by EMD Millipore (UK). Dulbecco's phosphate buffered saline (DPBS); RPMI-1640 medium, trypsin-versene (EDTA) solution and L-glutamine solution were obtained from Lonza BioWhittaker™ (UK). Keratinocyte serum free medium (KSFM) with L-glutamine and TrypLE™ Express were obtained from Gibco®, Life Technologies™ (UK). Rabbit polyclonal anti-human vimentin and rat monoclonal (DECAM-1) anti-human E-cadherin were supplied by abcam® (UK). Monoclonal phycoerythrin conjugated mouse IgG1 anti-human vimentin (clone RV202) and purified mouse IgG2a anti-E-cadherin (clone 36/E-Cadherin) were obtained from BD Pharmingen™ and BD Transduction Laboratories™ (UK) respectively. Alexa Fluor® 488 conjugated goat anti-mouse IgG, Alexa Fluor® 488 conjugated goat anti-rabbit IgG, Alexa Fluor® 568 conjugated goat anti-mouse IgG, , Alexa Fluor® 568 conjugated goat anti-rat IgG, LIVE/DEAD® Fixable Dead Cell Stain Kit, rabbit IgG isotype control and rabbit IgG isotype control was supplied by Invitrogen®, Life Technologies™ (UK). Mouse hybridoma anti-human HLA-A2 was generated locally by others from HB54 cell line obtained from the American type culture collection, USA. VECTASHIELD® mounting medium with 4', 6-diamidino-2-phenylindole (DAPI) was obtained from Vector Laboratories (USA). The FM3 cell line was originally obtained from Prof. G. Pawelec, University of Tübingen, Germany. The OPCT1 cell line was originally obtained from Onyvax, UK. Distilled and deionised water (ddH$_2$O) was produced locally by distillation and ion exchange filtration, resulting in a pH of 5.8 and a conductivity of < 1 μS/cm^{-1}.

5.2.2 Surface fabrication

Surfaces were fabricated as per the general method described in section 4.2.2.

5.2.3 Tissue culture of adherent human cell lines

FM3 culture conditions were RPMI-1640 growth medium supplemented with 1% L-glutamine and 10% FCS extract. Confluent cultures were passaged or introduced onto culture surfaces by removal of growth media, washing twice with DPBS and then 1x trypsin solution. After 5 min incubation, cells were aspirated and pelleted by centrifugation (3 min at 400 RCF), the trypsin solution was removed and the cells suspended in media. Cells (number determined by haemocytometer) were then introduced onto (ultra-violet (UV) sterilised for 15 min) culture surfaces or tissue culture flasks. OPCT1 culture conditions were KFSM medium supplemented with 1% L-glutamine and 2% bovine (FCS) extract. During passage, cells were treated with 1x TrypLE™ Express trypsin substitute but otherwise treated the same as FM3.

5.2.4 Enrichment & cell selection strategies

Two different strategies were used for cell enrichment, the first focussing on cell adhesion, the second based on surface induced cell response.

5.2.4.1 Enrichment by cell adhesion

FM3 and OPCT1 cells were seeded at a ratio of 1:1, at a density of 2.5^x10^3 cells per cm^3 to TCPS 24 well plates and allowed to adhere over a period of 24 h with 1 mL of RPMI and KFSM serum free media in a 1:1 ratio. The plates were then exposed to 160 RCF for a period of 5 min. Following this process the original media (and any detached cells) were aspirated and the cells treated with 200 µL of TrypleXpress for 30 min to remove the remaining adhered cells. After cells were stained for HLA-A2 (differentially expressed between OPCT1 and FM3) using method 5.2.6 and assessed by flow cytometry using method 5.2.9.

5.2.4.2 Enrichment by surface induced cell response

OPCT1 cells were seeded at a density of 2.5^x10^3 cells per cm^2 in the TCPS 24 well plate format. Cells were allowed to proliferate till confluence under normal culture conditions. Prior to confluence cells were treated with 200 µL of TrypleXpress for 30 min to remove the adhered cells after washing twice with 1 mL of PBS. Cells were then reseeded to the surfaces at their original concentration of 2.5^x10^3 cells per cm^3 for a second

round of expansion. Prior to the second confluence cell sub-populations were assessed by either flow cytometry (method 5.2.9) or immunofluorescence (method 5.2.7) to determine population changes over the preceding enrichment period.

5.2.5 Neutral red proliferation/viability assay

The assay was performed in the manner described in section 4.2.8.

5.2.6 Sub-population & cytoskeleton visualisation by immunostaining

The staining protocol for 24 well plates as described in section 4.2.10 was used. The dilution factor of the primary and secondary antibodies used is given in table 5.1.

Table 5.1: Antibodies and conditions for immunostaining

Antibody (Primary)	Dilution
Mouse hybridoma anti-human HLA-A2	1:20
Mouse anti-human E- cadherin	1:100
Rat anti-human E-cadherin	1:100
Rabbit polyclonal anti-human Vimentin	1:235.3
Secondary	
Goat anti-Mouse Alexa Flour® 488	1:1500
Goat anti-Mouse Alexa Flour® 568	1:1000
Goat anti-Rat Alexa Flour® 568	1:1000
Goat anti-Rabbit Alexa Flour® 488	1:1500

5.2.7 Light and immunofluorescence microscopy

Light microscopy was conducted using a Nikon Eclipse TS100 light microscope with 10x0.25 (WD 6.2), 20x0.40 (WD 3.0) and 40x0.55 (WD 2.1) objectives. Images were digitised with a Nikon DN100 Digital Net Camera with 0.7x magnification. Apoptotic cells when necessary were stained with 0.4% trypan blue solution in a ratio of one part dye to four parts media.

Immunofluorescence (IF) microscopy was conducted using a BX51 fluorescence microscope using 20x and 40x objectives (Olympus, UK). Images were digitised with a DF71 digital camera (Olympus, UK) controlled through CellF v.2.6 software (Olympus Soft Imaging Solutions GmbH, Germany). Cell sub-population size was determined

manually using ImageJ (v.1.7) Cell Counter plugin for at least four replicate images of each condition.

5.2.8 Confocal microscopy

Confocal micrographs were obtained using an SP5 Confocal Microscope (Leica, Germany). Scans for different excitation and emission channels were conducted sequentially to prevent crosstalk with 2-6 lines averaged during scanning. Scan resolution was 1024x1024, confocal aperture 1 AU and bidirectional scanning enabled.

5.2.9 Flow cytometry

Cells were detached from the surface using the standard conditions for that cell line (method 5.2.3). Upon release cells were washed once in DPBS and the concentration adjusted to 1^x10^6 cells per mL in 1 mL. A live dead stain was introduced; 1 µL of LIVE/DEAD® Fixable Dead Cell Stain Kit per tube, prepared at room temperature by reconstituting one vial of LIVE/DEAD® Fixable Dead Cell Stain with 50 µL of DMSO. Cells were then incubated for 30 min at room temperature before being washed once with DPBS. Fixation was performed for 15 min at 37°C using 1 mL of 2% paraformaldehyde. After fixation cells were permeabilised by incubation on ice for 30 min with 1 mL of ice cold MeOH. Cells were then blocked with two washes of blocking solution (0.5% (w/v) BSA fraction IV) in DPBS before incubation for 10 min in blocking solution. Cells were then stained for 1 h with one unit (5 µL) of monoclonal phycoerythrin conjugated mouse IgG1 anti-human vimentin (clone RV202) in 100 µL of blocking solution. After incubation cells were washed twice with blocking solution and once with isoton before immediate analysis performed using a Gallios™ flow cytometer (Beckman Coulter, UK). A live dead control was obtained by mixing at a ratio of 50:50, normally treated cells to cells killed by 30 min exposure to 57°C. An isotype control was used to correct for background staining. Initial cytometer method development and compensation was kindly provided by Dr. S. McArdle and Mrs C. Johnson. Analysis was performed using the Kaluza (v.1.2) software package (Beckman Coulter, UK).

5.2.10 Statistical testing

Statistical testing was conducted using the GraphPad Prism 6 (v.6.01) software package (GraphPad Software, USA). Significant features in the proliferation and enrichment data

were respectively determined using ANOVA with Bonferroni's multiple comparisons post-test or either unpaired two tailed t-test or one way ANOVA with repeated measures and Tukey's multiple comparisons post-test. In both cases the assumptions of normality and constant variance were assessed. In the following work all error unless otherwise stated is presented as standard error of the mean. The following notation is used to denote significance; (*) $P \leq 0.05$ significant, (**) $P \leq 0.01$, (***) $P \leq 0.001$ and (****) ≤ 0.0001.

5.3 Results & discussion

5.3.1 Selection using cell adhesion as the selective pressure

OPCT1 and FM3 differentially express the Human leukocyte antigen (HLA) HLA-A2 (OPCT1 negative, FM3 positive) which was used to distinguish them in co-culture (appendix C, fig. C1). After the enrichment procedure (method 5.2.4.1) cells were analysed by flow cytometry to determine if enrichment had occurred, fig. 5.2. Non-specific staining isotype controls are shown in appendix C, fig. C2.
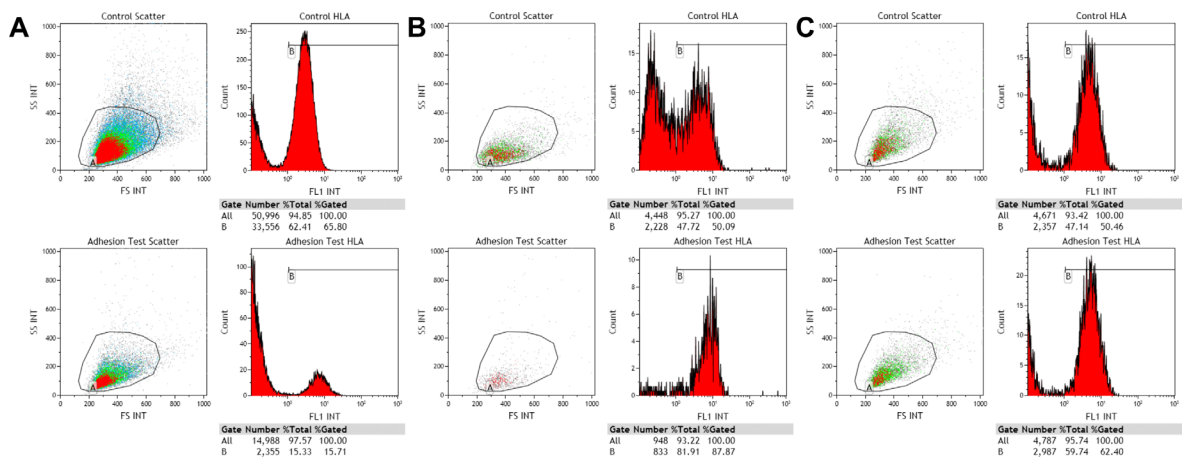
Figure: 5.2: Flow cytometry of adhesion based selection of cells from OPCT1 and FM3 co-culture. Histograms (A, B, C) show three independent replicates measuring HLA-A2 expression before (top) and after (bottom) enrichment. Non-specific staining isotype controls are shown in appendix C, fig. C2.

Initial results showed a clear change in population post-selection, with the enrichment of the HLA-A2 positive population FM3, fig. 5.2B. However selection was in an unexpected direction, the more weakly adherent (section 4.3.3) HLA-A2 positive FM3 population on TCPS was not expected to be enriched. Repetition of the experiment showed inconsistent results, in most cases no change was observed (fig. 5.2C), and changes when seen were not limited to one direction, fig. 5.2A, B.

Selection using adhesion characteristics between the two lines did not work as expected; despite the known adherence characteristics of these cell lines from previous work (section 4.3.3). Understanding why provided insight into how co-cultured cells perform in the tissue culture environment, in addition to the limitations of the method and culture system adopted. An initial concern was the requirement of different media between the two lines, however both lines were viable over a seven day period when cultured in either media or the composite media used for the study. However the potential for media effects to change the properties of the cells under investigation under non-standard conditions could not be excluded.

Additionally on observation of the cell lines in culture, it was noted that the distribution of the cells was not necessarily uniform; sedimentation may drive cells to a gradient from the centre to the edges of the well, fig. 5.3A. Variation in cell concentration has implications for the culture; firstly the generation of local micro-environments (gradients of ECM and cell contact) which make the culture non-uniform as cells respond differently at different densities (Iwasa *et al*., 2003). Additionally a cell gradient allows cells surrounded by other cells to move completely from the surface making contact purely to the membrane of underlying cells, avoiding the desired selective pressure. This is a problem inherent to the assumption of a 2+1D culture system (refer to section 1.3.3) when cells culture in 3D.

With cells in close proximity the potential also exists for cells to make contact with one another as cell-cell adhesion is possible though a number of mechanisms such as tight junctions (Gumbiner, 1996). The two different cell types may interact to change their respective properties; a weakly adhered cell may be more adhesive if in contact with a more strongly adherent cell type. The potential for the two distinct cell populations to conduct cell-cell contact through tight junctions was examined through confocal microscopy using E-cadherin to highlight tight junction formation; which was shown to be the case, fig. 5.3B.
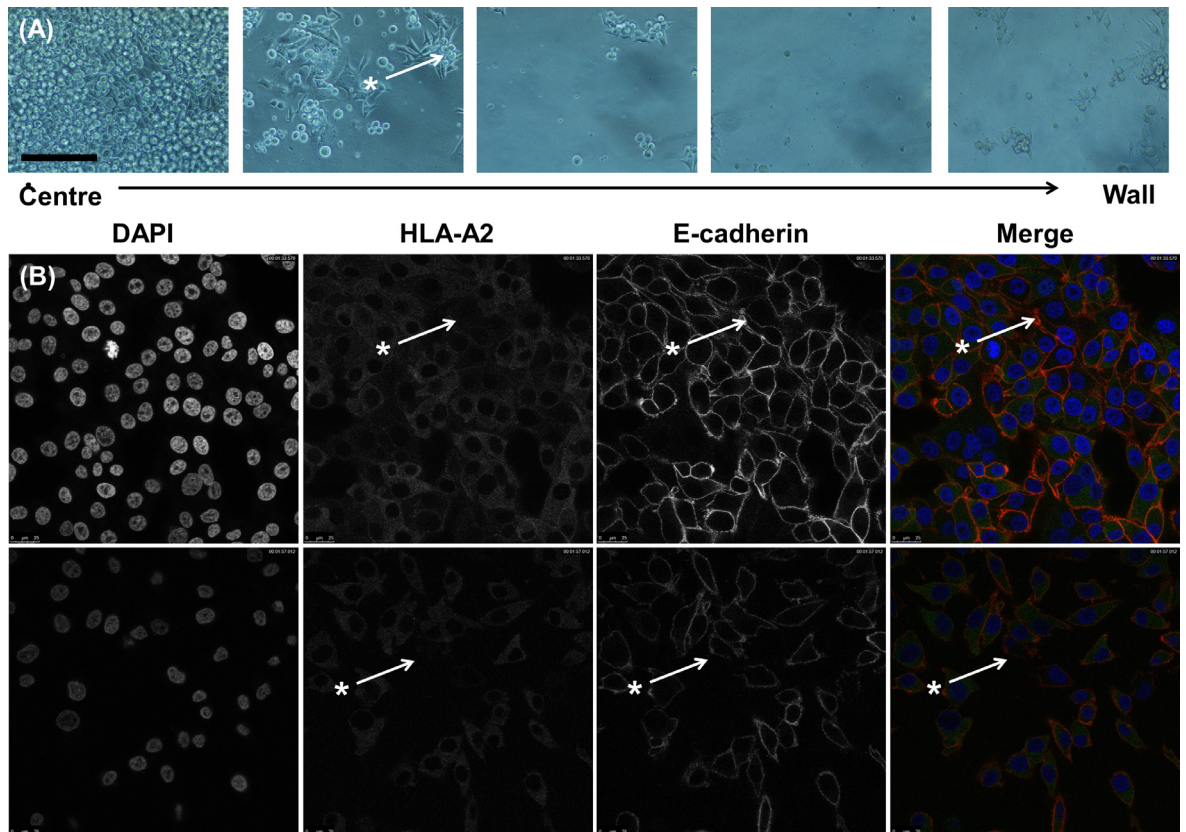
Figure: 5.3: Light micrographs of FM3 and OPCT1 co-culture across a tissue culture plate where differential deposition has occurred (A), highlighted region (*) shows an example of cell aggregation. Scale bar represents 40 μm. Confocal fluorescence micrographs (B) showing tight junction formation between FM3 (HLA-A2 positive) and OPCT1 (HLA-A2 negative) cells in co-culture. Regions highlighted (*) show cells of different HLA-A2 phenotypes demonstrating E-cadherin (tight junction) co-localisation. Non-specific staining isotype controls are shown in appendix C, fig. C3.

While this system was unsuccessful (or at least irreproducible), success in the area of selection through adhesive characteristics has been demonstrated recently by others using a microfluidic system using shear force instead of centrifugal force to separate human pluripotent stem cells from other cell types (Singh *et al*., 2013). However since the selective pressure is limited to the point of selection this method would suffer from the problems noted above in that the isolated population would be vulnerable to being lost once placed back in standard culture conditions and as such this strategy was discarded.

5.3.2 Selection using surface functionality as the selective pressure

With the failure of selection between multiple cell lines using the adhesion strategy, a different approach was selected. In the previous chapter it was shown that populations of OPCT1 cells show translocation of vinculin to the nucleus (fig. 4.10), this translocation is associated with nuclear translocation of β-catenin (adhesion protein involved in gene transcription) and is a marker that epithelial to mesenchymal (EMT) transition has occurred within the cell line (Simcha *et al*., 1998; Eger *et al*., 2000).

Work by Dunning-Foreman on OPCT1 demonstrated OPCT1 sub-populations that express a range of EMT markers that would suggest that EMT is occurring and mixed populations exist in the cell line (Dunning-Foreman, 2012). These markers included cytokeratin (intermediate filament associated with epithelial cells) positive and negative populations (Moll *et al*., 1982), fibronectin (extracellular matrix protein associated with mesenchymal cells, among others) expression with mesenchymal markers (Mani *et al*., 2008), N-cadherin (associated with mesenchymal cells, among others) expression (Mani *et al*., 2008; Zeisberg & Neilson, 2009) and CD44 expression (Mani *et al*., 2008). Expression of E-cadherin suppressor transcription factors associated with induced EMT, including Snail, Slug and Twist were also demonstrated (Casas *et al*., 2011; Dunning-Foreman, 2012; Mani *et al*., 2008).

Cells of an epithelial or mesenchymal phenotype are of considerable interest in cancer research due to the role mesenchymal cells are believed to play in metastasis, breaking away from the primary tumour to induce tumourogenesis at another site (Thiery *et al*., 2009). Within this the phenomenon of epithelial-mesenchymal transition (EMT) is of particular interest as it explains how cells from the primary tumour can potential escape to initiate a tumour elsewhere after undergoing EMT and the reverse process mesenchymal-epithelial transition (MET) (Thiery *et al*., 2009).

OPCT1 is a cell line which contains many different cell phenotypes; these can be readily identified morphologically using conventional microscopy, fig 5.4A, B, C. Two specific sub-populations of interest within OPCT1 include the epithelial like and mesenchymal like cells, which can be readily identified by the morphology they exhibit with epithelial cells clustering together with well-defined cell-cell contact and mesenchymal cells being loosely clustered with weak intra-cellular contact, fig. 5.4C (Gumbiner, 1996). This morphological assessment can be confirmed through the use of markers associated with epithelial cell types such as the cell-cell adhesion molecule E-cadherin and markers for mesenchymal cell

types such as vimentin, an intermediate filament (Korita *et al.*, 2010; Berx & van Roy, 2008). Epithelial like cells should express E-cadherin highly but not express vimentin highly and *vice versa* for mesenchymal cells, fig. 5.4D.
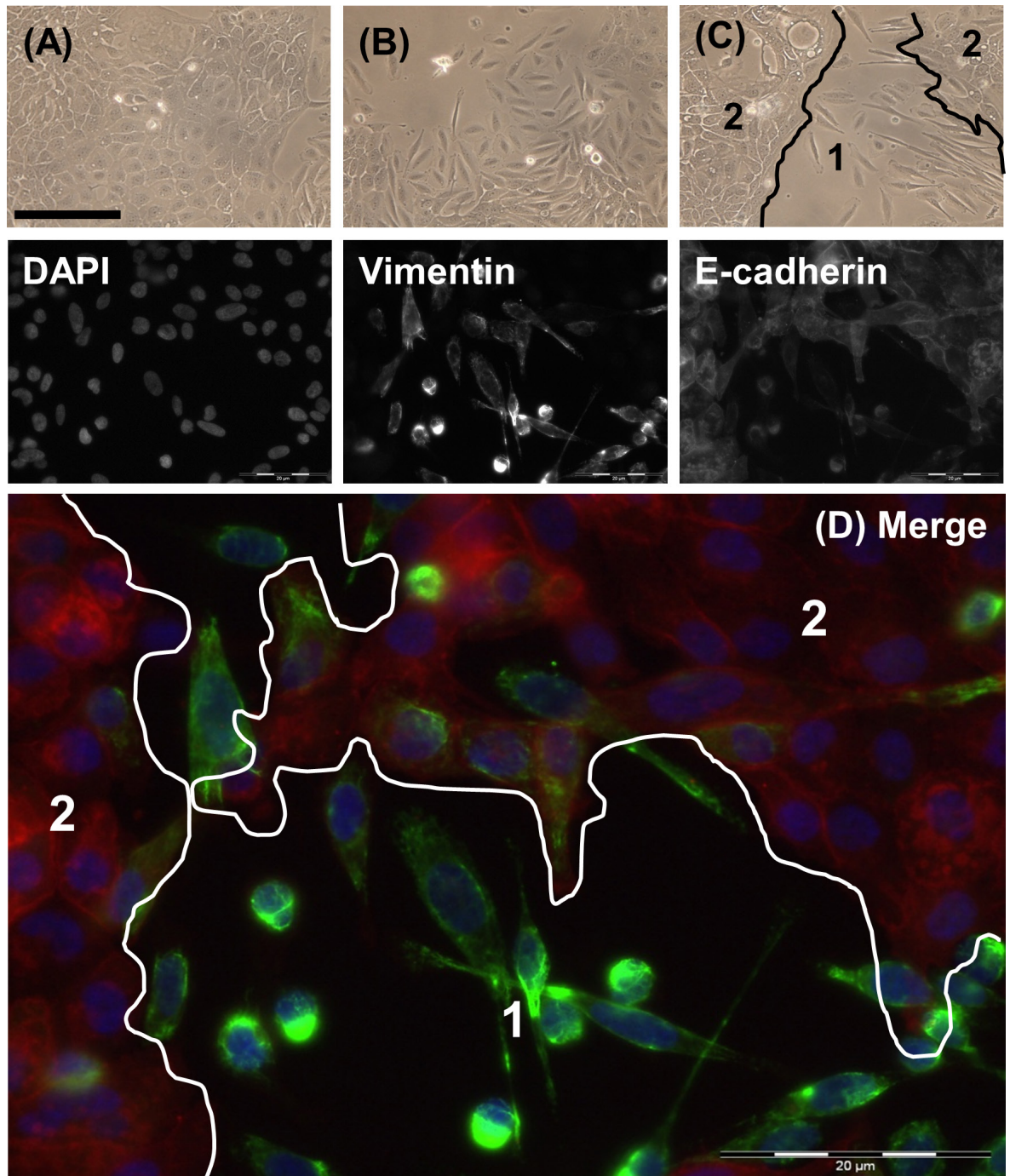
Figure 5.4: Light micrographs (A) and (B) illustrate some of the different morphological sub-populations of OPCT1, scale represents 45 μm. Micrograph (C) has been annotated to highlight the differences in morphology between the mesenchymal (1) and epithelial (2) populations. IF micrograph (D) highlights these different sub-populations through the differential expression of the EMT markers vimentin (green) and E-cadherin (red), blue

represents nuclear staining (DAPI). Non-specific staining isotype controls are shown in appendix C, fig. C4.

IF staining demonstrated that there are cell sub-populations within the OPCT1 cell line that match the supposed epithelial (fig. 5.4D2) and mesenchymal phenotypes (fig. 5.4D1). Close examination of the different sub-populations of OPCT1 by IF microscopy demonstrates a classical 'epithelial' population, fig. 5.5A. A tightly clustered group of cells with strong cell-cell contact with clear E-cadherin expression and no observable expression of vimentin. One phenotype observed (albeit in low abundance) represents an intermediate population of cells (fig. 5.5B) with both high E-cadherin and vimentin expression and cell-cell contact with clustering, if this represents cells undergoing a transitional activity like EMT or MET is unknown. The 'mesenchymal' population shows much greater diversity (fig. 5.5C, D, E and F) in morphology, which may represent in itself further sub-divisions. Overall, an elongated morphology can be observed (length may vary) with limited to no cell-cell contact or clustering and high expression of vimentin but low to no expression of E-cadherin. A difference in the morphology of the nucleus was also seen with a larger and more oval nucleus observed in mesenchymal populations. Finally a population exists that shows neither mesenchymal nor epithelial staining, but demonstrates epithelial characteristics of clustering and cell-cell contact (fig. 5.5G); again this represents a small sub-population of cells and may represent epithelial cells expressing a low level of E-cadherin.
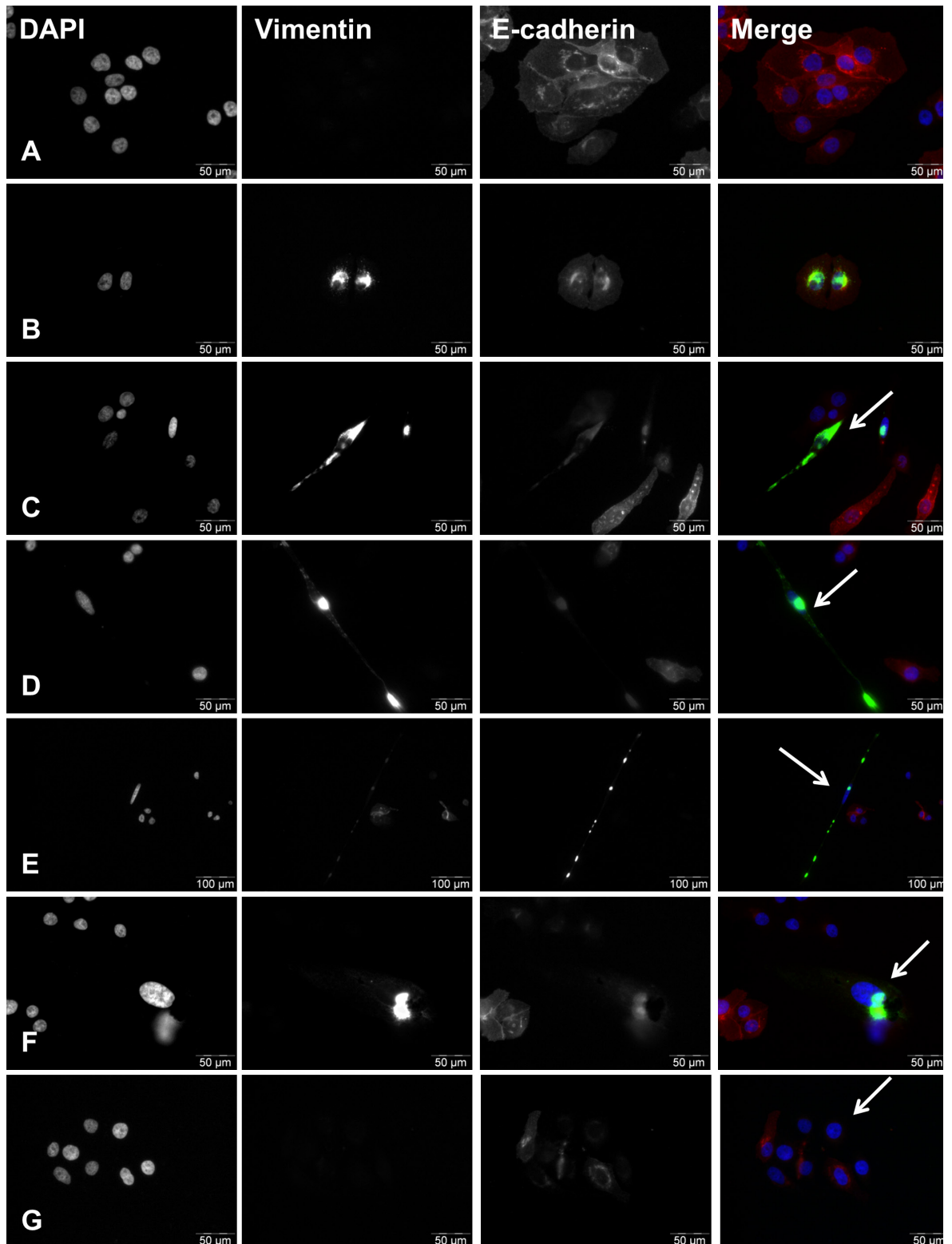
Figure 5.5: Immunofluorescence micrographs highlighting (note arrows) in detail the different sub-populations of OPCT1 based on the differential expression of vimentin (green) and E-cadherin (red), DAPI (blue) nuclear staining is also represented. Different cell populations represented by the micrograph series A-G. Non-specific staining isotype controls are shown in appendix C, fig. C4.

This diversity is problematic in terms of classifying cells during the process of enrichment, especially across different experimental procedures. For the purposes of this study the 'mesenchymal' population was considered as any population which shows high vimentin expression, 'epithelial' was defined as all else. This will result in the addition of the mixed phenotype (fig. 5.5B) to the 'mesenchymal' population; due to the small size of this population it should not be expected to impact on the study's conclusions. This will similarly be the case for the double negative phenotype (fig. 5.5G) included in the 'epithelial' population. Again as a minority population this should not be a significant issue and overall the methodology, though a simplification of the culture, should make assessment of cell populations robust, but these caveats must be considered when simple marker panels are used.

Fig. 5.5 demonstrated that a multitude of different cell populations exist within OPCT1 and that these sub-populations can be readily identified and monitored using existing markers. This makes OPCT1 an ideal model cell line for studying the changing cell populations in response to a perturbation such as a selective culture surface. Additionally current tissue culture materials are inadequate for the extended culture of cells of the 'mesenchymal' phenotype due to uncontrolled differentiation effects resulting in loss of the population over time, fig. 5.6. This makes the sub-populations of OPCT1 relevant to current problems in tissue culture (McMurray *et al*., 2011).
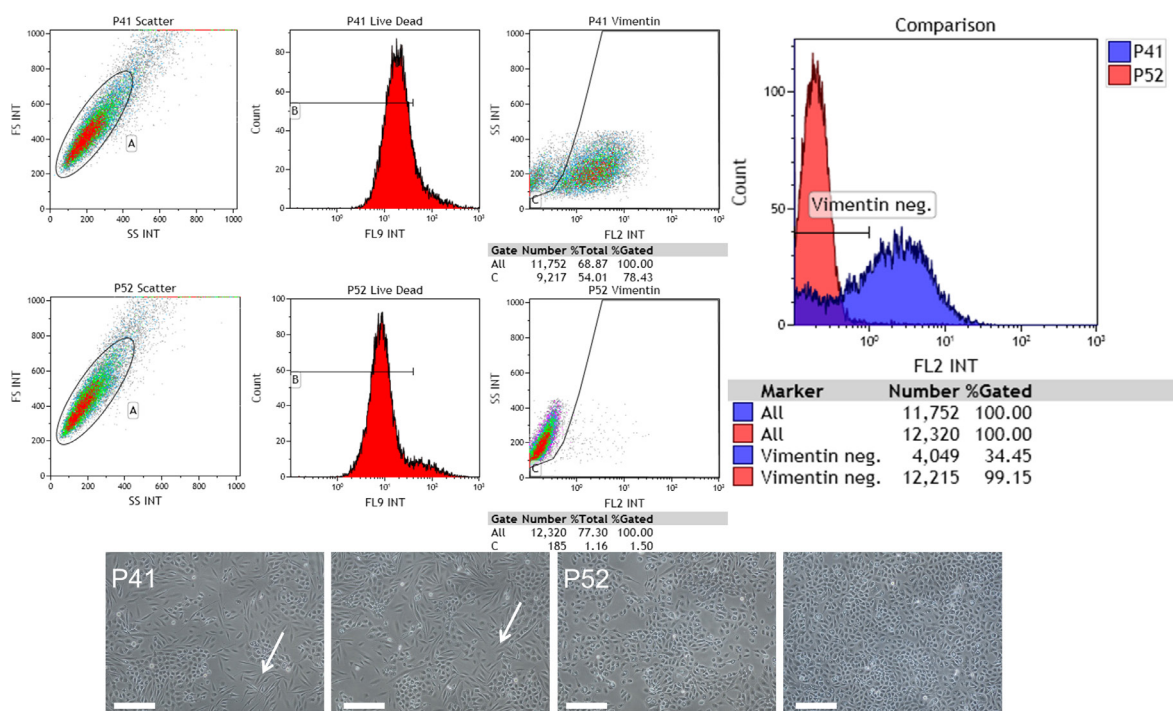
Figure 5.6: Loss of mesenchymal like (vimentin positive population) population from the OPCT1 cell line, observed over an extended period of culture under standard conditions. Representative micrographs are also given to highlight the morphological changes (note regions indicated by arrows) between passage 41 and 52, scale represents 30 μm. Non-specific staining isotype controls are shown in appendix C, fig. C5.

If a surface could be developed which could enrich for, isolate or sustain EMT related cell types then it would be of considerable interest to cancer researchers. The markers to distinguish these populations are known and readily available, so a second attempt at selection was attempted within the OPCT1 sub-populations, avoiding many of the detrimental effects seen in the previous study. A different selection method was applied, rather than adhesion, proliferation was attempted through the application of a 3-aminopropyl functionalised silica surface due to the positive influence seen on cell growth and adhesion in previous studies, the control surface being TCPS. The initial study on selection was performed as described in method 5.2.4.2 and the cell line was examined by light microscopy (fig. 5.7) to assess cell morphology.
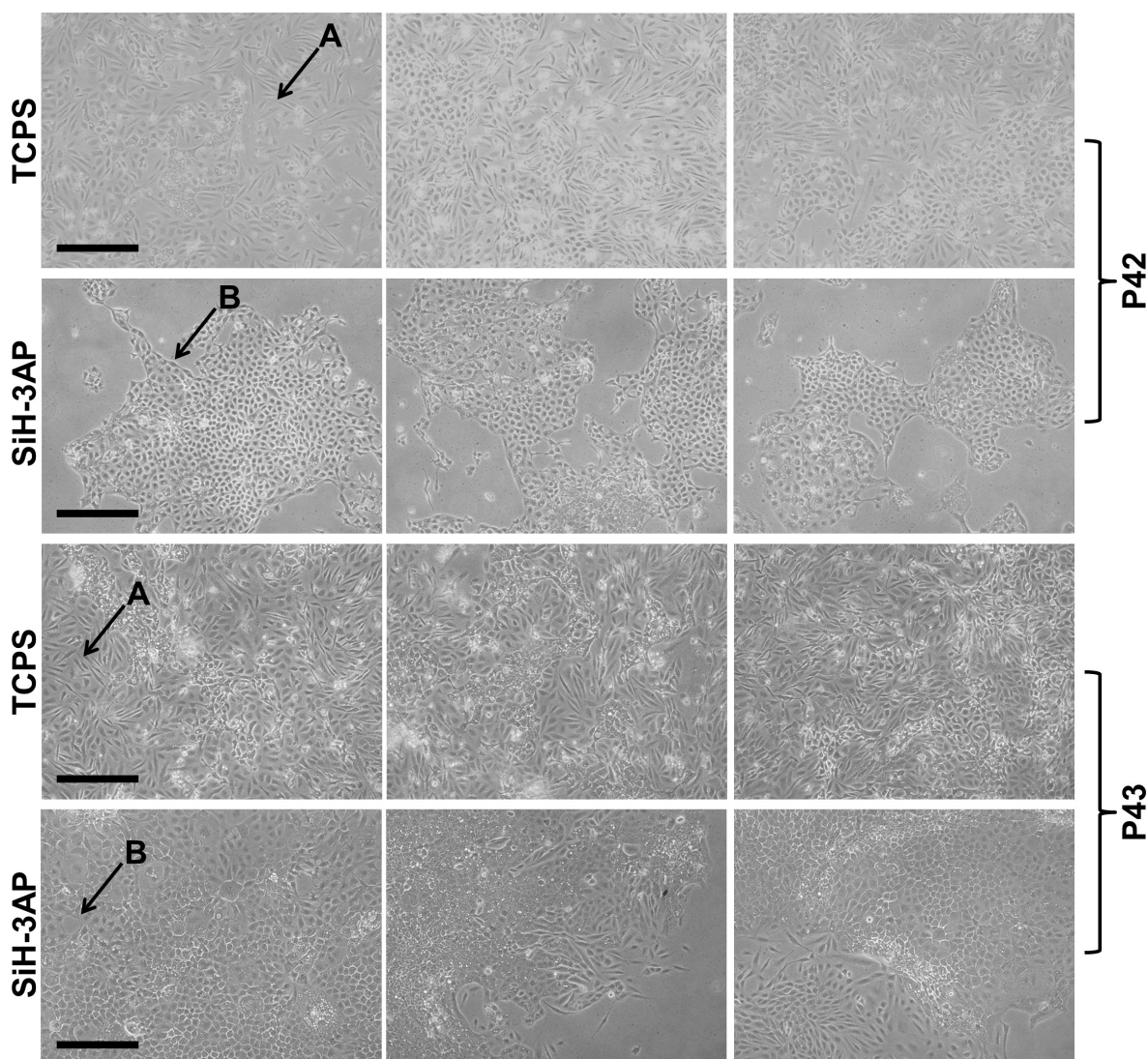
Figure 5.7: Representative light micrographs showing changes in OPCT1 sub-population morphology after a period of enrichment on different surfaces, scale represents 30 μm. Cells demonstrating mesenchymal (A) and epithelial (B) phenotypes are highlighted.

A discrete shift was noted between the cultures present on the different surfaces, fig. 5.7. It was observed that cells cultured on the 3-aminopropyl surface demonstrated a more uniform morphology rather than the mixture of cell types seen on TCPS. The morphology on the 3-aminopropyl surface demonstrated the tight clustering and cell-cell contact expected from an epithelial sub-population, fig. 5.7B. Unlike the TCPS surface few cells which could be described as mesenchymal (elongated, minimal cell-cell contact) could be seen, fig. 5.7A. IF microscopy was applied to determine if marker expression had changed in agreement to the morphological changes observed, fig. 5.8.

Figure 5.8: Representative IF micrographs (A) showing changes in the OPCT1 epithelial (red) and mesenchymal (green) sub-populations after a period of enrichment on the TCPS (control) and 3-aminopropyl (test) surfaces. The difference in populations (B) observed over seven replicate enrichments (n = 7). Non-specific staining isotype controls are shown in appendix C, fig. C4.

The IF data closely matched the morphological assessment, the enrichment showed a significant selective effect on the epithelial and mesenchymal populations within the OPCT1 line that was dependant on which culture surface had been used (fig. 5.8A). Cells cultured on TCPS showed a mixture of the two populations (mesenchymal population ~30% of the total), as expected and observed during conventional tissue culture practice. Cells growing on the 3-aminopropyl surface showed a strong selective response for the epithelial sub-population, mesenchymal population reduced ~10% of the total (fig. 5.8B). This trend in response was shown to be significant over multiple selection experiments; a selective material had been achieved. To confirm the result, a series of enrichment experiments were conducted and assessed using flow cytometry. This would potentially allow the quantification of the changes in large populations of cells to be assessed more accurately than by IF microscopy, fig. 5.9.
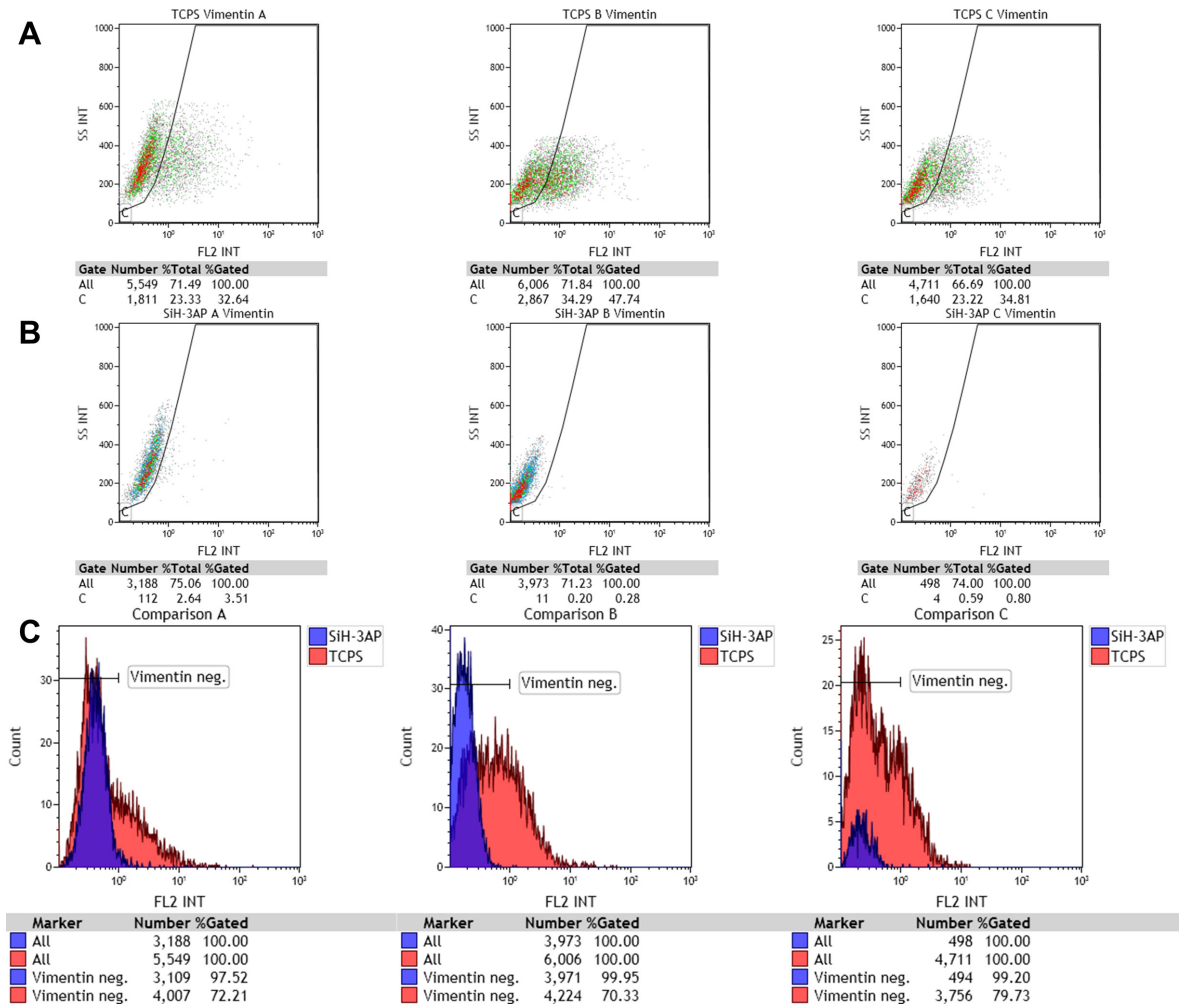
Figure 5.9: Analysis of flow cytometry data obtained after three replicate enrichment experiments using 3-aminopropyl surfaces. The scatter plot (A) is gated to visualise mesenchymal cells for the control (TCPS) post-enrichment, (B) mesenchymal cells on 3-aminopropyl surface post-enrichment and a comparative histogram (C). A loss of the vimentin positive population was seen post-enrichment. Non-specific staining isotype controls are shown in appendix C, fig. C6.

The flow cytometry analysis supported the conclusions of the IF study, after enrichment on the 3-aminopropyl surface the epithelial population was eliminated from the culture ~1.53% (n = 3) of the population from an initial population of ~38.39%. This equates to a 25 fold reduction in cell population in a two passage period (~two weeks in culture) though changes in the cultures were noticeable after seven days, fig. 5.7 P42.

5.3.3 Determining the selective property of the culture surface

With the determination of the direction and extent of the selective effects observed the question as to which surface property is responsible for driving selection in that particular direction arises. To try to resolve this, enrichment was repeated with an unmodified silica surface substituted for the 3-aminopropyl surface. The outcome of the enrichment on this additional surface is shown in fig. 5.10.
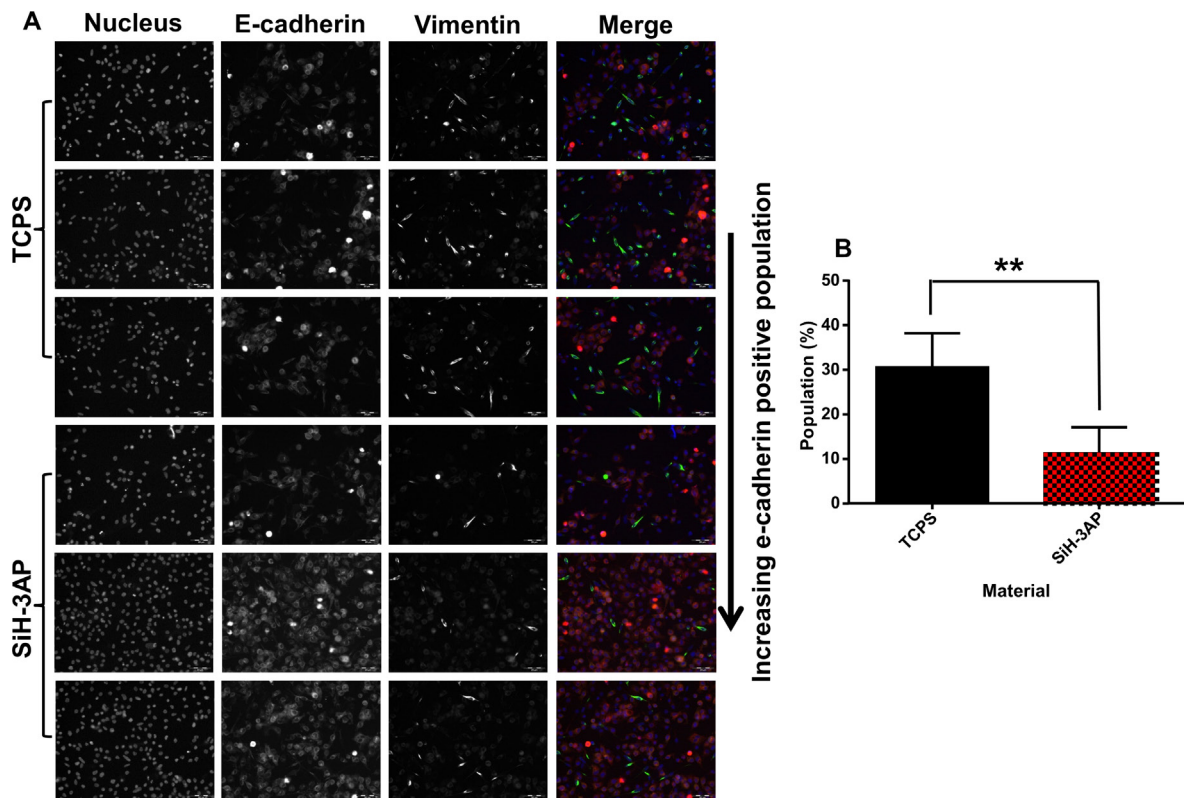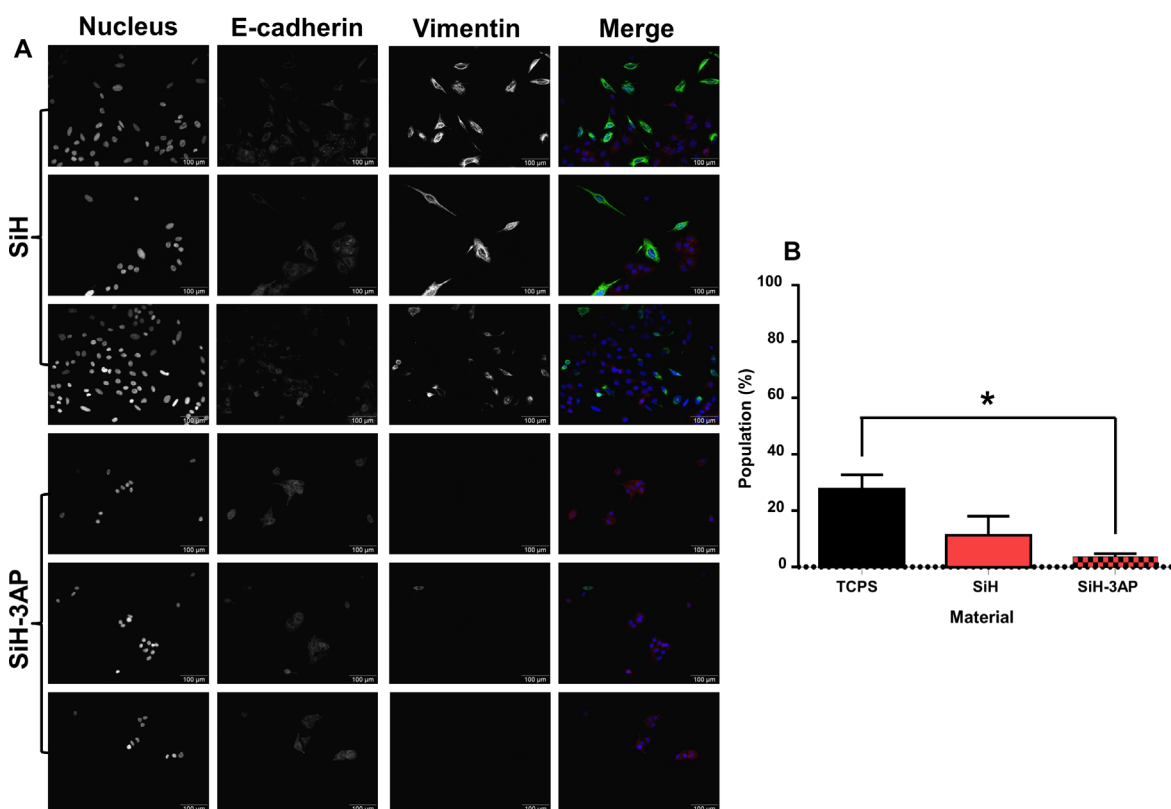

Figure 5.10: Representative IF micrographs (A) showing changes in the OPCT1 epithelial (red) and mesenchymal (green) sub-populations after a period of enrichment on SiH and SiH-3AP surfaces. The quantification of this data in terms of the mesenchymal population (n = 4) is shown in graph (B). Non-specific staining isotype controls are shown in appendix C, fig. C4.

As noted before a significant response was observed between TCPS and the 3-aminopropyl surfaces (fig. 5.10A), with a significant change (~28% to ~4%) in the mesenchymal population post-enrichment (fig. 5.10B). The silica surface was unable to produce the response of the 3-aminopropyl surface, though the reported difference was itself insignificant in comparison to the 3-aminopropyl surface. This is suggestive of the role of surface functionality as the driving force behind the selective effect. The similarity of the SiH and 3-aminopropyl modified surfaces in terms of surface energy (65.94 ± 0.03 and

61.58 ± 4.7 mN/m respectively) and RMS roughness (75.17 ± 1.56 and 71.62 ± 3.70 nm respectively) topology (table 4.2 and 4.3) adds additional weight to this hypothesis. This result is in contrast to other studies that have focussed on the role of topology (Connelly *et al*., 2010; McMurray *et al*., 2011) and mechanical properties like stiffness (Nava *et al*., 2012) on the influence of the culture, though some studies do show an influence of surface chemistry on cell differentiation through control of protein adsorption (Keselowsky *et al*., 2005), a process noted to be distinct on these surfaces (fig. 4.14). However this is dependent on the assumption that the selective effect is a transformative effect as described by the above studies rather than by any other mechanism (fig. 5.1), a case not yet proven in the case of the phenomena described in this study.

5.3.4 An alternative selectivity; enrichment for mesenchymal like cell populations

With a surface capable of very rapidly (within one-two passages) inducing a change in culture from a mixture of cells to ~1.53% of a single epithelial population, the question arises; can the reverse (selection or enrichment of the mesenchymal population) be induced? A control surface used during the IF studies of the epithelial enrichment demonstrated an interesting morphological phenomena, fig. 5.11.
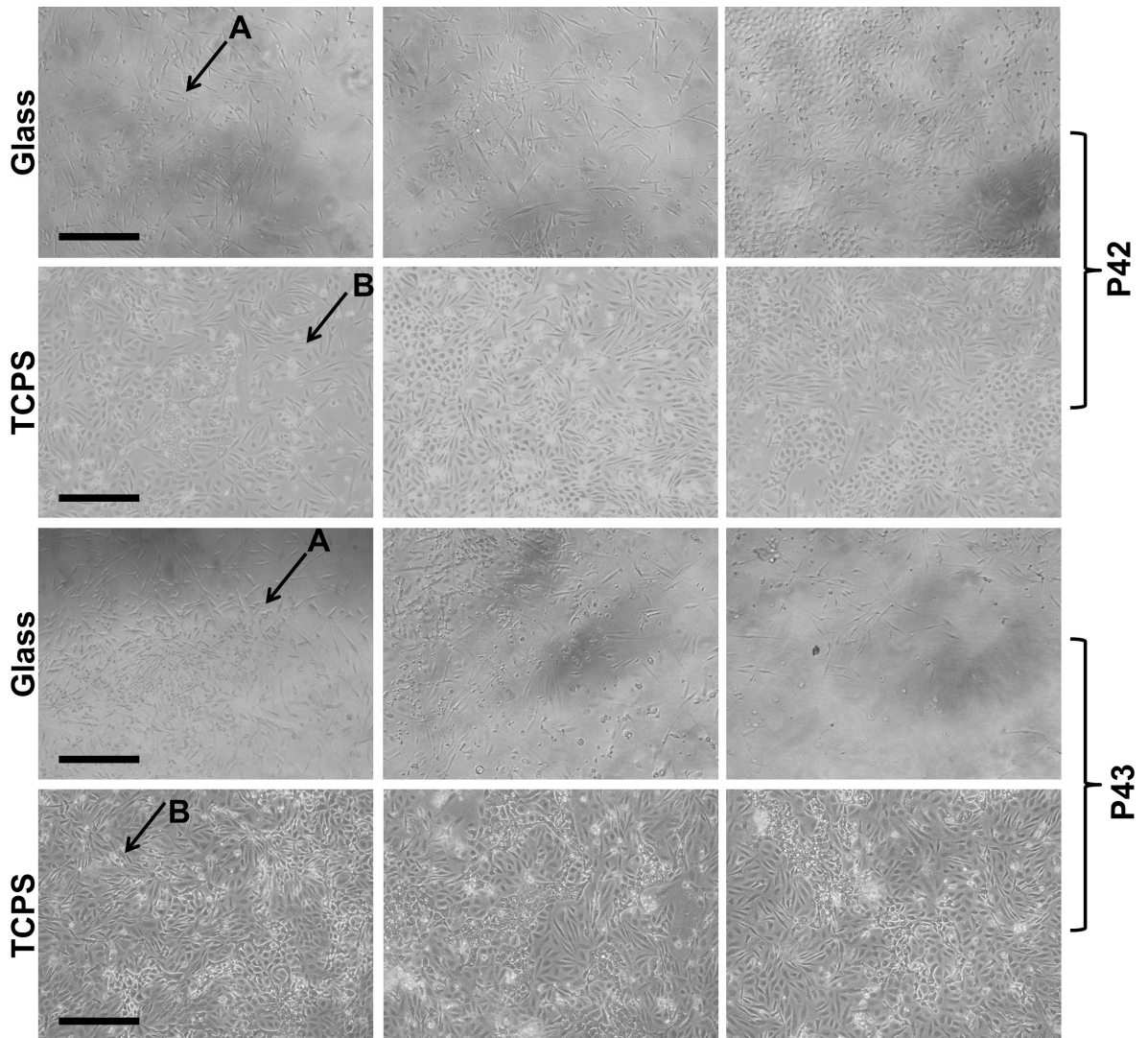
Figure 5.11: Representative light micrographs showing changes in OPCT1 sub-population morphology after a period of enrichment on glass and TCPS surfaces, scale represents 30 µm. Cells demonstrating mesenchymal (A) and epithelial (B) phenotypes are highlighted.

The morphology of the culture was shown to be distinct from that cultured using TCPS, fig. 5.11. This distinction manifested in the appearance of large numbers of cells of an elongated morphology with minimal cell-cell contact (fig. 5.11A), a morphology reminiscent of mesenchymal morphologies, fig. 5.6D, E. IF microscopy was again applied to determine if marker expression matched the morphology changes observed, fig. 5.12.
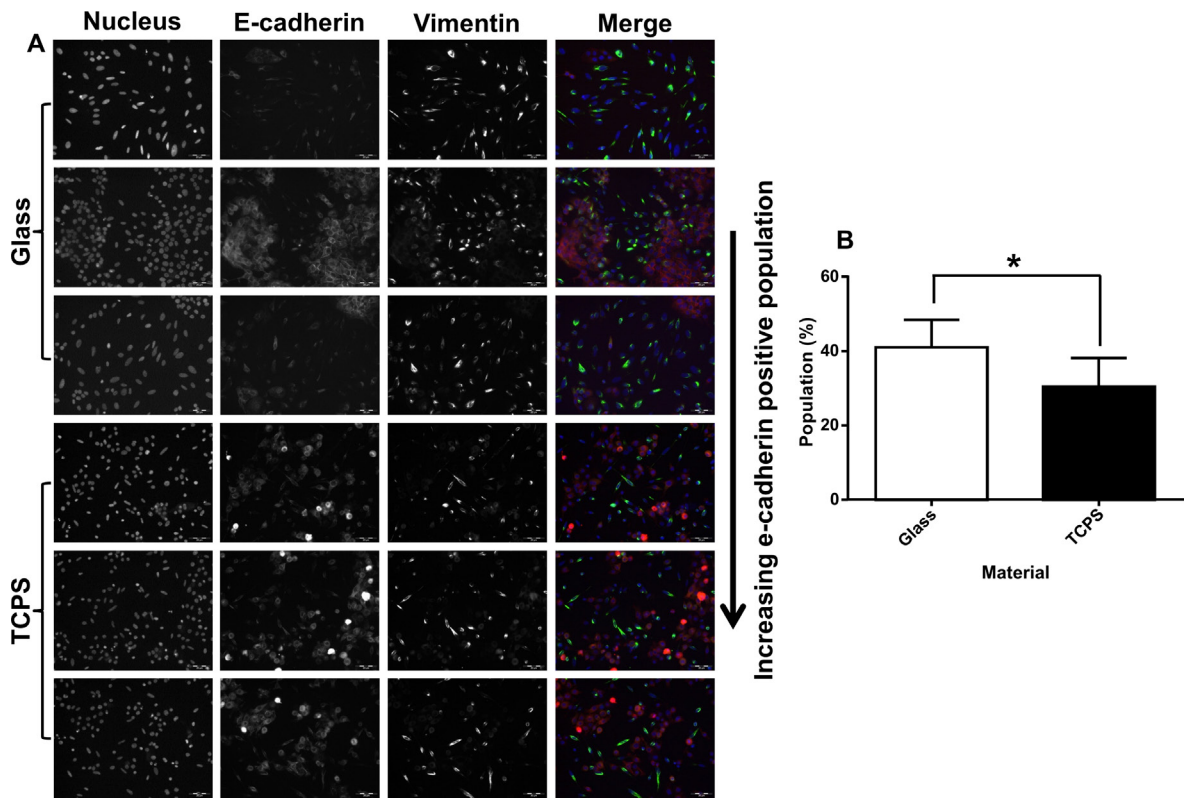
Figure 5.12: Representative IF micrographs (A) showing changes in OPCT1 sub-population morphology and marker (vimentin and E-cadherin) expression (B) after a period of enrichment on glass and TCPS surfaces (n = 4). Non-specific staining isotype controls are shown in appendix C, fig. C4.

The percentage of cells exhibiting vimentin expression was observed to be significantly higher than cells cultured on TCPS, fig. 5.12A, B. Despite showing a mixture of cells, the surface showed a distinct enrichment for the vimentin expressing mesenchymal like sub-population. Efforts to measure the population change using flow cytometry were unsuccessful; the population obtained resembled those on TCPS or SiH surface, fig. 5.13A (compare with fig. 5.9C, 5.10). Closer examination of the glass surface revealed what was occurring, fig, 5.13C.
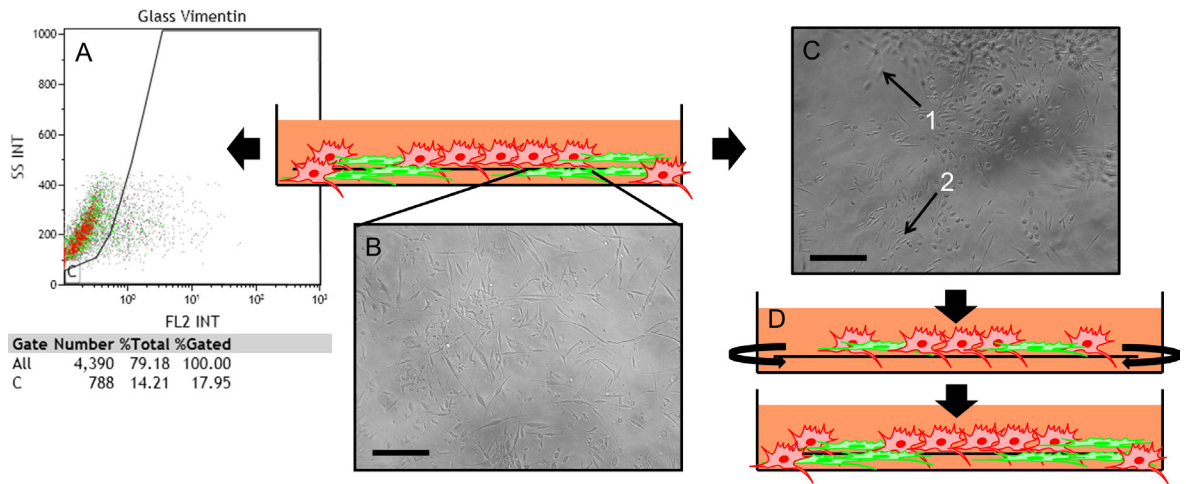
Figure 5.13: Flow cytometry data (A) derived from cells isolated from the top of the slide, no mesenchymal enrichment despite distinct morphological differences by light microscopy (B). Micrograph C shows focal plane off-set between epithelial (1) and mesenchymal (2) populations of OPCT1, schematic D shows resulting explanation of what occurs in culture to result in the mesenchymal phenotype enrichment observed.

Within the well the glass slide was displayed on the bottom, changes that were observed in culture were occurring on the lower surface; in a void between the TCPS surface and the lower face of the glass slide. This was demonstrated by focal off-set in light micrographs, fig. 5.13C. As such flow cytometry experiments on cells sampled from the top of the slide did not resemble the expected populations observed since the cells were derived from the wrong area of the well-plate.

What was understood to be occurring in culture was the creation of a distinct microenvironment on the underside of the glass slide. Cells migrating into the void are either of a mesenchymal phenotype exclusively (clustering epithelial cells perhaps unable to migrate as effectively into this space) that are sustained or cells that upon entering into the microenvironment are induced to undergo EMT (mesenchymal population not supported over time on TCPS or glass) and then sustained. A further experiment was conducted; the enrichment was induced in a medium with an absence of FCS, fig. 5.14.
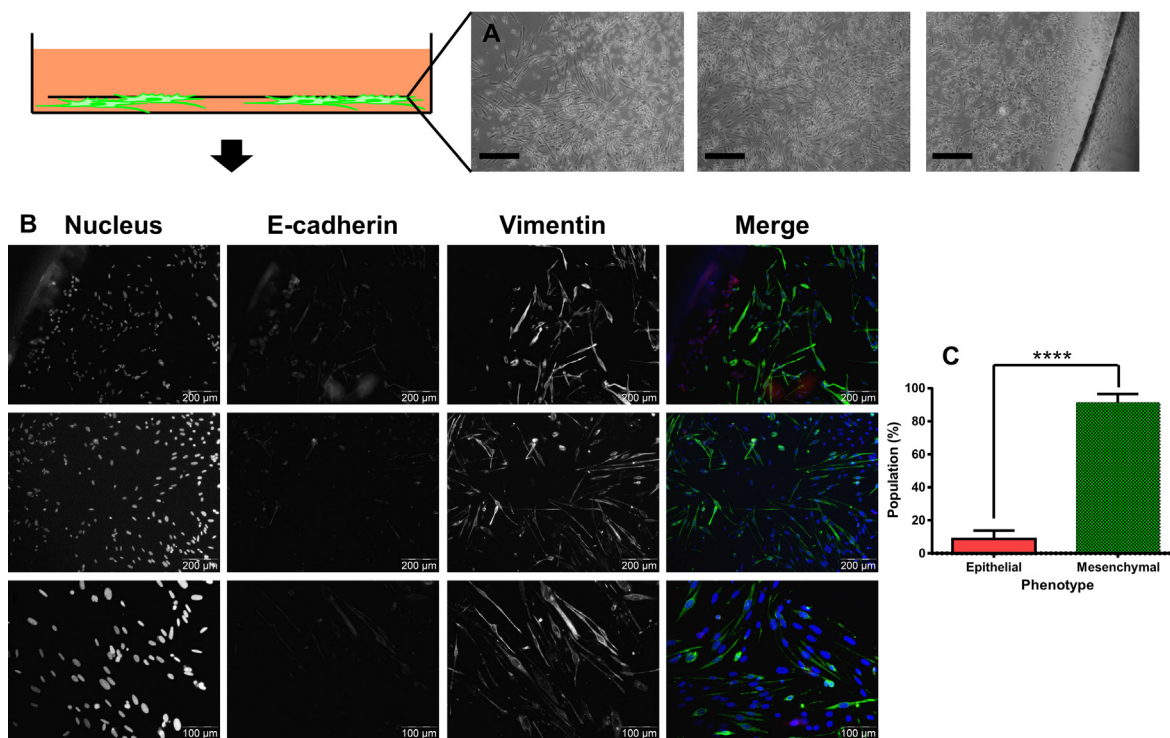
Figure 5.14: Representative light micrographs (A) show the distribution of mesenchymal cells across the surface from the edge of the slide inwards, scale represents 30 µm. Representative IF micrographs (B) visualise marker expression, which was quantified for 400 cells (graph C). Non-specific staining isotype controls are shown in appendix C, fig. C6.

In the absence of FCS, a population of cells were still capable of survival and migrating into the void below the disk. The majority of these cells as observed by light and IF microscopy were of a mesenchymal morphology or phenotype, cells clustering and expressing E-cadherin were rarely observed. This mesenchymal population was determined to be 91% ± 5.1% of the total population based on 400 cells. A mesenchymal population greater than any observed to date, table 5.2, including an OPCT1 culture on TCPS from an initial passage.

Table 5.2: Mesenchymal population determined by technique

Surface	IF (%)	FC (%)
TCPS/Initial passage	30.4 ± 7.8	38.4 ± 4.7/78.4
SiH-3-aminopropyl	7.5 ± 4.0	1.5 ± 1.0
SiH	11.3 ± 6.7	-
Glass/-FCS	41.0 ± 7.3/91 ± 5.1	17.95/-

160.

The further loss of the epithelial population in the absence of serum but the sustainment (and further enhancement) of the mesenchymal population in the void suggests a mechanism for this phenomena. Cells of a mesenchymal phenotype are not sustained or enriched on polystyrene or glass alone (fig. 5.8, 5.12), though within the void created through a glass insert, enrichment was observed (fig. 5.11, 5.12). If FCS is withdrawn the mesenchymal population in the void was enhanced further (fig. 5.14) and the epithelial population was further lost. Thus the mesenchymal phenotype can sustain itself in serum free conditions but the epithelial population cannot. The microenvironment formed under the disk in serum containing media likely acts as a low serum environment as the disk likely inhibits diffusion of serum proteins, favouring the mesenchymal population and inhibiting any epithelial cells that enter this environment or try to undergo MET within this environment. As such the mechanism achieved is likely based on attrition. Though the morphological differences observed in the mesenchymal population with the predominance of populations characterised by fig. 5.5D, E may suggest that the mesenchymal population and not just the epithelial population is influenced by this microenvironment.

5.4 Conclusions

Though initial attempts to achieve selection using adhesion as the selective force were unsuccessful, the process of understanding why selection did not work provided insight into the cellular processes occurring within culture as well as highlighting the importance of certain aspects of culture such as the local micro-environments.

With the application of a different selection mechanism, cell enrichment between epithelial and mesenchymal cells from mixed culture was successfully demonstrated in both directions. The studies conducted also suggest that functionality plays a role in the selection of the epithelial cells and that serum deprivation by mechanical obstruction results in a microenvironment that causes the attrition of epithelial cells and maintenance of mesenchymal cells. The final chapter will discuss the implications of the work, what is outstanding from the current studies in addition to the potential future directions of the work achieved.

5.5 References

1. Berx G & van Roy F. (2009). Involvement of Members of the Cadherin Superfamily in Cancer. *Cold Spring Harbor Perspect. Biol.*, 1(6):doi:10.1101/cshperspect.a003129

2. Casas E, Kim J, Bendesky A, Ohno-Machado L, Wolfe C.J & Yang J. (2011). Snail2 is an Essential Mediator of Twist1-Induced Epithelial Mesenchymal Transition and Metastasis. *Cancer Res.*, 71(1):245-54

3. Connelly J.T, Gautrot J.E, Trappmann B, Tan D.W, Donati G, Huck W.T & Watt F.M. (2010). Actin and serum response factor transduce physical cues from the microenvironment to regulate epidermal stem cell fate decisions. *Nat. Cell Biol.*, 12(7):711-8

4. da Costa D.S, Pires R.A, Frias A.M, Reis R.L & Pashkuleva I. (2012). Sulfonic groups induce formation of filopodia in mesenchymal stem cells. *J. Mater. Chem.*, 22(15):7172-8

5. Dunning-Foreman N.L. (2012). Investigating the properties of cancer stem cells and epithelial to mesenchymal transition in human prostate cancer. PhD. Nottingham Trent University

6. Eger A, Stockinger A, Schaffhauser B, Beug H & Foisner R. (2000). Epithelial Mesenchymal Transition by c-Fos Estrogen Receptor Activation Involves Nuclear Translocation of β-Catenin and Upregulation of β-Catenin/Lymphoid Enhancer Binding Factor-1 Transcriptional Activity. *J. Cell Biol.*, 148(1):173-87

7. Gumbiner B.M. (1996). Cell Adhesion: The Molecular Basis of Tissue Architecture and Morphogenesis. *Cell*, 84(3):345-57

8. Hawley T.S & Hawley R.G. (2004). Flow Cytometry Protocols. Humana Press. United States of America, 3rd Edition, ISBN 1-58829-234-7

9. Helou M, Reisbeck M, Tedde S.F, Richter L, Bar L, Bosch J.J, Stauber R.H, Quandt E & Hayden O. (2013). Time-of-flight magnetic flow cytometry in whole blood with integrated sample preparation. *Lab Chip*, 13(6):1035-8

10. Iwasa J, Ochi M, Uchio Y, Katsube K, Adachi N & Kawasaki K. (2003). Effects of Cell Density on Proliferation and Matrix Synthesis of Chondrocytes Embedded in Atelocollagen Gel. *Artif. Organs*, 27(3):249-55

11. Keselowsky B.G, Collard D.M & García A.J. (2005). Integrin binding specificity regulates biomaterial surface chemistry effects on cell differentiation. *Proc. Natl. Acad. Sci. U. S. A.*, 102(17):5953-5957

12. Kilian K.A & Mrksich M. (2012). Directing Stem Cell Fate by Controlling the Affinity and Density of Ligand–Receptor Interactions at the Biomaterials Interface. *Angew. Chem. Int. Ed.*, 51(20):4891-5

13. Korita P.V, Wakai T, Ajioka Y, Inoue M, Takamura M, Shirai Y & Hatakeyama K. (2010). Aberrant expression of vimentin correlates with dedifferentiation and poor prognosis in patients with intrahepatic cholangiocarcinoma. *Anticancer Res.*, 30(6):2279-85.

14. Lee J.H, Jung H.W, Kang I & Lee H.B. (1993). Cell behaviour on polymer surfaces with different functional groups. *Biomaterials*, 15(9):705-11

15. Mani S.A, Guo W, Liao M, Eaton E.N, Ayyanan A, Zhou A.Y, Brooks M, Reinhard F, Zhang C.C, Shipitsin M, Campbell L.L, Polyak K, Brisken C, Yang J & Weinberg R.A. (2008). The Epithelial-Mesenchymal Transition Generates Cells with Properties of Stem Cells. *Cell*, 133(4):704-15

16. McMurray R.J, Gadegaard N, Tsimbouri P.M, Burgess K.V, McNamara L.E, Tare R, Murawski K, Kingham E, Oreffo R.O.C & Dalby M.J. (2011). Nanoscale surfaces for the long-term maintenance of mesenchymal stem cell phenotype and multipotency. *Nature Mater.*, 10(8):637-44

17. Miltenyi S, Muller W, Weichel W & Radbruch A. (1990). High Gradient Magnetic Cell Separation With MACS. *Cytometry*, 11(2):231-8

18. Moll R, Franke W.W & Schiller D.L. (1982). The catalog of human cytokeratins: Patterns of expression in normal epithelia, tumors and cultured cells. *Cell*, 31(1):11-24

19. Nava M.M, Raimondi M.T & Pietrabissa R. (2012). Controlling self-renewal and differentiation of stem cells via mechanical cues. *J. Biomed. Biotechnol.*, 2012:797410

20. Ni M, Zimmermann P.K, Kandasamy K, Lai W, Li Y, Leong M.F, Wan A.C.A & Zink D. (2012). The use of a library of industrial materials to determine the nature of substrate-dependent performance of primary adherent human cells. *Biomaterials*, 33(2):353-64

21. Sallusto F & Lanzavecchia A. (1994). Efficient Presentation of Soluble Antigen by Cultured Human Dendritic Cells Is Maintained by Granulocyte/Macrophage Colony-stimulating Factor Plus Iuterleukin 4 and Downregulated by Tumor Necrosis Factor α. *J. Exp. Med.*, 179(4):1109-1118

22. Simcha I, Shtutman M, Salomon D, Zhurinsky J, Sadot E, Geiger B & Ben-Ze'ev A. (1998). Differential nuclear translocation and transactivation potential of beta-catenin and plakoglobin. *J. Cell Biol.*, 141(6):1433-48

23. Singh A, Suri S, Lee T, Chilton J.M, Cooke M.T, Chen W, Fu J, Stice S.L, Lu H, McDevitt T.C & García A.J. (2013). Adhesion strength–based, label-free isolation of human pluripotent stem cells. *Nat. Methods*, 10(5):438-44

24. Thiery J.P, Acloque H, Huang R.Y.J & Nieto M.A. (2009). Epithelial-Mesenchymal Transitions in Development and Disease. *Cell*, 139(5):871-90

25. Zeisberg M & Neilson E.G. (2009). Biomarkers for epithelial-mesenchymal transitions. *J. Clin. Invest.*, 119(6):1429-37

Chapter Six:

Moving to a Mechanistic Understanding of Cell Response & Selection Effects with Respect to Surface Property.

6.1 Introduction

Previous chapters have shown the development of a general process for the fabrication of silica surfaces on polystyrene in a manner that is suitable for application in the tissue culture environment. This system was used to present a range of different surface chemistries and the cell response to these different chemistries was assessed in terms of proliferation and toxicity, adhesion, motility and cytoskeletal morphology. Cell response in many cases was found to vary significantly depending on the surface functionality presented in culture. Finally a number of chemistries were applied to induce cell enrichment and their influences on the epithelial and mesenchymal sub-populations of OPCT1 were assessed, with selective effects observed.

While some conclusions can be drawn from the study as it stands, specifically in terms of the surface properties that permit positive cell responses in culture and those that are important in inducing a selective effect for some of the populations seen, many important questions remain as to how the differences in surface property influence the cell and how these influences culminate in the responses observed. Although the studies conducted to date have been successful with respect to the aims of the work in terms of being able to apply surface chemistry to a potentially useful cell selection problem in cancer biology, a detailed explanation remains elusive.

A specific question that remains largely unresolved concerns which surface properties direct the enrichment of mesenchymal cells? More broadly, how these surface properties influence the cell and through what biological pathways they act? Finally, why do different cells and proteins respond differently to the different functionalities presented and how does this relate to the characteristics of the cell and proteins involved? This chapter will try

to address these points through reference to what is known in the literature, experimental evidence collected during the course of this Ph.D. study, culminating in the proposal of directions for further experimental work.

6.2 Discussion

6.2.1 Implications for materials used in tissue culture & identifying a mechanism of cell-surface interaction/biocompatibility

As demonstrated in chapter one, many new materials have been developed over the past few decades for the culture of tissues and cells *in vitro*. From the initial crude use of existing glass vessels to the rise and ever expanding diversity of tissue culture plastics, each generation of tissue culture materials has been accompanied with improved culturing characteristics, in addition to improved economy and fabrication efficiency. These developments in materials science have often been accompanied with an improved understanding of the cell biology, specifically in terms of the interactions of cells and biomolecules associated with the process of cell-surface interaction, such as the interaction of extra-cellular matrix proteins with surfaces of varying chemical and physical properties (Curtis *et al.*, 1983; Steele *et al.*, 1995; Serra *et al.*, 2012).

The originality of the work as described in detail in chapter three is in the demonstration of silica materials applied as cell culture surfaces in which the wetting properties of said surfaces are of a hydrophilic and super-hydrophilic nature. Current materials and previous studies focus on the avocation of materials of moderately hydrophilic (35-40°) or intermediate (~90°) wetting characteristics (Saltzman & Kyriakides, 2007). While the low initial wetting property exhibited by the materials used for proliferation of FM3 melanoma cells was contrary to the established norms of tissue culture materials development, the suggested mechanism of biocompatibility is conventional; protein adsorption. That cell adhesion and proliferation correlates positively with protein adsorption would agree with our current understanding of cell-surface interactions (Koenig *et al.*, 2003), and the proliferation and survival dependence of adherent cell lines (Valentijn & Gilmore, 2004)

The contribution of this work to the field of *in vitro* materials science is that (at least for many adherent tumour cell lines, refer to chapter four) the range of wettability for materials used *in vitro* can be considerably expanded. So long as the adsorption of proteins

required for cell adhesion or the biological surface modification that inherently occurs within the biological environment is unimpeded. As an extension of this work, one could hypothesise that surfaces that offer low rates of protein adsorption or low protein loading may be poor culture surfaces; a hypothesis currently supported in the literature (Valentijn & Gilmore, 2004), though this may not apply for all adherent cell types, especially those of a diseased state or stem like nature (Lin & Chang, 2008; Miki & Rhim, 2008).

The desire to increase control over the cellular properties exhibited in culture (specifically cells of a stem like nature), has resulted in a demand for an increasing diversity of tissue culture materials (Miki & Rhim, 2008). The work presented in this thesis both reflects and validates that viewpoint by showing that materials divergent from tissue culture norms can be applied and acts to complete the characterisation of tissue culture surface performance across the wetting gradient, complimenting studies by others into the applicability of super-hydrophobic materials to *in vitro* tissue culture; who found a disruption of protein (FN) adsorption and a negative impact on the proliferation of most adherent cells such as fibroblasts, chondrocytes and osteosarcoma (Ballester-Beltran *et al*., 2011; Oliveira *et al*., 2011).

6.2.2 Understanding cell response to materials of diverse properties & identifying mechanisms for surface mediated exploitation of cell responses

Chapter four represented an extension of the work accomplished in chapter three and expanded the range of functionalities considered while also considering a larger cohort of cell lines and responses, though all lines are established in tissue culture practice, adherent in nature and understood to be tumour derived.

The observations of increased proliferative and adhesive performance for the 3-aminopropyl surface chemistry and generally poorer performance in these aspects for the methyl and phenyl functionalised materials combined with decreased protein adsorption, specifically with respect to fibronectin (FN) expanded on the protein adsorption and biocompatibility hypothesis given in chapter three. By identifying that FN adsorbs differentially between the surfaces and in a manner differing from other proteins like BSA, showed that specific proteins rather than the whole serum are important in understanding the cell response. Though this point is already well established (Allen *et al*., 2006;

Deligianni *et al.,* 2001; Curtis & Forrester, 1984), this biocompatibility effect (and serum adsorption hypothesis presented in chapter three) can be further demonstrated if serum and fibronectin alone is titrated onto a surface that has been identified as hostile to cell adhesion and proliferation, fig. 6.1.
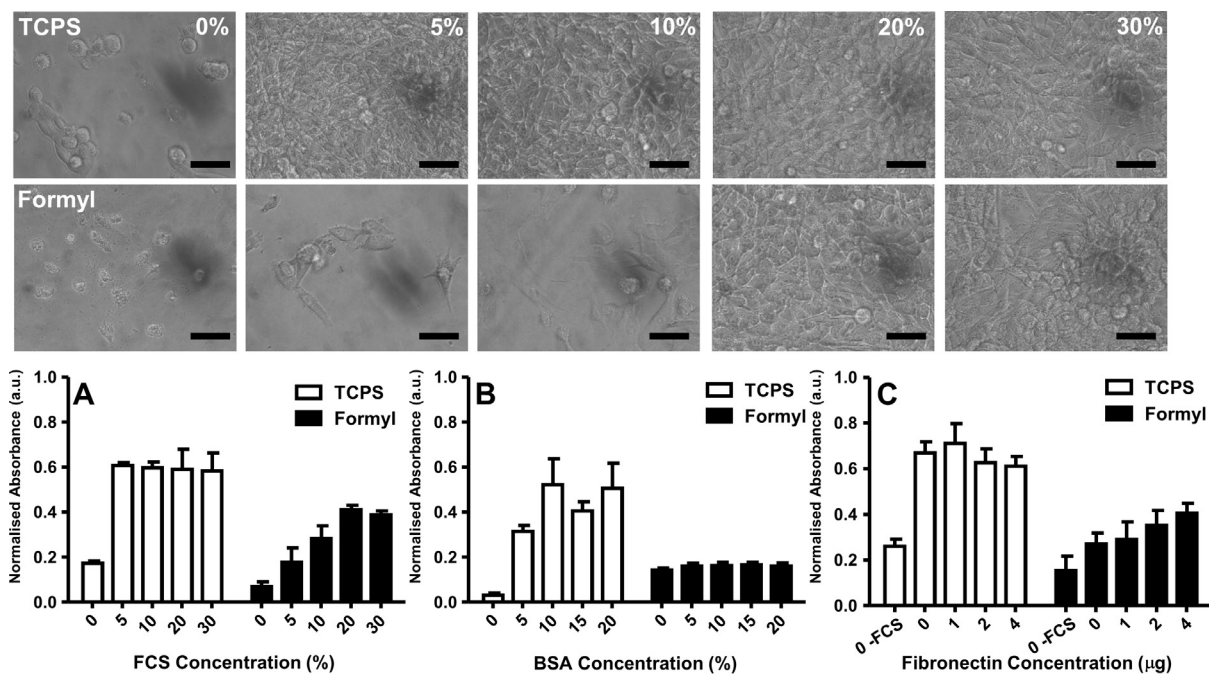
Table 6.1: Surface free energy of formyl modified 3-aminopropyl surface						
Sample	θ (°)	γ^{tot} [mN/m]	γ^{d} [mN/m]	γ^{p} [mN/m]	γ^{+} [mN/m]	γ^{-} [mN/m]
Formyl	63.0 ± 6.6	47.0 ± 5.6	39.1 ± 0.3	7.9 ± 3.4	2.3 ± 0.4	2.3 ± 1.4

Figure 6.1: Light micrographs of FM3 proliferation on TCPS and a SiH-formyl surface with increasing concentrations of serum. FM3 proliferation in the presence and absence of serum (A), varying concentrations of albumin (B), varying concentrations of FN (C, first sample representing no serum and no FN) are also shown. Scale represents 5 μm. Table 6.1 represents surface free energy and water wetting characteristics (θ) of the formyl surface used.

The protective effect of the serum is immediately observed, FM3 cell proliferation recovering as the percentage of serum in the media increases, fig. 6.1A. The main protein component of serum is known to be serum albumin (BSA) (appendix B, table B1); BSA was titrated into the growth medium in addition to 5% of serum to provide any necessary growth factors. However as serum albumin increases no protective effect is observed, even the growth of FM3 with the low dose of serum on TCPS appears to be disrupted, fig. 6.1B.

If BSA is substituted for FN the protective effect is restored, as is the performance of FM3 on TCPS, fig. 6.1C. This demonstrates that FN is at least one of the molecules in serum that is capable of rescuing cell adhesion and proliferation on a hostile surface.

The principal observation of chapter four was that though cell lines have conserved similarities (adhesion and proliferation on silica surfaces) some of the responses observed differed on interaction with differently functionalised materials. It was observed that cells and proteins responses can change subtly to the separately treated surfaces, specifically between cells from differing lineages. While this observation may seem superficial, it should be noted that these differences carry the hallmarks of being complicated events; themselves the product of interactions between different variables (serum presence and functionality for example). This observation supported the rational of the work; that different surface properties can influence different cell populations differently (albeit differences between cells of divergent types – melanoma *versus* adenocarcinoma). Once this is observed the difficulty for the development of a selective surface is in understanding the relationship between surface property and cell response and how to apply this to cell selection. In this respect, the positive proliferation but distinctly altered adhesion of the 3-aminopropyl surface made it the most interesting candidate for enrichment studies.

6.2.3 Exploiting cell-surface interaction to achieve a desired cell response

The identification of the 3-aminopropyl surface as a chemistry which directed the enrichment of epithelial cells is of considerable interest. Analogous studies related to this functionality have demonstrated that PGLA and PGA surfaces functionalised with 3-aminopropyl groups can support the growth of rat embryonic cardiomyocytes, (Natarajan *et al.*, 2008) but to the best of my knowledge no other researchers have shown incorporation of 3-aminopropyl groups may influence cancer cell sub-populations in such a manner, though others have shown that N-(2-aminoethyl)-3-aminopropyltrimethoxysilane could influence endothelial and primary osteogenic cell differentiation (Spargo *et al.*, 1994; Thomas *et al.*, 2002). Additionally others have shown that amino functionalised glass surfaces can induce osteogenesis and are not able to sustain the mesenchymal phenotype for human mesenchymal stem cells (Curran *et al.*, 2006; Curran *et al.*, 2010). Though currently limited to a single cell line, such a discovery is entirely novel and it would be of

considerable interest to see if such effects are noticed in other cell types of a similar phenotype. With the current preoccupation with cells of a 'stem-like' phenotype, the identification of a surface that enriches epithelial cells from co-culture is currently unique to this study.

While some evidence has been demonstrated that surface functionality acts as the driving force for this selective effect *versus* topology, it should be noted that changes were observed in the population of epithelial cells when using the unmodified silica surface alone in comparison to the control surface TCPS (though not to the extent of the 3-aminopropyl modified surface). That different surface properties may interact to influence the extent of the population changes observed cannot be ruled out, a greater range of surface characteristics would have to be trialled to better resolve the surface properties important for this type of enrichment.

The identification of functionality as a driver of controlled differentiation (if the mechanism is transformation) contrasts with comparable works where topology or stiffness is considered important (Nava *et al*., 2012). However in chapter four it was shown that differential protein adsorption occurs between the different surfaces, chapter one identified how protein adsorption can change surface properties. Differing amounts (multilayers etc.) or types of protein adsorbed to the surface may result in different mechanical properties at the surface which could result in a mechanotransduction mechanism for the surface 'signal' to change the characteristics of the populations in culture; very similar to what is expected from the literature. This possibility could potentially be studied through nano-indentation (Bassani *et al*., 2006).

Similarly the identification of a surface(s)/conditions capable of enrichment for the mesenchymal phenotype is of considerable worth due to the previously stated interest in cells with stem like properties. Other groups have shown that mesenchymal cells may be maintained for an extended period on modified surfaces, table 6.2. Studies using a known biological entity are excluded; those that remain revolve around two different mechanisms, interestingly split between the two divisions of surface treatment. Studies based on topological changes favour mechanotransduction, those based on chemical modification favour differential adsorption or formation of protein or other biomolecule cues (table 6.2 below). The mechanistic division should not technically exist as all processes (protein

adsorption, focal adhesion, cell tensioning etc.) are part of the same overarching mechanism; mechanotransduction (Ingber, 2006).

Though individual studies may wish to highlight particular elements as part of a detailed mechanism, which is perhaps missing from current studies despite identification of the separate components of mechanotransduction.

Though the resolution of a detailed mechanism in this work is required with respect to cell enrichment (epithelial attrition or transformation), the favoured concept of serum depletion leading to a more mesenchymal phenotype (such as when induced by stromal cell derived factor-1) is already established (Onoue et al., 2006). Serum depletion is common with many treatment regimens which induce EMT, such as dosage with TGF-β, since serum is suggested to contain factors which inhibit EMT (Onoue et al., 2006).

A criticism of the current work beyond its dependence on a single cell line is that though selective surfaces have been identified, the mechanism by which this selection occurs and its relationship to surface chemistry is poorly defined. While changes to surface properties after functionalisation have been characterised and are suggestive of the surface modification as described, a greater range of surface characteristics (varying loading of 3-aminopropyl groups to the silanol surface) would be desirable to better resolve the surface properties important for these types of enrichment.

With respect to this, the limitations of this first generation of surfaces used within the study become obvious. While wholly applicable to the application, future work investigating the mechanisms involved would benefit from the generation of surfaces where important surface chemistry properties can be studied in isolation from one another. For example, an atomically flat surface such as a mica plane with varying degrees of surface chemistry, up to complete coverage – such as that found with some self-assembled mono-layers. Such an approach would also be useful in resolving the influence of surface chemistry and topology (and any suspected interaction) on the adsorption of different biomolecules to the surfaces in culture, since these are believed to play a major role in cell-surface interaction and act as a mechanism for the transduction of surface property to cell response.

Table 6.2: Select studies on surfaces of a differentiating, selective or enriching nature

Surface	Cell	Mechanism	Outcome	Reference
Topological modification				
PMMA (120 nm pits, 300 nm space, off-set)	Osteoprogenitors & hMSC	Mechanotransduction	Controlled differentiation	Dalby *et al.*, 2007
PES fibres (283-1452 nm Ø)	Neural stem cells	-	Controlled differentiation	Christopherson *et al.*, 2009
PEG hydrogel	Muscle stem cells	Mechanotransduction (stiffness)	Controlled renewal	Gilbert *et al.*, 2010
PUA moulded groves/ridges (350 nm space, 500 nm height)	hMSC	Mechanotransduction	Controlled differentiation	Lee *et al.*, 2010
Planar PCL, PS, PC (120 nm pits, 300 nm spacing, off-set)	Osteoprogenitors & hMSC	Proliferation & mechanotransduction	hMSC maintenance	McMurray *et al.*, 2011
Chemical modification				
Self-assembled monolayer (SAM)	Immature osteoblast like cells	Protein (FN) adsorption & integrin specificity	Controlled differentiation	Keselowsky *et al.*, 2005
SAM	hMSC	-	Controlled differentiation	Curran *et al.*, 2006
Small functional group modified PEG hydrogel	hMSC	ECM mimic	Controlled differentiation	Benoit *et al.*, 2008
SAM	hMSC	Protein (FN) adsorption & integrin specificity	Controlled differentiation	Phillips *et al.*, 2010
SAM (70 nm Ø)	hMSC	Control focal adhesion	Controlled differentiation	Curran *et al.*, 2010
SAM	hMSC	Controlled adhesion & growth factor release	Controlled differentiation	Curran *et al.*, 2011
SAM	hMSC	Heparin mimic	Induced differentiation	da Costa *et al.*, 2012
Corning® Synthemax®, defined medium	hMSC	Removal undefined factors, greater adhesion & growth factors	Expansion & maintenance	Dolley-Sonneville *et al.*, 2013

As noted in chapter four the enhanced adsorption of proteins like FN which are relevant to cell-surface interaction pathways provides a potentially detailed mechanism for this transduction of surface property to cell response. Further exploration of these pathways at the protein and transcription level would need to be investigated, not to mention other relevant proteins, before further conclusions could be drawn. The potential that complex cell-responses can be induced through simply controlling the cells environment at the protein adsorption level through surface chemistry or topology is an elegant response to many of the problems faced in tissue culture and associated fields like biomaterials and tissue engineering (Allen *et al*., 2006). Specifically when considering what is known already about the surface controlled adsorption of proteins and the influence on cell response (Garcia *et al*., 1999), cellular micro-environments on dynamic materials and the potential hazards of the tethered cell signalling approach favoured today, which in many ways represents earlier tissue culture concepts where xenobiotic and artificial compounds under non-physiological conditions were more accepted (Allazetta *et al*., 2013; Carragee *et al*., 2011). This rational and the alternative is illustrated in fig. 6.2.

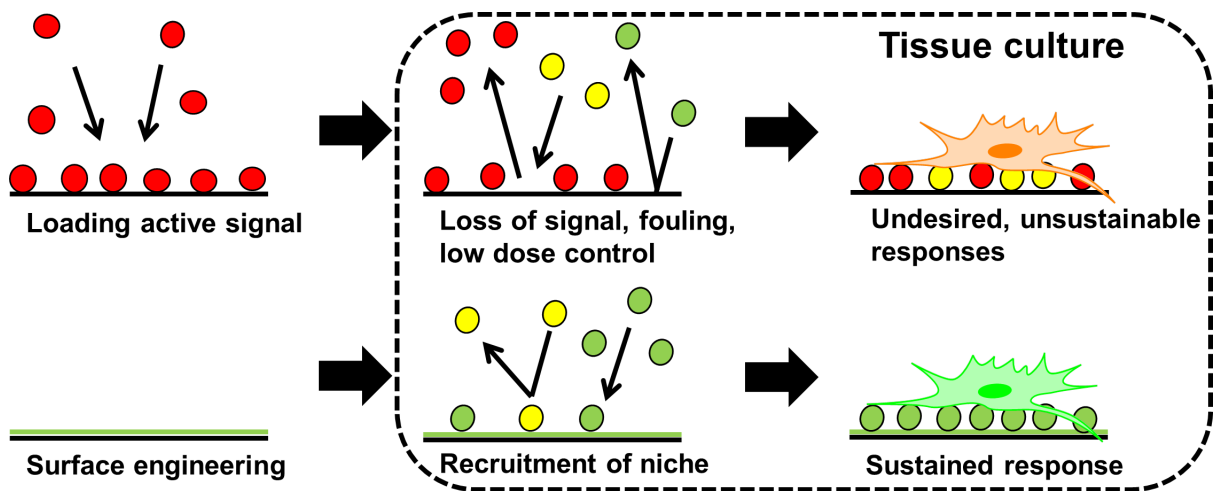**Figure 6.2:** Concept of a self-assembling engineered cell microenvironment and comparison to an engineered cell microenvironment.

6.3 Conclusions

The main conclusion of the study with respect to the initial aims can be summarised as follows; the culture surface can be used to direct the selection of specific cell sub-populations of interest. This selection may be conducted in complex *in vitro* environments

without special culture conditions (other than substitution of the conventional TCPS surface) and in the presence of multiple cell types.

Further conclusions which can be derived from this study are:

- Silica surfaces can be made suitable for the culture of human derived tumour cell lines and that the initial properties of the surface need not be so tightly defined with respect to biocompatibility since biological modifications occur in culture.

- Differently functionalised surfaces influence cell response and protein adsorption differently and this response varies between different cells and proteins. This presents many opportunities for the selection of materials with potentially selective effects.

- Cell-surface interaction is complicated and cell-responses observed independently may be modified (such as adhesion) when culture conditions are varied.

- Surface chemistry in addition to surface topology may be used to modify cell culture sub-populations in co-culture, the 3-aminopropyl surface chemistry significantly enriching the epithelial population while glass disks created microenvironments enrich the mesenchymal population.

This study represents a unique contribution to the existing body of scientific literature in that it is the first time that surfaces of these types have been applied to the culture of human derived tumour cell lines. This is also the first time to the best of my knowledge that surface directed cell selectivity has been achieved *in vitro* in the presence of multiple cell sub-populations. The potential offered by this concept, if it can be tuned to select for other cells of interest, would be very significant for the work of tumour biology, biomarker discovery and other biomedical fields where disease phenotypes exit within a larger population as well as other fields where a high degree of control over specific cell sub-populations is required, such as tissue and other biological engineering fields (Fisher *et al.*, 2013; Yeatts *et al.*, 2013).

6.4 Priorities & considerations for future work

Having successfully identified surfaces which can act selectively in culture, there is considerable scope for future studies surrounding the project, specifically with regard to the issues raised in the above discussion.

6.4.1 Greater understanding of the materials & how properties influence cell & protein responses.

One of the limitations of the current study is that the different materials presented in chapter four are understood in a largely qualitative nature in terms of their properties. While experimental evidence is presented to demonstrate that these materials do have different chemical properties, a greater level of characterisation such as determining the extent of surface coverage of the functionality is desirable and achievable even on chemically complex surfaces through greater application of techniques like XPS and secondary ion mass spectrometry (Kim *et al*., 2005).

The advantage of this characterisation is that it would allow another level of variability into the materials fabricated, as once the extent of modification can be quantified, efforts can be made to vary the functionality between materials, offering another route to tuning material properties and accordingly the response of different proteins and cells to the surfaces. This would allow fundamental information on precisely what materials properties are required to achieve a given outcome to be derived as well as defining how this is related to other material properties such as topology. The generation of functionality and topology gradients to quickly assess the responses of cells and proteins to different surface chemistries could also be explored.

6.4.2 Greater understanding of the cells response & how it differs between the different cell populations

Principally, a more detailed understanding how biological pathways can be influenced by different materials and as such the cells response and the mechanisms of transducing this response can be gained through pathway analysis. This can be done at a range of different levels, from the transcriptome, to the proteome and metabolome (Cranford *et al*., 2013). 'Omics' technologies such as sequencing, gene arrays and mass spectrometry involve the simultaneous study of many hundreds of different entities in the cell and how they change in relation to perturbations in their environment. Such global studies would be ultimately essential in understanding why cells respond in the manner they do to different surfaces. A current theme is to apply the Omics philosophy to materials

testing directly; to look at arrays of many different kinds of materials at once and compare the responses observed (Cranford *et al*., 2013).

A novel method to generate a more detailed understanding of biological interactions with the different silica surfaces is laid out below. Current technology permits the fabrication of the different surfaces in an array format; this can be used for tissue culture, once complete the responses of the cells can be examined in a massively parallel manner. This principle has been discussed in detail by Anderson *et al*., with respect to probing cell response to biomaterials using optical imaging and immunofluorescence (Anderson *et al*., 2005).

Such a methodology however has drawbacks, for example the number of compatible fluorescence probes limits the number of entities that can be examined to ≤10 at most. If the analysis system was based on an Omics technology such as mass spectrometry, then the number of entities assessed simultaneously would be considerably enhanced, the system would also be able to assess entities which were not anticipated to change, providing a more global 'a priori' approach.

With the advent of MALDI-Imaging the potential to relate a raster of mass spectra to a 2D coordinate could allow the application of mass spectrometry to 'biomaterial arrays'. However, currently the technology appears to be limited to the imaging of tissue sections, with limited exploration of other applications, such as imaging cells from tissue culture, with a direction towards drug protein co-localisation (Ait-Belkacem *et al*., 2012). The preliminary results of a culture compatible MALDI-Imaging biomaterials array are shown in fig. 6.3.
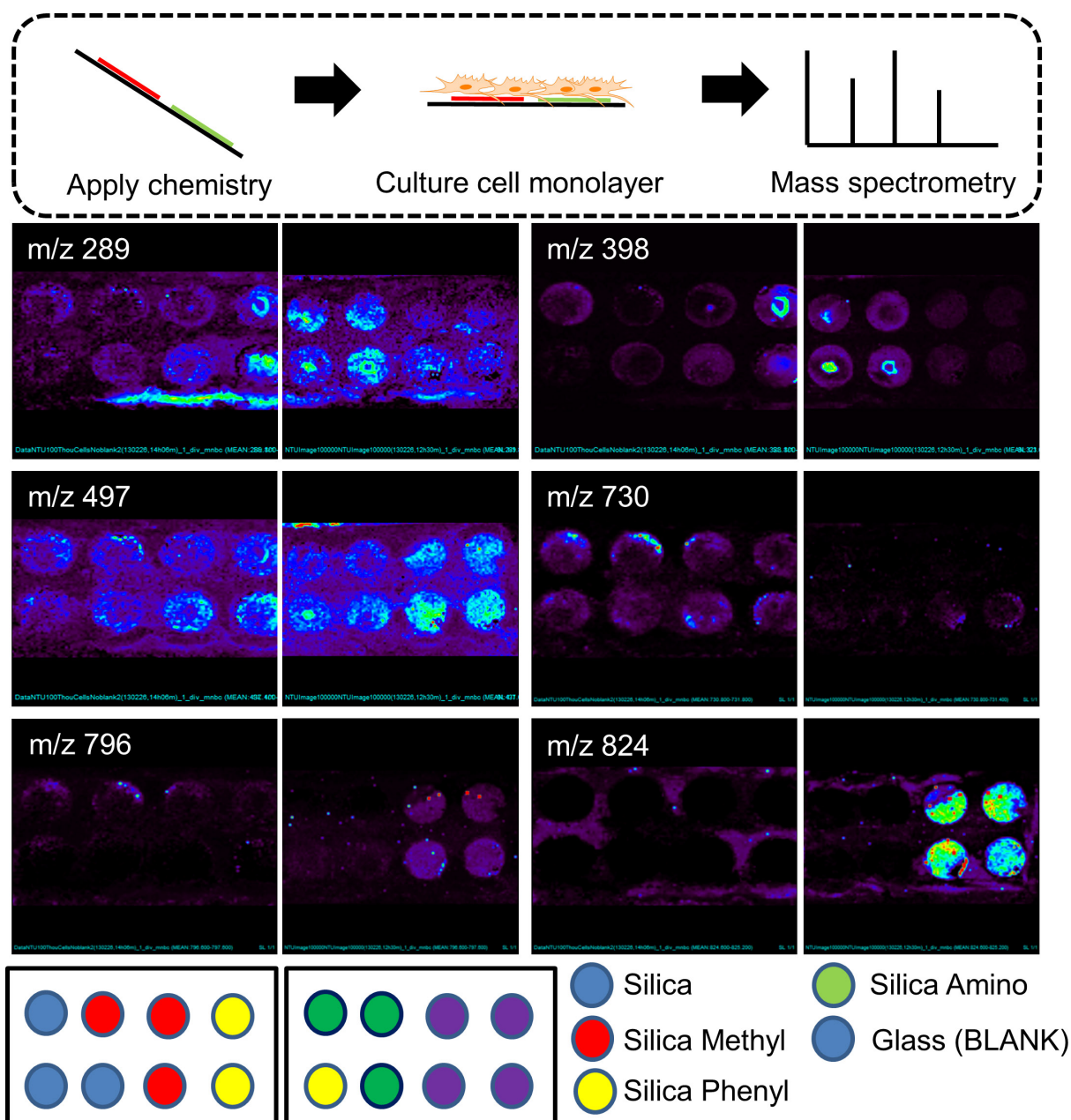
Figure 6.3: Concept of MALDI-Imaging materials shown above, an array of chemistry is applied to a suitable surface and a monolayer of cells culture atop the array. Array is then analysed through MALDI-Imaging mass spectrometry to identify differences in protein or lipid distribution, which can be correlated with the array. Preliminary data obtained with the assistance of Prof. M. Clench (Sheffield Hallam University), demonstrating differential lipid and protein *m/z* peaks correlating with different the functionalities used on the array.

As can be seen from fig. 6.4, the concept is capable of identifying cellular responses at the lipid level across the array. The potential of this technique to act as a high throughput

screening technology for cell-material interactions, in addition to cell protein interactions is very promising.

6.4.3 Application of selective materials in the cancer therapy development program

As materials with selective effects have been identified for populations relevant for cancer research, the possibility of applying these surfaces usefully in a therapy development program becomes a possibility; there are several potential areas such surfaces could be applied.

- The first application would be in general tissue culture practice within cancer research. The ability to derive and maintain different populations is potentially very useful, since it was already observed that conventional culture materials are unable to sustain certain sub-populations (derived from either cancerous or normal tissue), especially over extended periods (Colosimo *et al.*, 2013). This could also be applied to the culture of patient derived primary materials rather than just established cell lines as these are very difficult to maintain by conventional practice, potentially due to the inadequate materials used to isolate primary tissue *in vitro* (Wang & Shen, 2011). Such a strategy may improve the quality and applicability of *in vitro* cell models in cancer research as they currently suffer many limitations (Capes-Davis *et al.*, 2010; Domcke *et al.*, 2013). It should be borne in mind however that through work performed by others, there is a suggestion that certain sub-populations may be difficult to remove from culture since they are inherent to the cultures continued viability (Wang *et al.*, 2013)

- The second is in determining better the response of tumour sub-populations to known anti-cancer therapeutics, since it is acknowledged that different cancer sub-populations respond differently to known treatment regimens (Singh & Settleman, 2010). Since selective surfaces readily allow the isolation of one or more population of interest, they can be used to pre-condition a tumour population so only cells of interest in terms of drug response are carried through into the study. However the potential for interactions between the surface and drug variables in the cell response assay would make it difficult to incorporate the surfaces directly into

a study and make correlations with established assay materials like TCPS difficult to impossible.

- The final and potentially most interesting application would be in cancer vaccine development as a means to derive new biomarkers as therapeutic targets, since the surfaces may be used to isolate or enrich for specific cell sub-populations. As a result of selection or enrichment the biological 'noise' of other sub-populations would be reduced, so biomarker identification strategies may be able to more accurately resolve and associate biomarkers relative to the sub-population targeted. Targeted therapy, such as immunotherapy, being inherent to the strategies being employed today and in the near future to deal with problematic tumour sub-populations (Polzer & Klein, 2013).

6.5 References

1. Ait-Belkacem A, Sellami L, Villard C, DePauw E, Calligaris D & Lafitte D. (2012). Mass spectrometry imaging is moving toward drug protein co-localization. *Trends Biotechnol.*, 30(9):466-74

2. Allazetta S, Tanja C. Hausherr T.C & Lutolf M.P. (2013). Microfluidic Synthesis of Cell-Type-Specific Artificial Extracellular Matrix Hydrogels. *Biomacromolecules*, 14(4):1122-31

3. Allen L.T, Tosetto M, Miller I.S, O'Connor D.P, Penney S.C, Lynch I, Keenan A.K, Pennington S.R, Dawson K.A & Gallagher W.M. (2006). Surface-induced changes in protein adsorption and implications for cellular phenotypic responses to surface interaction. *Biomaterials*, 27(16):3096-108

4. Anderson D.G, Putnam D, Lavik E.B, Mahmood T.A. & Langer R. (2005). Biomaterial microarrays: rapid, microscale screening of polymer–cell interaction. *Biomaterials*, 26(23):4892-7

5. Ballester-Beltran J, Rico P, Moratal D, Song W, Mano J.F & Salmeron-Sanchez M. (2011). Role of superhydrophobicity in the biological activity of fibronectin at the cell–material interface. *Soft Matter*, 7(22):10803-11

6. Bassani R, Solaro R, Alderighi M, di Cesare D & Allegrini M. (2006). Nanoindentation with AFM. AITC-AIT 2006 International Conference on Tribology, ISBN: 88-902333-0-3

7. Benoit D.S, Schwartz M.P, Durney A.R & Anseth K.S. (2008). Small functional groups for controlled differentiation of hydrogel-encapsulated human mesenchymal stem cells. *Nature Mater.*, 7(10):816-23

8. Capes-Davis A, Theodosopoulos G, Atkin I, Drexler H.G, Kohara A, MacLeod R.A, Masters J.R, Nakamura Y, Reid Y.A, Reddel R.R & Freshney R.I. (2010). Check your cultures! A list of cross-contaminated or misidentified cell lines. *Int. J. Cancer*, 127(1):1-8

9. Carragee E.J, Hurwitz E.L & Weiner B.K. (2011). A critical review of recombinant human bone morphogenetic protein-2 trials in spinal surgery: emerging safety concerns and lessons learned. *Spine J.*, 11(6):471-91

10. Christopherson G.T, Song H & Mao H.Q. (2009). The influence of fiber diameter of electrospun substrates on neural stem cell differentiation and proliferation. *Biomaterials*. 30(4):556-64

11. Colosimo A, Russo V, Mauro A, Curini V, Marchisio M, Bernabò N, Alfonsi M, Mattioli M & Barboni B. (2013). Prolonged *in vitro* expansion partially affects phenotypic features and osteogenic potential of ovine amniotic fluid-derived mesenchymal stromal cells. *Cytotherapy*, 15(8):930-50

12. Cranford S.W, de Boer J, van Blitterswijk C & Buehler M.J. (2013). Materiomics: An - omics Approach to Biomaterials Research. *Adv. Mater.,* 25(6):802-24

13. Curran J.M, Chen R & Hunt J.A. (2006). The guidance of human mesenchymal stem cell differentiation *in vitro* by controlled modifications to the cell substrate. *Biomaterials*, 27(27):4783-93

14. Curran J.M, Stokes R, Irvine E, Graham D, Amro N.A, Sanedrin R.G, Jamil H & Hunt J.A (2010). Introducing dip pen nanolithography as a tool for controlling stem cell behaviour: unlocking the

potential of the next generation of smart materials in regenerative medicine. *Lab Chip*, 10(13):1662-70

15. Curran J.M, Pu F, Chen R & Hunt J.A (2011) The use of dynamic surface chemistries to control msc isolation and function. *Biomaterials*, 32(21):4753-60

16. Curtis A.S., Forrester J.V., McInnes C & Lawrie F. (1983) Adhesion of cells to polystyrene surfaces. *J. Cell Biol.*, 97(5):1500-6

17. Curtis A.S.G & Forrester J.V. (1984). The competitive effects of serum proteins on cell adhesion. *J. Cell Sci.*, 71:17-35

18. da Costa, Pires R.A, Frias A.M, Reis R.L & Pashkuleva I. (2012). Sulfonic groups induce formation of filopodia in mesenchymal stem cells. *J. Mater. Chem.*, 22(15):7172-8

19. Dalby M.J, Gadegaard N, Tare R, Andar A, Riehle M.O, Herzyk P, Wilkinson C.D & Oreffo R.O. (2007). The control of human mesenchymal cell differentiation using nanoscale symmetry and disorder. *Nature Mater.*, 6(12):997-1003

20. Deligianni D.D, Katsala N, Ladas S, Sotiropoulou D, Amedee J & Missirlis Y.F. (2001). Effect of surface roughness of the titanium alloy Ti-6Al-4V on human bone marrow cell response and on protein adsorption. *Biomaterials*, 22(11)1241-51

21. Dolley-Sonneville P.J, Romeo L.E & Melkoumian Z.K. (2013). Synthetic surface for expansion of human mesenchymal stem cells in xeno-free, chemically defined culture conditions. *PLoS One*. 8(8):e70263

22. Domcke S, Sinha R, Levine D.A, Sander A & Schultz N. (2013). Evaluating cell lines as tumour models by comparison of genomic profiles. *Nat. Commun.*, 4(2126): doi:10.1038/ncomms3126

23. Fisher R, Pusztai L & Swanton C. (2013). Cancer heterogeneity: implications for targeted therapeutics. *Br. J. Cancer*, 108(3):479-85

24. García A.J, Vega M.D & Boettiger D. (1999). Modulation of Cell Proliferation and Differentiation through Substrate-dependent Changes in Fibronectin Conformation. *Mol. Biol. Cell*, 10(3):785-98

25. Gilbert P.M, Havenstrite K.L, Magnusson K.E, Sacco A, Leonardi N.A, Kraft P, Nguyen N.K, Thrun S, Lutolf M.P & Blau H.M. (2010). Substrate elasticity regulates skeletal muscle stem cell self-renewal in culture. *Science*, 329(5995):1078-81

26. Ingber D.E. (2006). Cellular mechanotransduction: putting all the pieces together again. *FASEB J.*, 20(7):811-27

27. Keselowsky B.G, Collard D.M & García A.J. (2005). Integrin binding specificity regulates biomaterial surface chemistry effects on cell differentiation. *Proc. Natl. Acad. Sci. U. S. A.*, 102(17):5953-7

28. Kim J, Shon H.K, Jung D, Moon D.W, Han S.Y & Lee T.G. (2005). Quantitative Chemical Derivatization Technique in Time-of-Flight Secondary Ion Mass Spectrometry for Surface Amine Groups on Plasma-Polymerized Ethylenediamine Film. *Anal. Chem.*, 77(13):4137-41

29. Koenig A.L, Gambillara V & Grainger D.W. (2003). Correlating fibronectin adsorption with endothelial cell adhesion and signaling on polymer substrates. *J. Biomed. Mater. Res., Part A*, 64A(1):20-37

30. Lee M.R, Kwon K.W, Jung H, Kim H.N, Suh K.Y, Kim K & Kim K.S. (2010). Direct differentiation of human embryonic stem cells into selective neurons on nanoscale ridge/groove pattern arrays. *Biomaterials*, 31(15):4360-6

31. Lin R & Chang H. (2008). Recent advances in three-dimensional multicellular spheroid culture for biomedical research. *Biotechnol. J.*, 3(9-10):1172-84

32. McMurray R.J, Gadegaard N, Tsimbouri P.M, Burgess K.V, McNamara L.E, Tare R, Murawski K, Kingham E, Oreffo R.O & Dalby M.J. (2011). Nanoscale surfaces for the long-term maintenance of mesenchymal stem cell phenotype and multipotency. *Nat. Mater.*, 10(8):637-44

33. Miki J & Rhim J.S. (2008). Prostate cell cultures as *in vitro* models for the study of normal stem cells and cancer stem cells. *Prostate Cancer Prostatic Dis.*, 11(1):32-9

34. Natarajan A, Chun C, Hickman J.J & Molnar P. (2008). Growth and Electrophysiological Properties of Rat Embryonic Cardiomyocytes on Hydroxyl- and Carboxyl-Modified Surfaces. *J. Biomater. Sci., Polym. Ed.*, 19(10):1319-31

35. Nava M.M, Raimondi M.T & Pietrabissa R. (2012). Controlling self-renewal and differentiation of stem cells *via* mechanical cues. *J. Biomed. Biotechnol.*, 2012:797410

36. Oliveira S.M, Song W, Alves N.M & Mano J.F. (2011). Chemical modification of bioinspired superhydrophobic polystyrene surfaces to control cell attachment/proliferation. *Soft Matter*, 7(19):8932-41

37. Onoue T, Uchida D, Begum N.M, Tomizuka Y, Yoshida H, Sato M. (2006). Epithelial-mesenchymal transition induced by the stromal cell-derived factor-1/CXCR4 system in oral squamous cell carcinoma cells. *Int. J. Oncol.*, 29(5):1133-8

38. Phillips J.E, Petrie T.A, Creighton F.P & García A.J. (2010). Human mesenchymal stem cell differentiation on self-assembled monolayers presenting different surface chemistries. *Acta Biomater.*, 6(1):12-20

39. Polzer B & Klein C.A. (2013). Metastasis Awakening: The challenges of targeting minimal residual cancer. *Nat. Med.*, 19(3):274-5

40. Saltzman W.M & Kyriakides T.R, Principles Tissue Engineering, Academic Press, 3rd edn, 2007, p. 279

41. Serra M, Brito C, Correia C & Alves P.M. (2012). Process engineering of human pluripotent stem cells for clinical application. *Trends Biotechnol.*, 30(6):350-9

42. Singh A & Settleman J. (2010). EMT, cancer stem cells and drug resistance: an emerging axis of evil in the war on cancer. *Oncogene*, 29(34):4741-51

43. Spargo B.J, Testoff M.A, Nielsen T.B, Stenger D.A, Hickman J.J & Rudolph A.S. (1994). Spatially controlled adhesion, spreading, and differentiation of endothelial cells on self-assembled molecular monolayers. *Proc. Natl. Acad. Sci. U. S. A.*, 91(23):11070–4

44. Steele J.G, Dalton B.A, Johnson G & Underwood P.A. (1995). Adsorption of fibronectin and vitronectin onto Primaria™ and tissue culture polystyrene and relationship to the mechanism of initial attachment of human vein endothelial cells and BHK-2 1 fibroblasts. *Biomaterials*, 16(14):1057-67

45. Thomas C.H, Collier J.H, Sfeir C.S & Healy K.E. (2002). Engineering gene expression and protein synthesis by modulation of nuclear shape. *Proc. Natl. Acad. Sci. U. S. A.*, 99(4):1972-7

46. Valentijn A.J, Zouq N & Gilmore A.P. (2004). Anoikis. Biochem. Soc. Trans., 32(Pt3):421-5.

47. Wang Y, Bronshtein T, Sarig U, Nguyen E.B, Boey F.Y.C, Venkatraman S.S & Machluf M. (2013). A Mathematical Model Predicting the Coculture Dynamics of Endothelial and Mesenchymal Stem Cells for Tissue Regeneration. *Tissue Eng. Part A*, 19(9-10):1155-64

48. Wang Z.A & Shen M.M. (2011). Revisiting the concept of cancer stem cells in prostate cancer. *Oncogene*, 30(11):1261-71

49. Yeatts A.B, Choquette D.T & Fisher J.P. (2013). Bioreactors to influence stem cell fate: augmentation of mesenchymal stem cell signaling pathways via dynamic culture systems. *Biochim. Biophys. Acta*, 1830(2):2470-80

Appendix A
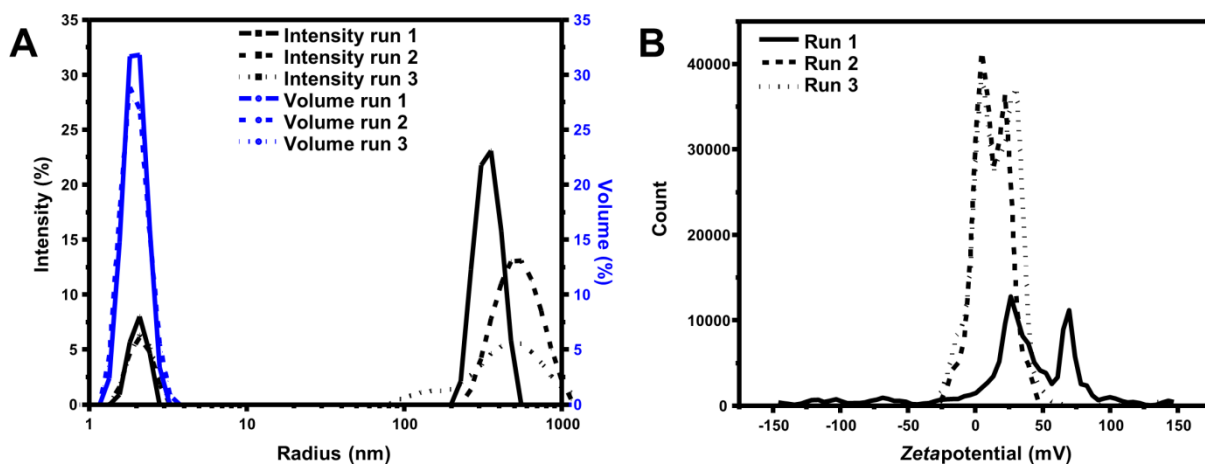
Figure A1: Volume and intensity data (A) obtained by DLS of 25 mg/mL lysozyme dispersed in 0.1 M phosphate buffer (pH 7.6). *Zeta* potential measurements (B) of 25 mg/mL lysozyme dispersed in 0.01 mM HCl.

Table A1: Size & *zeta* potential measurements of lysozyme

DLS measurements of protein size (0.1 M phosphate buffer, pH 7.6)					
Run	Ø (nm)	Width (nm)	PdI	Avg. *Zeta* (mV)	Mob (μmcm/Vs)
1	4.127	0.499	0.745	-	-
2	4.263	0.688	1	-	-
3	4.324	0.720	1	-	-
Zeta potential measurements (1 mM HCl)					
1	-	-	-	8.36	0.557
2	-	-	-	10.3	0.689
3	-	-	-	11.1	0.742
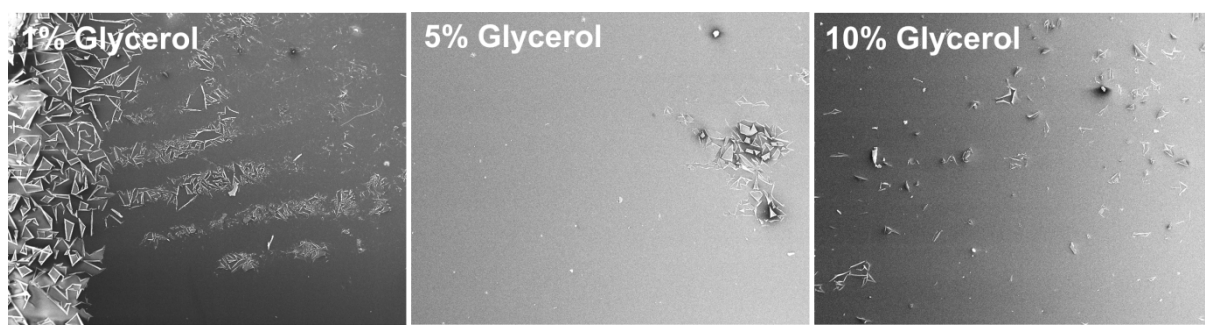
Figure A2: Influence of glycerol drying control additive on silica film cracking post-drying. Addition of 5% glycerol to the hydrolysis solution eliminated cracking.

Appendix B
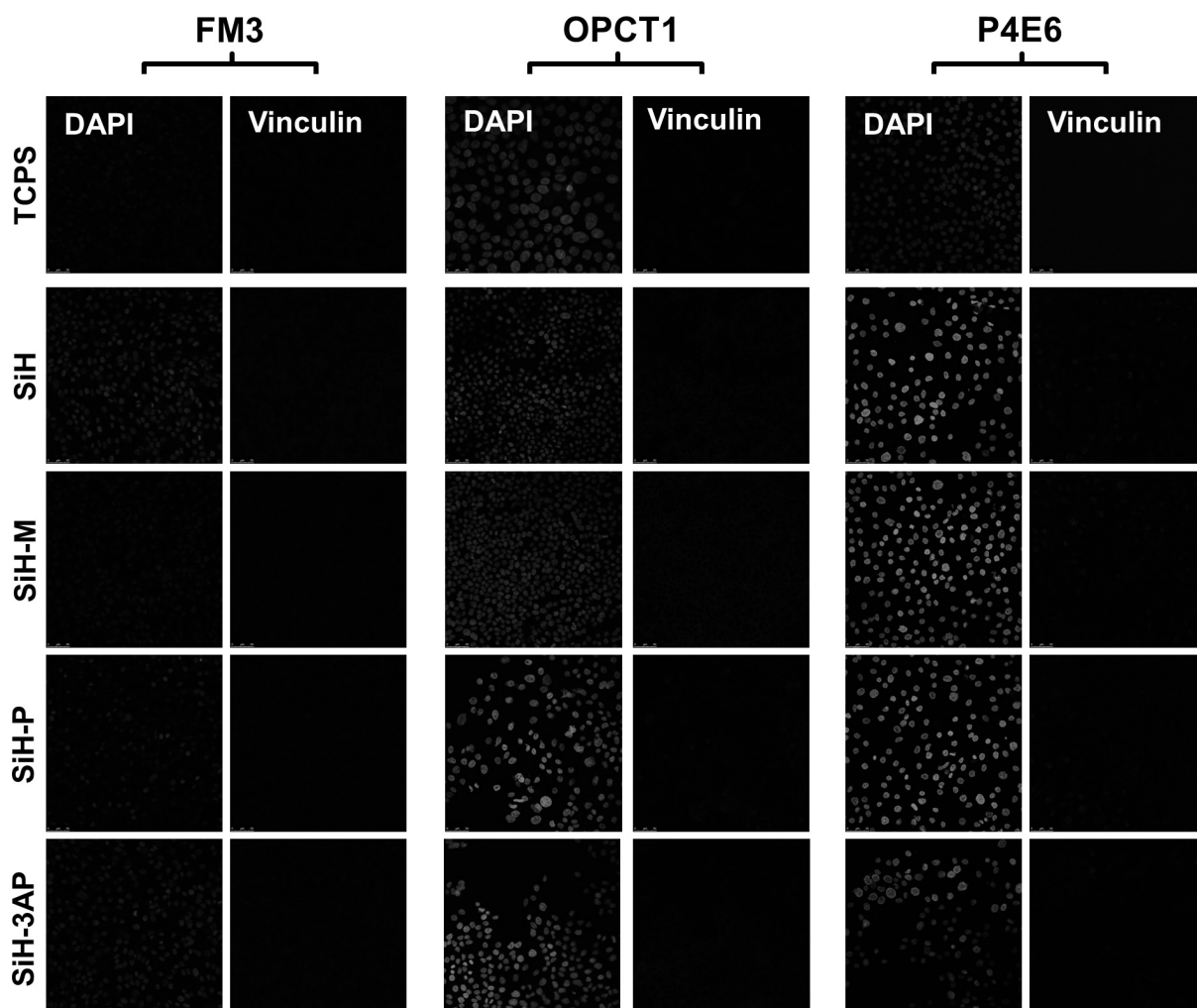
Figure B1: Isotype controls for non-specific background staining of goat anti-mouse IgG conjugated to Alexa Fluor® 488 antibody for the FM3, P4E6 and OPCT1 cell lines on different surfaces. DAPI staining of cell nuclei is also shown.

Table B1: General properties of foetal calf serum

pH	7.25
Osmolarity	309 mOsm/L
Endotoxin	0.24 EU/mL

Chemical composition			
Sodium	135 mMol/L	Gamma GT	6 IU/L
Potassium	12.7 mMol/L	Cholesterol	34 mg/mL

Chemical composition

Chloride	99 mMol/L	Bilirubin	0.2 mg/mL
Uric acid	2.9 mg/mL	Glucose	125 mg/mL
Calcium	14.3 mg/mL	Urea	41 mg/mL
Phosphorous	10.8 mg/mL	Creatinin	2.9 mg/mL
Alkaline phosphatase	220 IU/L	Triglyceride	60 mg/mL
LDH	489 IU/L	Haemoglobin	15.51 mg/mL
SGOT	31 IU/L	Iron	0.194 mg/mL
SGPT	<6 IU/L		

Protein composition

Total protein	3.79 g/100 mL	Globulins	0.78 g/100 mL
Albumin	1.57 g/100 mL	Globulins	0.05 g/100 mL
Globulins	1.4 g/100 mL	IgG	0.45 g/100 mL

Table B2: General properties of RPMI-1640 media

pH	6.9-7.4
Osmolarity	270-293 mOsm/L
Endotoxin	0.24 EU/mL

Chemical composition (mg/mL)

$Ca(NO_3)_2 \cdot 4H_2O$	100	L-Methionine	15
KCl	400	L-Penylalanine	15
$MgSO_4 \cdot 7H_2O$	100	L-Proline	20
NaCl	6000	L-Serine	30
$NaHCO_3$	2000	L-Threonine	20
$Na_2HPO_4 \cdot 7H_2O$	1512	L-Tryptophan	5
Glucose	2000	L-Tyrosine	20
Glutathione (reduced)	1	L-Valine	20
Phenol red·Na	5	p-Aminobenzoic acid	1
L-Arginine	200	d-Biotin	0.2
L-Asparagine·H_2O	50	D-Ca Pantothenate	0.25
L-Aspartic acid	20	Choline Chloride	3
L-Cystine	50	Folic acid	1
L-Glutamic acid	20	i-Inositol	35
Glycine	10	Nicotinamide	1
L-Histidine	15	Pyridoxine·HCl	1

Chemical composition (mg/mL)			
Hydroxy L·Proline	20	Riboflavin	0.2
L-Isoleucine	50	Thiamine·HCl	1
L-Leucine	50	Vitamin B12	0.01
L-Lysine·HCl	40		

Appendix C
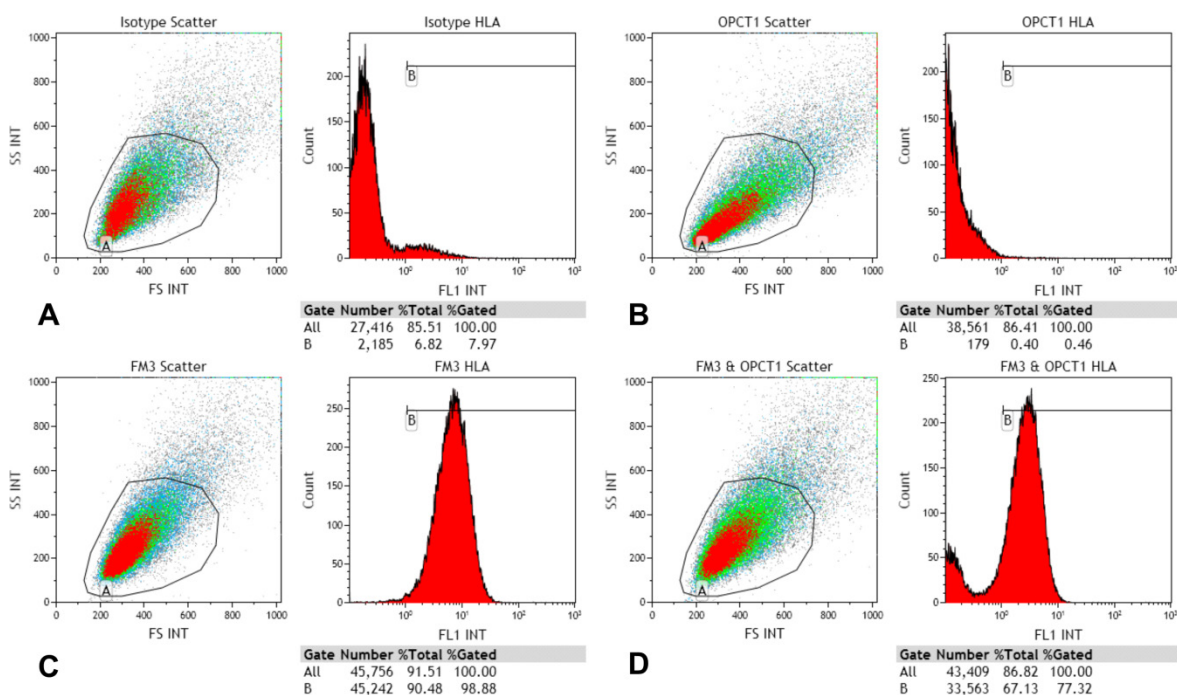
Figure C1: Differential expression of HLA-A2 by OPCT1 (B) and FM3 (C) cell lines by flow cytometry. Non-specific staining isotype control identified ~8% of the FM3 population acquired the HLA-A2 antibody non-specifically (A). Histogram generated by staining FM3 and OPCT1 from co-culture (D) demonstrates both populations can be resolved.
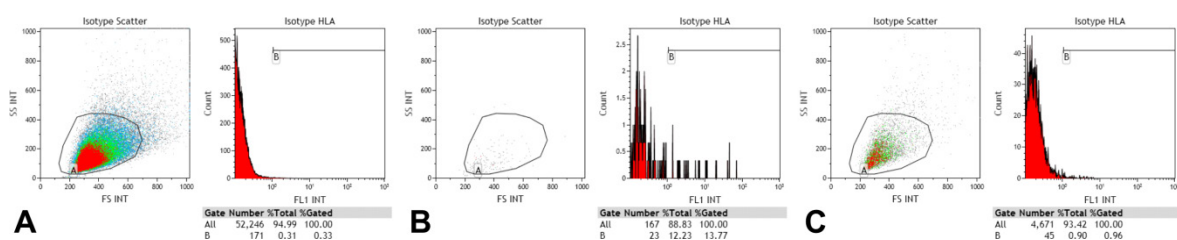
Figure C2: Non-specific isotype control for goat anti-mouse IgG conjugated to Alexa Fluor® 488 antibody obtained during attempts to enrich by adhesion, obtained by flow cytometry.

Figure C3: Non-specific isotype controls for goat anti-mouse IgG conjugated to Alexa Fluor® 488 and goat anti-rat IgG conjugated to Alexa Fluor® 568 antibodies obtained by confocal microscopy. DAPI staining of the cell nucleus is also shown.

Figure C4: Non-specific isotype controls for goat anti-rabbit IgG conjugated to Alexa Fluor® 488 and goat anti-mouse IgG conjugated to Alexa Fluor® 568 antibodies obtained by confocal microscopy. DAPI staining of the cell nucleus is also shown.

Figure C5: Non-specific isotype control for mouse anti-human vimentin antibody with live dead staining for the OPCT1 cell lines obtained by flow cytometry.

Figure C6: Non-specific isotype control for mouse anti-human vimentin antibody with live dead staining for the OPCT1 cell lines obtained by flow cytometry.
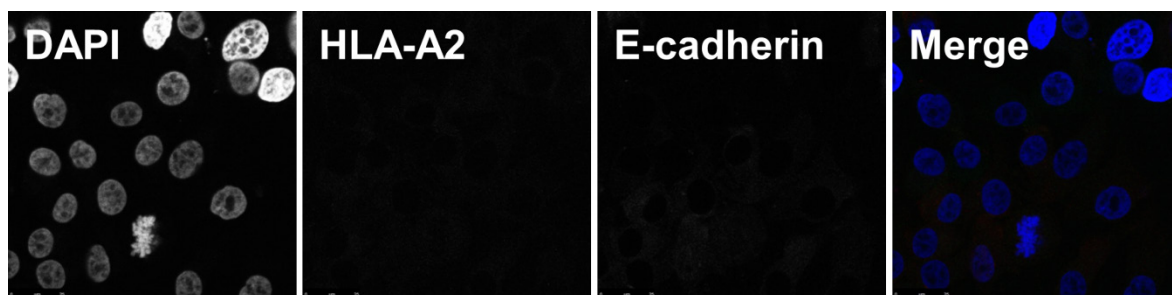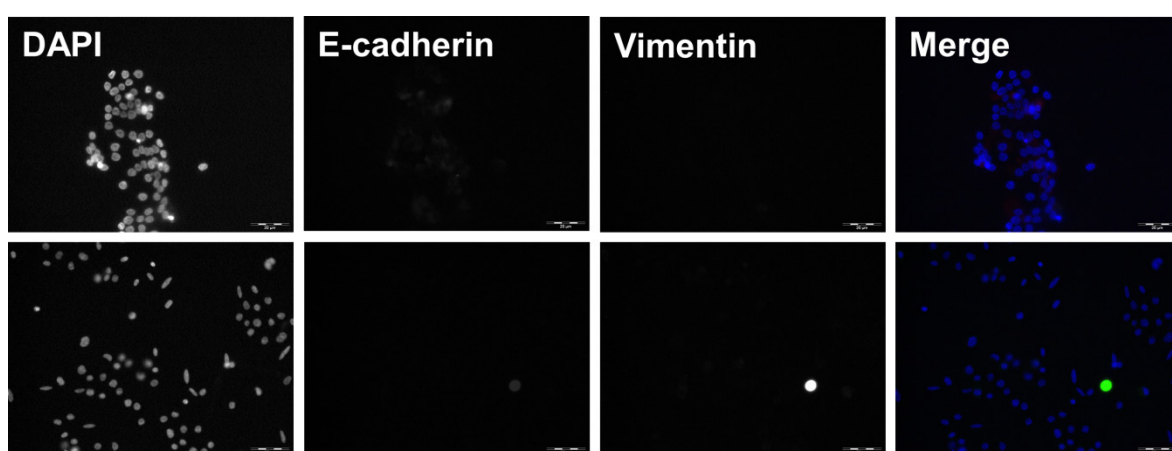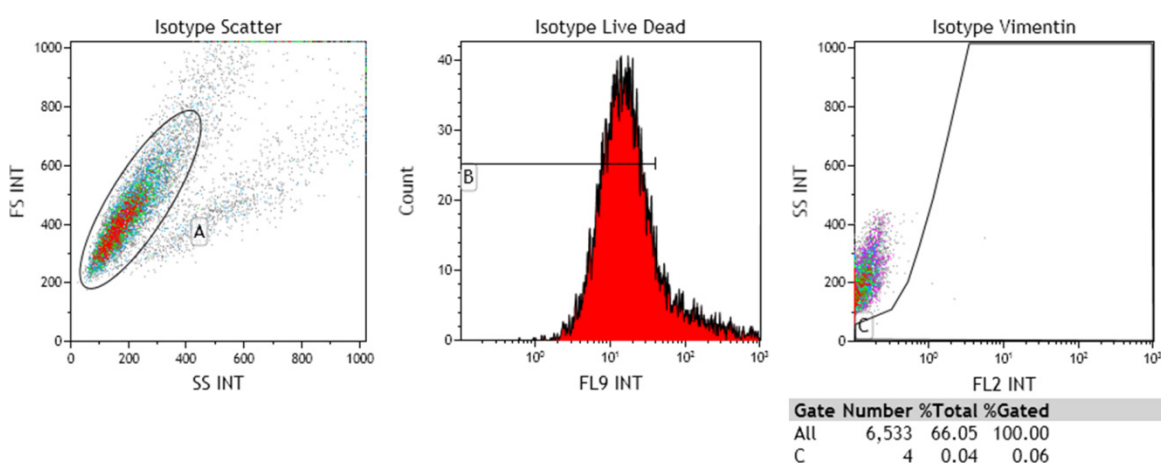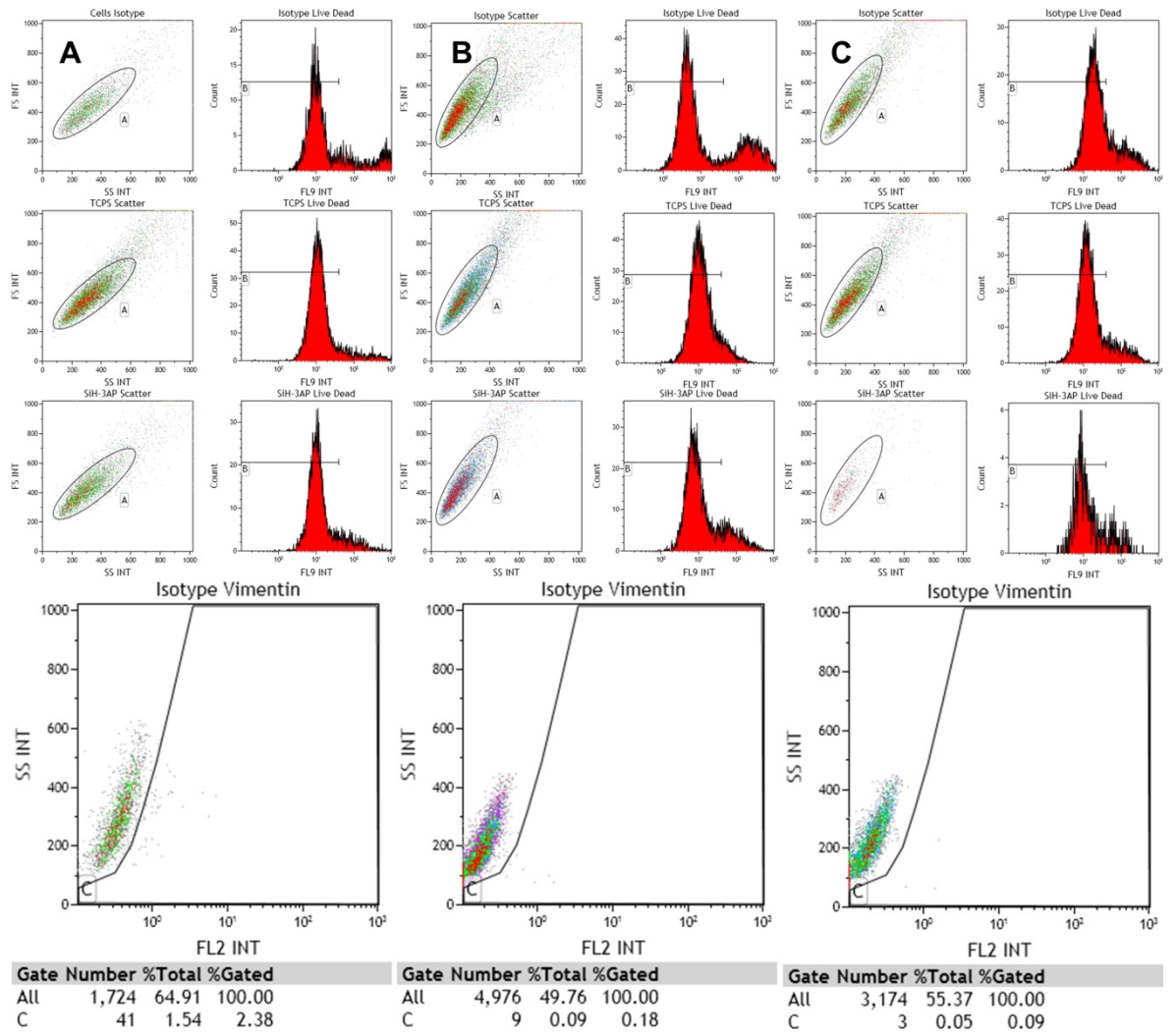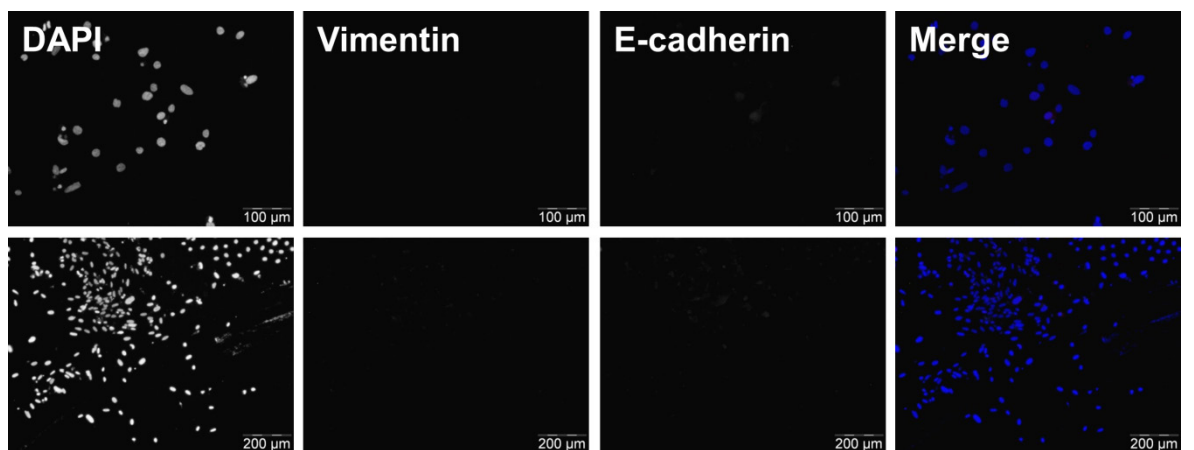

Figure C7: Non-specific isotype controls for goat anti-rabbit IgG conjugated to Alexa Fluor® 488 and goat anti-mouse IgG conjugated to Alexa Fluor® 568 antibodies for the OPCT1 cell line obtained by immunofluorescence.

Appendix D

Materials & methods

Materials

Tissue culture polystyrene in a 96 well format was obtained from Sarstedt (UK). Polyaniline hydrochloride, ammonium persulphate, glutaric dialdehyde, lysozyme, sodium phosphate monobasic, sodium phosphate dibasic, 3-amino-7-dimethylamino-2-methylphenazine hydrochloride (Neutral Red dye), 0.4% trypan blue solution, 3-aminopropyltriethoxysilane (APTEOS) and tetramethoxysilane (TMOS) were obtained from Sigma-Aldrich® (UK). Bovine foetal calf serum (FCS), 1 M hydrochloric acid, methanol, 96 well chamber slides and glacial acetic acid were obtained from Thermo Fisher Scientific (UK). EtOH was supplied by Hayman Speciality Products (UK). Dulbecco's phosphate buffered saline (DPBS); RPMI-1640 media, trypsin-versene (EDTA) solution and L-glutamate solution were obtained from Lonza BioWhittaker™ (UK). Keratinocyte serum free media (KSFM) with L-glutamine and TrypLE™ Express were obtained from Gibco®, Life Technologies™ (UK). The FM3 cell line was originally obtained from Prof. G. Pawelec, University of Tübingen, Germany. The OPCT1 cell line was originally obtained from Onyvax, UK. Distilled and deionised water (ddH$_2$O) was produced locally by distillation and ion exchange filtration, resulting in a pH of 5.8 and a conductivity of $< 1\mu S/cm^{-1}$.

Surface fabrication

Surfaces were fabricated in the manner described in section 4.2.2. Formyl modified surfaces were fabricated through the further functionalisation of the SiH-3AP surface through treatment with 2% glutaric dialdehyde for a period of 2 h at 57°C. Arrays for MALDI imaging were fabricated using 96 well chamber slides, the well plastic removed after culture for MALDI imaging.

Surface free energy measurement

Measurements were performed in the manner described in section 4.2.5.

Tissue culture

Cells were cultured in the manner described in section 5.2.3. For MALDI imaging array OPCT1 cells were seeded at an initial density of 1^x10^5 cells per well and cultured for a period of 48 hours.

Neutral red assay

The assay was performed in the manner described in section 4.2.8.

Light microscopy

Light microscopy was performed in the manner described in section 5.2.7.

MALDI imaging

MALDI imaging was performed on arrays which were removed from culture and washed twice with PBS before being washed once with ddH_2O to remove salts. The arrays were applied with a CHCA matrix before MALDI-imaging was performed using an ABSciex QTof MALDI mass spectrometer. Instrument operation and sample preparation was kindly conducted by Prof. M. Clench (Sheffield Hallam University, UK). Data analysis was performed using the BioMap 3.8.04 software to identify differentially expressed peaks across the array. Data was subjected to normalisation using the divide function of BioMap with the matrix peak at *m/z* 417 as the reference.

Glossary

°	Degrees	DOPA	L-3,4-dihydroxyphenylalanine
2+1D	Pseudo two dimensional	DPBS	Dulbecco's phosphate buffered saline
3D	Three dimensional		
A	Absorbance	DRIFTS	Diffuse reflectance infrared Fourier transform spectroscopy
A_0	Correlation function baseline		
ABCB5	ATP-binding cassette sub-family B member 5	ε	Extinction coefficient
		ECM	Extracellular matrix
ACTT	Adoptive cell transfer therapy	EDTA	Ethylenediaminetetraacetic acid
ADP	ADP	EDXa	Energy dispersive X-ray analysis
AFM	Atomic force microscope		
AMP	AMP	ELISA	Enzyme-linked immunosorbent assay
Å	Angstrom		
ANOVA	Analysis of variance	EMT	Epithelial to mesenchymal transition
APC	Antigen presenting cell		
APTEOS	3-aminopropyltriethoxysilane	ERK	Extracellular signal-regulated kinases
Arg	Arginine		
Asp	Asparagine	EtOH	Ethanol
ATP	Adenosine-5-triphosphate	EU	Endotoxin units
ATR	Attenuated total reflectance	exp	Exponential
AU	Arbitrary units	F	Test statistic
Avg	Average	FAC	Focal adhesion kinase
B	Correlation function intercept	FACS	Fluorescence assisted cell sorting
BE	Binding energy		
BSA	Bovine serum albumin	f-actin	Filamentous actin
c	Concentration	FADD	Fas-associated protein with death domain
C	Correlation function		
C1s	Photoelectrons from carbon 1s subshell	Fb	Fibrinogen
		FCS	Foetal calf serum
Cav	Caveolin	FLIP	FLICE-like inhibitory protein
CD	Cluster of differentiation	FN	Fibronectin
CSC	Cancer stem cell	FSP	Fibroblast-specific protein 1
D	Diffusion coefficient	FTIR	Fourier transform infrared
DAPI	4,6-diamidino-2-phenylindole	G_0	G zero cell cycle phase
ddH_2O	Distilled & deionised water	G_1	Gap 1 cell cycle phase
Δk	Variation of light intensity	GDA	Glutaric dialdehyde
DLS	Dynamic light scattering	Gl	Gas liquid interface
DNA	Deoxyribonucleic acid	Gly	Glycine

HLA	Human leukocyte antigen	O1s	Photoelectrons from oxygen 1s subshell
hMSC	Human mesenchymal stem cell		
hv	Light	P	Probability
ICP-OES	Induction coupled plasma – optical emission spectroscopy	P#	Passage
		p53	Tumour protein 53
IF	Immunofluorescence	PANI	Polyaniline
Ig	Immunoglobulin	PAP	Prostatic acid phosphatase
IL	Interleukin	PBMC	Peripheral blood mononuclear cell
IR	Infrared		
IU	International unit	PBS	Phosphate buffered saline
JNK	c-Jun N-terminal kinase	PC	Polycarbonate
K/k	Rate	PCL	Polycaprolactone
Kα	K-alpha X-ray	PdI	Polydispersity index
k_B	Boltzmann's constant	PEG	Polyethylene glycol
KE	Kinetic energy	PES	Polyethersulfone
KSFM	Keratinocyte serum free media	PGA	Polyglycolide
L	Path length	PGLA	Poly(lactic-co-glycolic acid)
LDH	Lactate dehydrogenase	pH	Power of hydrogen
Lsi1	Low silicon rice1 protein	pI	Isoelectric point
LYZ	Lysozyme	PMMA	Poly(methyl methacrylate)
m/z	Mass to charge ratio	Ppi	Pyrophosphate
MACS	Magnetically assisted cell sorting	ppm	Parts per million
		PS	Polystyrene
MALDI	Matrix assisted laser desorption ionisation	PTEOS	Phenyltriethoxysilane
		PUA	Poly(urethane acrylate)
MAPK/ERK	Signalling pathway	Q	Tetra-functional condensation species
MEK	Mitogen-activated protein kinase kinase		
		R^2	Coefficient of determination
MeOH	Methanol	RAS	Ras protein family
MET	Mesenchymal to epithelial transition	RC	Remaining cells
		RCF	Relative centrifugal force
MS	Mass spectrometry	RGD	Arg-Gly-Asp integrin binding site
MSMS	Tandem mass spectrometry		
MTEOS	Methyltriethoxysilane	R_H	Hydrodynamic radius
n	Refractive index	RLU	Relative light unit
N/n	Replicate number	RMS	Root mean squared
N1s	Photoelectrons from nitrogen 1s subshell	RNA	Ribonucleic acid
		RPMI	Roswell Park Memorial Institute medium
Ø	Diameter		
		$S_\#/T_\#$	Electronic states

193.

SAM	Self-assembled monolayer	WHO	Would health organisation
SD	Standard deviation	Wt.%	Weight percentage
SE	Standard error	X	Dimension
SEM	Scanning electron microscopy	XPS	X-ray photoelectron spectroscopy
SG	Solid gas interface		
SGOT	Aspartate aminotransferase	Y	Dimension
SGPT	Serum glutamic pyruvate transaminase	Z	Dimension
		ZO-1	Tight junction protein ZO-1
Si	Silicon	γ^d	Dispersive component of surface energy
Si2p	Photoelectrons from silicon 2p subshell		
		γ^p	Polar component of surface energy
SiG	Glycerol incorporating silica		
SiH	Super-hydrophilic silica	γ^{tot}	Surface free energy
SiH-3AP	APTEOS functionalised SiH	γ^-	Basic component of the polar component of surface energy
SiH-M	MTEOS functionalised SiH		
SiH-P	PTEOS functionalised SiH	γ^+	Acidic component of the polar component of surface energy
SL	Solid liquid interface		
α-SMA	α-smooth muscle actin	δ	In-plane bending vibration
sol	Solution	η	Viscosity
Src	Src family kinase	θ	Plane angle
T	Time	λ_0	Laser wavelength
t	Temperature	ρ	Rocking bond vibration
TACSTD	Tumour-associated calcium signal transducer	γ/τ	Out-of-plane bending vibration
		τ	Time constant
TBS	Tris-buffered saline	ω	Wagging bond vibration
T-cell	T lymphocyte	π	Pi mathematical constant
TCPS	Tissue culture polystyrene		
TEM	Transmission electron microscope		
TEOS	Tetraethoxysilane		
TGF-β	Tumour growth factor		
TMOS	Tetramethoxysilane		
Tris	Tris(hydroxymethyl) aminomethane		
TWEEN	Polysorbate		
UV-Vis	Ultra-violet visible		
ν	Bond stretching vibration		
ν_a	Out-of-phase ν		
ν_s	In-phase ν		
WD	Working distance		

Communications

Publications

- Hickman G.J, Rai A, Boocock D.J Rees R.C & Perry C.C. (2012). Fabrication, characterisation and performance of hydrophilic and super-hydrophilic silica as cell culture surfaces. J. Mater. Chem., 22:12141-12148

- El hadad A.A, Barranco V, Jiménez-Morales A, Peón E, Hickman G.J, Perry C.C & Galván J.C. Organic-inorganic hybrid sol-gel thin films modified with nanocrystalline hydroxyapatite particles; *in-vitro* bioactivity and corrosion protection performance. Manuscript in preparation

Oral presentations

- <u>Hickman G.J</u>, Boocock D.J Rees R.C & Perry C.C. (2013). Interactions of Cancer Cells & Inorganic Materials; Selective Culture of Tumour Sub-populations. 11th International Conference on Materials Chemistry (MC11)

- <u>Hickman G.J</u>, Boocock D.J Rees R.C & Perry C.C. (2013). Surface Directed Enrichment of Epithelial Cell Population from Co-Culture. UK Society for Biomaterials 13th Annual Conference

- <u>Hickman G.J</u>, Boocock D.J Rees R.C & Perry C.C. (2012). Interactions of Cancer Cells & Inorganic Materials; Demonstrating a Selective Surface. Royal Society of Chemistry Special Interest Group Biomaterials 7th Annual Meeting

Poster presentations

- <u>Hickman G.J</u>, Boocock D.J Rees R.C & Perry C.C. (2012). Super-Hydrophilic Silica Surfaces for Tissue Culture. UK Society for Biomaterials 12th Annual Conference

- <u>Hickman G.J</u>, Boocock D.J Rees R.C & Perry C.C. (2011). Interactions of Cancer Cells & Inorganic Materials; Towards a Selective Surface. 10th International Conference on Materials Chemistry (MC10)

- <u>Hickman G.J</u>, Rai A, Boocock D.J Rees R.C & Perry C.C. (2011). Investigation into the effects of biomimetic silica surfaces on the culture of melanoma cell lines using proteomic methods. 8th East Midlands Proteomics Workshop